

LOCAL ATMOSPHERIC CIRCULATIONS AND THE  
MESOCLIMATE OF DURBAN

*by*

ROBERT ARTHUR PRESTON-WHYTE, B.A. (Hons), M.A. (Natal)

*Submitted in partial fulfilment of  
the requirements for the degree of  
Doctor of Philosophy in the Depart-  
ment of Geography, University of  
Natal, Durban*

1970

## CONTENTS

	Page
Table of Contents	ii
List of Figures	vi
List of Tables	xv
List of Symbols	xviii
Preface	xix
 PART I	
INTRODUCTION	1
 CHAPTER 1 : TOPOGRAPHIC SETTING, WEATHER AND CLIMATE	2
1.1 Topographic setting	2
1.2 Weather and climate	8
1.2.1 <i>Characteristics of pressure systems</i>	8
1.2.2 <i>Characteristics of weather systems</i>	10
1.2.2.1 Anticyclones	10
1.2.2.2 Cyclones	11
1.2.2.3 Coastal lows	13
1.2.2.4 Berg winds	18
1.2.3 <i>Characteristics of climate</i>	20
1.2.3.1 Wind	20
1.2.3.2 Temperature and humidity	24

	Page
CHAPTER 2 : OBSERVATION AND ANALYSIS	31
2.1 Introduction	31
2.2 Instrumentation and location	31
2.2.1 <i>The measurement of wind by balloons</i>	31
2.2.2 <i>The measurement of wind by anemometer</i>	36
2.2.3 <i>The measurement of temperature and humidity by motor vehicle traversing</i>	38
2.2.4 <i>Lapse rate measurements by tethered balloon</i>	40
2.3 Harmonic analysis	41
PART II CHARACTERISTICS OF LOCAL WIND SYSTEMS	44
CHAPTER 3 : SEA BREEZES	45
3.1 Introduction	45
3.2 General characteristics	45
3.3 Frequency of occurrence	48
3.4 Inland penetration	50
3.5 Depth and velocity characteristics	59
3.6 Surging	67
3.7 The effect of gradient winds	69
CHAPTER 4 : LAND BREEZES	78
4.1 Introduction	78
4.2 General characteristics	78
4.3 Frequency of occurrence	83
4.4 Depth	85
4.5 Land breeze and mountain-plain wind interaction	90

		Page
4.6	The effect of gradient winds	97
4.7	Seaward penetration	100
CHAPTER 5 :	DRAINAGE WINDS	102
5.1	Theoretical models	102
5.2	Onset	106
5.3	Damming and channelling	106
5.4	Depth	111
5.5	Surging	116
5.6	The effect of gradient winds	118
5.7	Dissipation	121
PART III	THE EFFECT OF LOCAL CIRCULATIONS UPON SELECTED CLIMATIC ELEMENTS	125
CHAPTER 6 :	THE DIURNAL VARIATION OF RAINFALL AT DURBAN	126
6.1	Introduction	126
6.2	Theories of nocturnal rainfall	127
6.3	Characteristics of the diurnal variation of rainfall	129
6.4	A model for low intensity nocturnal precipitation over Durban	137
6.5	Evening thunderstorms over Durban	141
CHAPTER 7 :	WIND AS A FACTOR IN THE FORM OF DURBAN'S HEAT ISLAND	152
7.1	Introduction	152



	Page
7.2 The urban setting	156
7.3 Land breeze - drainage wind modification of the temperature field	156
7.4 Sea breezes and the urban temperature field	159
7.5 Gradient wind modification of the temperature field	162
7.6 Comparison of mean summer and winter reduced temperature	165
7.7 A spatial model of the urban heat island	167
CHAPTER 8 : PHYSIO-CLIMATIC VARIATIONS IN THE DURBAN AREA	172
8.1 Introduction	172
8.2 The spatial variation of temperature	176
8.3 The spatial variation of vapour pressure	178
8.4 A spatial model of physio-climatic variations	183
PART IV CONCLUSIONS	187
CHAPTER 9 : SUMMARY AND CONCLUSIONS	188
REFERENCES	204

## LIST OF FIGURES

Figure		Page
1.1	Altitudinal zones of Natal.	3
1.2	Relief and location map of the Durban area.	3
1.3	Map to show physiographic regions of the coastal belt at Durban:	5
	1. Bluff ridge	
	2. Coastal alluvial flats	
	3. Coastal sand ridge	
	4. Hill and valley region	
	5. Interfluve region	
	6. Pinetown basin	
	7. Dissected valley-gorge region	
	8. Kloof plateau	
1.4	Relief and location map of the Pinetown basin.	5
1.5	Map and topographic section to show relief and location along the Mgeni - Mlazi River interfluve.	7
1.6	Surface and upper air charts to describe the passage of a cold front over South Africa on selected days between 17-21.5.66.	14
1.7	Variations of daily minimum temperature ( $^{\circ}\text{C}$ ) and rainfall (mms) over South Africa with the passage of a cold front, 17-21.5.66.	15
1.8	January 1967 vertical time section at Durban to show 24 hour height changes (metres) of constant-pressure surfaces.	17
1.9	July 1967 vertical time section at Durban to show 24 hour height changes (metres) of constant-pressure surfaces.	17
1.10	Time sections to show wind components (m/sec) normal to the coast (u), parallel to the coast (v) and wind directions during the passage of a coastal low, 30.6.69. Positive u components	19

		Page
2.5	Winter 1968 location of 0400-0500 temperature recording stations in the Pinetown basin.	39
3.1	Profiles and horizontal components of balloon trajectories to show the onset of the sea breeze on 6.12.67 at station 17, Cowies Hill.	49
3.2	Profiles and horizontal components of balloon trajectories to show the onset of the sea breeze on 6.12.67 at station 19, Botha's Hill.	51
3.3	Profiles and horizontal components of balloon trajectories to show the onset of the sea breeze on 8.1.68 at station 20, Cato Ridge.	51
3.4	Profiles and horizontal components of balloon trajectories to show the onset of the sea breeze on 16.1.68 at station 21, Mpushini.	52
3.5	Velocity isopleths (m/sec) to show the inland migration of the sea breeze on 6.12.67.	54
3.6	Section to show variations in the height of the zero wind component, 4.1.68. Velocity isopleths in m/sec.	54
3.7	The penetration of the sea breeze beyond station 21 on 11.1.68. Velocity isopleths in m/sec.	55
3.8	Possible interaction between sea breezes and valley winds suggested by strengthened on-shore components of air movement on 26.1.68 at station 21. Velocity isopleths in m/sec.	55
3.9	The variation in pressure over Natal and the adjacent Indian Ocean and changes in the speed and direction of upper winds at 1400 on 11.1.68. Pressure over the land is reduced to 850 milli-bars; over the sea to mean sea level.	58
3.10	Time section to show wind direction and onshore (positive) and offshore (negative) wind components in m/sec on 28.11.68 at station 2.	60
3.11	Computed vertical cross-section perpendicular to the coast to show the development of the sea breeze. $u$ , component of air movement normal to the coast positive onshore, $w$ , component of vertical air movement positive upwards, $\theta$ potential temperature ( $^{\circ}\text{A}$ ) (after Fisher, 1961).	61

	show onshore air movement, positive $v$ components air movement directed down the coast.	
1.11	Autographic records to show the occurrence of a Berg wind and passage of a coastal low.	21
1.12	Mean wind speeds (mph) for each month at Louis Botha airport, Durban (after S.A. Weather Bureau, 1960).	23
1.13	February, June and October mean wind speeds (mph) for each hour at Louis Botha airport, Durban (after S.A. Weather Bureau, 1960).	23
1.14	Isopleth graphs showing monthly variations of mean hourly wind speed (mph) at Stamford Hill (station 13), Louis Botha airport (station 15) and Reservoir Hills (station 12) (partly after S.A. Weather Bureau, 1960).	25
1.15	Isopleth graphs showing monthly variations of mean hourly temperature ( $^{\circ}\text{C}$ ) and mean hourly relative humidity (%) at Durban Weather Bureau (after S.A. Weather Bureau, 1954).	26
1.16	Diurnal variation of temperature lapse rate ( $^{\circ}\text{C}$ ) on 28.7.67 at station 18.	27
1.17	Diurnal variation of temperature lapse rate ( $^{\circ}\text{C}$ ) from 3-12.7.66 at station 18.	27
1.18	Tephigram showing mean temperature lapse rates for December, March, June and September, 1964-1966 at Durban.	28
1.19	Tephigrams showing mean temperature lapse rate and standard deviations for the period 1964-1966 at Durban.	28
2.1	Map to show location of observing stations in the Durban area. Double theodolite stations are connected by a solid line.	35
2.2	Map to show the location of balloon observing stations north-west of Durban.	35
2.3	Summer 1968-69 and winter 1968 location of midday temperature recording stations in the Durban area.	37
2.4	Winter 1968 location of 0400-0500 temperature re- cording stations in the Durban area.	39

		Page
4.3	Wind roses for station 14 and 15, July 1963.	84
4.4	Time section to show depth (ft), velocities (m/sec) and direction characteristics of the land breeze and transition zone to the gradient wind. Observations on 4-5.7.67 from station 18.	86
4.5	Time section to show variations in the depth of the land breeze. Observed on 15-16.7.68 from station 1.	87
4.6	Time section to show lack of direction shear separating the land breeze from upper winds. Observed on 26-27.7.67 from station 18.	89
4.7	Section to show the inland migration of the land breeze on 16.6.67. Velocity isopleths in m/sec.	89
4.8	Land breeze - mountain-plain wind interaction on 1.7.68 in the Durban area. Velocity isopleths in m/sec.	91
4.9	Sections to show the existence of mountain-plain winds independent of the land breeze on 8.7.68. Velocity isopleths in m/sec.	93
4.10	Mountain-plain wind - land breeze interaction on 10.7.68 between Durban and Cato Ridge. Velocity isopleths in m/sec.	93
4.11	Mountain-plain wind - land breeze interaction on 12.7.68 between Durban and Cato Ridge. Velocity isopleths in m/sec.	95
4.12	Mean profiles of the land breeze - mountain-plain wind for July 1968 at stations 10, 17, and 19.	95
4.13	Time section to show depth (ft), velocity (m/sec) and direction characteristics of the land breeze under post-frontal conditions. Observations on 5-6.7.67 from station 18.	96
4.14	Time section to show depth (ft), velocities (m/sec) and direction characteristics of the land breeze under post-frontal conditions. Observations on 3-4.7.67 from station 18.	98
4.15	Seaward penetration of the land breeze under fine weather conditions. Balloon releases on 27.6.63 from stations 16 and 2.	99

		Page
3.12	Time section to show depth (ft), velocity (m/sec) and direction characteristics of the sea breeze on 7.7.67 at station 18.	63
3.13	Time section to show depth (ft), velocity (m/sec) and direction characteristics of the sea breeze recorded on 3.12.68 at station 2.	65
3.14	Mean profiles of onshore wind components (m/sec) measured on 28.11.68 and 3.12.68 from station 2.	66
3.15	Velocity spectra of the sea breeze, 0920-1220, on 28.11.68 at station 2.	68
3.16	Velocity spectra of the sea breeze, 0955-1150 on 3.12.68 at station 2.	68
3.17	Inland migration of the sea breeze with weak north-east gradient winds on 16.1.68. Velocity isopleths in m/sec.	70
3.18	Inland migration of the sea breeze with strong north-east gradient winds on 22.1.68. Velocity isopleths in m/sec.	70
3.19	Time section to show depth (ft), velocity (m/sec) and direction characteristics of the sea breeze under post-frontal conditions. Observations on 20.1.69 from station 2.	71
3.20	Time section to show depth (ft), velocity (m/sec) and direction characteristics of the sea breeze under post-frontal conditions. Observations on 5.7.67 from station 18.	73
3.21	Time section to show backing of the sea breeze as north-east gradient winds are reinstated. Observations on 6.7.67 from station 18, velocity isopleths in m/sec.	74
3.22	Time section to show a possible frontal onset of the sea breeze on 26.7.67 at station 18. Velocity isopleths in m/sec.	75
4.1	Profiles and horizontal components of balloon trajectories to show the onset of the land breeze on 1.7.68 at station 19, Botha's Hill.	81
4.2	Profiles and horizontal components of balloon trajectories to show the onset of the land breeze on 12.7.68 at station 20, Cato Ridge.	82

		Page
5.1	Comparison between wind speeds (m/sec) and direction on 7.7.64 at stations 4 and 14. Temperatures (°C) recorded at station 4.	107
5.2	Time sections to show drainage winds on 17.7.63 at stations 4 and 8. Wind speed isotachs in m/sec; pecked lines indicate transitional boundaries.	107
5.3	Time section to show the onset of south-west drainage winds at station 9. Velocity isopleths in m/sec.	109
5.4	Relief and location map of the Richards Bay area.	110
5.5	Time section to show depth (ft), velocity (m/sec) and direction characteristics of drainage winds recorded on 25-26.5.68 from station 22 at Richards Bay.	110
5.6	Comparison of drainage wind speeds at 6 ft (m/sec) measured on 15-16.7.68 at station 1 and 9-10.7.69 at station 2.	113
5.7	Time section to show depth (ft), velocity (m/sec) and direction characteristics of the drainage wind on 11.7.69 in the Mgeni River valley at station 2.	114
5.8	Comparison of the mean offshore wind component profile in the drainage wind-land breeze (dots) with the Prandtl profile (solid line), 11.7.69.	114
5.9	Time section to show depth (ft), velocity (m/sec) and direction characteristics of the drainage wind in the Mgeni River valley with upper north-north-east gradient winds. Observations on 9-10.7.69 from station 2.	115
5.10	Comparison of the mean offshore wind component profile in the drainage wind (dots) with the Prandtl profile (solid line) 9-10.7.69.	115
5.11	Velocity spectra of the drainage wind, 0205-0405 on 11.7.69 at station 2.	117
5.12	Drainage wind - gradient wind interaction over the sea. Balloon release on 1.7.63 from station 2.	119
5.13	Backing of the drainage wind with time observed on 19-20.5.67 from station 2.	119

		Page
5.14	Time section to show weakening of the drainage wind over Natal Bay. Observations on 9.7.63 from station 8. Wind speed isotachs in m/sec; pecked lines indicate transitional boundaries.	122
6.1	Mean hourly rainfall amount in mms (solid line) and mean frequency of occurrence (dashed line) at Louis Botha airport, Durban, 1958-67.	131
6.2	Mean hourly rainfall amount (mms) by month at Louis Botha airport, Durban, 1958-67.	131
6.3	Percentage frequency hourly rainfall occurrences by month at Louis Botha airport, Durban, 1958-67.	132
6.4	Median and upper quartile rainfall plotted against mean hourly rainfall (mms) recorded in December, January and February at Louis Botha airport, Durban, 1958-67. The straight line indicates equal values of upper quartiles or medians and means.	135
6.5	Median and upper quartile rainfall plotted against mean hourly rainfall (mms) recorded in June, July and August at Louis Botha airport, Durban, 1958-67. The straight line indicates equal values of upper quartiles or medians and means.	135
6.6	Diagrammatic model showing the influence of land breeze and mountain-plain winds upon nocturnal precipitation over the coast.	138
6.7	Mean annual rainfall distribution normal to the coast at Durban (after S.A. Weather Bureau, 1965).	140
6.8	Track of thunderstorms which move towards Durban from the interior of Natal.	143
6.9	Model of a large isolated thunderstorm or squall-line element embedded in an environment in which the wind backs with height (after Newton, 1960).	145
6.10	Diagrammatic model showing the movement of a thunderstorm towards the coast following the retreating convergence zone between onshore and offshore winds.	146
6.11	Surface, 500 mb and 300 mb charts, upper air dry bulb and dew point temperatures and velocity (m/sec) and direction characteristics of the sea breeze on 9.1.69 at Durban.	148





		Page
6.12	Autographic records during the passage of a thunderstorm past Durban on 9.1.69.	149
7.1	Residential density, work zone and recreational regions in the Durban area (after Davies, 1960; Davies and Rajah, 1965).	155
7.2	Isotherms ( $^{\circ}\text{C}$ ) of mean minimum temperature, July 1968 in the Durban area.	157
7.3	Isotherms ( $^{\circ}\text{C}$ ) of mean minimum temperature in the Pinetown basin, July 1968.	157
7.4	Isotherms ( $^{\circ}\text{C}$ ) of mean midday corrected temperatures under north-east sea breeze conditions, November-February 1969.	161
7.5	Isotherms ( $^{\circ}\text{C}$ ) of mean midday corrected temperatures under southerly wind conditions, November-February 1969.	163
7.6	Isotherms ( $^{\circ}\text{C}$ ) of mean midday corrected temperatures, November-February 1969.	164
7.7	Isotherms ( $^{\circ}\text{C}$ ) of mean midday corrected temperatures, June 1969.	164
7.8	Location of section lines for the harmonic analysis of mean spatial temperatures over Durban.	168
8.1	Isotherms ( $^{\circ}\text{C}$ ) of mean midday uncorrected temperatures, November-February 1969.	175
8.2	Isotherms ( $^{\circ}\text{C}$ ) of mean midday uncorrected temperatures, June 1969.	175
8.3	Section to show the reduction of mean summer temperature ( $^{\circ}\text{C}$ ) and vapour pressure (mbs) with distance inland from the Berea crestline.	177
8.4	Mean midday vapour pressure isopleths under north-east sea breeze conditions, November-February 1969.	177
8.5	Mean midday vapour pressure isopleths under southerly wind conditions, November-February 1969.	179
8.6	Mean midday vapour pressure isopleths, November-February 1969.	181
8.7	Mean midday vapour pressure isopleths, June 1969.	181

		Page
8.8	Mean midday isopleths of the Temperature-Humidity Index, November-February 1969.	184
9.1	Relief and location map of the Hillcrest scarp region.	193
9.2	Model to show stages of mountain wind deepening and overflow onto the Kloof-Hillcrest plateau.	193
9.3	The movement of atmospheric pollution from a single source by local circulations and gradient winds on the Natal coast.	201
9.4	Diagrammatic model to show nocturnal local air circulations during winter in the Durban area.	201

## LIST OF TABLES

Table		Page
1.1	Details of the configuration of the Durban area.	4
1.2	Configuration details of valleys through the Berea ridge.	4
1.3	Details of the configuration of the Pinetown basin.	6
1.4	Percentage frequency of stable discontinuities over Durban (after Taljaard, 1955).	11
1.5	Frequency per month of the movement of cold fronts past Durban, 1965-67 (after S.A. Weather Bureau daily synoptic charts).	12
1.6	Frequency per month of the movement of coastal lows past Durban, 1965-67 (after S.A. Weather Bureau daily synoptic charts).	18
1.7	Mean wind speeds in mph for each direction at Stamford Hill airport, Durban (after S.A. Weather Bureau, 1960).	22
3.1	Mean hourly wind speed ( $\bar{U}$ ) in mph and the mean hourly land-sea temperature difference ( $\Delta T$ ) in $^{\circ}\text{C}$ during February and July at Durban (after S.A. Weather Bureau, 1954, 1960; Wellington, 1955).	47
3.2	Frequency of wind directions per 500 for the 12 daytime hours at station 13, Durban (after S.A. Weather Bureau, 1960).	50
3.3	Mean height in geopotential metres of the 850 mb surface during January 1969 at weather stations in the Transkei, East Griqualand and Natal (after Durban Meteorological Office daily 1400 synoptic charts).	57
3.4	December to February wind resultants over Durban (after S.A. Weather Bureau Rawin data, 1965-66).	64

		Page
4.1	Mean hourly wind speeds in mph and the mean hourly land-sea temperature difference ( $\Delta T$ ) in $^{\circ}\text{C}$ during February and July at Durban (after S.A. Weather Bureau, 1954, 1960; Wellington, 1955).	80
4.2	Monthly frequencies (per cent) of land breezes recorded from June 1967 to May 1968 at station 12.	85
4.3	Examples of pre-dawn directions and depths (ft) of the land breeze over Durban.	85
5.1	Volume ( $\text{m}^3$ ) of air transported by drainage winds of varying speed (m/sec) past the section line in Fig. 2.1.	111
6.1	30 year (1921-50) rainfall normals for Durban Point (after Climate of South Africa, 1950).	130
6.2	Frequency of raindays during specified hours recorded at Louis Botha airport, Durban, 1958-67.	133
6.3	Percentage frequency of rainfall intensities (mm/hr) between 0700-1800 and 1900-0600 in January and July at Louis Botha airport, Durban, 1958-67.	134
6.4	Percentage frequency of occurrence and percentage contribution to total monthly rainfall of 10 hour continuous rainfall at Louis Botha airport, Durban, 1958-67.	136
6.5	Frequency of occurrence at Durban Heights of wind components normal to the coast during periods of rainfall from July to December, 1967.	141
7.1	Percentage frequency of wind observations from December to February at Durban (after Weather on the coasts of Southern Africa, 1941).	160
7.2	Seasonal range and mean extreme temperatures ( $^{\circ}\text{C}$ ) along the east-west section, G-H, through the heat island.	165
7.3	Mean seasonal temperature differentials, $\Delta T^{\circ}\text{C}$ , between the seashore, heat island, and Berea crest, along the section line G-H.	166

		Page
7.4	Spatial distribution of mean summer and winter reduced temperature ( $^{\circ}\text{C}$ ) expressed by Equation 7.1. $S_k$ denotes cumulative percentage contribution to the total variance.	169
8.1	Spatial variation of mean summer Temperature-Humidity Index. $S_k$ denotes cumulative percentage contribution to the total variance.	185

## LIST OF SYMBOLS

$a$	amplitude
$A, B$	lengths of parallel sides of trapezium
$C$	cloudiness
$d$	distance
$e$	vapour pressure
$exp$	exponent
$h$	height of maximum wind component
$H$	depth of wind system
$k$	wave number
$L$	free lift
$N$	number of observations
$p, q$	harmonic constants
$S$	percentage contribution to variance
$t$	time
$T, T_d$	dry bulb temperature
$T_w$	wet bulb temperature
$\bar{T}_s$	space mean temperature
$\Delta T$	temperature differential between land and sea
$\overline{THI}_s$	space mean Temperature-Humidity Index
$\bar{U}$	mean wind speed
$u$	x component of wind velocity
$v$	y component of wind velocity
$U_m$	maximum wind speed
$V$	rate of ascent
$W$	balloon weight
$z$	height, perpendicular distance between parallel sides of a trapezium
$\sigma$	standard deviation
$\phi$	phase angle

## PREFACE

Rapid urban and industrial growth along the Natal coast has occurred with little concern for characteristics of local climate. In general, industrial growth has taken place without taking into account the potential for pollution transportation during the winter season; urban areas have developed without consideration for the vital need in sub-tropical latitudes to maintain adequate mixing of the lower atmosphere. The apparent inadequacy in planning for climate has partly been due to a lack of understanding of the nature and characteristics of local wind systems. The motivation for this study stems, therefore, from the need to evaluate the influence of land-sea and topographically-induced wind systems upon certain aspects of weather and climate on the Natal coast.

During summer, moist and relatively cool air is advected almost daily over the Natal coast by the sea breeze. Observations of spatial and temporal variations of these winds were made in the period 1963-69 from recording stations in the Durban area and along a 40-mile transect approximately normal to the coast at Durban. Comparable observations have not as yet been made in South Africa nor have there been attempts to examine the influence of sea breezes upon selected climate and weather phenomenon. In this latter connection the role of the sea breeze is examined in two separate fields in this study, namely urban climatology and thunderstorm development.

Climatic discomfort caused by the combined effect of high temperatures and humidities on the Natal coast, is at a maximum in urban areas. Since these areas are also highly populated, a need exists to evaluate the ability of the sea breeze to reduce urban

temperatures by advection of cooler air over the area, by eddy diffusion of heat or by displacement of urban temperatures away from poorly ventilated areas. Thus climatic discomfort in these areas may also be reduced. Detailed observations of the influence of the sea breeze, in particular, and wind in general, upon the spatial variation of temperature, humidity and human comfort were, therefore, undertaken in the Durban area. It is believed that this is the first time an attempt has been made to describe the spatial distribution of a comfort index in an urban area. The results should be of interest to the architect and town planner.

The sea breeze, strengthened by gradient and valley winds, is shown to penetrate at least 40 miles inland. In accordance with this, it is suggested that the inland invasion of marine air takes place in response to lowered pressure in adjacent inland areas in southern Natal and provides the moisture required to feed thunderstorms which develop in this area. These storms subsequently move towards the coast following the retreating convergence zone between winds with an onshore and offshore component of motion and reach Durban after sunset.

Land breezes are best developed in winter. Observational techniques were similar to those employed in the sea breeze study and provide the only detailed examination of spatial and temporal variations of land breezes in South Africa. Until recently the nature and characteristics of topographically-induced winds in Natal were also a relatively unexplored feature of local atmospheric circulations. However, Tyson (1967) has examined local winds in certain Natal valleys and his prediction that mountain-plain winds reach the coast during the night is also examined in this study.

While the relatively weak and shallow land breeze may be of secondary importance when compared with the sea breeze, it would be a mistake to underestimate the importance of these winds upon certain



aspects of coastal climate. In particular the tendency for land breezes to initiate cloud and precipitation at night is examined while the potential for the transportation of atmospheric pollution by these winds is also briefly discussed.

A study of the diurnal variation of precipitation at Durban reveals a high frequency of low intensity precipitation at night. The nature of this precipitation differs in both frequency and amount from high intensity rainfall which is the product of thunderstorm and frontal activity. It is suggested in this study that the land breeze plays a dominant role in providing the buoyancy necessary to cause nocturnal drizzle precipitation from shallow stratus cloud.

The thesis is divided into four parts. Part I examines details of the physiography, weather, climate, observational methods and analysis techniques. Because of the variability of weather on the coast of Natal that section is dealt with in more detail than would have been deemed necessary for a similar study inland. Without knowledge of the characteristics of the atmospheric circulation, the behaviour of local wind systems in relation to large scale systems could not be adequately discussed.

In Part II land and sea breezes and topographically-induced wind systems are examined in detail. Emphasis is placed not only on the observational characteristics of these winds such as onset, depth, velocity gradient, surging, relation to gradient winds and dissipation but also on their relation to theoretical models of the relevant wind system.

The influence of local wind systems upon selected climatic elements is dealt with in Part III. Characteristics of the diurnal variation of precipitation are examined in Chapter 6. Rainfall frequencies and amounts are shown to be highest in the first half

of the night and a model is developed to explain the influence of land breezes and mountain-plain winds upon low intensity but high frequency nocturnal rainfall. High intensity but low frequency rainfall produced by thunderstorms also occurs soon after sunset and a further model is advanced to explain this phenomenon in relation to the sea breeze.

The effect of air movement upon the spatial variation of temperature, humidity and a discomfort index in both summer and winter is examined in Chapters 7 and 8. The relationship between these elements has permitted the development of an empirical model to predict values across the city of mean midday summer and winter temperatures as well as discomfort index values.

In Part IV the most significant aspects relating to the study as a whole are summarised. In conclusion the potential for the transport of pollutants by land breezes and topographically-induced winds is briefly discussed as an aid to planning and simple spatial models are given showing generalised air movement and ventilation characteristics in the Durban area and along the Natal coast.

I am deeply conscious of the assistance I have received in all stages of the study. Part of the fieldwork was financed by a generous grant from the Council for Scientific and Industrial Research. The nature of the work required numerous fieldworkers and I am grateful to the many students who assisted me in this respect. In particular I wish to thank E. Wattleworth, D. Grant and C. Henzi. I am also indebted to Mr. Kleyweg of the Durban Meteorological Office for making weather records available, Mr. Hurrypursad whose assistance in the darkroom was invaluable, Miss K. Mack who persevered with the draft typing with considerable patience and Mrs. Foster-Storey who typed the thesis. Grateful thanks are also extended to Professor P.D. Tyson for some most

stimulating discussions. Finally I must express my appreciation to Professor R.J. Davies for his considerable assistance in the preparation of the thesis.

PART I

INTRODUCTION

## CHAPTER 1

## TOPOGRAPHIC SETTING, WEATHER AND CLIMATE

## 1.1 Topographic setting

The Natal coastal belt, defined here as the area lying below 2,000 ft in altitude, widens from 15 miles at Durban to 35 miles at Richards Bay and 60 miles at St. Lucia Bay (Fig. 1.1). South of Durban, incision by rivers through granite and resistant sandstone has produced deep, narrow valleys which extend to the coast; to the north the coastal strip becomes increasingly low-lying and river valleys shallow and wide. The coast is not indented but its smooth line is broken at Durban by a steep-sided sand ridge, known as the Bluff, which diverges from the normal line of the Natal coast at an angle of about  $14^{\circ}$ . Similar sand deposits line the coast and in places stand as ridges above the beach zone.

The Bluff ridge, which extends seawards at Durban, rises above 250 ft in altitude and dominates the coastal topography in this area (Fig. 1.2). The ridge forks 3.2 miles from its head and is approximately paralleled 0.9 miles to the west by the Wentworth ridge. West of these coastal ridges a further ridge, known as the Berea, parallels the coast and rises above 400 ft in altitude. Due to the divergence of the Bluff ridge from the line of the coast, the corridor between the coastal and Berea ridges widens towards the sea in the north. At Jacobs the distance between the base of the Wentworth and Berea ridges, taken as the 50 ft contour, is 0.3 miles. The corridor then widens to 1.8 miles at Umbilo, 2.2 miles at Congella and 3.5 miles at the northern end of the Bluff.

Natal Bay lies between the Bluff and Berea ridges and is

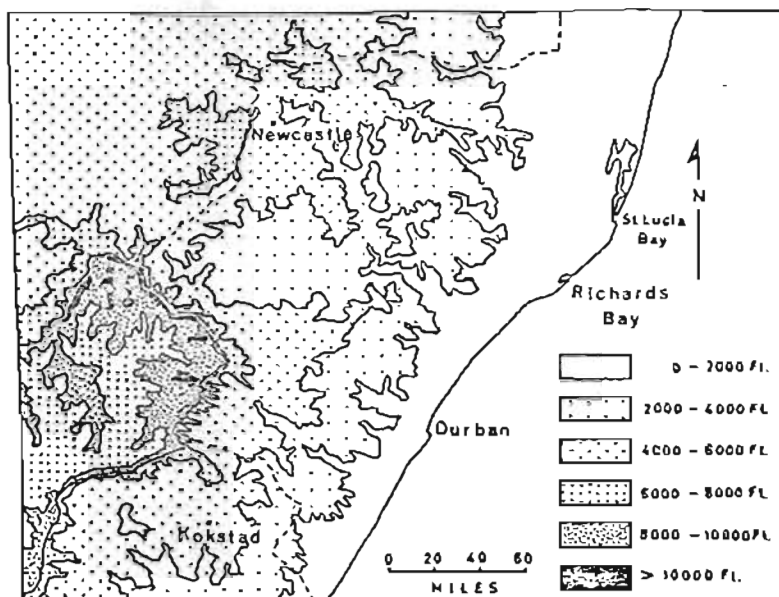


Fig. 1.1 : Altitudinal zones of Natal

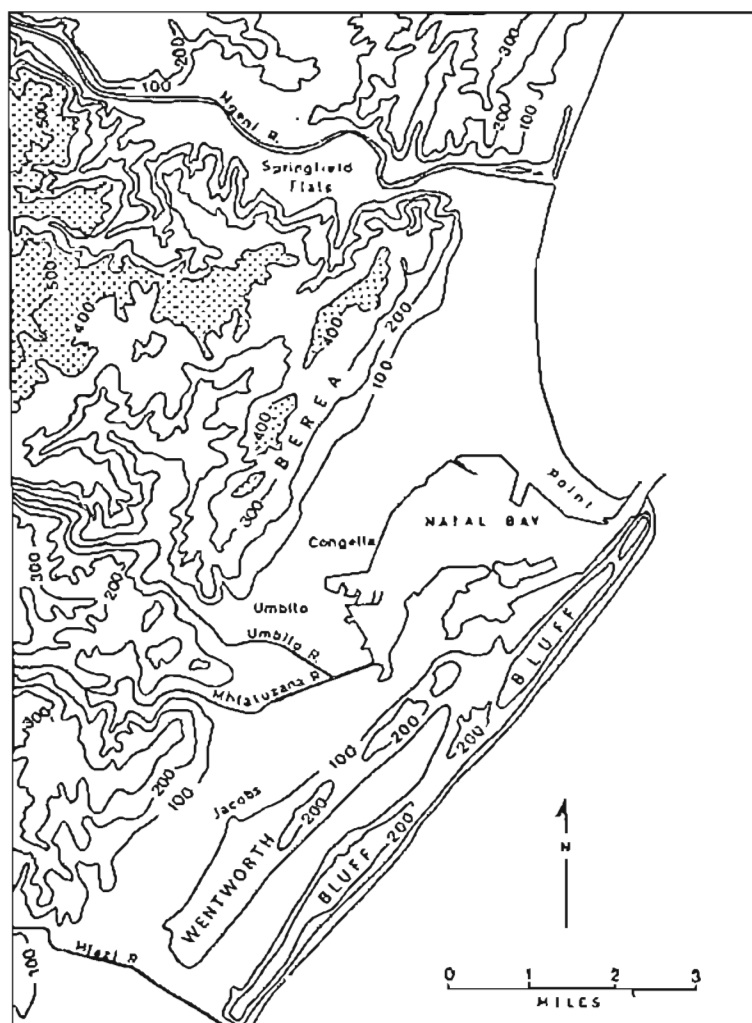


Fig. 1.2 : Relief and location map of the Durban area

enclosed to the north by a curved spit called the Point. The floor of the corridor between the ridges is flat and low-lying and consists largely of alluvium deposited by the Umbilo and Mhlatuzana Rivers which enter the bay in the south and the Mgeni River which entered the bay prior to 1860 in the north. This latter river has since changed its course to drain into the sea 3.5 miles north of Natal Bay. Further details of the configuration and geometry of the Durban area are given in Table 1.1.

Table 1.1: Details of the configuration of the Durban area

	Approximate Slope (deg)		Approximate Altitude (ft)	Trend (deg)
Berea ridge	(east facing)	7	440	30
Bluff ridge	(west facing)	39	290	38
Wentworth ridge	(west facing)	18	270	38-45

Rivers in the Durban area have entrenched narrow valleys through the Berea ridge. Table 1.2 shows that the Mgeni River valley through the ridge is the most narrow and is referred to in this study as the Springfield Gap.

Table 1.2: Configuration details of valleys through the Berea ridge

	Width (ft) at 200 ft contour	Trend (deg)
Mgeni River	1950	90
Umbilo River	2250	140
Mhlatuzana River	2400	120

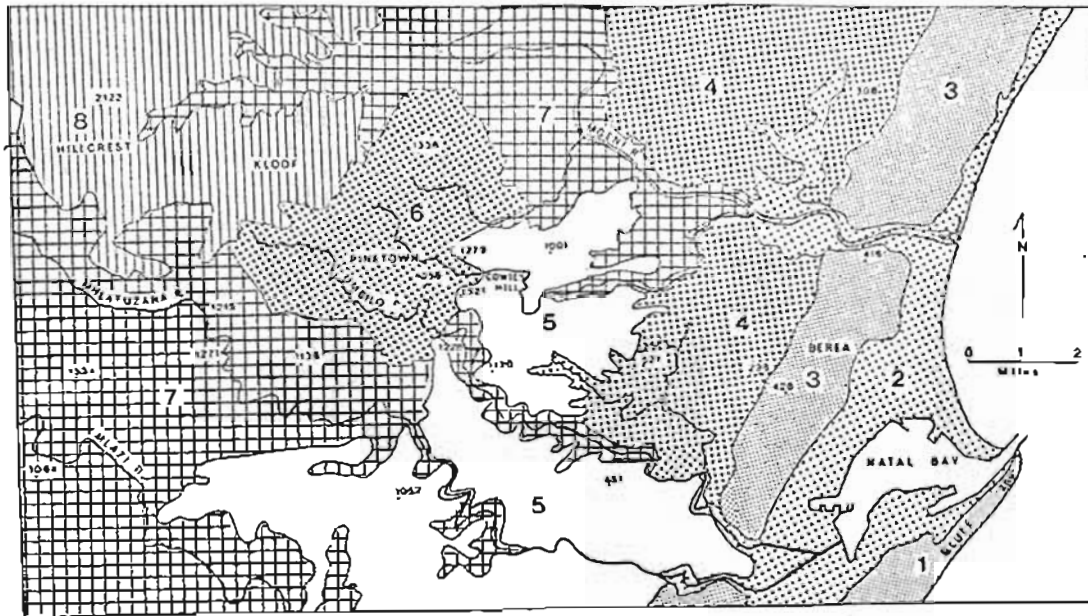


Fig. 1.3 : Map to show physiographic regions of the coastal belt at Durban:

1. Bluff ridge
2. Coastal alluvial flats
3. Coastal sand ridge
4. Hill and valley region
5. Interfluvial region
6. Pinetown basin
7. Dissected valley-gorge region
8. Kloof plateau

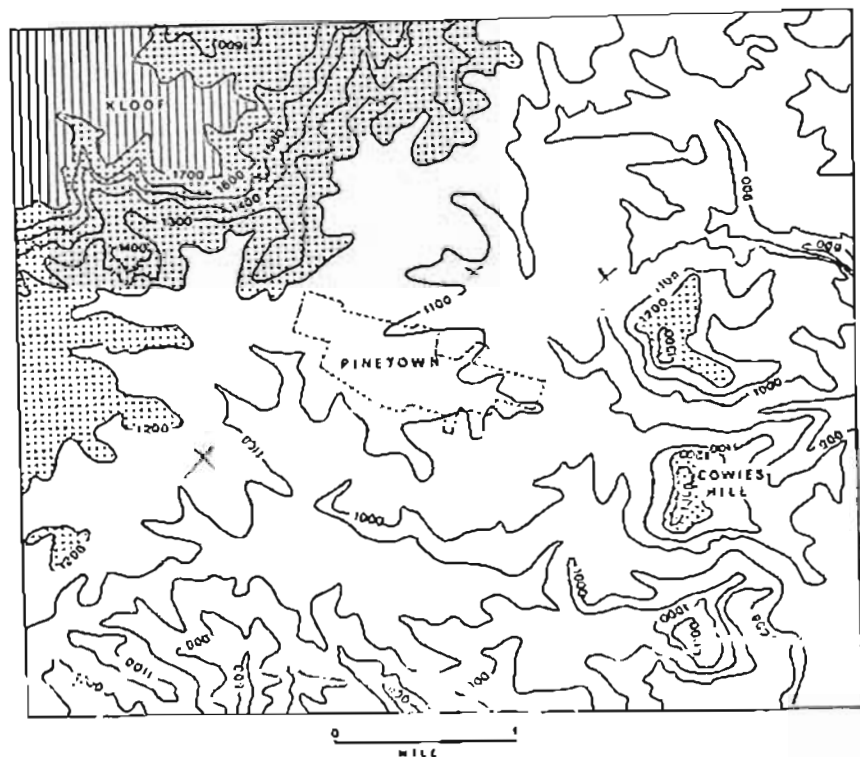


Fig. 1.4 : Relief and location map of the Pinetown basin





West of the Berea ridge a low-lying hill and valley region slopes up to interfluvial heights separated by entrenched east-west valleys (Fig. 1.3). The interfluves rise gently to 1,300 ft east of the Pinetown basin, the average elevation of which is about 1,100 ft. A sharp escarpment rising to above 1,700 ft forms the western edge of the Pinetown basin above which the Kloof-Hillcrest plateau extends westward for some 5.5 miles.

The Pinetown basin is partly cut off from the sea by the 1,300 ft Cowies Hill ridge. Fig. 1.4 shows that the floor of the basin also constitutes the watershed between north flowing tributaries of the Mgeni River and south flowing tributaries of the Umbilo River. Details of the configuration of the basin are given in Table 1.3.

Table 1.3: Details of the configuration of the Pinetown basin

Approximate Slope (deg)		Width (miles)		Approximate Altitude (ft)	
		between 1,100-1,200 ft contours		at crest of scarp	
SE	W	N-S	E-W	E	W
15	18	2.0	1.7	1,300 <sup>396</sup>	1,700 <sup>518</sup>

In common with much of the geology west of the Berea, the Kloof-Hillcrest plateau is cut across Table Mountain Sandstone. The resistance to weathering and erosion of the quartzitic strata in this stratigraphic series is responsible for the steep-sided nature of the valleys which the rivers have cut as they adjusted to base level. Consequently the Mgeni River flows about 1,700 ft below the crest of the planed, gently seaward sloping Kloof-Hillcrest plateau region although only some 12 miles from the coast.

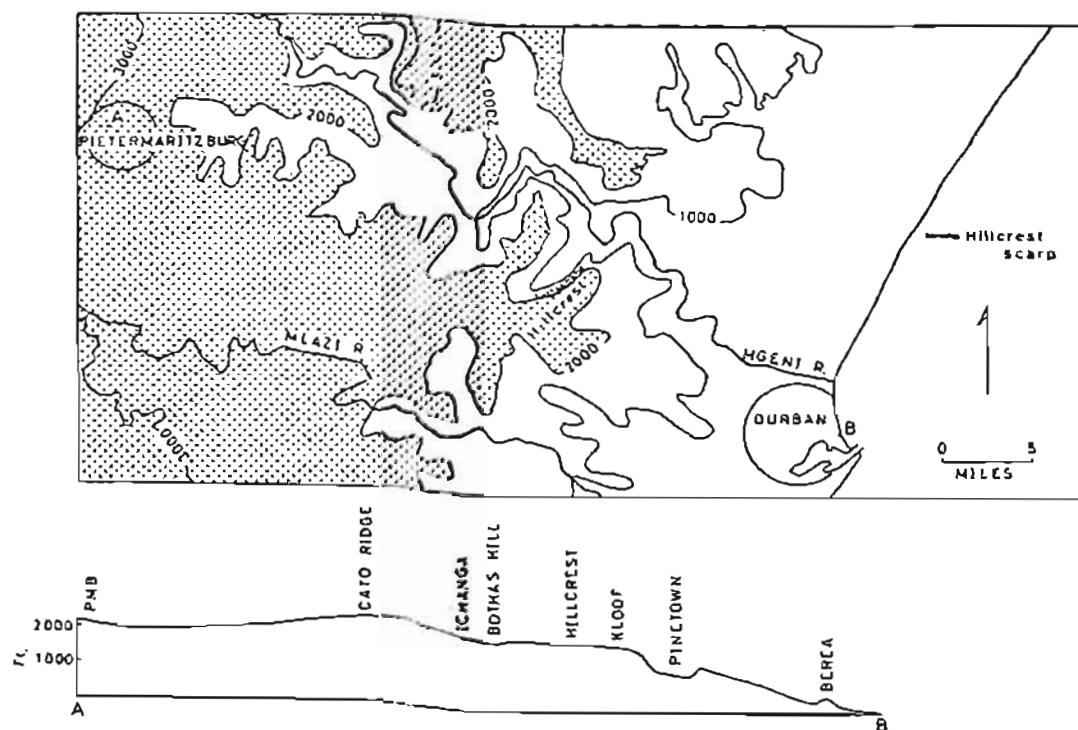


Fig. 1.5 : Map and topographic section to show relief and location along the Mgeni - Mlazi River interfluvium

The north-west margin of the Kloof-Hillcrest plateau is bounded by the steep-sided slope of the west-facing Hillcrest fault-line scarp (Fig. 1.5). Below this scarp lies a highly dissected region drained by the Mgeni River. The interfluvial region between the Mgeni River to the north and the Mlazi River to the south extends almost to Pietermaritzburg as an upland area between 2,000-2,500 ft.

## 1.2 Weather and climate

### 1.2.1 *Characteristics of pressure systems*

Atmospheric circulations over the Natal coast are primarily influenced by sub-tropical anticyclones. These are most numerous along  $36^{\circ}\text{S}$  in summer,  $32^{\circ}\text{S}$  in winter and  $34^{\circ}\text{S}$  in the intermediate seasons (Taljaard, 1967). A seasonal meridional oscillation of the mean position of the Indian Ocean high is largely due to interhemispherical mass transport, which is responsible for a pressure rise from January to July in the southern hemisphere and a fall in the latter half of the year. Vowinckel (1955) shows that from January to April, mass flux from northern to southern hemispheres between longitude  $0^{\circ}\text{E}$  and  $90^{\circ}\text{E}$ , bypasses the still overheated African continent and is transported to the middle latitudes where, over the Indian Ocean, an extensive pressure rise results. By April, however, the cooling African sub-continent is able to accommodate the mass transport from the north and a pressure rise begins in sub-tropical latitudes to reach a maximum intensity in July.

The increase of pressure over Southern Africa is accompanied by a movement of the Indian Ocean high into the western part of this ocean and it reaches about  $65^{\circ}\text{E}$  in June (Vowinckel, 1955). This makes it the only maritime sub-tropical high pressure cell whose centre of gravity moves into the western part of an ocean. van Loon (1961)

attempts an explanation of this phenomenon by suggesting that the circulation over Australasia may influence the seasonal movement of the Indian Ocean high. Rapid cooling of the Australian continent in winter produces a source of cold air over the land with a relatively warm surrounding sea contributing to what amounts to a warm source. A split in the upper westerlies results, an occurrence marked by the development of highs further south than elsewhere in the southern hemisphere and by cold pools and depressions at upper levels. It may be possible, therefore, to connect the mean zonal high pressure oscillation in the Indian Ocean with the development and disappearance of the split in the westerlies over Australasia.

The intensity of the winter anticyclone in the Indian Ocean is greater than is to be found with anticyclones over all the other oceans (Vowinckel, 1955). This characteristic, together with the westward and northward shift of the mean position of the high, exerts a profound effect upon the nature and characteristics of winter climate on the Natal coast. Lengthy spells of warm, dry, cloudless weather which accompany anticyclonic cells provide ideal conditions for the development of land breezes and topographically-induced wind systems. These local winds also provide a mechanism for the transport, rather than dispersal, of atmospheric contaminants which collect beneath subsidence or radiation inversions. However, in this season frontal depressions also penetrate further north than in summer to produce weather along the Natal coast which is more characteristic of temperate than of sub-tropical latitudes. The development of local wind systems is then inhibited by the strong winds, cloud and possible rain that accompanies these depressions while accumulated atmospheric pollution is rapidly dispersed.

During summer the inter-hemispherical mass flux is reversed and movement is towards the northern hemisphere. This is succeeded by a weakening of the Indian Ocean high pressure cell and is accompanied by an eastward shift of the centre of gravity of the high to  $88^{\circ}\text{E}$  by

December (Vowinckel, 1955) as well as by a southerly displacement of the axis of the belt. This latter movement is primarily responsible for a reduction in summer of the frequency with which cold fronts penetrate into sub-tropical latitudes. However, throughout this season the lower atmosphere along the Natal coast is well mixed due largely to strengthened sea breezes and gradient winds and weaker subsidence inversions.

## 1.2.2 *Characteristics of weather systems*

### 1.2.2.1 Anticyclones

The Indian Ocean high must not be regarded as a permanently established element but rather as a composite of eastward moving individual cells. The movement of these anticyclones in the Indian Ocean belt occurs along a more restricted latitudinal zone than is to be found in the other oceans (Taljaard, 1967). In summer, for instance, the belt is only 8-12° wide with highest frequencies of anticyclone centres at 37°S (Taljaard and van Loon, 1963). Many of these cells skirt the Cape and south-east coast of South Africa, while the remainder extend ridges eastward across the continent. The longevity of these cells is remarkable and attempts to trace their lifespan have suggested periods of up to 24 days.

Subsidence from anticyclones result in the development of temperature inversions or quasi-isothermal layers at the boundary between cool, moist surface air and drier, warmer upper air<sup>1</sup>. At Durban two such stable discontinuities are frequently present. The

---

<sup>1</sup> Taljaard, Schmidt and van Loon (1961) define an inversion as "a rise in temperature exceeding 0.5°C over an interval of 50 mbs in an upward direction" and a quasi-isothermal layer as "one in which the lapse rate is less than the saturated adiabatic lapse rate but in which the increase in temperature with height does not exceed 0.5°C per 50 mbs."

upper, generally above 700 mbs divides continentally modified tropical air from overlying superior air, while the lower divides tropical or polar maritime air from overlying continentally modified tropical air (Taljaard, 1955). In Table 1.4 stable discontinuities in summer are shown to increase in frequency from the surface to 800 mbs but to decrease upwards in winter. This indicates a high frequency of near-surface inversions in winter which differ from nocturnal inversions by their presence throughout the day or for as long as the anticyclone persists.

Table 1.4: Percentage frequency of stable discontinuities over Durban (after Taljaard, 1955)

Elevation (mbs)	Winter	Summer
1000	34.3	4.9
950	13.0	12.9
900	11.8	16.5
850	9.5	19.7
800	9.9	21.7
750	7.0	8.8
700	2.1	2.2

#### 1.2.2.2 Cyclones

In general the sub-tropical anticyclone belt overlaps the zone of cyclonic activity on its poleward side. However, in the western Atlantic Ocean a deviation from this pattern occurs. In winter, cyclogenesis is most frequent in the belt between 25°S and 35°S which is north of the zone occupied by most anticyclonic centres (Taljaard and van Loon, 1962). From these latitudes cyclones move west-north-west to east-south-east in the Atlantic Ocean in a belt

which stretches from approximately  $22^{\circ}\text{S } 55^{\circ}\text{W}$  to  $40^{\circ}\text{S } 20^{\circ}\text{E}$ . The mean winter track of cyclones crosses the anticyclonic belt in mid-Atlantic so that only the effect of a trailing cold front is likely to be experienced along the south and east coasts of Southern Africa.

Summer cyclones exhibit the same directional characteristics as in winter. However, cyclogenesis now occurs more frequently between  $55^{\circ}\text{S}$  and  $70^{\circ}\text{S}$  which is in accordance with the southward displacement of the pressure belts. The northern limit of the belt of high frequency cyclogenesis stretches from about  $40^{\circ}\text{S}$  off the coast of South America to  $50^{\circ}\text{S}$  in mid-Indian Ocean (Taljaard and van Loon, 1963).

The seasonal meridional oscillation of the mean position of the sub-tropical high pressure belt is reflected in the frequency of northward penetration of cold fronts<sup>1</sup>. Table 1.5 shows that over a 3 year sample period, the highest frequency of cold fronts which passed Durban occurred in the winter months and the lowest frequency in the summer months.

Table 1.5: Frequency per month of the movement of cold fronts past Durban 1965-67 (after S.A. Weather Bureau daily synoptic charts)

J	F	M	A	M	J	J	A	S	O	N	D
0.3	2.3	1.8	3.8	3.0	4.0	4.5	4.0	3.8	4.0	2.8	2.3

<sup>1</sup> In order to reduce confusion over the identification of cold fronts, Taljaard, Schmidt and van Loon (1961) have suggested that they conform to 'a narrow sloping layer with a vertical extent of at least 3 kms, across which the temperature changes sharply in a horizontal direction by an average of at least  $3^{\circ}\text{C}$  in sub-tropical regions'. Thus a cold front is quantitatively defined in terms of its vertical extent and horizontal temperature gradient.

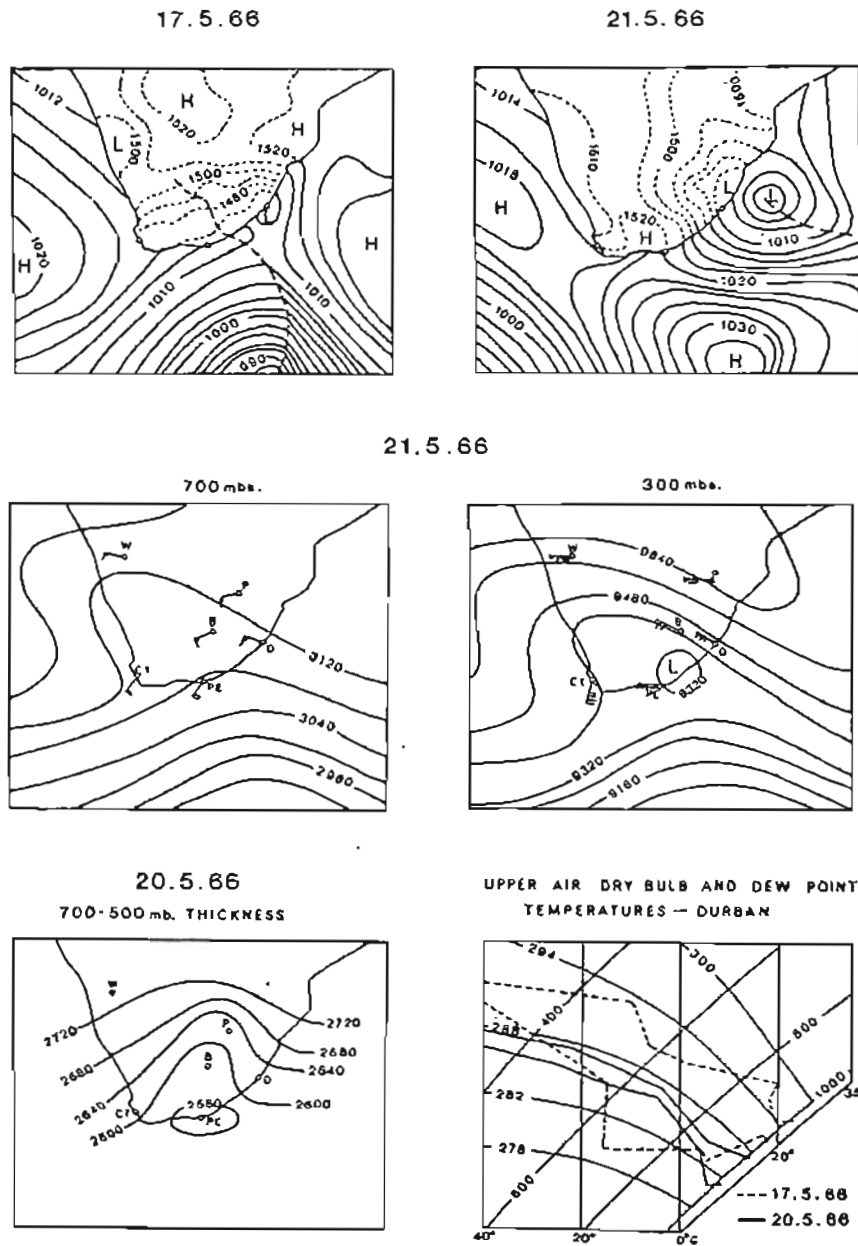
An example of atmospheric circulations and weather characteristics associated with the passage of a cold front over South Africa is given in Figs. 1.6 and 1.7. At the surface the passage of the cold front which moved eastward across the country between 17 - 21 May 1966, could be recognised by a temperature discontinuity. However, to understand the severity of the weather changes which accompanied the surface front, characteristics of the upper air wave pattern must be examined.

By 21 May, a deep trough was located over the country. Cold but dry air was being circulated over the South African plateau so that no precipitation occurred. Between 17 - 20 May similar cooling but with a corresponding increase in the moisture content of the air is shown to occur above 400 mbs at Durban. This was associated with deepening of an almost stationary low off the Natal coast. Divergence at 300 mbs to accommodate lower level convergence into the low was assisted by 110 knot wind over Durban. Precipitation under these conditions was continuous and heavy along the Natal coast on 20 and 21 May.

#### 1.2.2.3 Coastal lows

The term 'coastal low' is used for the relatively small and shallow low pressure systems, or pressure minima, which develop over and move in close proximity to the coast of Southern Africa between Walvis Bay and Lourenco Marques. At the surface the passage of a low is represented by a sudden change in temperature, pressure, wind direction and wind speed. Prior to the arrival of the low at Durban the temperature rises, the pressure falls and the pressure gradient steepens so that north-east gradient winds freshen and may blow strongly. When this wind moderates the front is imminent and is generally introduced by strong and gusty winds from the south-west. Temperature now falls rapidly and pressure rises.





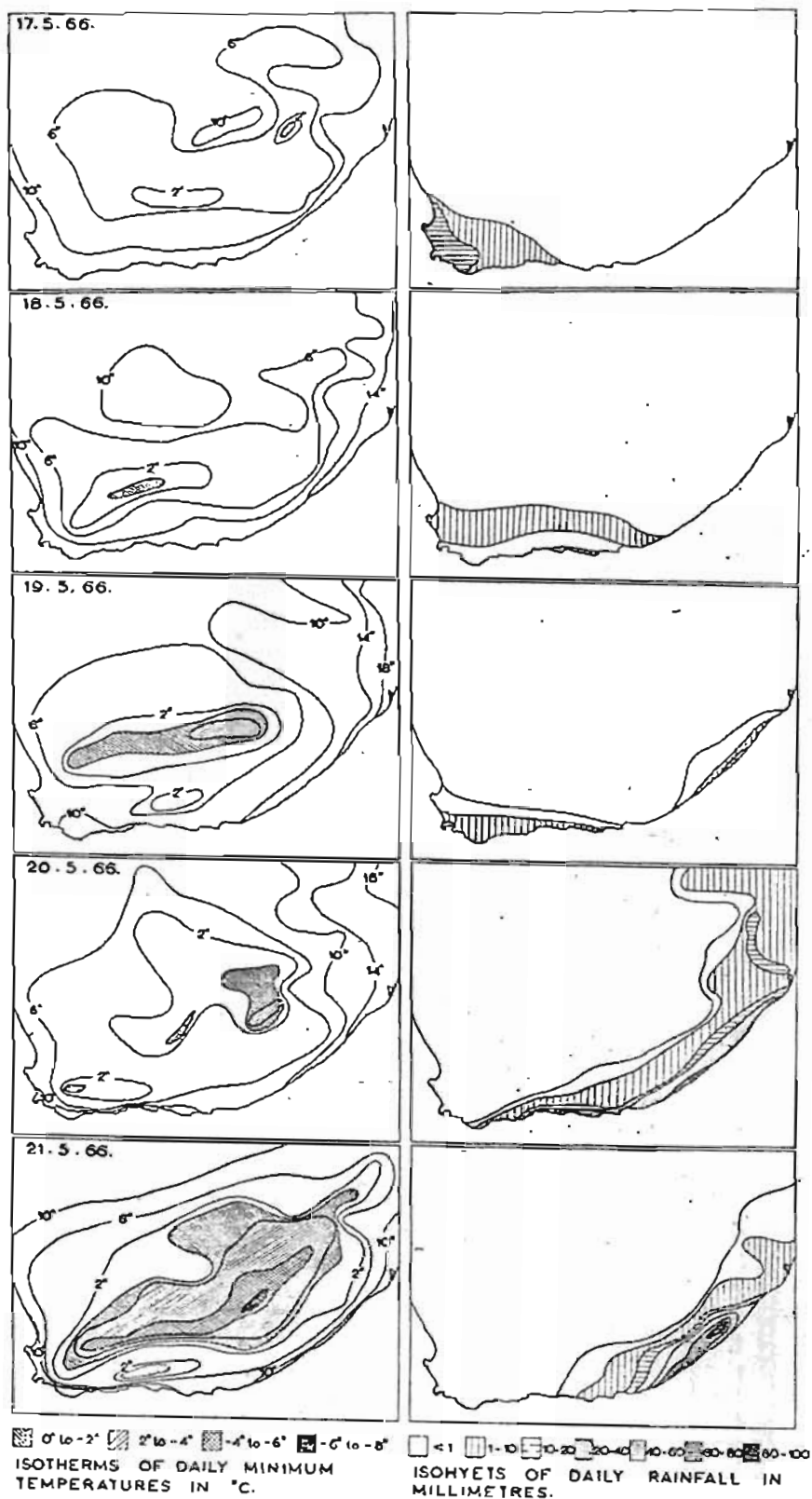
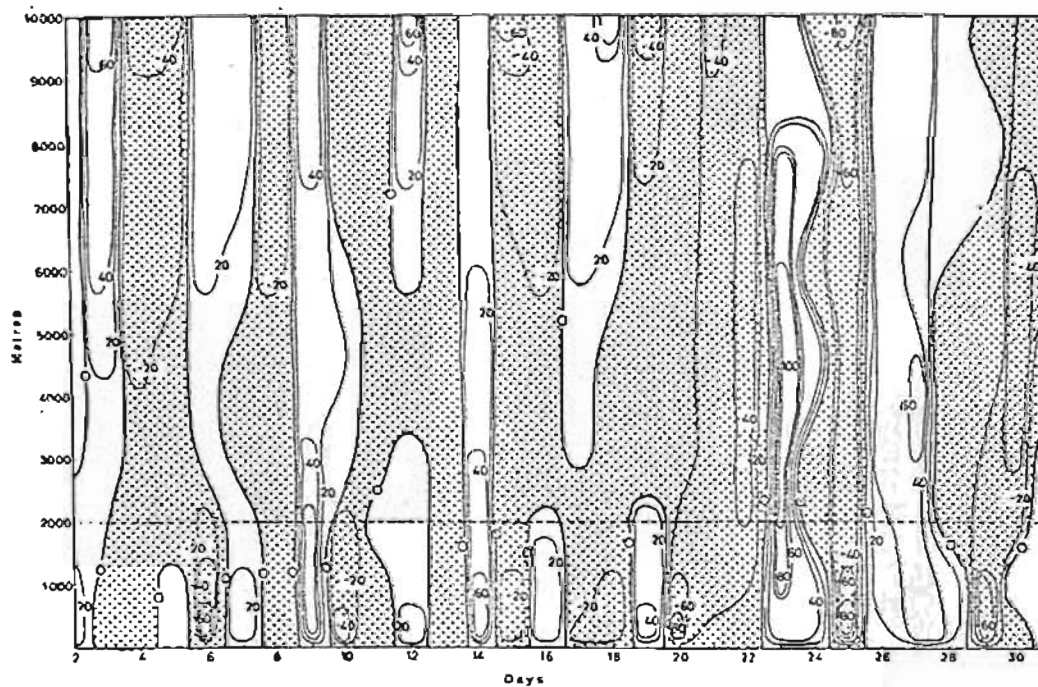


Fig. 1.7 : Variations of daily minimum temperature (°C) and rainfall (mms) over South Africa with the passage of a cold front, 17-21.5.66

1  
No satisfactory explanation of these lows exist. Hattle (1944) and van Lingen (1944) envisaged lows as endowed with fronts and represented them as waves travelling along a 'semi-permanent south-east coast front'. This front is defined as the discontinuity between mild Indian Ocean tropical maritime air and warmer continental or subsided air.

Taljaard, Schmidt and van Loon (1961) have examined coastal lows in relation to pseudo-frontal characteristics ahead of cold fronts and describe the existence of a 'leader front' along which cool tropical maritime air displaces relatively warmer tropical continental or subsided air. The movement of a leader front ahead of the cold front along the south and east coasts of Southern Africa frequently coincides with the presence of a pressure minimum situated over the coast. This pressure minimum is found to coincide with the lowest elevation of the disturbed sub-tropical inversion and, therefore, represents the position of greatest subsidence and divergence. The low indicates that divergence above the level of the inversion is in excess of convergence near the surface.

Although coastal lows are clearly related to the nature and movement characteristics of the large scale pressure patterns, they are not necessarily linked with cold fronts on the Natal coast. As summer approaches the frequency of occurrence of coastal lows increases while that of cold fronts decreases. Table 1.6 shows that in summer the monthly frequency of these lows is considerably higher than the cold front frequencies given in Table 1.5 and in all seasons they are responsible for repeated weather changes along the Natal coast. Since lows are associated with a decrease in air temperature they may also be recognised by variations in the height of the surface in response to the hydrostatic balance requirements in cold air. This is demonstrated in Figs. 1.8 and 1.9 by a comparison of constant pressure surfaces in January and July 1967 at Durban. The seasonal variations in occurrence of lows is shown by more height changes below 2000 m in the former



1.8 : January 1967 vertical time section at Durban to show 24 hour height change (metres) of constant-pressure surfaces

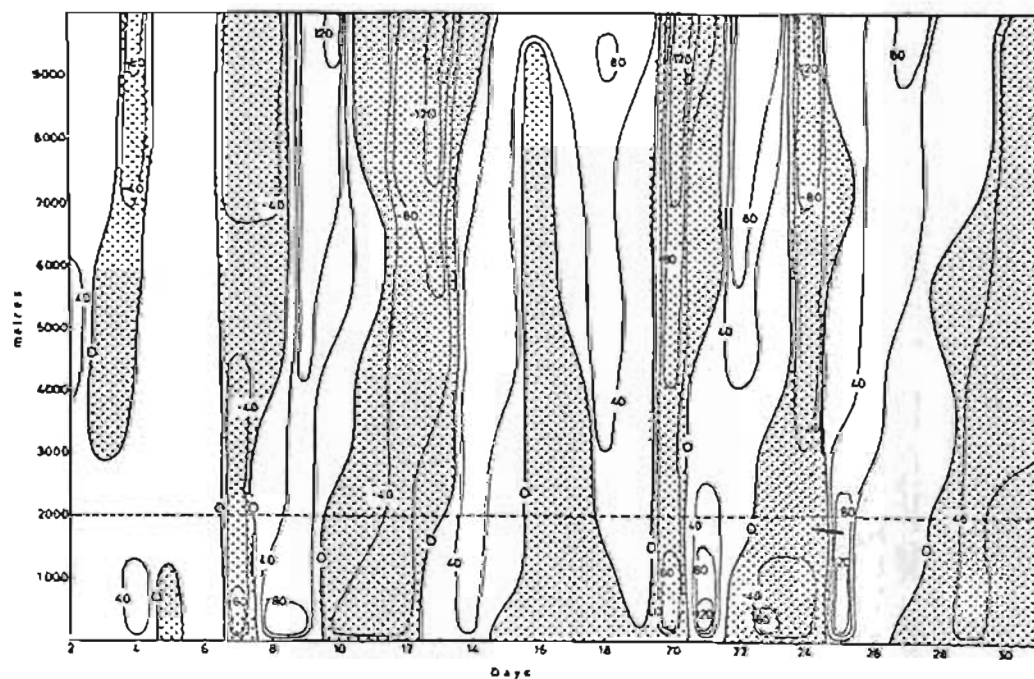


Fig. 1.9 : July 1967 vertical time section at Durban to show 24 hour height changes (metres) of constant-pressure surfaces

than in the latter month.

Table 1.6: Frequency per month of the movement of coastal lows past Durban 1965-67 (after S.A. Weather Bureau daily synoptic charts)

J	F	M	A	M	J	J	A	S	O	N	D
9.0	8.3	6.0	7.3	6.8	7.0	6.3	6.8	7.5	8.0	5.8	9.0

/ The model presented by Taljaard, Schmidt and van Loon (1961) offers an explanation of coastal lows which are linked to cold fronts. However, lows independent of cold fronts still defy a satisfactory explanation as to their origin and subsequent behaviour. The fact that coastal lows are preceded by upper winds with an offshore component may be a pointer to the required solution. Their existence mainly over the sea also suggests that upper air divergence, which maintains the low, cannot cope with increased convergence produced by frictional inflow over the land.

#### 1.2.2.4 Berg winds

The domination of the atmospheric circulation over Southern Africa by a semi-permanent high pressure cell explains the occurrence of west to north-west air flow of continentally modified maritime air and continentally modified superior air in the upper air over Durban (Taljaard, 1955). These winds contribute to yet another pre-frontal characteristic, namely the Berg wind. These winds occur mainly from April to September and produce the curious anomaly that the highest temperature of the year may occur in the winter season.

A Berg wind is a hot, dry wind blowing from the interior, a condition commonly associated with a high pressure pattern with weak pressure gradients over the interior and an advancing depression over the coast. In the transitional zone between anticyclone and advancing depression, pressure gradients, which trend parallel to the



coast, are steepest and subsidence and divergence occurs. The increased wind velocities break down the sub-tropical inversion and air, already warmed by subsidence, is transferred downwards by turbulence (Jackson, 1947; Tyson, 1964).

A typical example of air movement characteristics under Berg wind conditions is shown in Fig. 1.10. Throughout the morning and early afternoon north-westerly winds prevailed to 5,000 ft and the offshore (negative) component of air movement is, therefore, considerably greater than the component parallel to the coast. Under these conditions large positive departures of temperature usually occur with height, humidity is low, skies are clear and turbulence active. Berg wind conditions ceased with the arrival of the coastal low, which is shown to be shallow, of the order 2,000-3,000 ft, with strong negative components of air movement parallel to the coast.

Autographic records which show the occurrence of a Berg wind and a coastal low are given by Fig. 1.11. Winds backed during the morning from north to north-west and this was accompanied by a sharp rise in temperature, fall in relative humidity and steadily decreasing pressure. At about 1120 the wind backed sharply to south-south-west with the arrival of a 30 mph wind. It is apparent that the temperature immediately fell while the relative humidity and surface pressure as suddenly rose.

### 1.2.3 *Characteristics of climate*

#### 1.2.3.1 Wind

Mean monthly surface wind speeds at Durban reflect seasonal variations in pressure gradients of the large-scale pressure systems, the intensity of local circulations and stability characteristics of

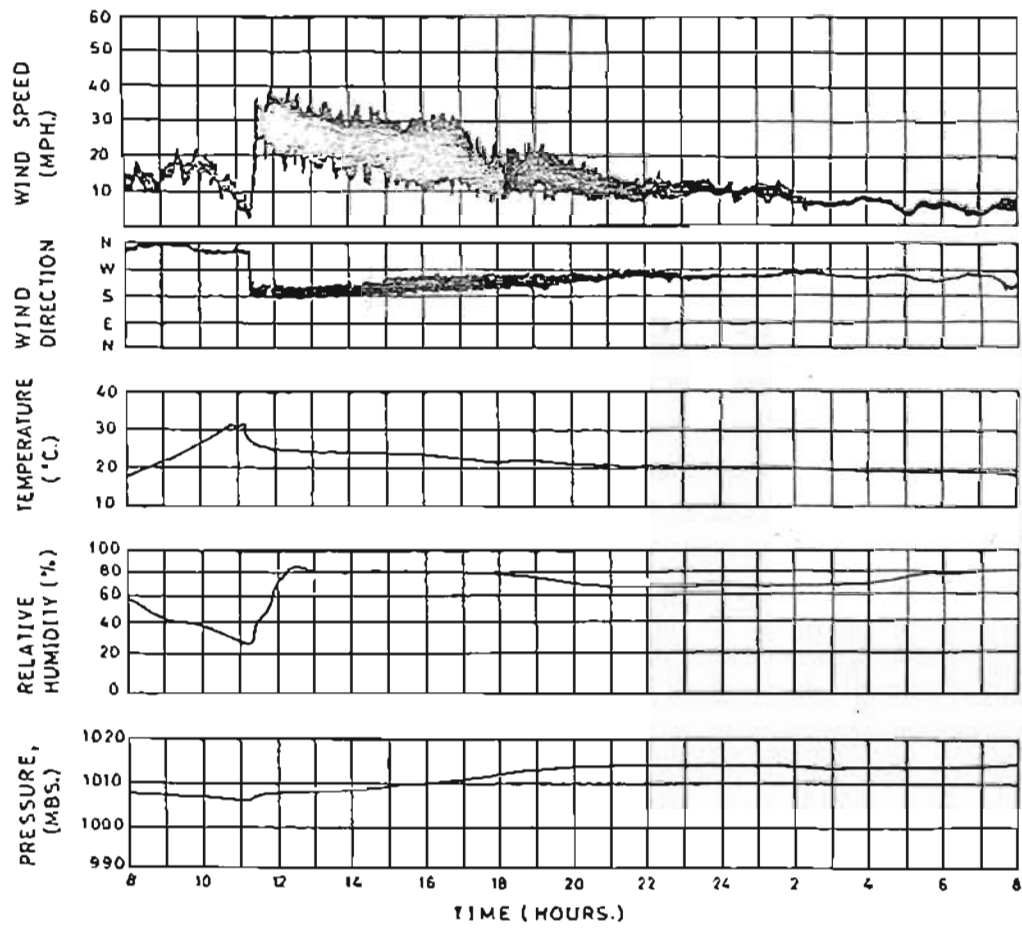


Fig. 1.11 : Autographic records to show the occurrence of a Berg wind and passage of a coastal low



air layers near the ground. Mean wind speeds are lowest between May and June when the frequency and intensity of anticyclones over the Natal coast is at a maximum (Fig. 1.12). Relatively higher mean wind speeds during the warm season, November to April, are due to steeper pressure gradients of the large-scale pressure systems as well as to stronger north-east sea breezes. Highest mean wind speeds occur from September to October, a transitional period at the end of winter which is associated with a reduction in the stability of the winter anticyclone and an increase in the northward penetration of frontal disturbances. Mean wind speeds in January and July for each direction are given in Table 1.7.

Table 1.7: Mean wind speeds (mph) for each direction  
at Stamford Hill airport, Durban (after  
S.A. Weather Bureau 1960)

Wind direction	January	July
N	5.6	4.7
NNE	9.4	9.3
NE	10.2	8.4
ENE	8.1	6.7
E	5.9	5.5
ESE	5.2	4.4
SE	5.8	5.1
SSE	8.1	6.9
S	13.8	11.5
SSW	15.6	15.7
SW	9.6	10.8
WSW	6.3	8.0
W	5.7	6.5
WNW	4.9	6.2
NW	4.8	5.7
NNW	4.0	4.2

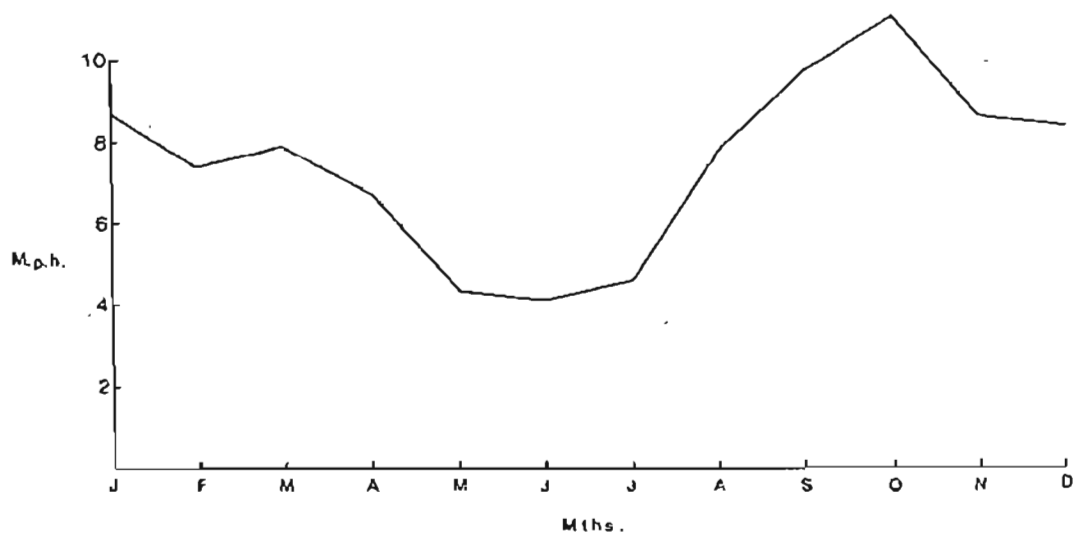


Fig. 1.12 : Mean wind speeds (mph) for each month at Louis Botha airport, Durban (after S.A. Weather Bureau, 1960)

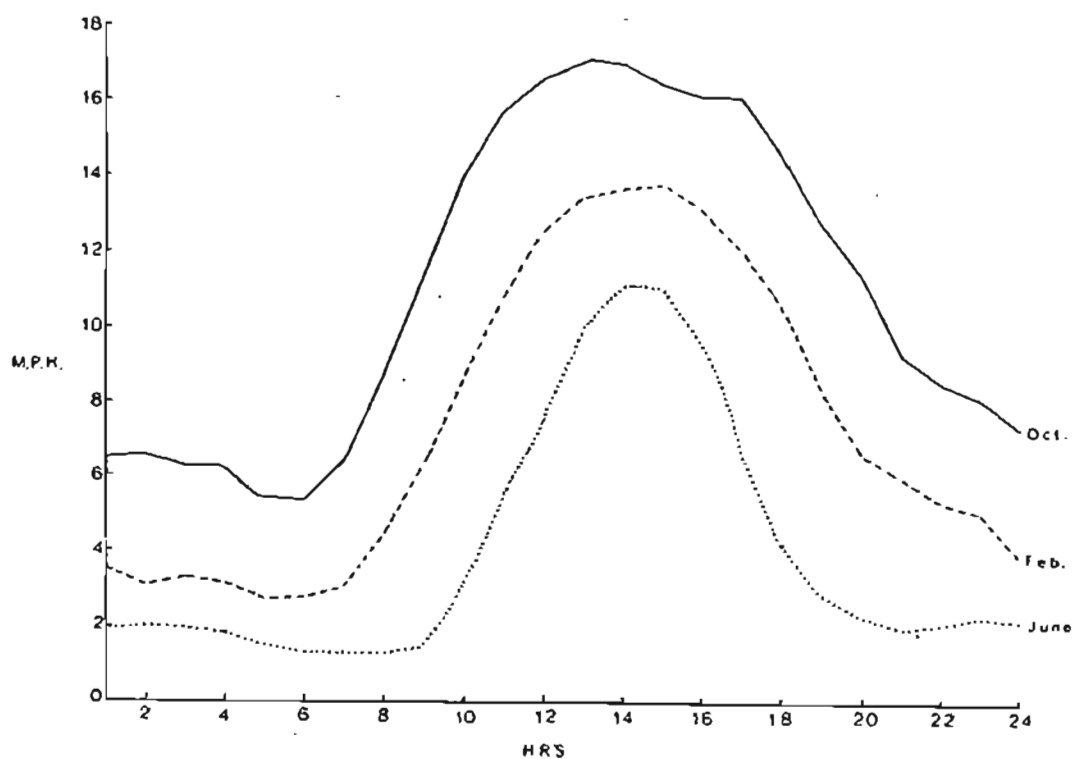


Fig. 1.13 : February, June and October mean wind speeds (mph) for each hour at Louis Botha airport, Durban (after S.A. Weather Bureau, 1960)

The diurnal variation of wind speed undergoes a slight change in amplitude rather than in phase during the year (Fig. 1.13). Maximum wind speeds occur at about 1400 but mean wind speeds at all times are highest in October and lowest in June. High nocturnal mean wind speeds in October, relative to other months, are due to strong south-west winds which blow at the rear of frontal depressions and may persist throughout the night.

Wind measurements are also affected by exposure. Fig. 1.14 shows that mean wind speeds are consistently higher at station 15 (Louis Botha airport, see Fig. 2.1) where channelling of south-west or north-east winds occurs, than at station 13 (Stamford Hill airport). On the other hand station 12, at a height of 932 ft was exposed to winds on all sides and in the summer season recorded higher mean wind speeds than station 15.

#### 1.2.3.2 Temperature and humidity

February is the warmest and July the coolest month (Fig. 1.15). In summer vapour pressure and, therefore, relative humidity is high, particularly at night, when little nocturnal cooling at constant pressure soon causes the air to approach saturation. With high near surface absolute humidities the atmosphere is also kept warm at night by absorption and re-radiation of long wave radiation. By day, eddy diffusion of heat by the sea breeze is mainly responsible for lowering surface temperature but addition of moisture to the atmosphere by this wind maintains a relatively low saturation deficit, particularly near the coast.

*This, fact plus the daytime radiation effect cancels the cooling effect from the sea breeze to a large extent.*

The winter months are cool and dry. Of interest is the occurrence of lowest relative humidity at 1000 in June. This is a period of calm and rapid surface heating, transitional between the land and sea breeze circulation.

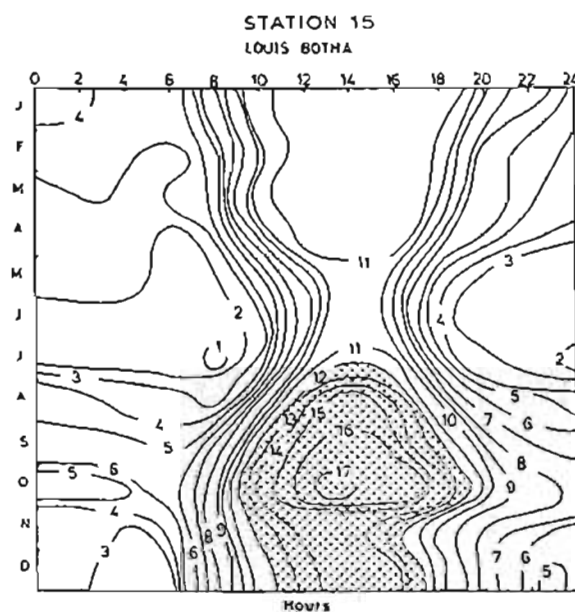
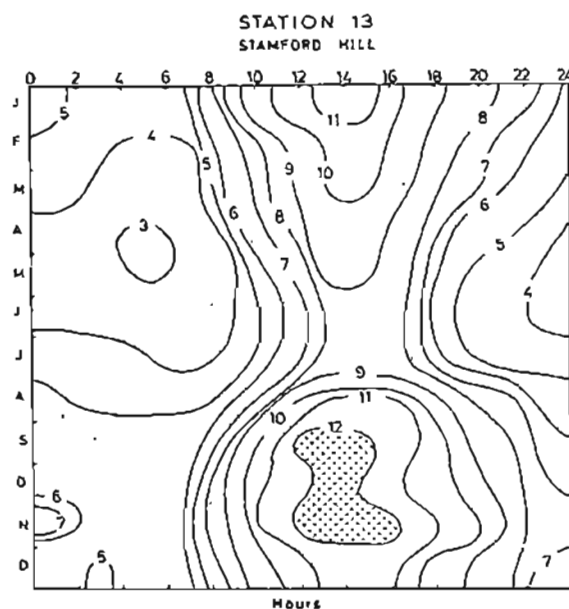
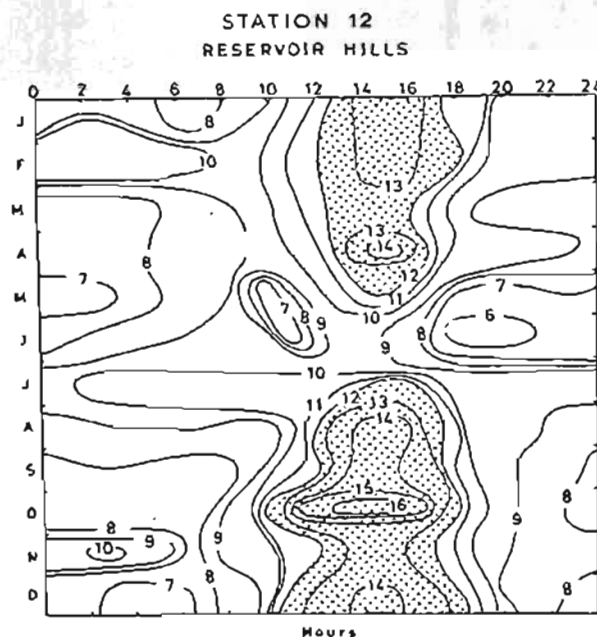


Fig. 1.14 : Isopleth graphs showing monthly variations of mean hourly wind speed (mph) at Stamford Hill (station 13), Louis Botha airport (station 15) and Reservoir Hills (station 12) (partly after S.A. Weather Bureau 1960)

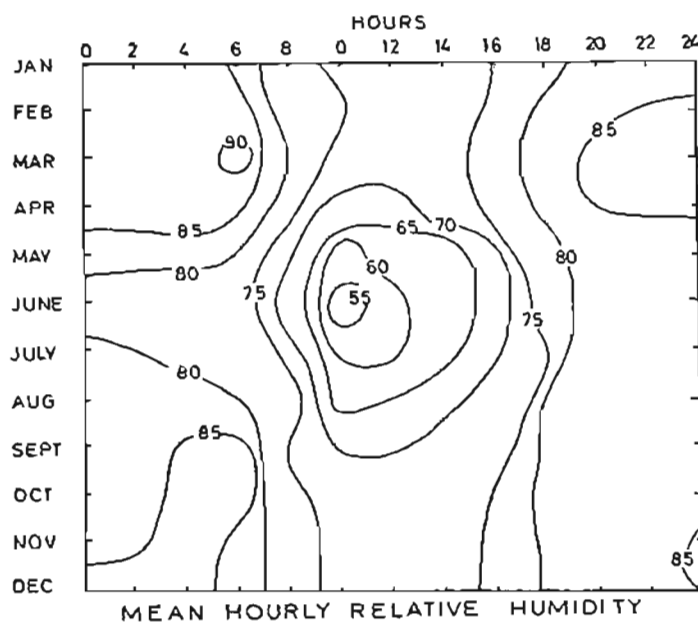
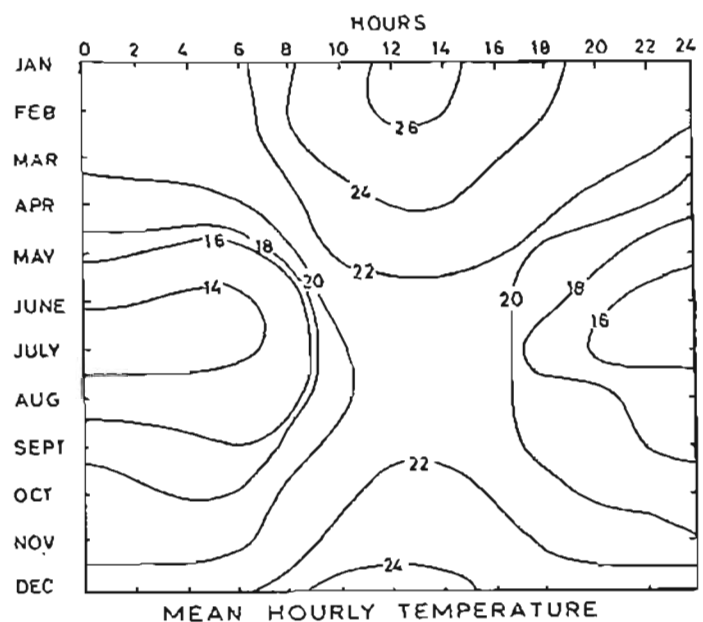


Fig. 1.15 : Isopleth graphs showing monthly variations of mean hourly temperature ( $^{\circ}\text{C}$ ) and mean hourly relative humidity (%) at Durban Weather Bureau (after S.A. Weather Bureau 1954).

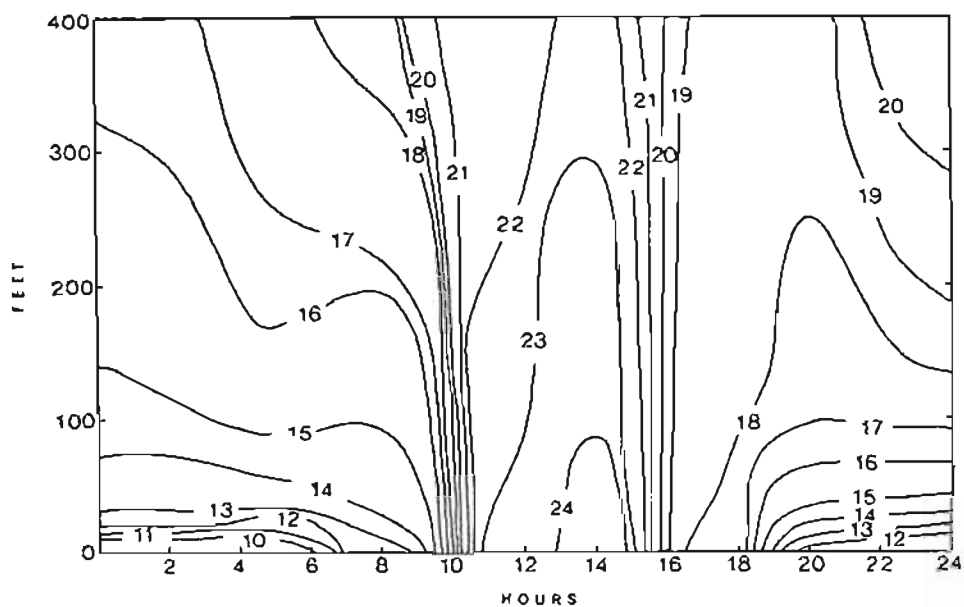


Fig. 1.16 : Diurnal variation of temperature lapse rate ( $^{\circ}\text{C}$ ) on 28.7.67 at station 18

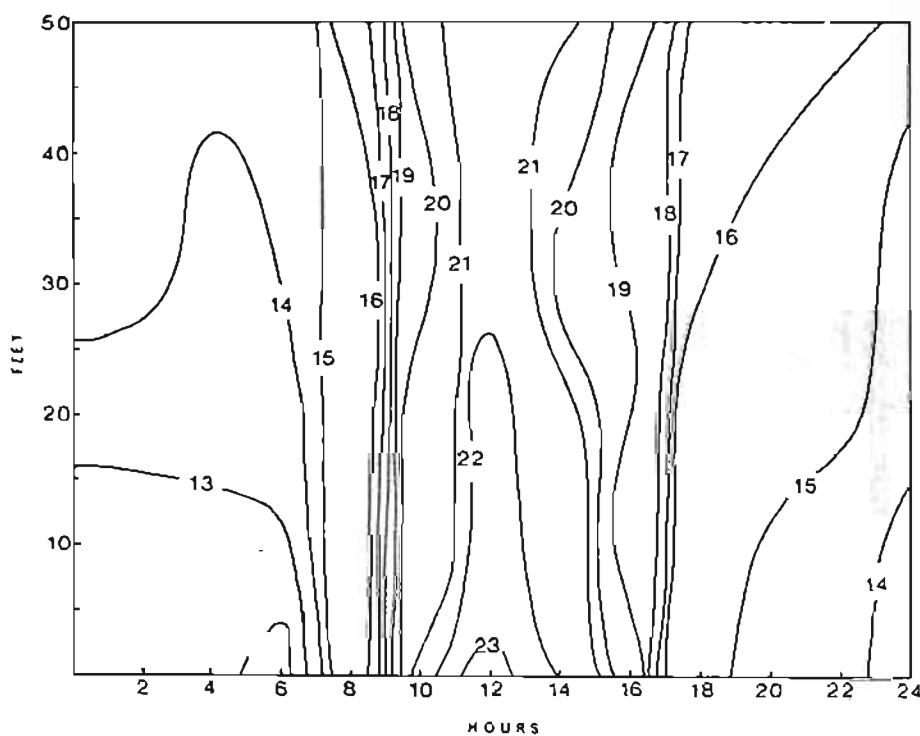


Fig. 1.17 : Diurnal variation of temperature lapse rate ( $^{\circ}\text{C}$ ) from 3-12.7.66 at station 18

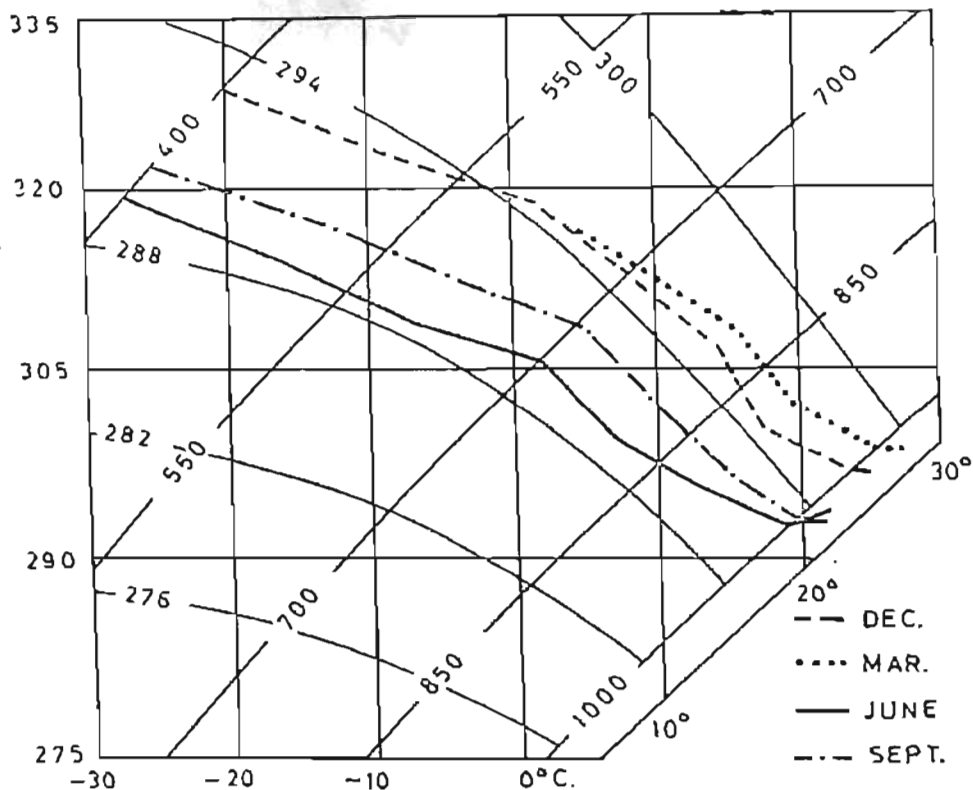


Fig. 1.18 : Tephigram showing mean temperature lapse rates for December, March, June and September, 1964-1966 at Durban

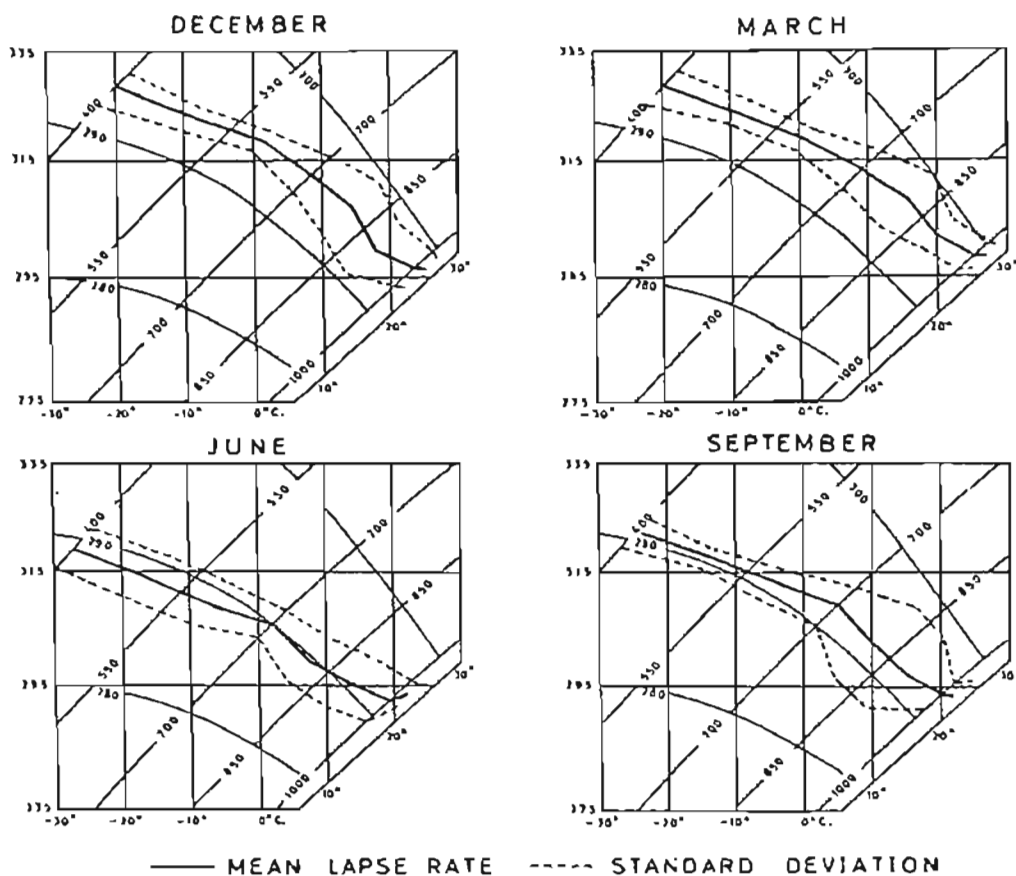


Fig. 1.19 : Tephigrams showing mean temperature lapse rate and standard deviations for the period 1964-1966 at Durban

In fine weather produced by anticyclones, rapid surface cooling takes place at night with the subsequent development of steep near-surface temperature inversions. Winter lapse rate measurements on 28 July 1967 to 400 ft at station 18 (see Fig. 2.2) in Pinetown showed that on this occasion the inversion broke down at about 1000 and reformed at about 1700 under clear sky and low wind conditions (Fig. 1.16). Below 50 ft, mean lapse rates over a 10 day period, which included calm and unsettled weather conditions, indicated a similar pattern with the exception of an earlier inversion breakdown (Fig. 1.17).

The seasonal variation of temperature is not confined to the surface alone but extends throughout the atmosphere. Fig. 1.18 shows that below 500 mbs atmospheric temperatures undergo a reduction of  $5^{\circ}\text{C}$  to  $7^{\circ}\text{C}$  between summer and winter. Variability about the mean temperature is caused by the passage of coastal lows and cold fronts in winter and coastal lows in summer. In winter atmospheric cooling by cold fronts is expected to take place throughout the atmosphere and a quasi-constant standard deviation occurs at all levels (Fig. 1.19). In autumn this does not take place to the same extent. Although the winter anticyclone is weakening in this season, near-surface subsidence inversions still exist and the breakdown of the inversion by more frequent coastal lows produces a high standard deviation below 700 mbs. During summer and spring subsidence inversions are weak or lacking altogether and this effect is less obvious.

\* \* \* \* \*

Characteristics of the weather and climate along the Natal coast have been dealt with in more detail than might seem necessary for a study of local circulations. However, weather along this coastline is so variable at all seasons and the influence of



travelling depressions upon local winds is so marked that without an introductory reference to large scale weather systems, the nature of local wind systems could not be appreciated in their correct context.

## CHAPTER 2

### OBSERVATION AND ANALYSIS

#### 2.1 Introduction

The measurement of local climatological elements does not necessarily require a long-term period of observations before certain conclusions can be reached concerning time and space variations of the parameters. This reasoning has been recognised by Geiger (1965) and has been applied by Fisher (1960) and Frizzola and Fisher (1963) in the study of sea breezes, Tyson (1967a) in a study of topographically-induced wind systems and Goldreich (1969) in a study of urban temperatures. The analysis of short-term measurements of certain climatic elements has also been applied in this study. Local circulations were recorded at intervals during July 1963 and over a 4-year period from 1966-69. The measurement of spatial temperature variations were made during July 1968 and between November 1969 to February 1970. In addition hourly precipitation records extending over a 10-year period from 1958-67 were obtained from Louis Botha airport.

#### 2.2 Instrumentation and location

##### 2.2.1 *The measurement of wind by balloons*

Wind measurement by balloons depends upon theodolite observations at regular intervals. Both the single and double theodolite methods were adopted with the choice of method dependent upon the particular requirements in terms of tracing air movement.

The single theodolite method relies upon a constant rate

of balloon ascent. A balloon to which a pre-determined weight is attached, is filled with hydrogen until it floats. Upon removal of the weight the balloon is no longer in equilibrium with its surroundings and rises with a lift determined by the removed weight. The rate of ascent is expressed by the equation

$$V = \frac{qL^{\frac{1}{2}}}{(L + W)^{\frac{1}{3}}} \quad (2.1)$$

where  $V$  denotes rate of ascent in ft/min,  $W$  weight of the balloon in grams,  $L$  free lift in grams and  $q$  a constant taken as 275 for balloons with a diameter less than 90 inches (HMSO 1959).

The pilot balloon theodolite records the angular position of the balloon at a particular instant by means of its azimuth and elevation. The former term denotes the direction of the point on the ground immediately below the balloon measured in degrees from true north; the latter term gives the angular height of the balloon above the ground. Since the height of the balloon is known from the rate of ascent, the application of trigonometrical ratios fixes the balloon position at each reading. Both direction and speed of air movement may be obtained from the balloon trajectory, the latter calculated from the balloon displacement per unit time.

Results obtained using the single theodolite method are subject to errors, caused by departures from the computed rate of ascent of the balloon, which may be caused by vertical responses to isolated buoyant currents or downdrafts and to heating of the balloon. Error is also accumulated under strong wind conditions. The accuracy of the single theodolite method has been examined by Arnold (1948) and Ayers (1958) who compared this method to double theodolite measurements which served as a standard. A mean error in speed of approximately 1.0 m/sec and a height error of between 10 and 15 per cent was generally found.

Balloon releases at regular time intervals using the single theodolite method varied from 5-60 minutes depending upon the measurement requirements. For instance, measurements aimed at recording wind surge characteristics by day or night required 5-10 minute releases, while over a 10-12 hour period local wind conditions could be adequately described by 30-60 minute releases. 5 gram balloons were used with an average rate of ascent of 350 ft/min by day and 200 ft/min by night.

A primary concern of this study being the measurement of land and sea breeze characteristics, wind speeds obtained from single theodolite measurements were converted to onshore (positive) and offshore (negative) wind components. In all cases the orientation of the coastline was taken as  $32^{\circ}$ . The variation of these components is described by velocity isopleths in metres per second on vertical time or space sections. Wind direction to sixteen compass points is also accommodated on these diagrams.

The double theodolite method requires a theodolite positioned at each end of a base line. Upon release of the balloon, readings of azimuth and elevation are simultaneously taken at consecutive time intervals. The base line was drawn on a map with scale 1:18,000 and this line was used to plot intersecting azimuth angles thus giving the fix of balloon positions in the horizontal plane. Wind speeds were calculated from the spacing of balloon positions at time intervals while wind direction was given by the horizontal displacement of the balloon. Since the elevation angle and horizontal distance from the balloon release points was known, the height of the balloon at each reading was calculated from tangent tables.

The main disadvantage of the double theodolite method is the difficulty, along the Natal coast, of locating suitable base lines in the horizontal plane approximately normal to the wind

direction<sup>1</sup>. However, a constant rate of balloon ascent is not assumed and changes in balloon height, due to diffusion of gas or vertical displacement of the balloon, is measured. This method was used at times when it was necessary to record the characteristics of low-level air movement and on these occasions balloons were adjusted to maintain a constant elevation or to ascend at a gentle rate. Since the main concern of the double theodolite method was to record drainage winds rather than land or sea breezes, only true wind speeds were represented on vertical time sections.

Low-level balloon flights using the double theodolite method require a slow rate of balloon ascent. To prevent the effect of radiational heating, a balloon developed from a transparent polythene material called Melinex was used during the day. This material, which is transparent to solar radiation and absorbs heat to an insignificant degree in the infra-red wavelengths, proved most satisfactory. Diffusion through the non-extensible Melinex balloon was negligible and could be ignored as a force calculated to affect buoyancy within the period the balloon was likely to remain visible. A double rubber 30 gram balloon was also used to counteract diffusion, the inner balloon containing hydrogen and the outer balloon air. The rate of loss of buoyancy would be initially zero, the gas escaping from the inner balloon being held in the outer balloon. The escape of gas through the outer balloon envelope only proceeds when an appreciable concentration is built up in the interspace (Lucas, Spurr and Williams, 1957).

Night ascents required a light attached beneath the balloon. The weight of battery powered lights proved prohibitive while the intensity of light thus generated decreases with time. Instead candle

---

<sup>1</sup> Another severe practical limitation of the double theodolite method is the number of fieldworkers required for its operation.

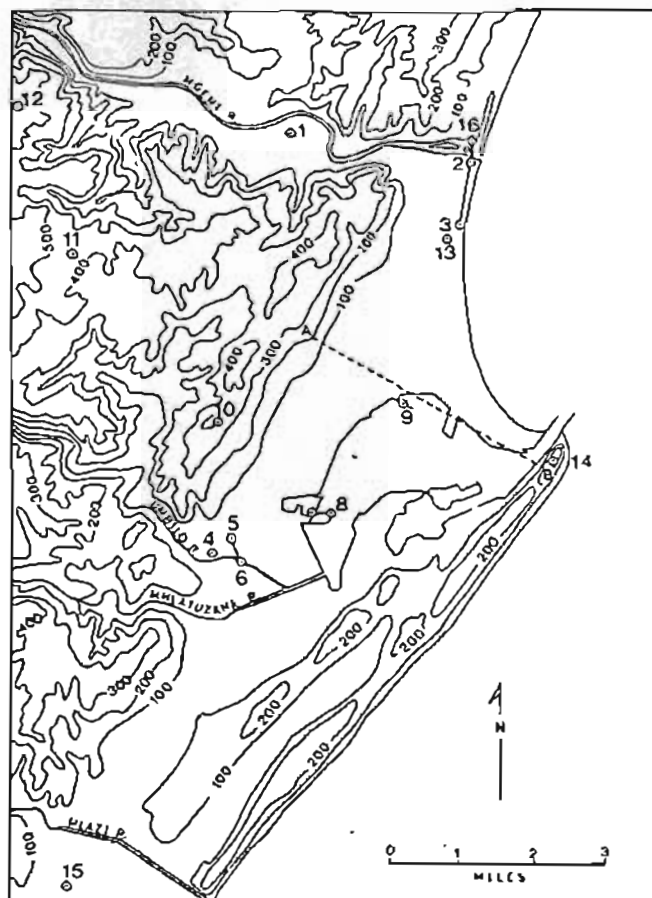


Fig. 2.1 : Map to show location of observing stations in the Durban area. Double theodolite stations are connected by a solid line

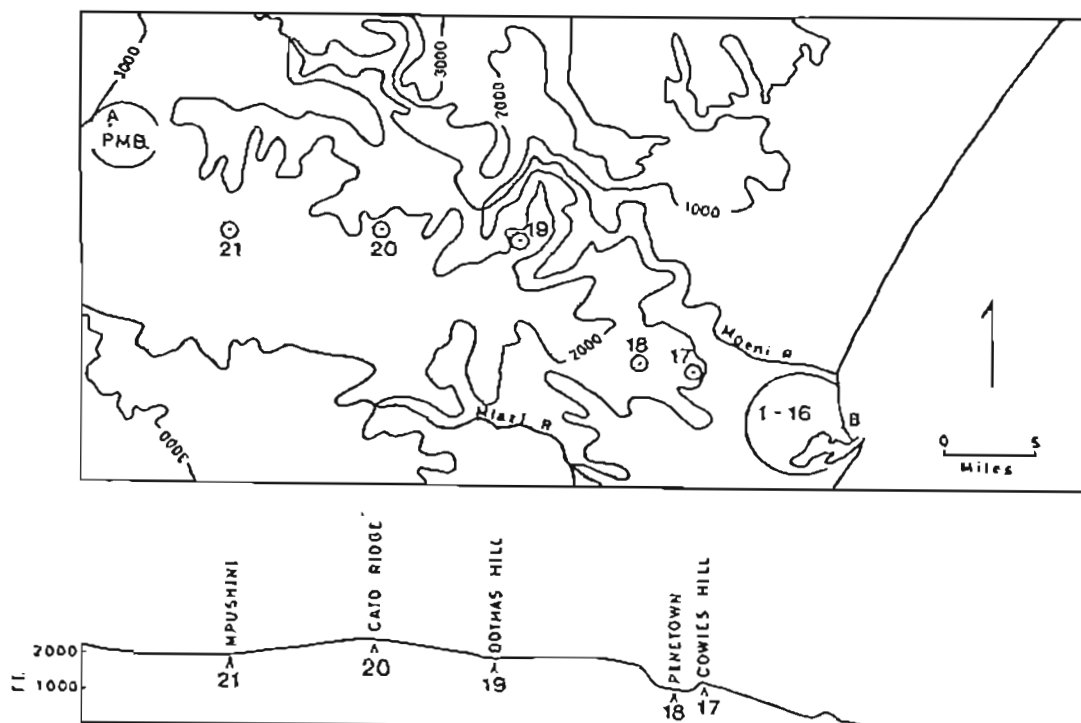


Fig. 2.2 : Map to show the location of balloon observing stations north-west of Durban

lanterns, in which the intensity of light emitted remains constant until the candle is extinguished, were used in preference. It was also hoped that the increase in buoyancy credited to the balloon by the wasting candle would help counteract the loss by radiational cooling. The lantern was suspended about 6 ft beneath the balloon to prevent heating effects.

By day solar heating of the balloon caused an additional component to the rate of ascent but diffusion of gas through the rubber membrane partly counteracted this effect. However, as balloons were tracked for only 10-15 minutes it was felt that the error thus accumulated was within reasonable limits.

Air movement in the Natal Bay area was observed by the single and double theodolite method and base lines and theodolite stations are shown in Fig. 2.1. Theodolite stations were also located in the Mgeni River valley to record topographically-induced wind systems and at sites along a line approximately normal to the coastline and extending 36 miles inland (Fig. 2.2). The latter stations were located on the interfluvial area between the Mgeni River valley to the north and the Mlazi River valley to the south. These stations were sited to record land and sea breezes and were located as far as possible away from the influence of wind circulations developed in deep valleys.

#### 2.2.2 *The measurement of wind by anemometer*

1. Casella anemometers were used for the measurement of low velocity nocturnal air flow in the Mgeni and Umbilo River valleys (stations 1, 2, 4). The instruments were mounted at the end of cross-bars fixed to an aluminium mast 3 ft and 18 ft above the ground. A sensitive wind vane was mounted on the opposing end of each crossbar. Recordings of wind speed and direction were taken at 5 minute intervals.

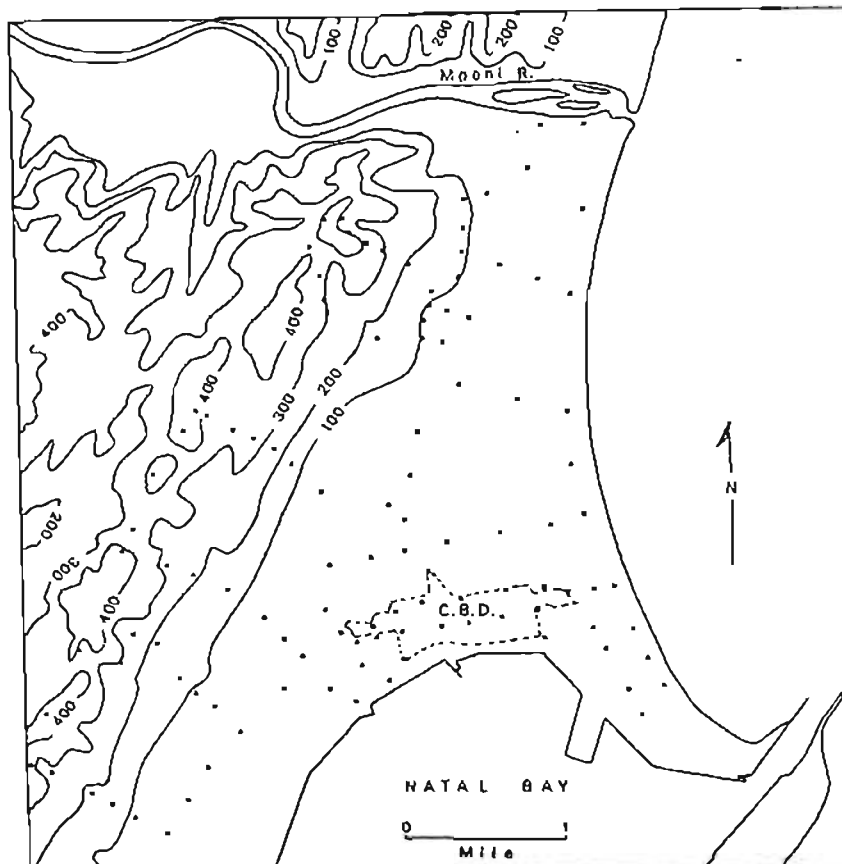


Fig. 2.3 : Summer 1968-69 and winter 1968 location of midday temperature recording stations in the Durban area



2. A Lamprecht anemometer was used to obtain 12 months' uninterrupted record from June 1967 to May 1968 at station 12.

2.2.3 *The measurement of temperature and humidity by motor vehicle traversing*

With limited resources, motor vehicle traversing is the most effective method of gathering a suitable array of temperature and humidity data and this method was adopted for data collection in Durban. Two thermistors, one to record dry bulb and one wet bulb temperature, were housed in an aluminium tube with length 8 ins and diameter 2.4 ins. The tube was mounted beside the front left-hand door of a rear-engined motor vehicle 54 ins above the ground and 7 ins from the vehicle. Adequate protection from the direct rays of the sun was provided by the tube and ventilation of the thermistors was achieved through the movement of the vehicle. Readings were taken only when the vehicle was in motion at speeds between 20 and 30 mph.

A potentiometer (a helipot graduated 0-1000 was used in this case) balanced the voltage between a standard resistor on one leg of a transistorised resistance bridge circuit and the thermistor. The helipot readings were then calibrated to degrees centigrade against a standard mercury thermometer. Frequent checks were carried out against sudden deviations of the thermistor from the original calibration but no significant change was perceived over the field-work period.

Temperatures were recorded by day at 110 stations along a 26 mile traverse shown in Fig. 2.3. The traverse was started at 1230 and took approximately one hour to complete. Since temperatures at the beginning and end of the traverse seldom differed significantly, no correction was applied to reduce temperatures to a common time.

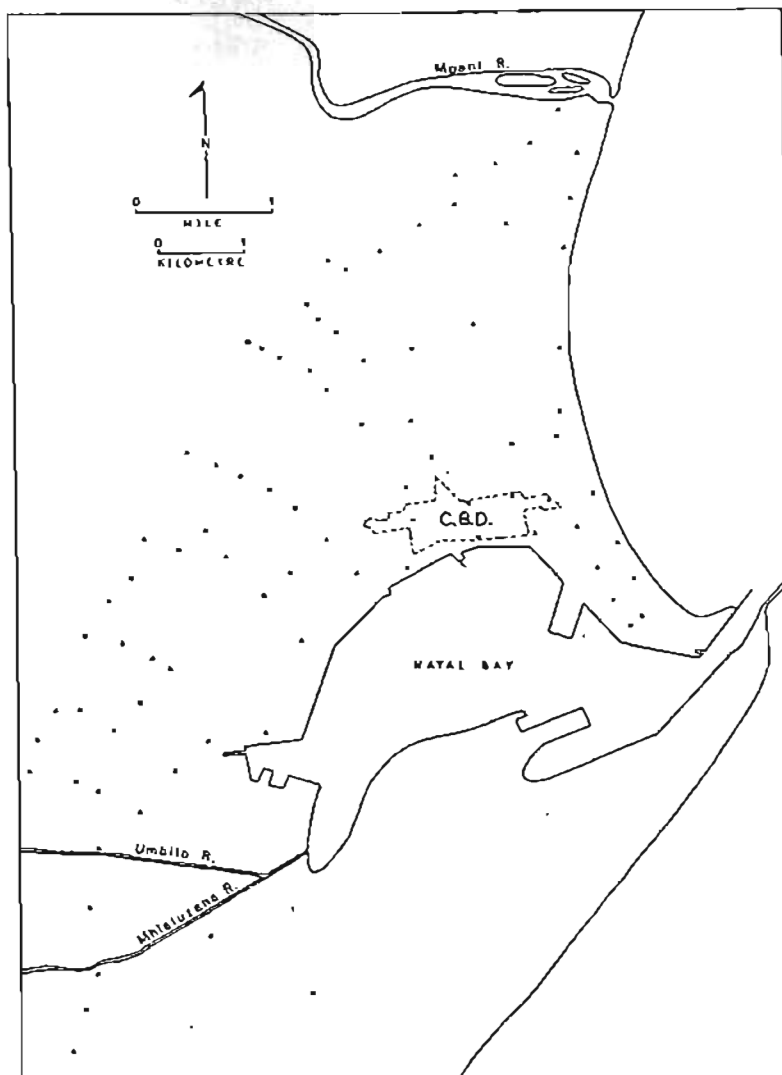


Fig. 2.4: Winter 1968 location of 0400-0500 temperature recording stations in the Durban area

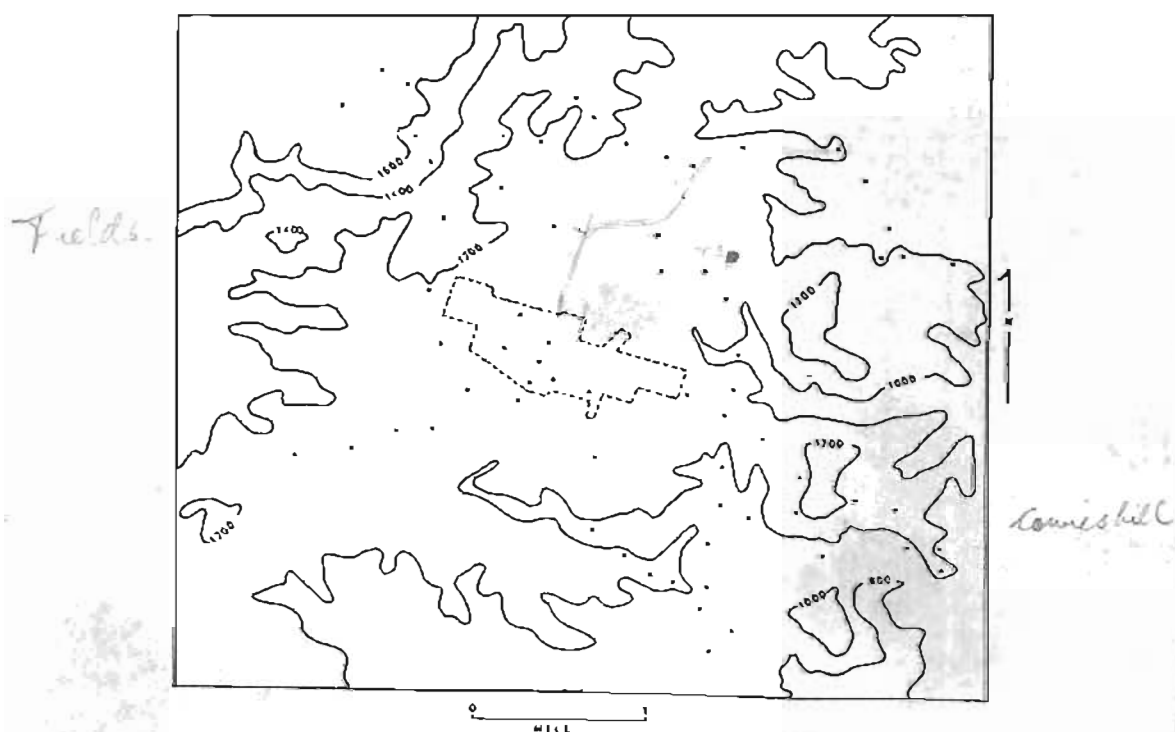


Fig. 2.5: Winter 1968 location of 0400-0500 temperature recording stations in the Pinetown basin

Over a summer period from late November 1968 to early February 1969, 28 daily traverses were run in continuous spells of about one week irrespective of weather conditions. Winter measurements were carried out over 10 days during June 1969. In both seasons the frequency distribution of temperature shows an almost normal distribution and it is felt that the data represent a reasonably good estimate of mean midday temperature over Durban.

The spatial variation of minimum temperature over Durban was recorded by 5 traverses during July 1968 at 86 stations along a 39 mile route shown in Fig. 2.4. These traverses were started at 0400 and run only under calm, clear cloudless conditions.

Traverses in the Pinetown basin were recorded at 66 stations along a 24 mile route shown in Fig. 2.5. This fieldwork was carried out in July 1968 and maximum (midday) and minimum (pre-dawn) temperatures were recorded over 10 days. 70

#### 2.2.4 *Lapse rate measurements by tethered balloon*

Lapse rate measurements were accomplished by the suspension of a radiosonde beneath a Kytoon which was tethered at the surface in the Pinetown basin at station 18. Similar measurements could not easily be made in Durban due to the danger to commercial aircraft. Movements of an artificially ventilated bi-metallic strip within the radiosonde, caused by variations in air temperature, were converted to morse code and transmitted to a receiver at the surface. Temperatures were thus recorded at 25 ft intervals and the Kytoon was able to lift the instrument to 400 ft in certain conditions. This technique is complicated by wind. The Kytoon does not fly vertically under these conditions and an elevation angle measured by theodolite is required to obtain the correct height.

### 2.3 Harmonic analysis

Harmonic analysis is a standard technique and has been clearly outlined by Conrad and Pollak (1950), Brooks and Carruthers (1953) and Panofsky and Brier (1963). The technique permits any curve described by an array of data arranged in a natural time or space sequence to be expressed as the algebraic sum of a series of sine functions. Each sine wave is successively called the first harmonic which has one maximum and one minimum, the second harmonic, with two maxima and two minima, etc. The harmonics are objectively described by values of wave amplitude and phase angle. In each case the total abscissal length of the harmonic remains the same and phase angles are obtained by shifting the curve to the left thus changing the values at which maxima or minima occur.

This technique has been widely used to define periodic fluctuations within a time or space series (Sutton 1953, Bryson 1957, Sabbagh and Bryson 1962, Horn and Bryson 1960, McGee and Hastenrath 1966, Tyson 1968a, 1968b, 1969a). Tyson (1969b) points out that the method consists of representing fluctuating data by a series of sine functions such that the variate  $X_t$  at time  $t$  is

$$X_t = \bar{X} + \sum_{k=1}^{N/2} a_k \sin \left( \frac{2\pi kt}{N} + \phi_k \right) \quad (2.2)$$

where  $\bar{X}$  denotes the mean of the series  $\bar{X}_t$  ( $t=0, \dots, N-1$ ),  $\pi = 180$  degrees,  $a_k$  denotes the amplitude of the  $k$ th harmonic with phase angle  $\phi_k$  and  $N$  the total length of the period.  $a_k$  and  $\phi_k$  are determined from

$$a_k = (p_k^2 + q_k^2)^{\frac{1}{2}} = \frac{p_k}{\sin \phi_k} \quad (2.3)$$

and

$$\tan \phi_k = \frac{p_k}{q_k} \quad (2.4)$$

where

$$p_k = \frac{2}{N} \sum_{t=0}^{N-1} X_t \cos \frac{2\pi kt}{N} \quad (2.5)$$

and

$$q_k = \frac{2}{N} \sum_{t=0}^{N-1} X_t \sin \frac{2\pi kt}{N} \quad (2.6)$$

except in the case where  $k = N/2$  when  $p$  is half the value given in Equation 2.5 and  $q$  is zero.

If the variance components of the harmonics describing an observed curve are summed together the curve is closely fitted. However, the variance component of each harmonic is independent of the other harmonics so that the contribution of the variance of the first harmonic to the total variance indicates the degree to which the first harmonic, specified by the parameters amplitude and phase angle, fit the observed curve. The variance contributed by individual harmonics to the total variance is given by

$$\frac{a_k^2}{2\sigma_k^2} \quad (2.7)$$

except in the case of  $N/2$  harmonics where the variance contribution is twice the value given by Equation 2.7. Since the variance contribution of each wave to the total variance is known, a variance

spectrum may be obtained by plotting the variance ratio against the frequency ( $k/N$ ) or period ( $N/k$ ) of each harmonic.

\* \* \* \* \*

Harmonic analysis was applied to obtain an objective description of both temporal and areal variations of selected climatic elements. All calculations were performed on the I.B.M. 1130 computer at the University of Natal. Periodic surges in land and sea breeze velocities obtained from balloon releases at 5 minute intervals were examined by applying this method to an array of wind speed measurements arranged in a natural series. The spatial character of mean summer and winter temperatures and summer discomfort index values over Durban was also examined by this technique. In this case the data array was obtained from temperature or discomfort index measurements at regular intervals along a base line. An expression was then developed to describe the variance contribution of each harmonic to the total variance. Summation of each harmonic function provides a close fit to the spatial variation of these elements along the base line.

## PART II

### CHARACTERISTICS OF LOCAL WIND SYSTEMS

## CHAPTER 3

### SEA BREEZES

#### 3.1 Introduction

During summer, moist and relatively cool air over the sea is advected almost daily over the Natal coast by the sea breeze. The characteristics of the circulation in terms of adjustment to the rotation of the earth and seasonal variations in the depth of the system have been described by Jackson (1954). To add to this work summer variations in the depth and velocity of the sea breeze at the coast as well as characteristics of its inland penetration have been examined. It is recognised, however, that the sea breeze is seldom unaffected by gradient winds of the large scale pressure systems and by topographically-induced winds in the dissected coastal hinterland.

#### 3.2 General characteristics

The occurrence of a sea breeze during both summer and winter is a predictable event in fine weather conditions. In summer the sea breeze prevails for about 11 hours from 0900 until 2000; in winter the duration of this wind is reduced to 7 or 8 hours and it blows from about 1000 or 1100 until 1800 (Weather on the Coasts of Southern Africa 1941).

An exact treatment of the problem of developing a sea breeze model was first attempted by Jeffreys (1922) who considered land-sea circulations as antitriptic winds in which only the frictional and pressure gradient forces are significant. That this early



model does not conform more closely to reality is due to neglect of the influence of the earth's rotation. Jackson (1954) points out that as the sea breeze circulation on the Natal coast grows with time, the wind backs from east to north-east to make a small angle with the coastline. This observation is in agreement with the theoretical model developed by Haurwitz (1947) which shows the rotation of the sea breeze with time under the influence of the Coriolis force and observations by Staley (1957, 1959), Dexter (1958) and Fisher (1960).

Surface friction seems to be an important consideration in the variation of sea breeze velocities during the day. In the simple solenoidal model developed by Bjerknes et al (1933), the sea breeze must be expected to set in at the time of maximum surface heating and reach its greatest velocity when the temperature gradient changes from onshore to offshore. This is far from reality and the effect of friction was suggested by Godske (1934) to be an important contributing factor to closer agreement between the phase difference between the time of maximum land-sea temperature difference and maximum velocities in the sea breeze circulation. This idea was examined in more detail by Haurwitz (1947) who showed, using Bjerknes' circulation theorem, that by varying the friction term the maximum sea breeze velocities could be made to occur at different time intervals after the time of maximum land-sea temperature difference had been reached. He concluded that from friction terms observed on land, the maximum sea breeze should occur about 3 hours after the maximum land-sea temperature difference. Table 3.1 shows that mean hourly wind speeds recorded in February at Durban occur at 1400, approximately at the time of maximum temperature difference between land and sea. This shows that the friction terms used by Haurwitz, although they do not give close agreement with observations, are clearly acting in the correct direction.

A clearly defined and dramatic 'frontal' type onset of the

Table 3.1: Mean hourly wind speed ( $\bar{U}$ ) in mph and the mean hourly land-sea temperature difference ( $\Delta T$ ) in  $^{\circ}\text{C}$  during February and July at Durban (after S.A. Weather Bureau, 1954, 1960; Wellington, 1955)

Time	February		July	
	$\bar{U}$	$\Delta T$	$\bar{U}$	$\Delta T$
8	2.7	-0.7	1.6	-4.6
9	3.3	0.3	1.9	-1.9
10	3.9	1.0	2.2	0.5
11	4.5	1.4	2.6	1.5
12	4.9	1.7	3.0	1.8
13	5.1	1.9	3.5	2.0
14	5.3	1.9	3.7	2.0
15	5.2	1.6	3.8	1.7
16	5.0	1.2	3.6	1.2
17	4.7	0.7	3.3	-0.1
18	4.5	0	2.8	-1.5

sea breeze is not characteristic of the circulation on the Natal coast nor is it to be found in the humid tropics where, according to Kimble (1946), steep land-sea temperature gradients are not common. Instead Wexler (1946) points out that the highest frequency of frontal type sea breezes occurs in temperate latitudes. The absence of a frontal onset over the Natal coast is largely due to gradient winds over the sea which, due to frictional inflow or isobaric orientation, blow onshore once the land breeze has subsided. Cooler sea air is then advected over the land and this inhibits the development of a steep temperature gradient over the coast, particularly as the land-sea temperature difference is already small. The basic ingredients for the occurrence of a well-developed sea breeze front are offshore gradient winds which advect strongly heated land air towards a markedly cooler sea so that a steep temperature gradient is established.

Sea breeze circulations are considerably affected by

latitude. In low latitudes where gradient winds and the Coriolis force is weak and surface heating is strong, the sea breeze circulation may dominate daytime air movement over the coast. In middle latitudes gradient winds invariably affect the sea breeze, either as a strengthening or as a weakening influence, while the Coriolis force is more effective in rotating the wind during the day towards a small angle with the coastline thus reducing the on-shore component of air movement while strengthening the component parallel to the coast. The Natal coast lies in sub-tropical latitudes midway between low and middle latitudes so that it is not surprising that the characteristics of both latitude zones should be found in the sea breeze circulation.

### 3.3 Frequency of occurrence

At its onset the sea breeze blows east-north-east to north-east as the example in Fig. 3.1 indicates. Table 3.2 shows the high frequency of these wind directions during both January and July the only other directions with comparable frequencies being south, south-south-west and south-west. These latter directions are, however, due to the passage of frontal systems past Durban. Although these post-frontal winds are associated with high wind speeds which tend to subdue the sea breeze circulation, a variation of wind direction is nevertheless usually evident during the day as winds back from south-south-west and south-west to south-south-east and south-east.

The sea breeze occurs more frequently in summer than in winter. The highest path taken by the summer sun is only  $6^{\circ} 20'$  from the zenith so that surface heating is more intense and of longer duration than during winter when the maximum angle of the mid-winter sun is  $53^{\circ} 20'$  from the zenith. The sea breeze can only set in when land temperatures exceed those over the sea. Consequently, reduced

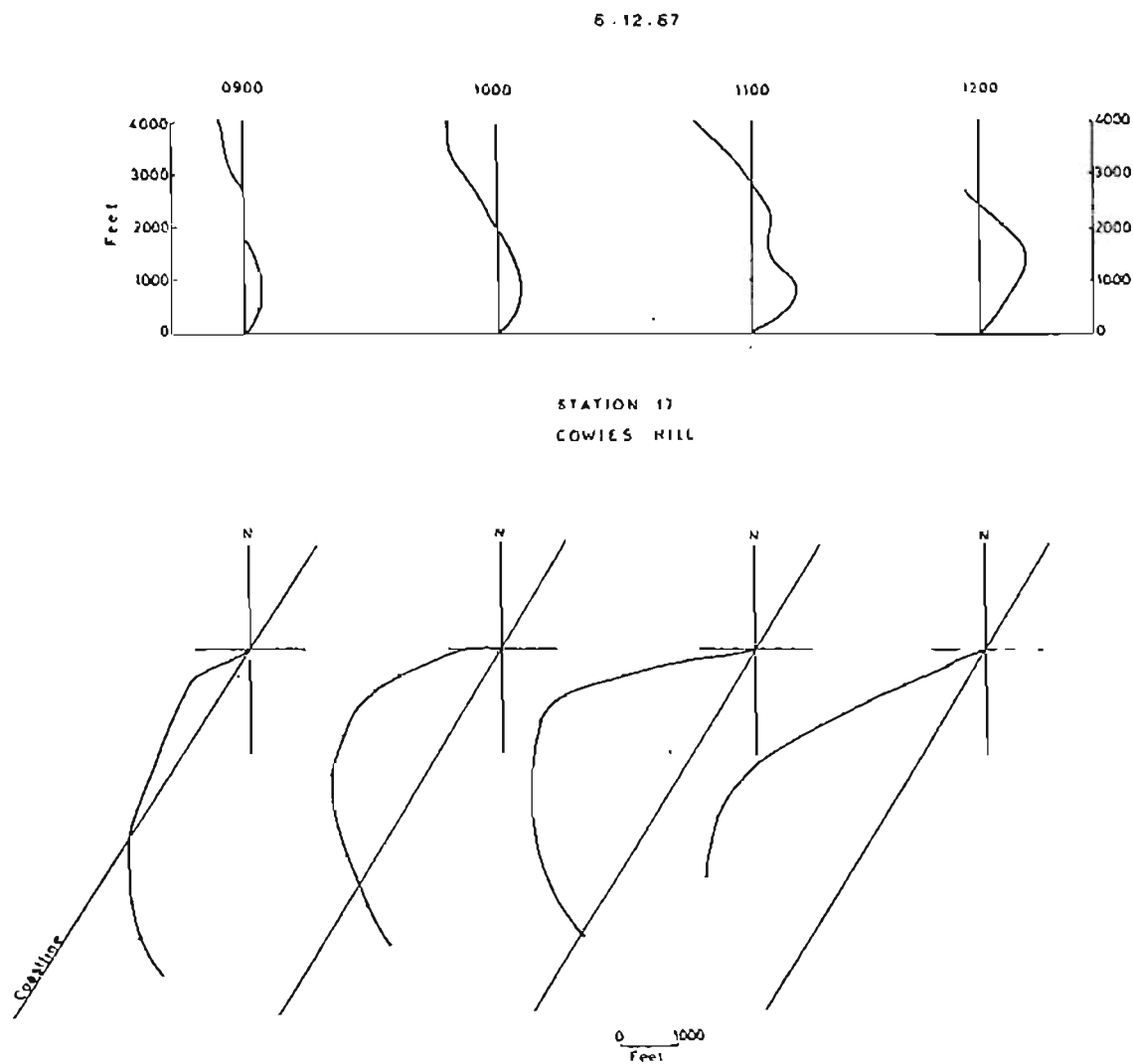


Fig. 3.1 : Profiles and horizontal components of balloon trajectories to show the onset of the sea breeze on 6.12.67 at station 17, Cowies Hill

Table 3.2: Frequency of wind direction per 500 for the 12 daytime hours only at station 13, Durban (after S.A. Weather Bureau 1960)

	January	July
N	3.1	8.3
NNE	49.1	40.9
NE	74.7	59.2
ENE	53.8	18.1
E	11.0	6.9
ESE	8.9	6.4
SE	19.3	11.3
SSE	23.6	14.1
S	49.4	32.2
SSW	79.9	51.8
SW	40.6	36.7
WSW	5.5	11.6
W	0.4	3.4
WNW	0.6	7.4
NW	1.6	19.7
NNW	1.4	19.8
CALM	75.9	153.2

surface heating in winter tends to inhibit the growth and duration of a sea breeze circulation. That conditions are more favourable for the continued existence of an offshore temperature gradient during winter mornings, is suggested by the relatively high July frequency of occurrence of offshore north-west and north-north-west winds.

#### 3.4

#### Inland penetration

The diurnal variation of wind direction at the coast, which varies from offshore at night to onshore during the day, may be found to occur throughout Natal. Tyson (1966, 1968a) has described the development of a mountain-plain wind during the night and valley winds during the day and he suggests that both these

6.12.67

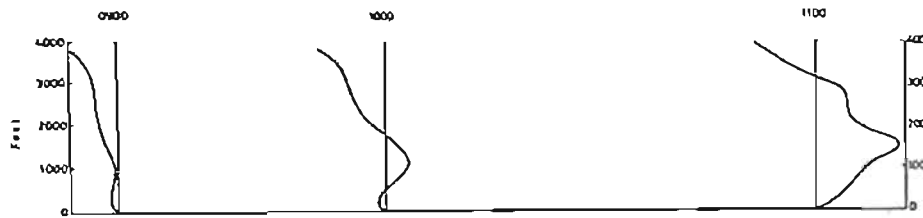
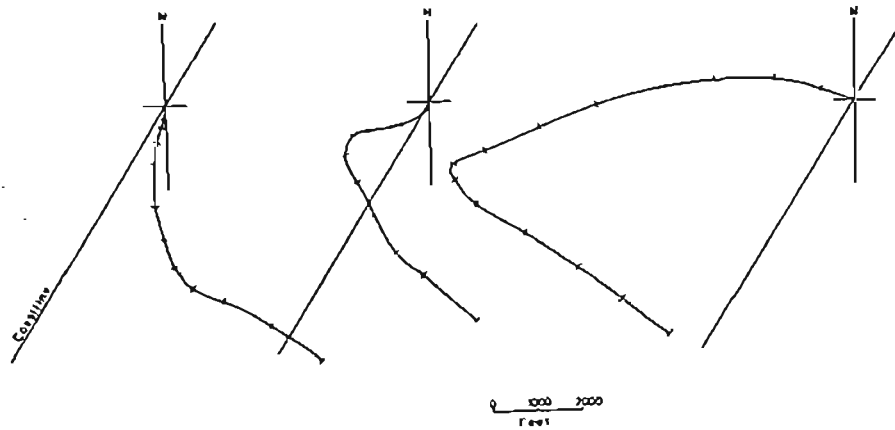
STATION 18  
BOTHAS HILL

Fig. 3.2 : Profiles and horizontal components of balloon trajectories to show the onset of the sea breeze on 6.12.67 at station 19, Bothas Hill

8.1.68

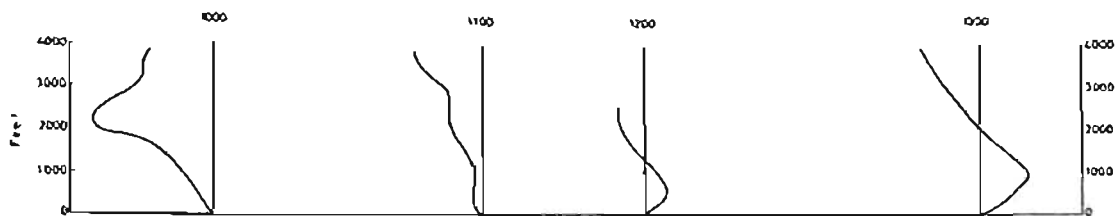
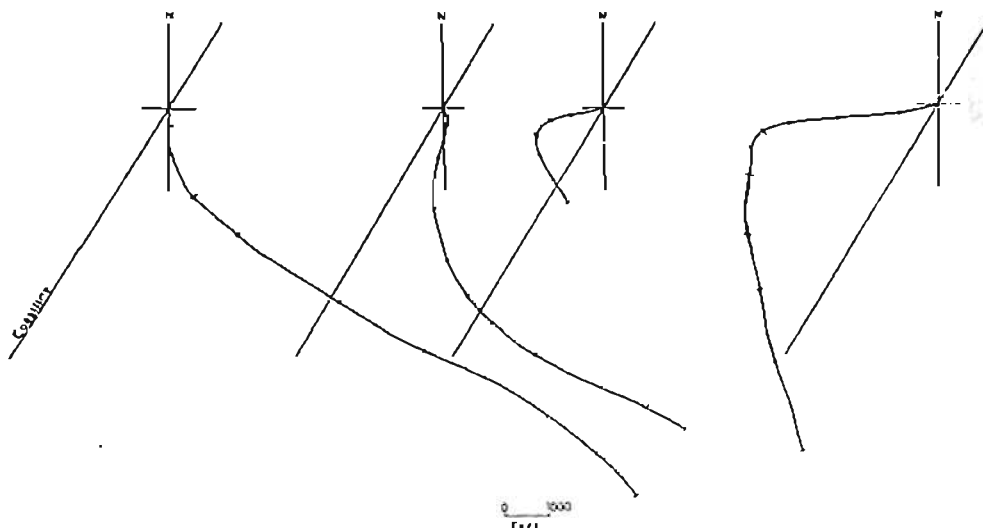
STATION 19  
CATO RIDGE

Fig. 3.3 : Profiles and horizontal components of balloon trajectories to show the onset of the sea breeze on 8.1.68 at station 20, Cato Ridge



16.1.68

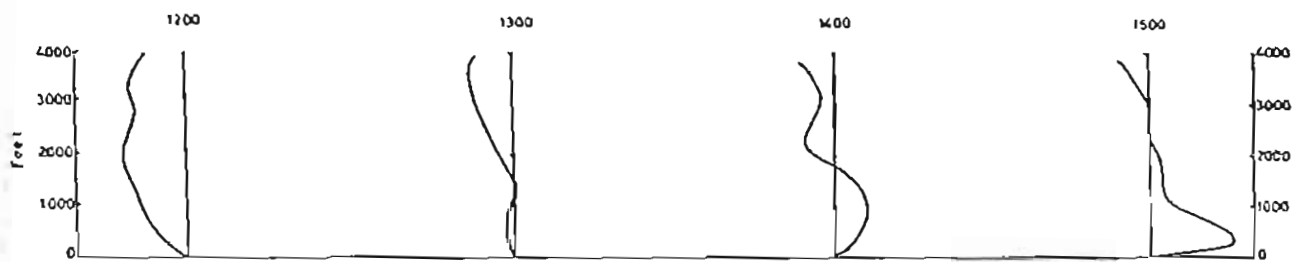
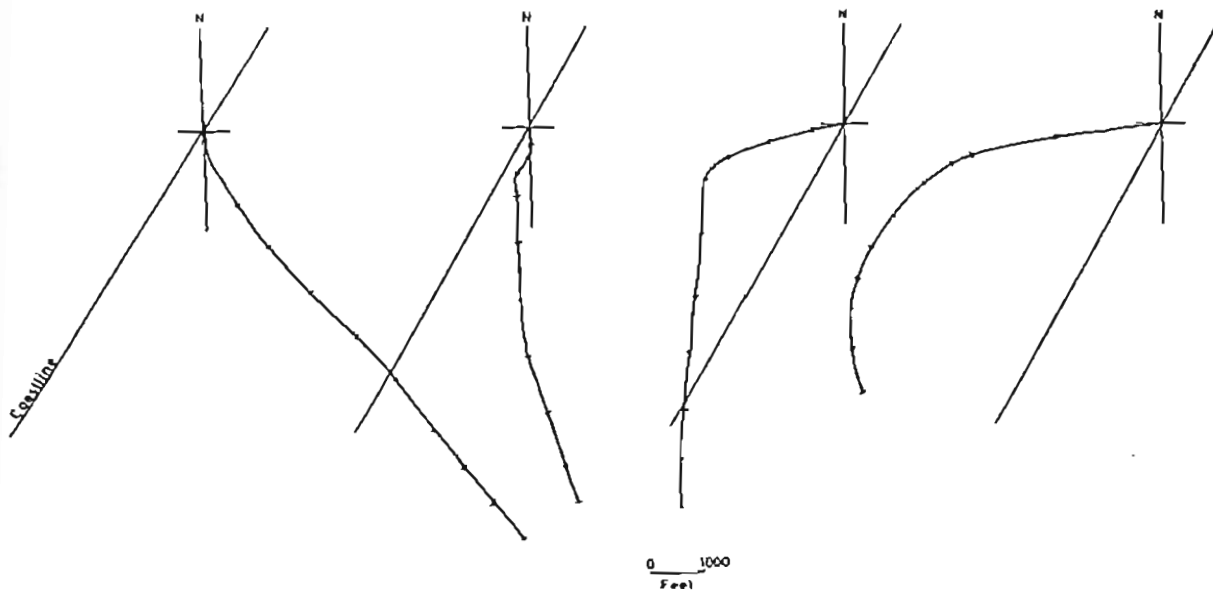
STATION 21  
MPUSHINI

Fig. 3.4 : Profiles and horizontal components of balloon trajectories to show the onset of the sea breeze on 16.1.68 at station 21, Mpushini

winds extend across Natal from the Drakensberg to the coast. However, these circulations are topographically-induced and to them must be added the effect of land-sea circulations and gradient winds. It will be shown in a later chapter that the land breeze does not extend more than 20 miles inland as a separate circulation. However, the sea breeze may under suitable conditions and strengthened by gradient winds, extend considerably further. This is depicted in Figs. 3.2, 3.3 and 3.4 which show the onset and development of an onshore circulation at recording stations situated progressively further inland as far as Mpushini (station 21).

The sea breeze circulation penetrates without difficulty to above the Kloof plateau. Fig. 3.5 shows that by 0900 on 6 December 1967, the shear line, marked by a wind shift between onshore east-north-east winds and offshore northerly winds, lay between stations 17 and 19. By 1000 the sea breeze had extended beyond station 19 although on this occasion a shallow northerly wind still persisted at the surface. No dramatic frontal change accompanied the wind shift and onshore winds were weak at first but strengthened later. Maximum onshore wind components tended to occur over the coastal area and to weaken progressively with distance inland.

The depth of the onshore wind system increases in the vicinity of station 17 and this must be partly attributed to the abrupt 700 ft altitude rise from the Pinetown basin to the Kloof plateau surface. A particularly good example of this deepening from observations made on 4 January 1968 is shown in Fig. 3.6.

Having ascended onto the Kloof plateau the wind shear advances across the Mlazi - Mgeni River interfluvium and reaches Pietermaritzburg on occasions. Fig. 3.7 shows that on 11 January 1968, onshore winds, possibly of marine origin, passed station 21 by 1000. In general the rate of movement of the shear line varies



6 12 67

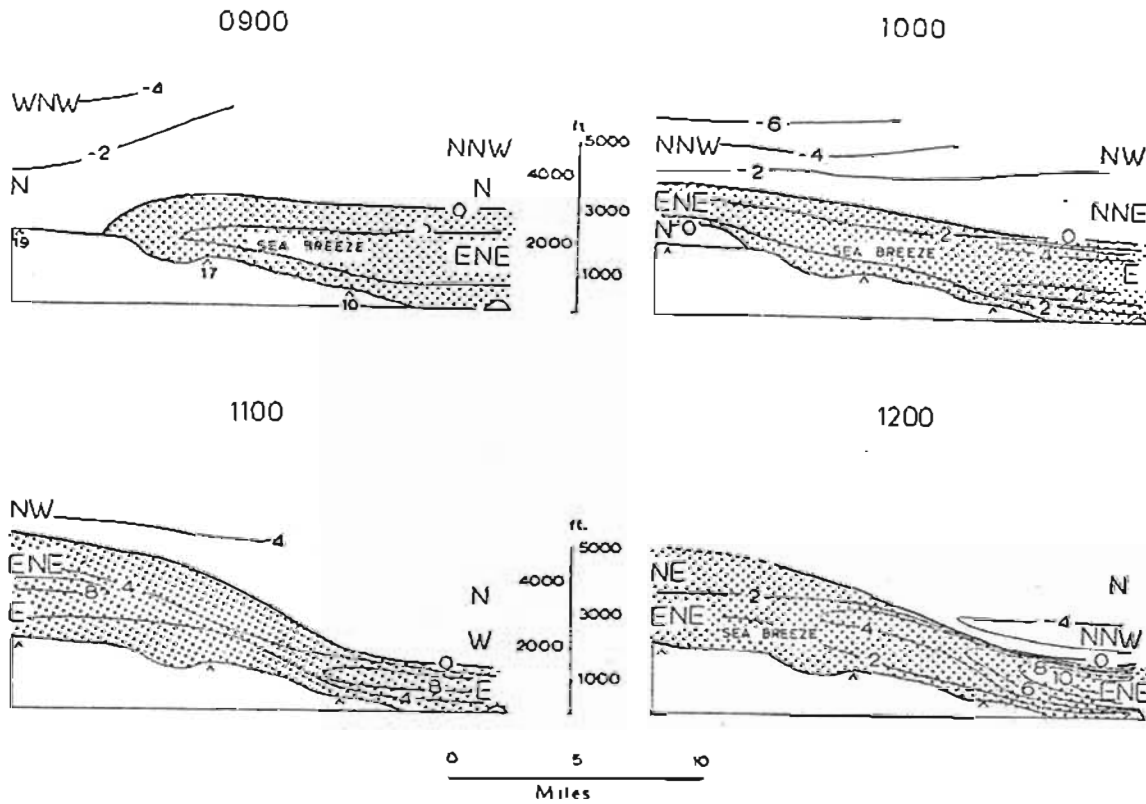


Fig. 3.5 : Velocity isopleths (m/sec) to show the inland migration of the sea breeze on 6.12.67

4. 1. 68.

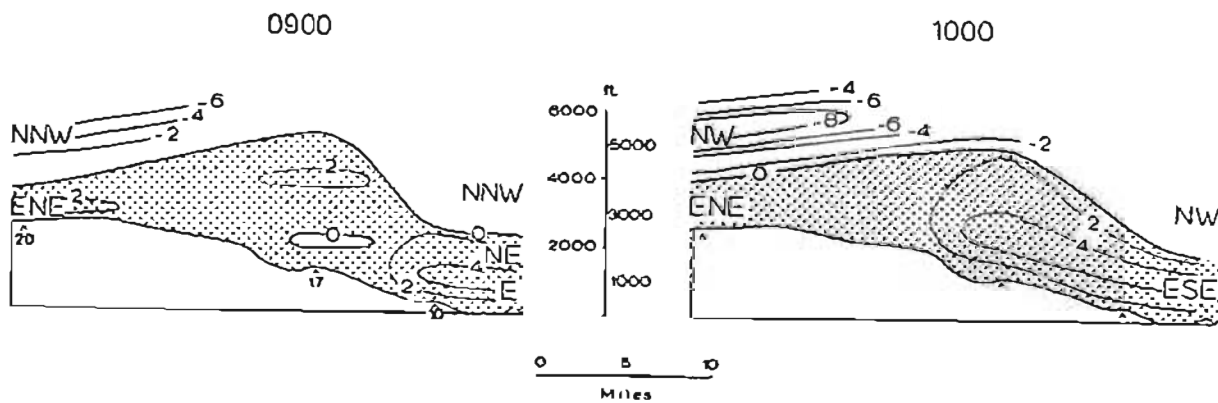


Fig. 3.6 : Section to show variations in the height of the zero wind component, 4.1.68. Velocity isopleths in m/sec

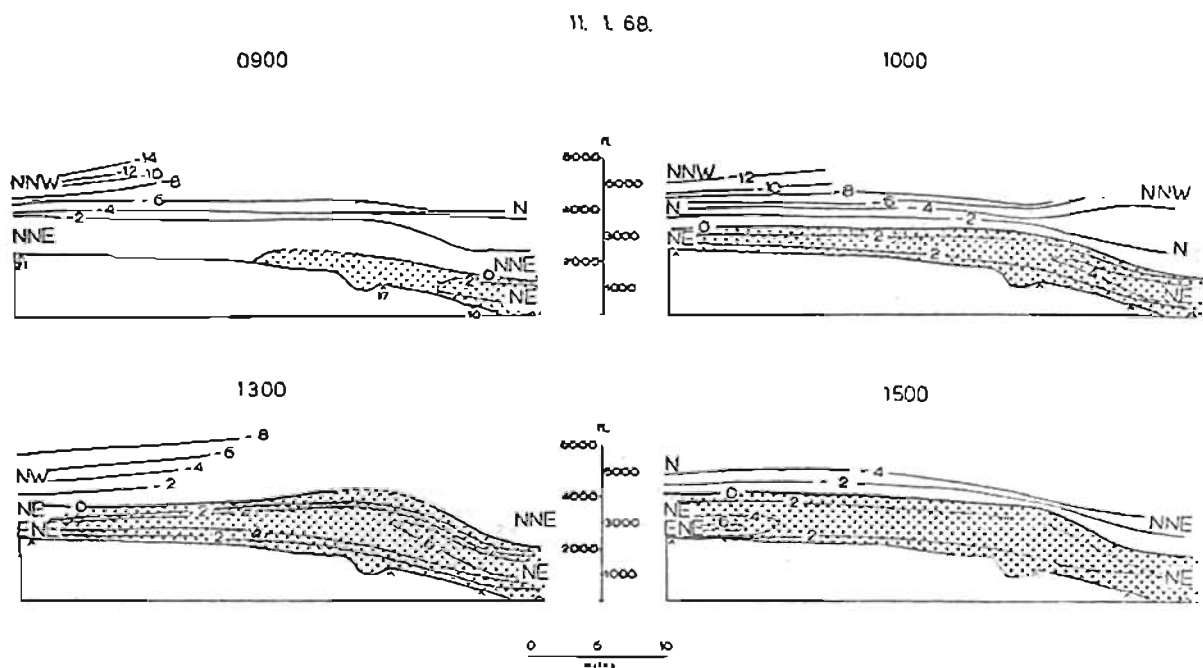


Fig. 3.7 : The penetration of the sea breeze beyond station 21 on 11.1.68. Velocity isopleths in m/sec

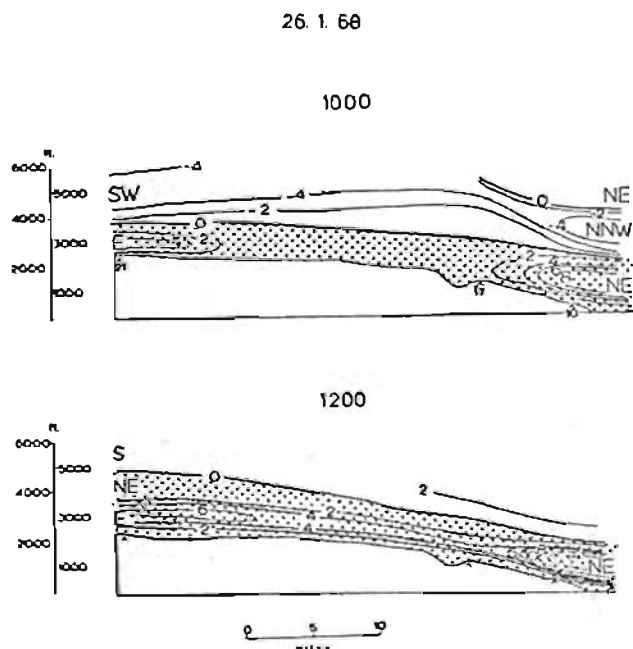


Fig. 3.8 : Possible interaction between sea breezes and valley winds suggested by strengthened onshore components of air movement on 26.1.68 at station 21. Velocity isopleths in m/sec

considerably from the relatively rapid advance of about 8 m/sec recorded in this example to much slower rates of about 4 m/sec. The onshore air layer deepened during the morning and by 1500 the height of zero wind component was 1,700 ft at station 21 and 1,500 ft at station 10 with a familiar bulge in the height of zero wind component over station 17 where the layer was 2,400 ft deep. Onshore wind components were stronger seaward of station 17 at 1000 and 1300 and this suggests that the main energy of the sea breeze circulation and probably the zone of strongest land-sea temperature gradient was concentrated in this area. By 1500, however, backing of the wind in response to the Coriolis force weakened the onshore wind components near the coast.

Although the sea breeze circulation appears to be strong and deep enough to move across the Kloof plateau, it is suggested that further inland penetration is accomplished by the additional assistance of other wind systems. By 1500 on 11 January 1969, east-north-east winds at station 21 showed a strong onshore component relative to the coastal area and seem, therefore, to be the product of forces generated other than by the sea breeze circulation. Valley winds which deepen to above ridge level (Tyson, 1968a) offer one explanation; another may be sought in the combined effect of sea breezes and gradient winds particularly as onshore circulations have been traced from the coast. A more probable conclusion, however, is that these winds represent the combined effect of all three wind systems.

Valley winds which influence air movement over station 21 would be generated mainly in the Mgeni River valley. As these winds deepen to above the level of the interfluvium which separates the Mgeni and Mlazi River valleys, entrainment into the combined onshore gradient wind and sea breeze system would occur. Observations on 26 January 1968 shown in Fig. 3.8 indicate north-east winds at the coast but easterly winds near the surface further inland. It is suggested

that in this case east is the resultant wind direction between deepening valley winds and the gradient wind-sea breeze system.

Unlike an advancing sea breeze front, which is associated with strong vertical currents usually identified by cloud (Leopold, 1949), the moving shear line in Natal is not accompanied by cloud development. However, vigorous cumulus growth in the Kloof plateau area, coupled with a tendency for the altitude of zero wind component to increase in this area, does suggest a zone of strong vertical motion 10-15 miles inland from the coast.

The movement of a shear line separating onshore from offshore wind components was not traced beyond station 21. However, from observations by Tyson (1963a) it seems likely that much of this onshore air movement is integrated, near the surface, into a regional valley wind which by day blows east-south-east to south-east over Natal.

It is difficult to evaluate the influence of pressure systems in Natal upon these local wind systems. In particular the presence of a lee depression in East Griqualand and southern Natal may be recognised by consistently lower pressures recorded at Kokstad than at Umtata, Cedara or Estcourt (Table 3.3).

Table 3.3: Mean height in geopotential metres of the 850 mb surface during January 1969 at weather stations in the Transkei, East Griqualand and Natal (after Durban Meteorological Office daily 1400 synoptic charts)

Umtata	Kokstad	Cedara	Estcourt
501	480	494	492

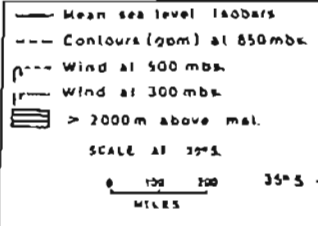


Fig. 3.9 : The variation in pressure over Natal and the adjacent Indian Ocean and changes in the speed and direction of upper winds at 1400 on 11.1.68. Pressure over the land is reduced to 850 millibars; over the sea to mean sea level

An example of 1400 synoptic conditions on 11 January 1968 shows that although pressures reduced to 850 mbs were generally low over eastern South Africa, lowest pressures over the land were to be found over the interior of southern Natal and East Griqualand (Fig. 3.9). Although this low may reflect pressure variations over a much larger area than the Natal interior, it was probably intensified by the development of a lee depression caused by strong north-west winds blowing over the Drakensberg. This low may produce a monsoon effect and be responsible for an added component of onshore winds towards the Natal interior.

### 3.5 . Depth and velocity characteristics

The depth and velocity of the sea breeze is characterised by day to day variations. This may be attributed in particular to:

- (a) Changes in the strength and direction of the prevailing gradient wind. This is of particular significance on the east coast of South Africa where the high frequency of coastal lows produce a wind shift from north-east to south-west every few days.
- (b) Changes in lapse rate. When unstable atmospheric conditions persist near the surface, heat generated by radiational warming of the land is spread through a deeper layer than under stable conditions and this would tend to restrict the development of a steep thermal pressure gradient. However, cloud development is also characteristic of unstable air and the release of the latent heat of condensation may more than counteract the initial reduction of a land-sea pressure gradient.
- (c) Variations in surface heating. The formation of a cloud

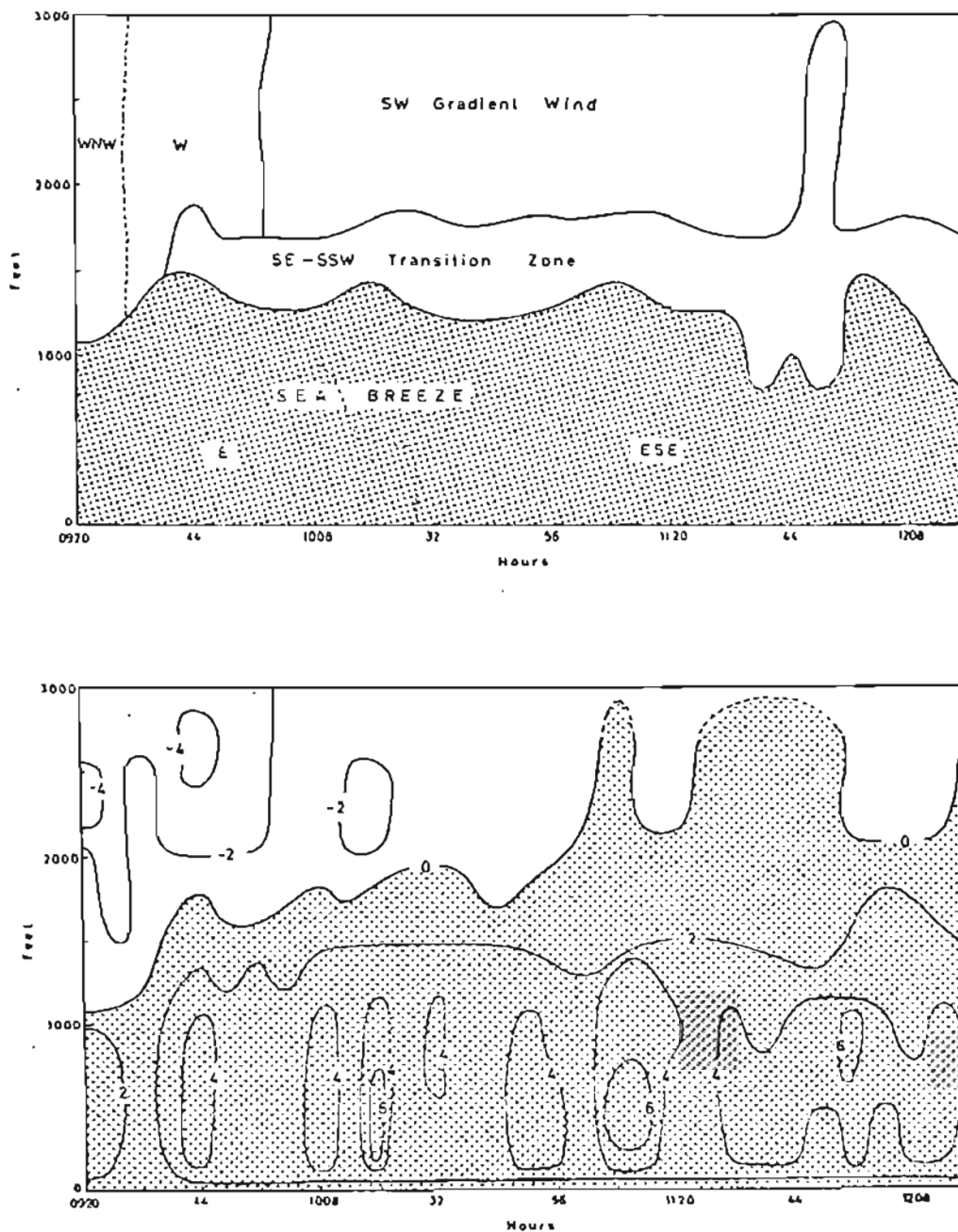


Fig. 3.10 : Time section to show wind direction and onshore (positive) and offshore (negative) wind components in m/sec on 28.11.68 at station 2

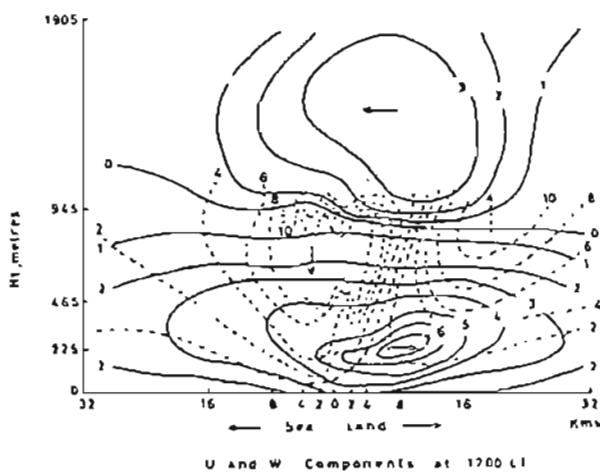
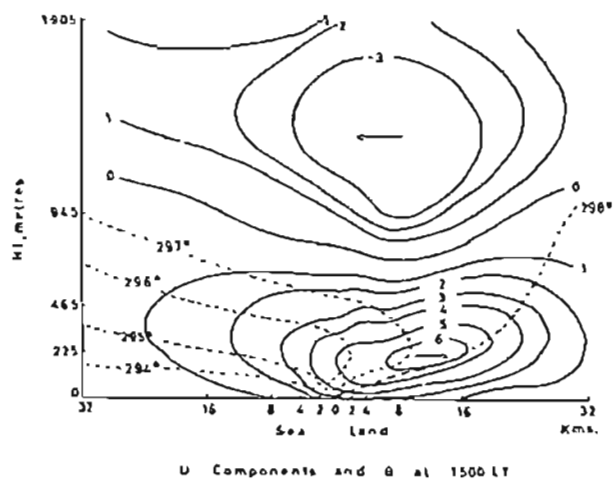
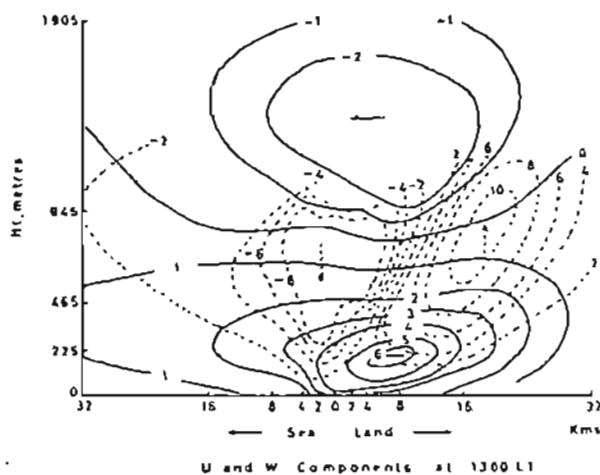
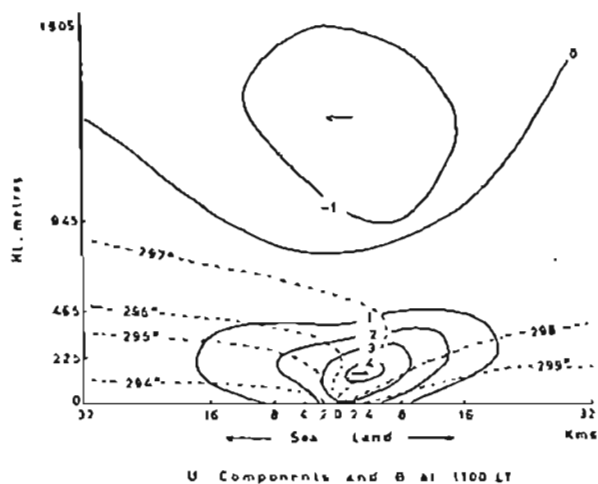


Fig. 3.11: Computed vertical cross-section perpendicular to the coast to show the development of the sea breeze.  $u$ , component of air movement normal to the coast positive onshore,  $w$ , component of vertical air movement positive upwards,  $\theta$  potential temperature ( $^{\circ}\text{A}$ ) (after Fisher, 1961)



cover over the land soon after sunrise retards surface heating and thus inhibits the sea breeze circulation. Nocturnal rainfall, a common phenomenon at Durban, not only cools the air layer near the ground but also delays the daytime rise in temperature while the saturated soil dries out.

Certain variables remain unchanged, however, and they must exert a considerable influence upon the sea breeze. These include:

- (a) The topography which is deeply incised by rivers flowing north-west to south-east. Topographically-induced up-valley winds must strengthen the sea breeze particularly in the lower layers.
- (b) With the exception of urban areas the landscape is largely grass-covered so that the rate of surface heating affected by this factor would not differ significantly from area to area.

In fine weather the sea breeze deepens steadily over the coast. Fig. 3.10 shows that a well-developed sea breeze circulation, recorded on 28 November 1968 from station 2, deepened from 1,100 ft at 0920 to 2,700 ft by 1220 at a rate of 9 ft/min. On this occasion east and east-south-east winds near the surface were due to the influence upon the sea breeze of low-level gradient winds over the sea which were veering in response to an advancing coastal low. The height of zero wind component at 1100 was about 2,000 ft and it is interesting to note that this is in approximate agreement with the model developed by Fisher (1961) for a sea breeze circulation at this hour (Fig. 3.11). Fisher used sea breeze observations from the New England coast as a basis for the integration of non-linear sea breeze equations at consecutive time intervals.

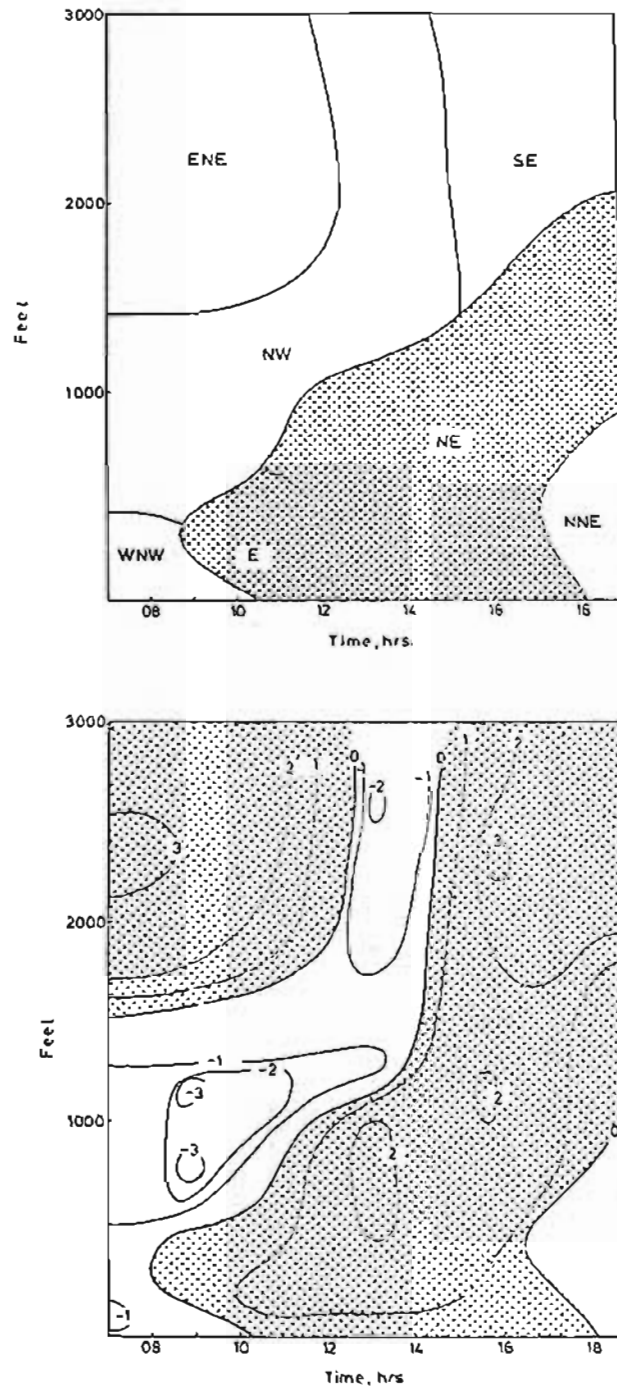


Fig. 3.12 : Time section to show depth (ft), velocity (m/sec) and direction characteristics of the sea breeze on 7.7.67 at station 18

From components of mean winds normal to the coast observed from pilot balloon ascents at Durban, Jackson (1954) concludes that in summer the onshore air current is between 2,000 and 3,000 ft. In addition this height was found to vary in accordance with the stability of the upper air with shallow sea breezes associated with low-level subsidence inversions. The infrequent occurrence of onshore winds above 3,000 ft is also shown in Table 3.4 which indicates resultant wind directions computed from December to February 1965-66 1400 radiosonde ascents at Durban. Resultant winds are easterly at 1000 mbs and northerly at 900 mbs.

Table 3.4: December to February wind resultants over Durban (after S.A. Weather Bureau Rawin data 1965-66)

Pressure (mbs)	Mean Height (ft)	Resultant Direction (deg)
1000	353	92
900	3335	356
800	6628	302

The increased stability of the upper air during winter and the greater frequency of subsidence inversions at levels lower than those characteristic of summer (Taljaard, 1955) means that in general sea breezes would be shallower in winter than in summer. Fig. 3.12 shows that on 7 July 1967 the onshore east and north-east wind deepened over station 18 from 200 ft at 0845 to 2,000 ft at 1800 at a rate of 3.24 ft/min. At 1300 the height of zero wind component was some 1,740 ft below that predicted by Fisher for a similar hour.

Despite the gradual deepening of the sea breeze circulation over the coast during the day, the zone of maximum onshore wind

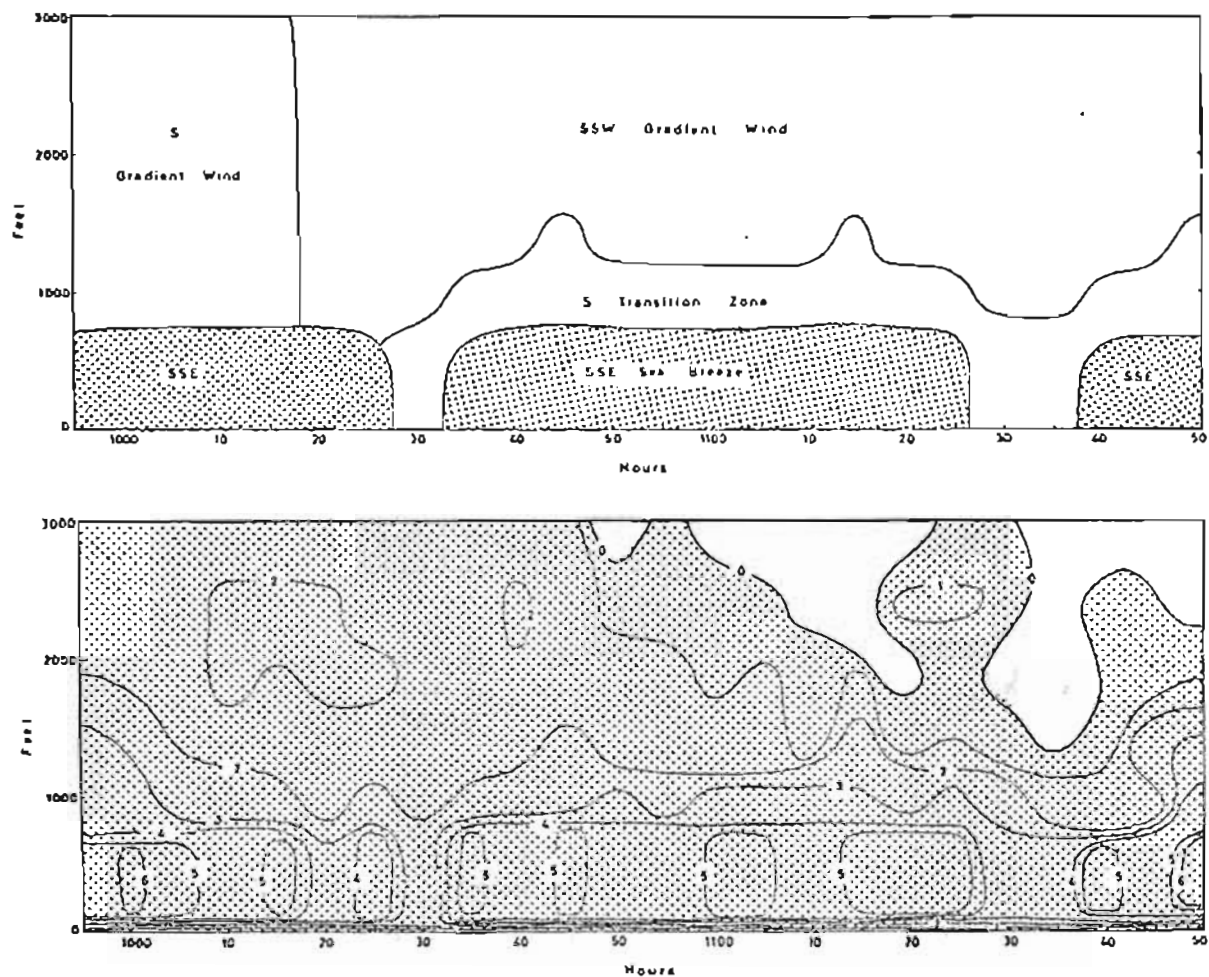


Fig. 3.13 : Time section to show depth (ft), velocity (m/sec) and direction characteristics of the sea breeze recorded on 3.12.68 at station 2

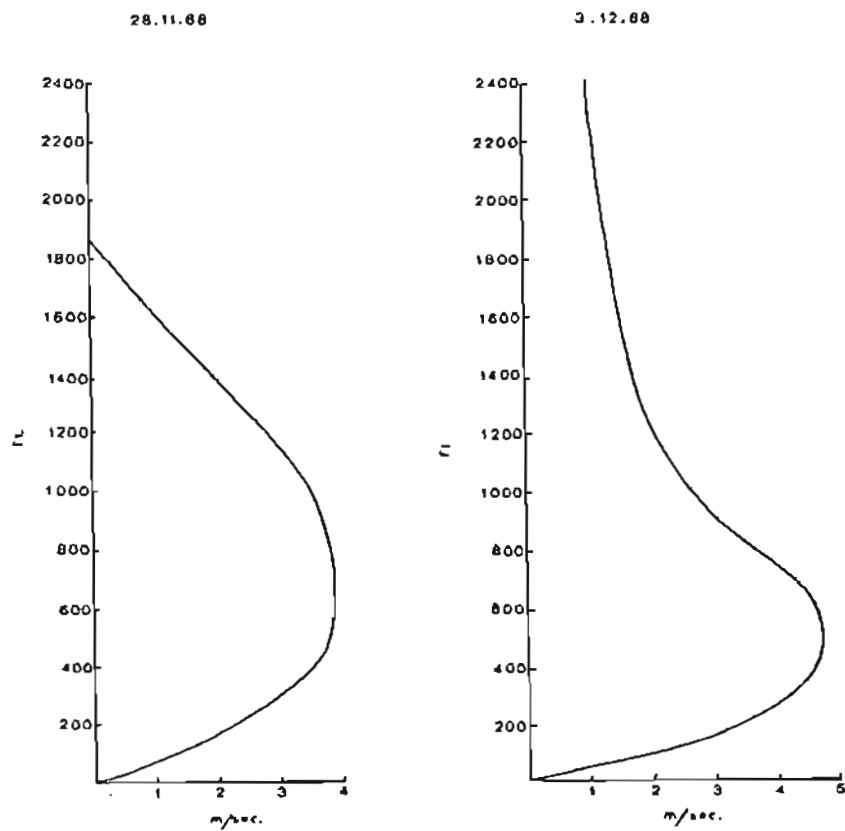


Fig. 3.14 : Mean profiles of onshore wind components (m/sec) measured on 28.11.68 and 3.12.68 from station 2

components remains approximately constant. This is apparent in Figs. 3.10 and 3.13 and mean values of the components shown in Fig. 3.14 indicate that maximum velocities were located between 500 and 1,000 ft. In the model developed by Fisher (1961) maximum onshore components are located between 640 ft and 1,300 ft.

On some occasions the wind profile rather than the zero wind component is an important indicator of the presence of a sea breeze circulation. On 3 December 1968 (Fig. 3.13) a fluctuating zero wind component was clearly not associated with the sea breeze but was due to slight variations of the gradient wind away from a direction parallel to the coast. Upper gradient winds suppressed any tendency of the sea breeze to deepen and its existence could only be recognised by maximum onshore components below 1,000 ft.

### 3.6 Surging

In the zone of maximum onshore wind components in Fig. 3.10 and Fig. 3.13, clearly recognisable surges are present. This aspect of the sea breeze appears to have received very little attention although Wallington (1959) has recognised surges at the sea breeze front over south-east England and Pearce (1962) describes 10 minute pulses in sea breeze velocities from anemogram recordings. Pulsating variations in the wind at inland stations are also recognised in the model developed by Pearce (1962) although they do not seem to appear in similar models developed by Fisher (1961) and Estoque (1962). Pearce cites surge-type solutions found by Ball (1960) to be associated with the Coriolis terms in the equations of motion as a possible explanation of this phenomenon. However, it may also be suggested that as onshore components of air movement due to the sea breeze and gradient winds increase, temperatures in the lower layer of the atmosphere may be temporarily lowered by advection of cooler sea air over the land and to eddy diffusion of heat. The

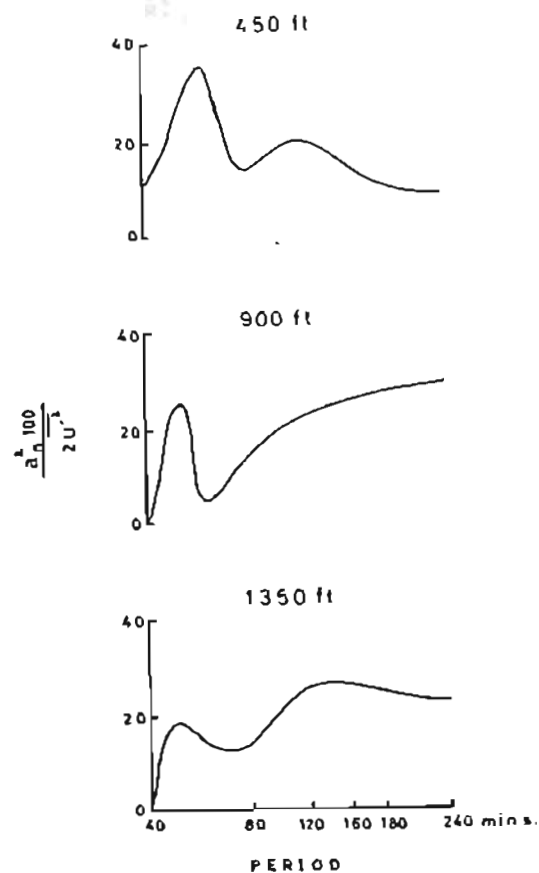


Fig. 3.15 : Velocity spectra of the sea breeze, 0920-1220, on 28.11.68 at station 2

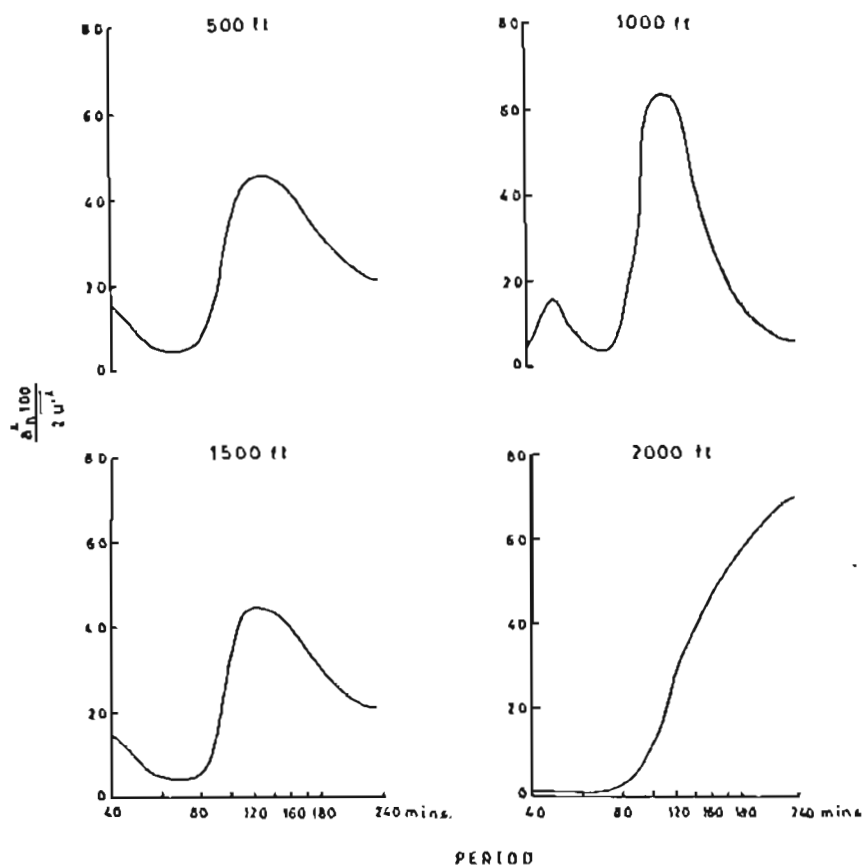


Fig. 3.16 : Velocity spectra of the sea breeze, 0955-1150 on 3.12.68 at station 2

sea breeze component of the onshore air movement may then be temporarily weakened by reduced baroclinity. A return to the previous velocities takes place as a surge and this awaits upon the renewal of the pre-existing temperature gradient by surface heating.

The process described above could account for periodic surges in the sea breeze and since surging seems to take place as a low frequency velocity oscillation it can be described by harmonic analysis. A variance spectrum is obtained by plotting the variance ratio given by Equation 2.7 against the period of each harmonic. By this method wind speed measurements on 28 November 1968 and 3 December 1968 from station 2 give periods of 60 and 120 minutes (Figs. 3.15 and 3.16). The period would, however, be expected to vary from day to day with changes in direction and speed of gradient winds and variations in the land-sea temperature gradient.

### 3.7 The effect of gradient winds

Prevailing directions of gradient winds along the Natal coast are north-east and south-west. The former is the result of air circulation about eastward moving highs; the latter due to the orientation of post-frontal pressure gradients. The sea breeze circulation is superimposed upon these winds and the nature and characteristics of the resultant wind is considerably determined by the speed and directional characteristics of the gradient wind.

When the pressure gradient about a prevailing high is slack, low velocity north-east gradient winds result and it is under these conditions that characteristics of the sea breeze can be best observed. Subsidence and upper air stability are usually associated with these pressure gradient conditions so that a shallow sea breeze must be expected. The inland penetration of the shear line between



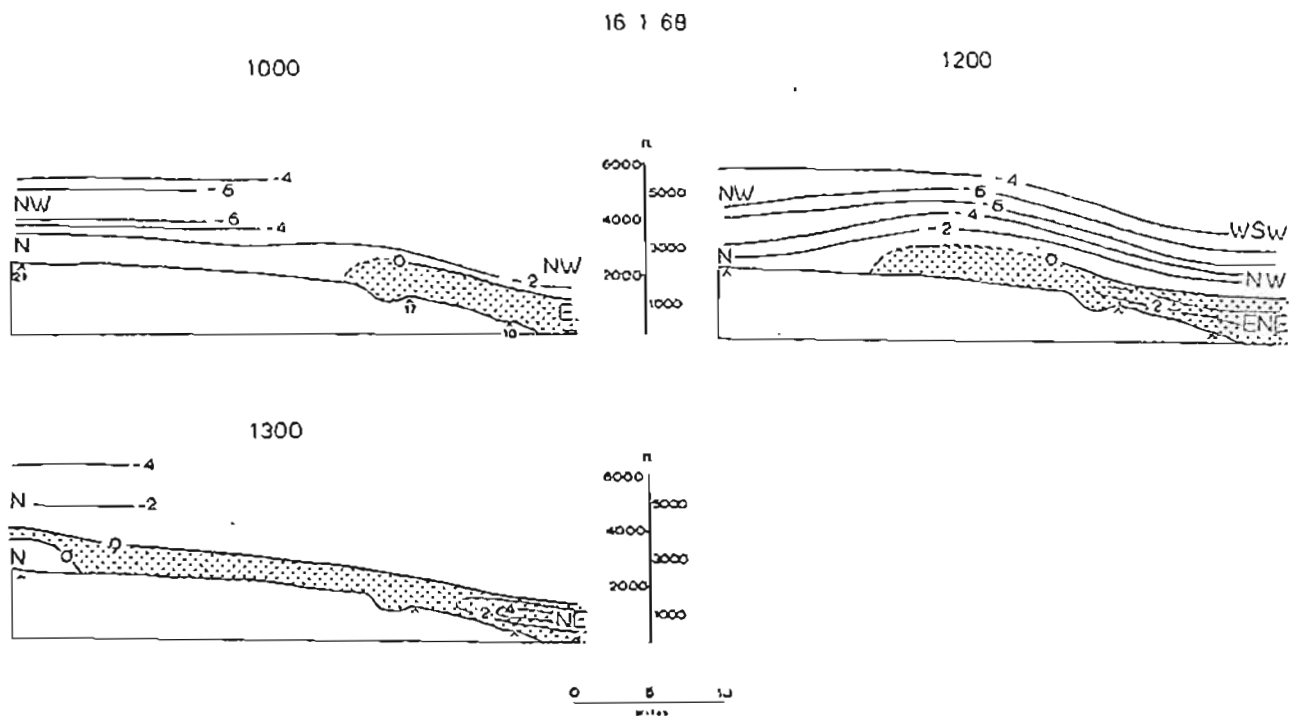


Fig. 3.17 : Inland migration of the sea breeze with weak north-east gradient winds on 16.1.68. Velocity isopleths in m/sec

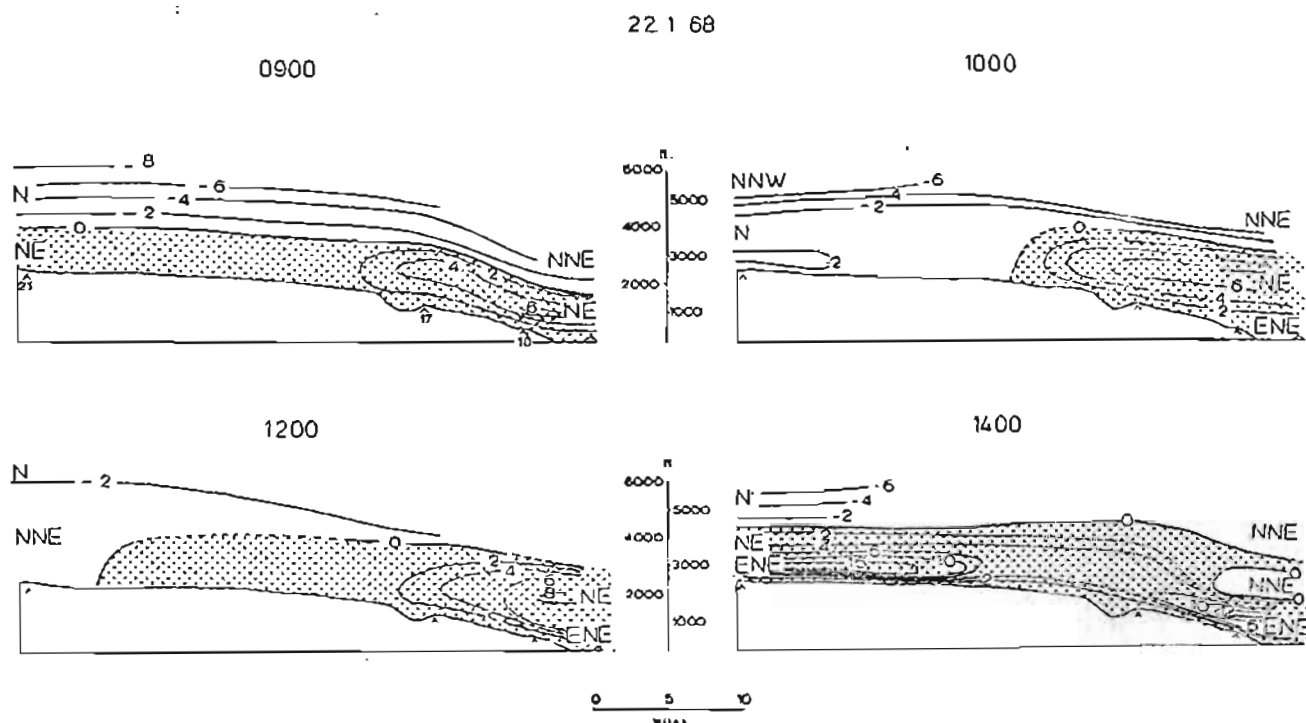


Fig. 3.18 : Inland migration of the sea breeze with strong north-east gradient winds on 22.1.68. Velocity isopleths in m/sec

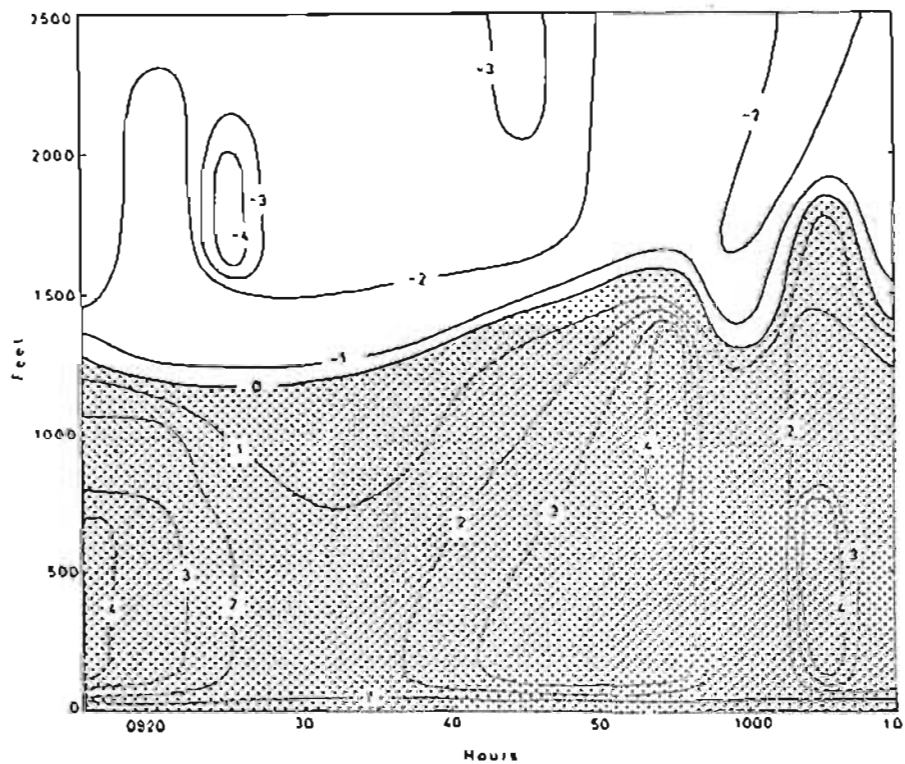
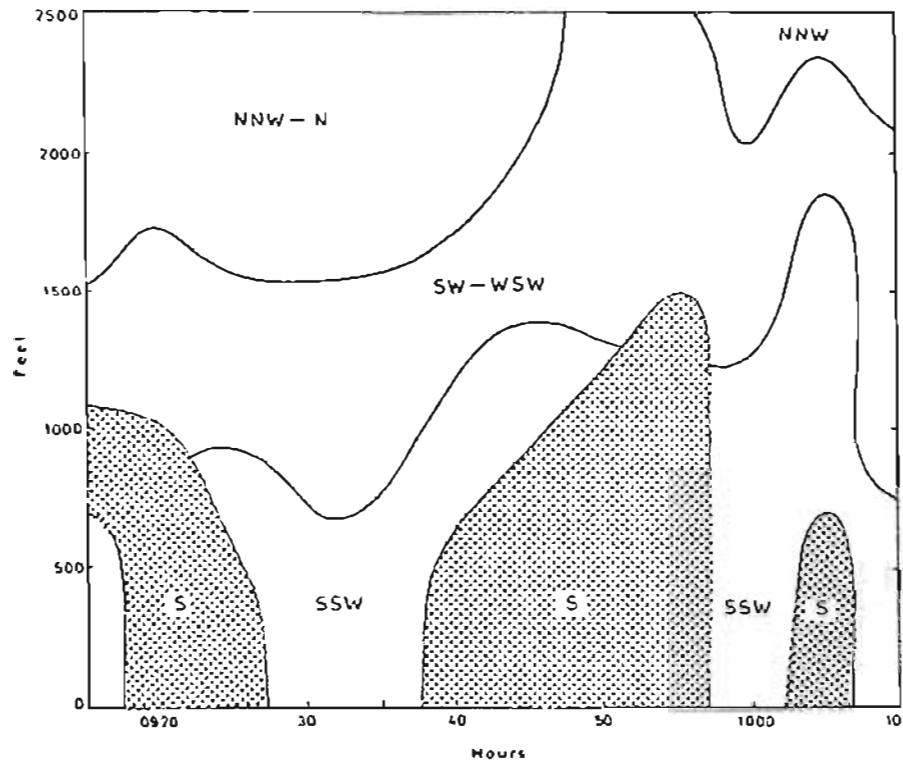


Fig. 3.19 : Time section to show depth (ft), velocity (m/sec) and direction characteristics of the sea breeze under post-frontal conditions. Observations on 20.1.69 from station 2

onshore and offshore wind components is slow and the velocity of onshore wind components weak. However, in the vicinity of the coast, growth of the sea breeze circulation generates progressively stronger onshore winds. On 16 January 1968 each of these characteristics were observed from balloon ascents (Fig. 3.17).

As a cold front advances north-east up the Natal coast, pressure gradients steepen and north-east gradient winds blow strongly. Under these conditions it is difficult to separate the weakened sea breeze components from the gradient wind. Observations on 22 January 1968 shown in Fig. 3.18 suggest that pressure gradients steepened sharply after 1200 as a low advanced up the coast, so that by 1500 the principal component of onshore east-north-east winds was derived from pre-frontal gradient winds rather than from land-sea or topographically-induced wind systems.

Post-frontal south-west winds are usually strong and turbulent and are associated with cool near-surface atmospheric temperatures. Cloud is common and rain may fall. Warming of the land is inhibited by these weather conditions so that only a weak sea breeze is usually apparent. Observations on 20 January 1969 shown in Fig. 3.19 indicated the periodic occurrence of a possible sea breeze effect as stronger onshore components of air movement appeared in the form of surges. These southerly winds were then overcome by south-south-west gradient winds.

On other occasions such as 5 July 1967 (Fig. 3.20) a sea breeze blew south-south-east from 1030 having backed from west-south-west and south-south-west. Maximum onshore components occurred at 1400 approximately at the time of greatest land-sea temperature difference. It is interesting to note that a clearly defined west-south-west return current prevailed above the sea breeze with maximum offshore wind components in phase with maximum onshore wind components.

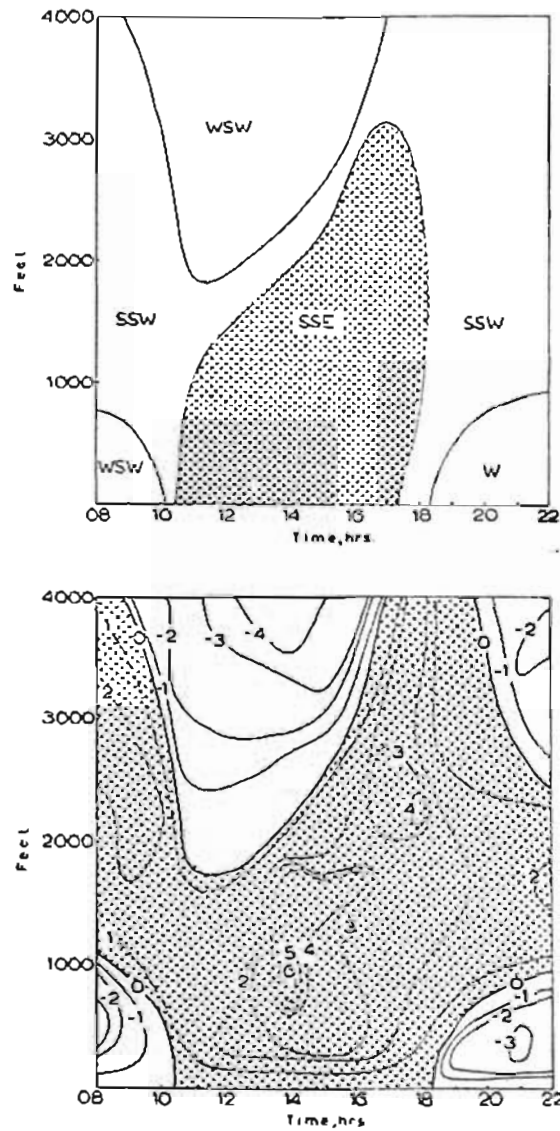


Fig. 3.20 : Time section to show depth (ft), velocity (m/sec) and direction characteristics of the sea breeze under post-frontal conditions. Observations on 5.7.67 from station 18

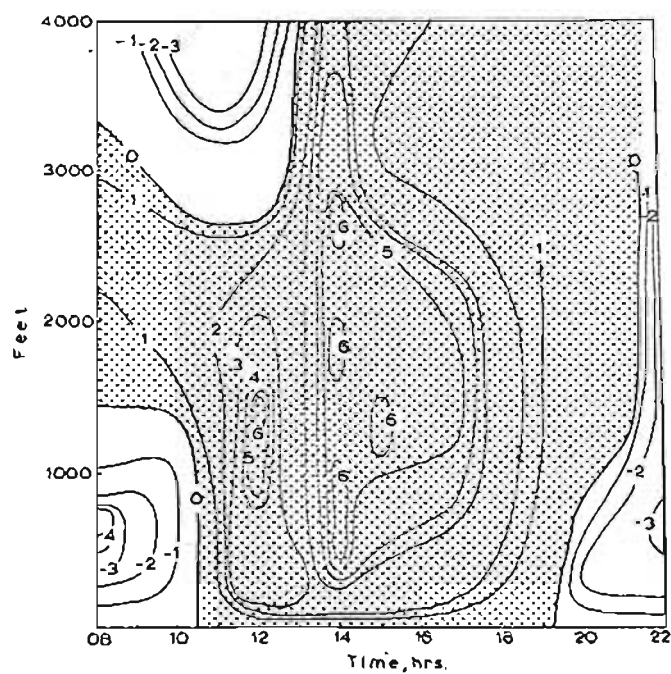
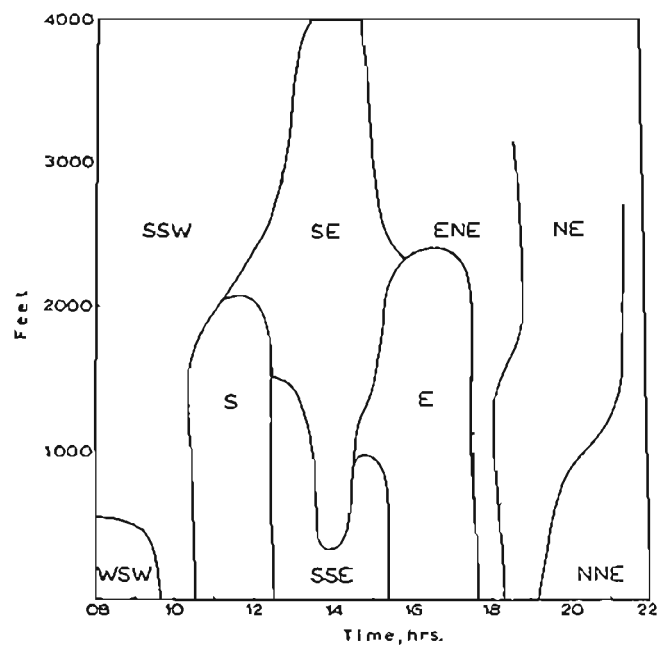
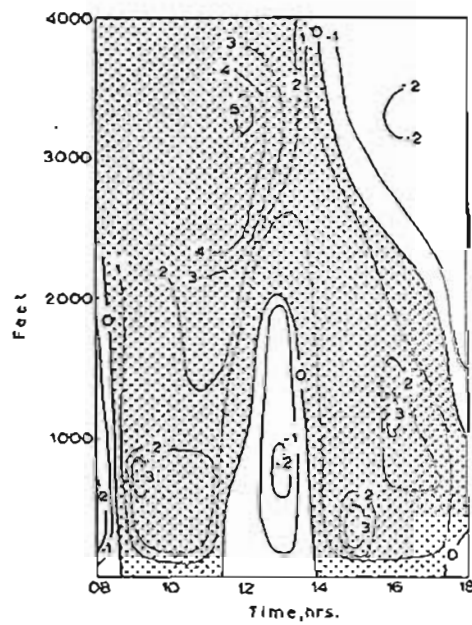
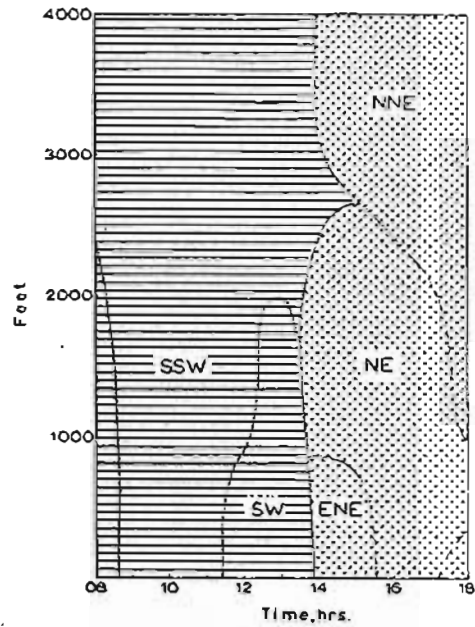


Fig. 3.21 : Time section to show backing of the sea breeze as north-east gradient winds are reinstated. Observations on 6.7.67 from station 18, velocity isopleths in m/sec



3.22 : Time section to show a possible frontal onset of the sea breeze on 26.7.67 at station 18. Velocity isopleths in m/sec

Anticyclonic cells which move eastward behind cold fronts cause gradient wind directions to return to north-east and bring warmer, clearer weather. It is not unusual, therefore, for winds to back through about  $225^{\circ}$  from an offshore west-south-west land breeze direction in the early morning towards an offshore north-north-east direction in the evening. Such an occurrence is shown in Fig. 3.21.

Less usual is the swift change in wind direction from south-west to north-east. Observations on 26 July 1967 indicated in Fig. 3.22, show that onshore south-south-west and offshore south-west winds prevailed until 1400 abruptly followed by onshore north-east winds. The model developed by Estoque (1962) and observations by Koschmeider (1941) suggest that in this case the advection of warmer land air towards the sea by offshore winds tends to produce a strong horizontal temperature gradient within a thick layer of the atmosphere and, therefore, a correspondingly steep pressure gradient near the surface. The sea breeze arrives as a local front when the onshore pressure gradient exceeds that generating the south-west wind. It must be emphasised, however, that this case is also associated with a return of the gradient wind system towards the prevailing north-east direction.

\* \* \* \* \*

The influence of the sea breeze upon certain climatic elements is considerable and this topic is examined in greater detail in later chapters. However, at this stage it should be noted that during the summer months, the cool, strengthened sea breeze lowers the level of climatic discomfort and displaces the urban heat island away from the Durban central business district. It is suggested that these winds are also indirectly associated with the

occurrence of evening thunderstorms over the Natal coast. Finally, ventilation of the atmosphere by the sea breeze lowers the level of atmospheric pollution.



## CHAPTER 4

### LAND BREEZES

#### 4.1 Introduction

It has generally been assumed that the seaward movement of cool air along the Natal coast at night is due to a land breeze circulation alone (Weather on the Coasts of Southern Africa 1941; Jackson 1954). However, Tyson (1966) has suggested that mountain winds, which originate in the deeply incised Drakensberg valleys, deepen and ultimately reach the coast as a mountain-plain wind where it is taken for or superimposed upon the land breeze. In addition drainage winds, which are confined to river valleys along the Natal coast, contribute an additional component to the offshore circulation. The purpose of this and the following chapter is to examine the nature and characteristics of these wind systems and to evaluate the contribution of each to the total offshore air movement.

#### 4.2 General characteristics

In contrast to the sea breeze circulation the land breeze has received little attention. In general it is assumed that the sea breeze mechanism also functions for the land breeze with the replacement of land surface heating by surface cooling so that a baroclinic atmosphere is maintained between land and sea surfaces and the circulation around isobaric-isosteric solenoids is reversed from onshore to offshore. The circulation has not been simulated by the integration of non-linear land breeze equations performed at consecutive time increments and few comments are to be found regarding the influence of friction and the earth's rotation upon this

circulation.

At night thermal stability in the land breeze layer inhibits turbulence so that surface land temperature, which relative to daytime is less affected by vertical diffusion of heat, cools further below the sea temperature than it rises above it by day. This occurs during both the warmest and coolest months although Table 4.1 shows that in July the maximum nocturnal land-sea temperature difference,  $\Delta T$ , exceeds the February value by a factor of 1.97. Throughout the night and in both months, negative  $\Delta T$  values are greater than positive daytime values (see also Table 3.1). This characteristic has also been recognised by Kimble (1946) who points out that even in the wet tropics land-sea temperature differences are greater by night than by day.

The land breeze is universally acknowledged as being weaker than the sea breeze and Kimble (1946) gives mean values of 1.0 m/sec for the tropics and Jackson (1954) 3.5 m/sec for the Natal coast. Paradoxically, the land breeze, both in summer and in winter prevails for a longer period than the sea breeze. Table 4.1 shows that the summer  $\Delta T$  value at Durban is negative for 14 hours; the winter value for 17 hours. The duration of the sea breeze is usually less than 10 hours while the land breeze prevails for about 13 hours in summer and 16 hours in winter. This is in approximate agreement with Kimble (1946) who gives average duration times at Batavia of 9 hours for the sea breeze and 14 hours for the land breeze.

While it is acknowledged that a critical negative land-sea temperature gradient is necessary to initiate the land breeze, it is not possible to state exactly what the value must be locally. Nonetheless, under ideal conditions  $\Delta T$  increases during the night and once started land breeze velocities should undergo a corresponding increase and reach maximum values at dawn. Mean winter wind speeds in Table 4.1 show a slight tendency towards this condition. After

Table 4.1: Mean hourly wind speeds ( $\bar{U}$ ) in mph and the mean hourly land-sea temperature difference ( $\Delta T$ ) in  $^{\circ}\text{C}$  during February and July at Durban (after S.A. Weather Bureau, 1954, 1960; Wellington, 1955)

Time	February		July	
	$\bar{U}$	$\Delta T$	$\bar{U}$	$\Delta T$
16	9.8	+1.2	8.2	+1.1
17	9.2	+0.6	7.5	-0.1
18	8.8	0	6.4	-1.5
19	8.0	-0.5	5.3	-2.7
20	7.5	-0.9	4.9	-3.4
21	6.9	-1.3	4.7	-3.9
22	6.3	-1.6	4.2	-4.4
23	5.6	-1.9	4.1	-4.9
24	5.2	-2.2	4.1	-5.1
01	4.5	-2.4	3.9	-5.6
02	4.1	-2.6	4.1	-5.8
03	4.1	-2.9	4.2	-6.0
04	3.6	-3.1	4.1	-6.2
05	3.7	-3.3	4.2	-6.5
06	3.7	-3.3	3.9	-6.5
07	3.7	-2.6	3.7	-6.5
08	5.2	-0.7	3.7	-4.6
09	6.5	+0.3	4.2	-1.9
10	7.7	+1.0	5.0	+0.4

sunrise, surface heating reduces  $\Delta T$  and the land breeze weakens. Under fine winter weather conditions on the Natal coast a period of stagnation with a duration as long as 90 minutes commonly preceeds the onset of the sea breeze.

Although the sea breeze circulation cannot be adequately described without recognition of the Coriolis parameter, the land breeze is usually regarded as a purely antitriptic wind. Munn (1966) points out that the air trajectories at night are rarely of sufficient length to make the Coriolis force worth consideration while relatively low velocities also reduce the effectiveness of this

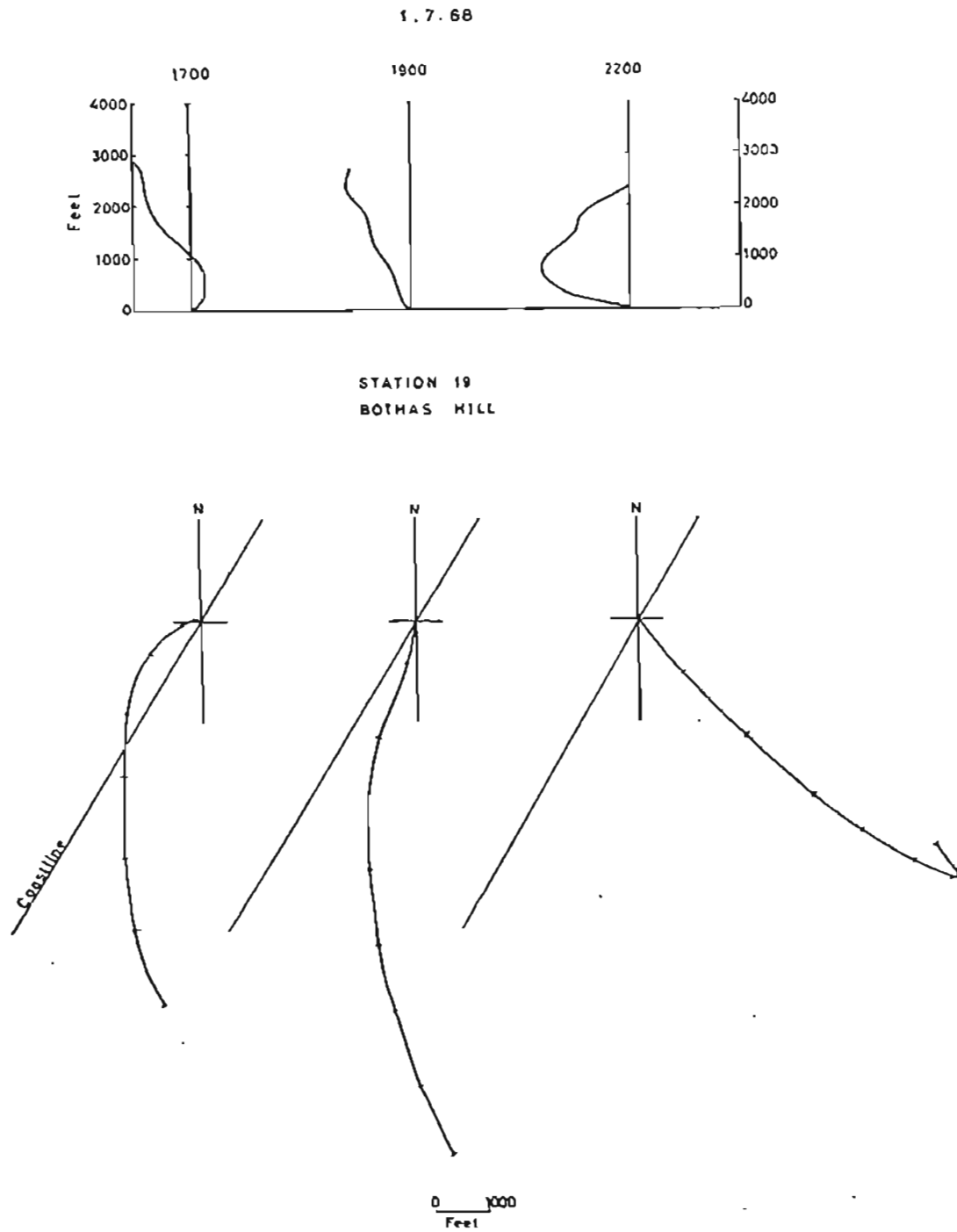


Fig. 4.1 : Profiles and horizontal components of balloon trajectories to show the onset of the land breeze on 1.7.68 at station 19, Bothas Hill

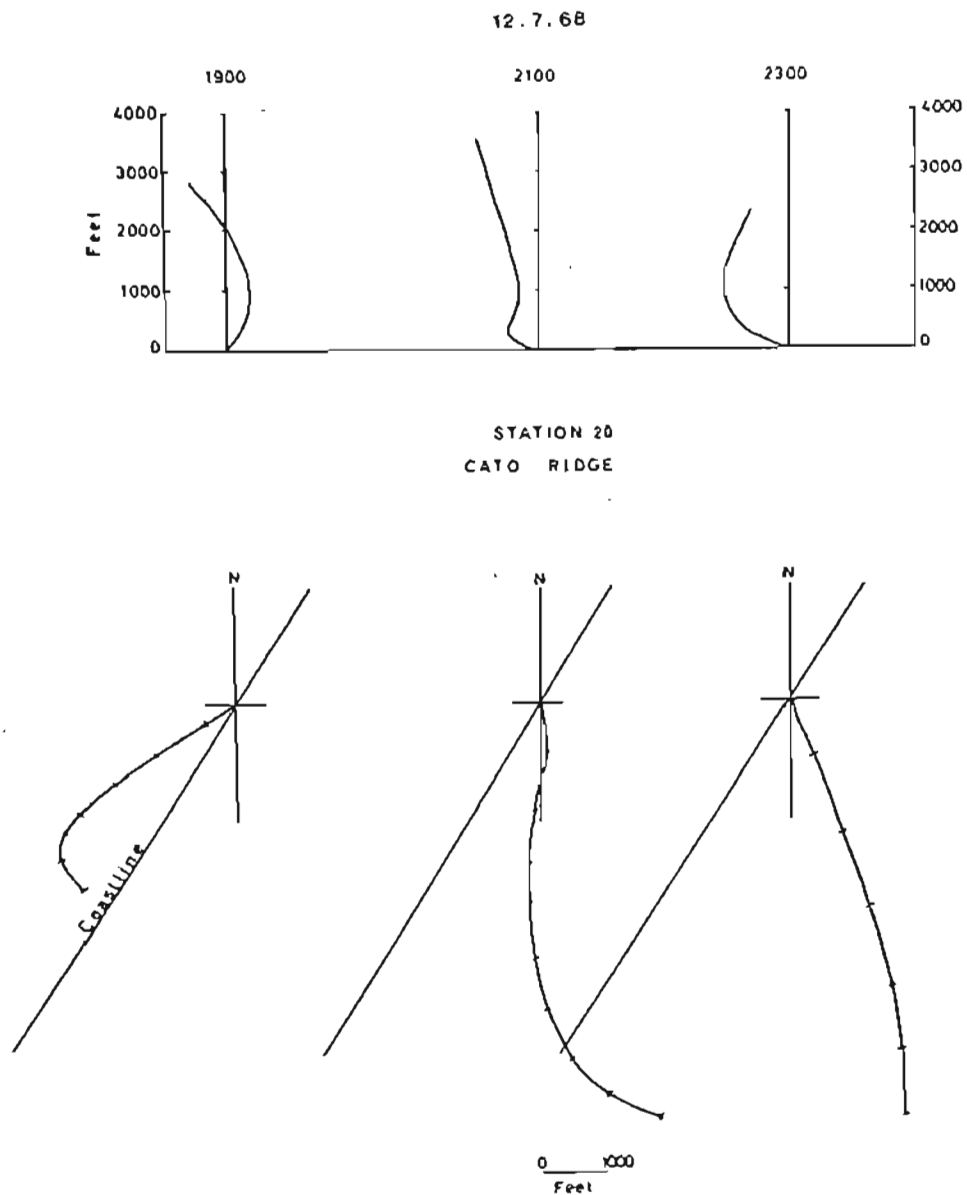


Fig. 4.2 : Profiles and horizontal components of balloon trajectories to show the onset of the land breeze on 12.7.68 at station 20, Cato Ridge

parameter.

#### 4.3 Frequency of occurrence

The land breeze on the Natal coast is here defined as a cool nocturnal wind with speeds not exceeding 4.5 m/sec at the surface and with an offshore direction which ranges from  $248^{\circ}$  to  $360^{\circ}$ . North-west is the most common direction (Figs. 4.1 and 4.2) but gradient winds frequently cause the land breeze to fluctuate within the above limits. The stipulation that wind speeds must not exceed 4.5 m/sec reduces the possibility of a north-westerly Berg wind being mistaken for a land breeze.

Weather Bureau measurements at Louis Botha airport (station 15) are unsuitable for frequency measurements of the land breeze since in fine weather thermal stability near the surface results in the suppression of turbulence so that wind speeds are usually less than the 1.3 m/sec recording threshold of the Dynes anemometer. Comparison of wind records from the Bluff signal station (station 14) and Louis Botha airport shown in Fig. 4.3 clearly indicate the infrequent penetration of the land breeze into the valley between the Bluff and Berea ridges. Wind data was, therefore, obtained from a Lamprecht anemometer which was set up at station 12 and maintained for 12 months from June 1967 to May 1968.

The frequency of land breezes per month is shown in Table 4.2. The highest frequencies occur in the winter months, the frequency in July 1967 exceeding that in January by a factor of 3.7. Land breeze occurrences numbered 197<sup>16</sup> over the 12 month period of which 38 per cent prevailed over the three winter months May, June and July and only 14 per cent over November, December and January. During the spring and autumn months 23 per cent prevailed in the former and 25 per cent in the latter season.

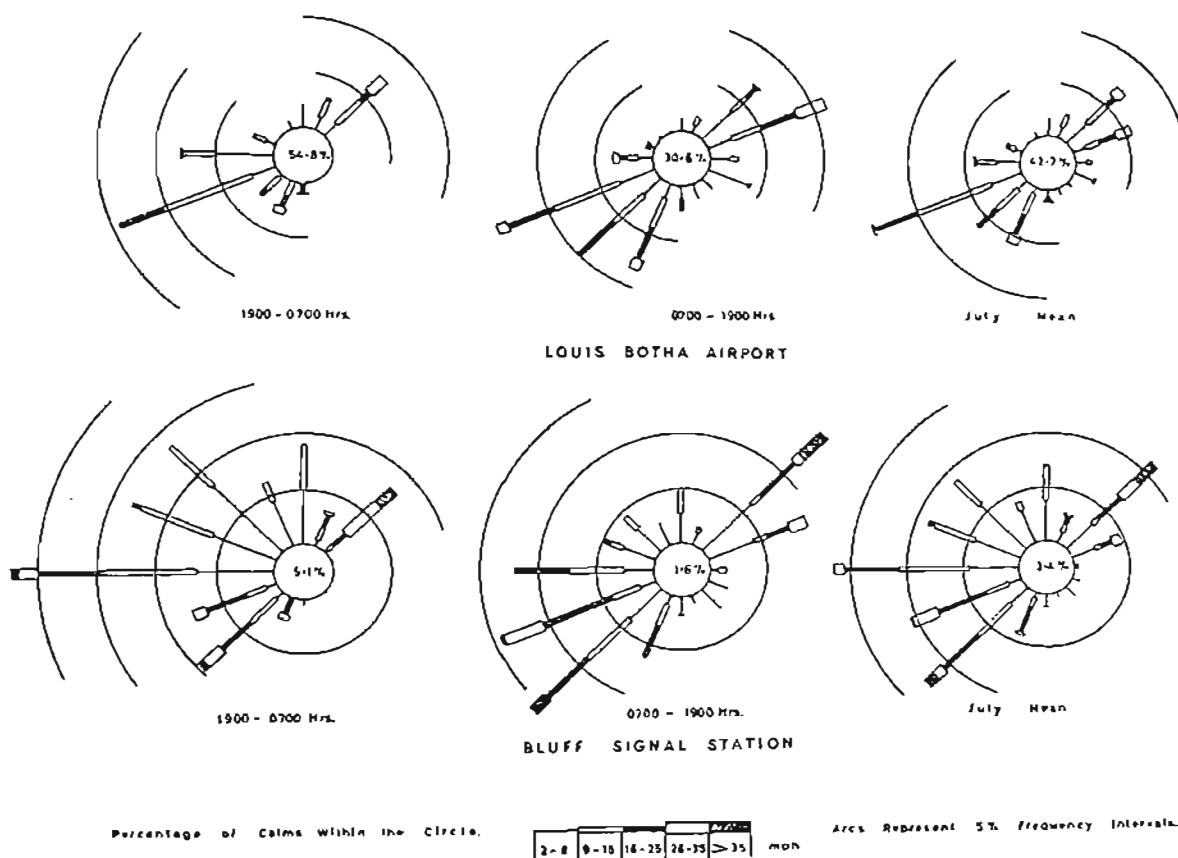


Fig. 4.3 : Wind roses for stations 14 and 15, July 1963



Table 4.2: Monthly frequencies (per cent) of land breezes recorded from June 1967 to May 1968 at station 12

J	J	A	S	O	N	D	J	F	M	A	M
80	84	48	37	55	33	32	23	32	55	73	74

#### 4.4 Depth

The stable stratification found over the land at night and the lack of thermally induced turbulence ensures that the land breeze system is shallow. Both Kimble (1946), who takes examples from the East Indies, and Wexler (1946) from the Black Sea, give observed depths of 500-600 ft. However, in a theoretical model developed by Schmidt (1947) for equatorial regions, the depth of the land breeze is placed at about 1,300 ft. Pre-dawn depth evaluations at Durban, carried out using the double theodolite method with balloons set to ascend at a slow rate, indicate that in fine weather the mean depth of the land breeze lies approximately midway between these two heights (Table 4.3).

Table 4.3: Examples of pre-dawn directions and depths (ft) of the land breeze over Durban

Date	Land Breeze Direction	Depth	Upper Wind Direction
27.6.63	WNW	700	SE
6.7.63	NW	950	NNE
7.7.63	W	500	SW
8.7.63	W	1000	NE
10.7.63	W	950	S
15.7.63	NW	850	N
16.7.63	W	700	SE
17.7.63	W	600	SE
MEAN		781	



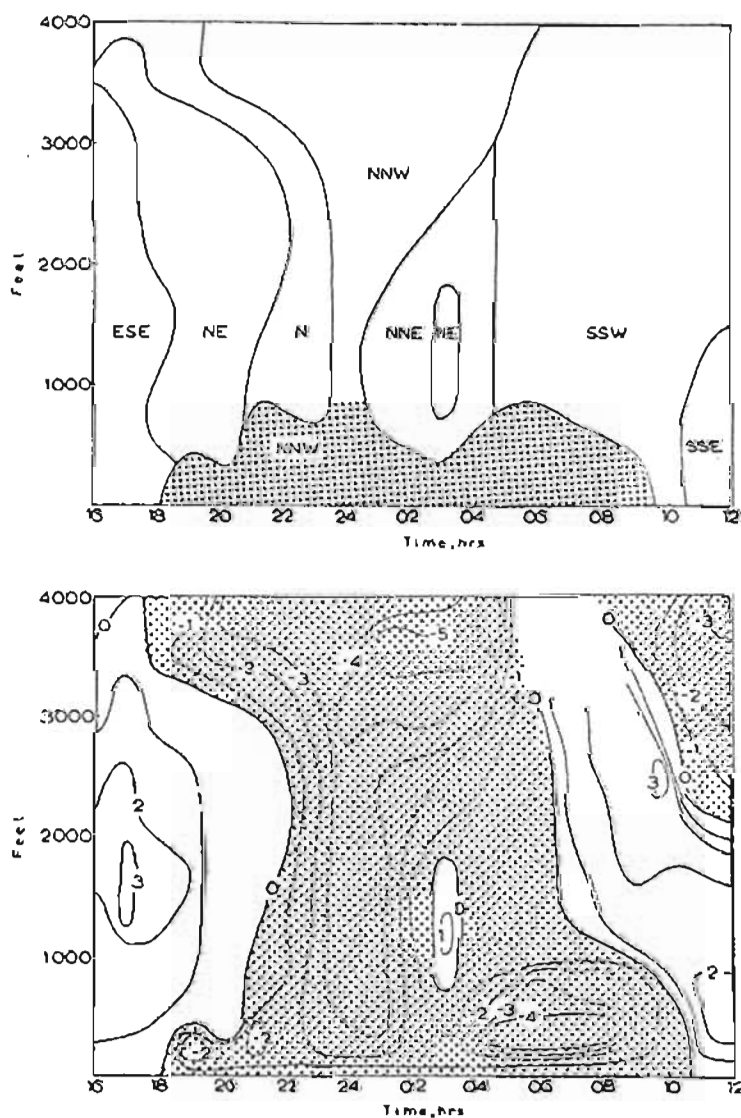


Fig. 4.4 : Time section to show depth (ft), velocities (m/sec) and direction characteristics of the land breeze and transition zone to the gradient wind. Observations on 4-5.7.67 from station 18

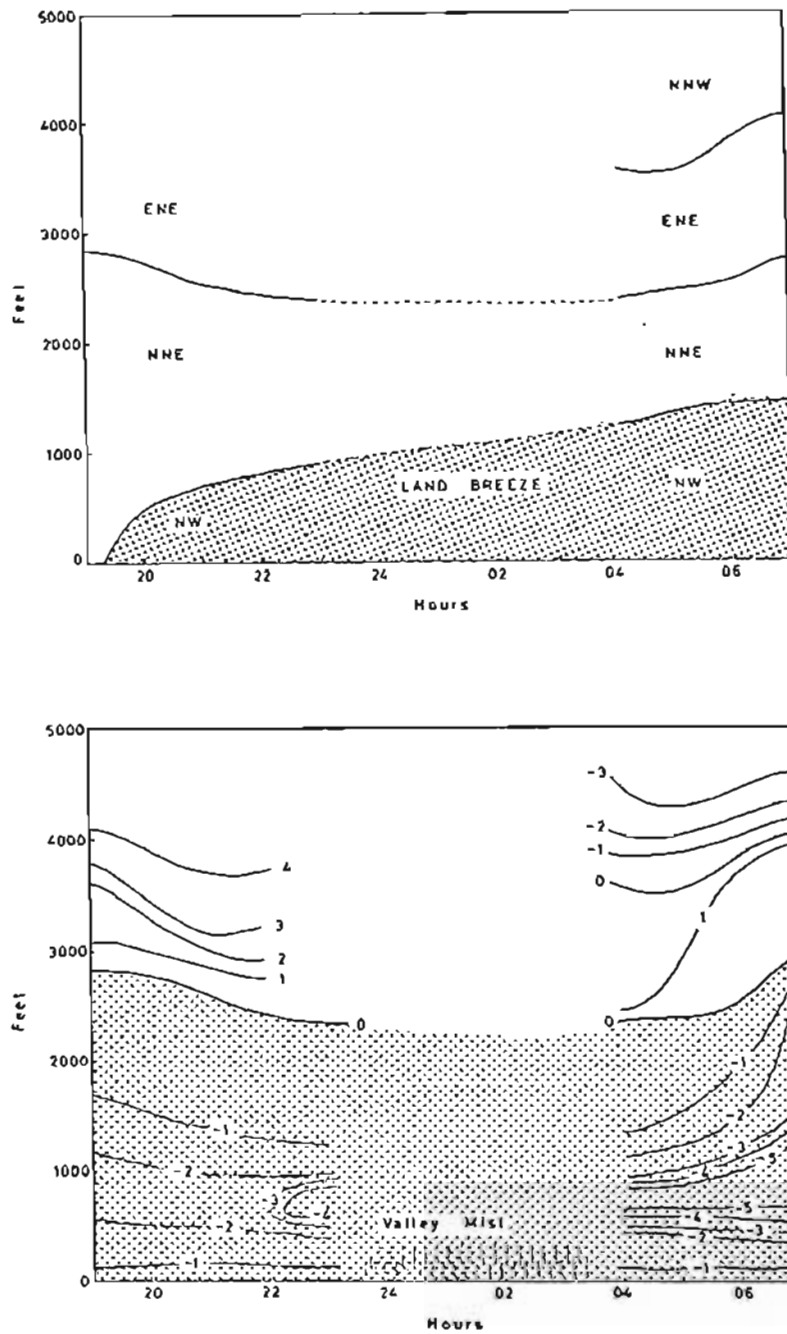
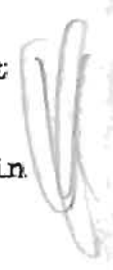


Fig. 4.5 : Time section to show variations in the depth of the land breeze. Observed on 15-16.7.68 from station 1

The land breeze does not always deepen at a constant rate and it is more commonly found that the upper level of this wind is periodically depressed by turbulence in the gradient wind above. For example, on 4-5 July 1967 (Fig. 4.4) the land breeze set in at the surface at station 18 soon after 1800 but onshore gradient winds persisted above 400 ft until 2030. Deepening of the land breeze was accompanied by initial backing of the upper gradient winds to north and north-north-west which later veered to north-north-east and north-east. With each change in gradient wind direction the upper level of the north-north-west land breeze was temporarily lowered. After being reduced to 350 ft at 0300 the depth of the north-north-west land breeze increased to 850 ft by 0600 and maximum offshore wind components were also recorded during this early morning period.

The ceiling of the land breeze is not always clearly defined by a direction shear and Fig. 4.5 shows that a transition zone between upper gradient winds and the land breeze may exist in which veering with height is accompanied by reduced offshore wind components. On other occasions a direction shear separating the land breeze from upper gradient winds is often found to be lacking altogether. For example, Fig. 4.6 shows north-west winds which extend from the surface to above 4,000 ft. On this occasion the onset of the land breeze was retarded by north-east gradient winds which blew strongly during the day in response to a steepening pressure gradient ahead of an approaching depression. Consequently the offshore wind backed slowly during the night to north-west by 0100. By 0500 the influence of the approaching low on the land breeze is shown by further backing to west-south-west at the surface and south-south-west by 0830. In this case the upper north-west wind is probably a gradient wind blowing in response to the isobaric pattern about an approaching depression. However, Tyson (1966) has suggested that at night these winds may receive an added component due to a mountain-plain wind system. It is maintained that mountain winds originate in



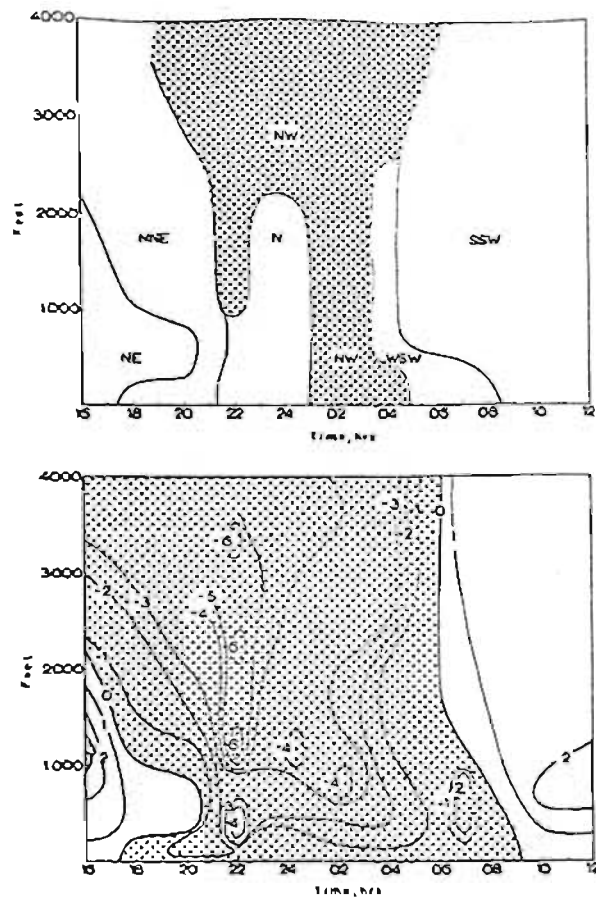


Fig. 4.6 : Time section to show lack of direction shear separating the land breeze from upper winds. Observed on 26-27.7.67 from station 18

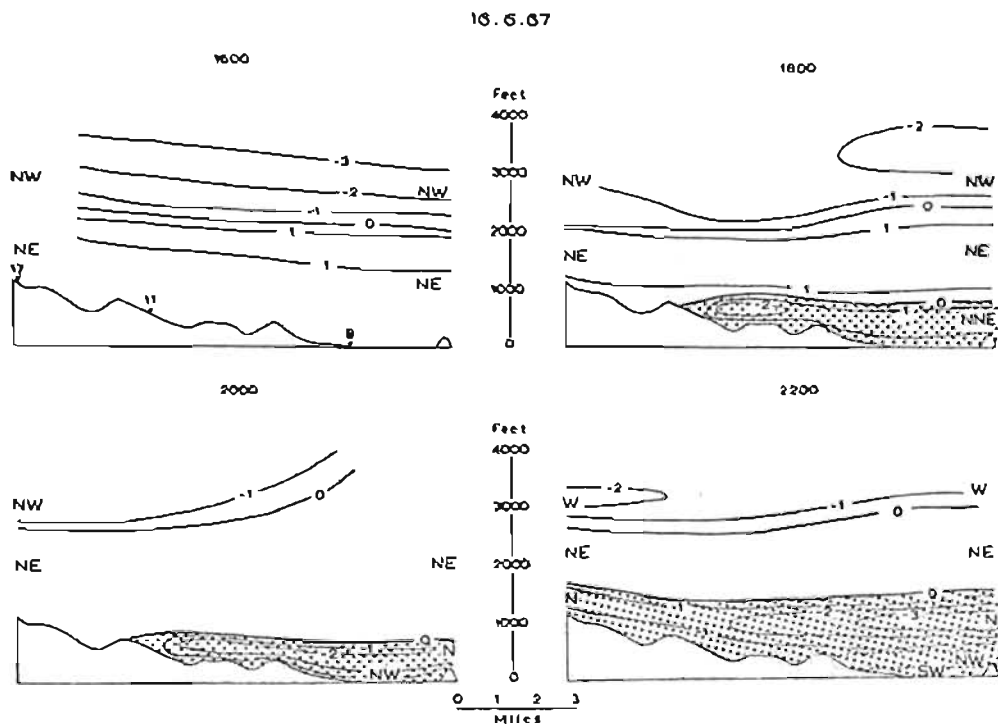


Fig. 4.7 : Section to show the inland migration of the land breeze on 16.6.67. Velocity isopleths in m/sec

deeply incised Drakensberg valleys by the combination of drainage winds in individual valleys which deepen to above ridge level. The integration of these local mountain winds with a regional mountain to plain circulation takes place in response to the development of a pressure gradient between the mountain and coastal areas. These winds may deepen to 3,000 ft and blow for 3-4 hours after sunrise in winter. If these winds can be recognised at the coast, the conceptual framework of the nocturnal circulation along the Natal coast would require revision.

#### 4.5 Land breeze and mountain-plain wind interaction

Tyson (1966) has recognised mountain-plain winds at recording stations situated between Cato Ridge and the Drakensberg and suggests that these winds penetrate to the coast as a regional offshore wind. The lack of published literature concerning the nature and characteristics of the land breeze on the Natal coast made this a justifiable conclusion at the time. In addition his hypothesis was strengthened by the observation of a one hour lag between onset times of the mountain-plain wind at Cato Ridge which is situated 27 miles inland and the land breeze at the coast.

Observations in the coastal area during the course of this study show that in the early hours of the night the mountain-plain wind cannot be mistaken for the land breeze. Simultaneous wind measurements at 3 and at times 4 recording stations aligned normal to the coast, show beyond reasonable doubt that the land breeze circulation is initially independent of the mountain-plain wind. A typical example shown in Fig. 4.7 indicates that an offshore component of air movement replaced onshore north-east winds between 1600-1800 on 16 June 1967 and that these winds had backed to north-west by 2000. By 2200 the height of zero wind component had deepened and northerly winds with an offshore component extended further inland.

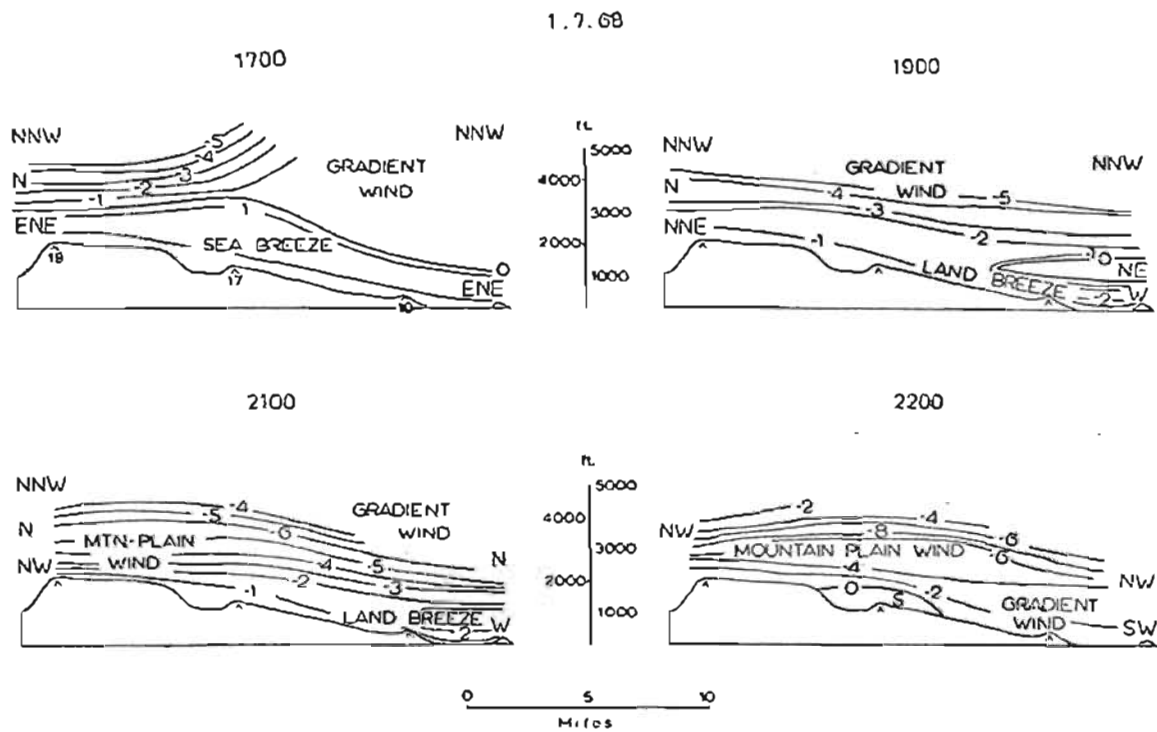


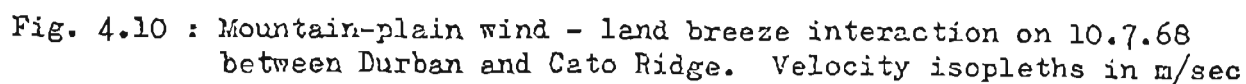
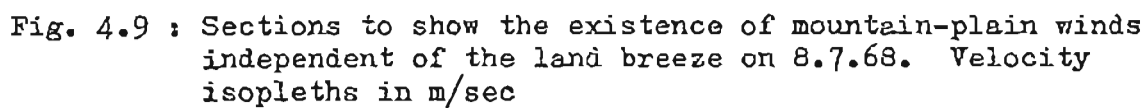
Fig. 4.8 : Land breeze - mountain-plain wind interaction on 1.7.68 in the Durban area. Velocity isopleths in m/sec

The problem of classifying the northerly wind is here apparent and two possible explanations may be advanced:

- (a) That it represents a transitional zone between a north-west land breeze and a north-east gradient wind above.
- (b) That it is a mountain-plain wind.

In order to achieve greater understanding of the interaction between the land breeze and mountain-plain wind, observation stations were located further inland than in the previous example. Once again the initial independence of the land breeze was established and Fig. 4.8 shows the replacement of an east-north-east sea breeze by a westerly land breeze over the coast and inland to station 17 by 1900 on 1 July 1968. Although wind components were offshore at station 19, the north-north-east wind direction suggests that no mountain-plain wind had as yet reached this point. Between 1900 and 2100, however, cold air draining down the Mgeni valley deepened until it ultimately extended to the level of the Kloof-Hillcrest plateau region. By 2100 the north-west mountain wind had enveloped the plateau area, deepened to 340 ft, and merged with the land breeze. Similar results were obtained by Tyson (1966) who found that the overflow of a mountain wind onto the Cato Ridge plateau was accompanied by a temperature drop at the surface and intensification and deepening of the nocturnal inversion. Although winds recorded at station 19 were unaccompanied by lapse rate measurements, the mountain-plain wind is distinguished from upper gradient winds by a direction shear between north-west and northerly winds at 2100. By 2200 an approaching low had suppressed the land breeze near the coast but the mountain-plain wind with maximum component velocities at about 2,500 ft prevailed above low-level south-westerly winds.

On occasions when north-east or north-north-east gradient





winds over the coast are strong, the land breeze is subdued and the mountain-plain wind does not reach the coast as a recognisable circulation. For instance on 8 July 1968 onshore gradient winds persisted until 2100 at the coast despite the appearance over the Kloof-Hillcrest plateau of a shallow north-west mountain-plain wind (Fig. 4.9). By 2200 this circulation had not advanced seaward and the cool north-west air current was entrained into the stronger north-north-east gradient wind instead.

The existence of a mountain-plain wind over the Kloof-Hillcrest plateau is explained by the deepening during the night of the stream of cold air drainage in the Mgeni River valley until this air is able to overflow along the Hillcrest scarp region and ultimately envelope the plateau. It has been mentioned that Tyson (1966) has observed a similar characteristic at Cato Ridge but it is interesting to note that the rate of deepening and, therefore, the time of overflow at Cato Ridge (station 20) and Botha's Hill (station 19) varies. Fig. 4.10 shows that on 10 July 1968 the mountain-plain wind set in at Cato Ridge at 2100 while winds at Botha's Hill were still approximately parallel to the coast, i.e. north-north-east. On 12 July 1968, however, the mountain-plain wind had appeared over the Kloof-Hillcrest plateau by 2000 and only became recognisable at Cato Ridge by 2300 (Fig. 4.11).

Deepening of mountain-plain winds above plateau level may lead to coalescence of these winds with the land breeze and ultimately the development of a regional mountain wind system which extends to the coast. It becomes difficult at this point to ascertain the degree to which the land breeze retains its identity. Mean profiles of the land breeze - mountain-plain wind calculated from simultaneous balloon releases from stations 10, 17 and 19 (Fig. 4.12) indicate a velocity maximum at 400 ft at station 10 which exceeds that at station 17 by a factor of 1.85. This suggests that low-level offshore wind speeds receive an added component over the coast from

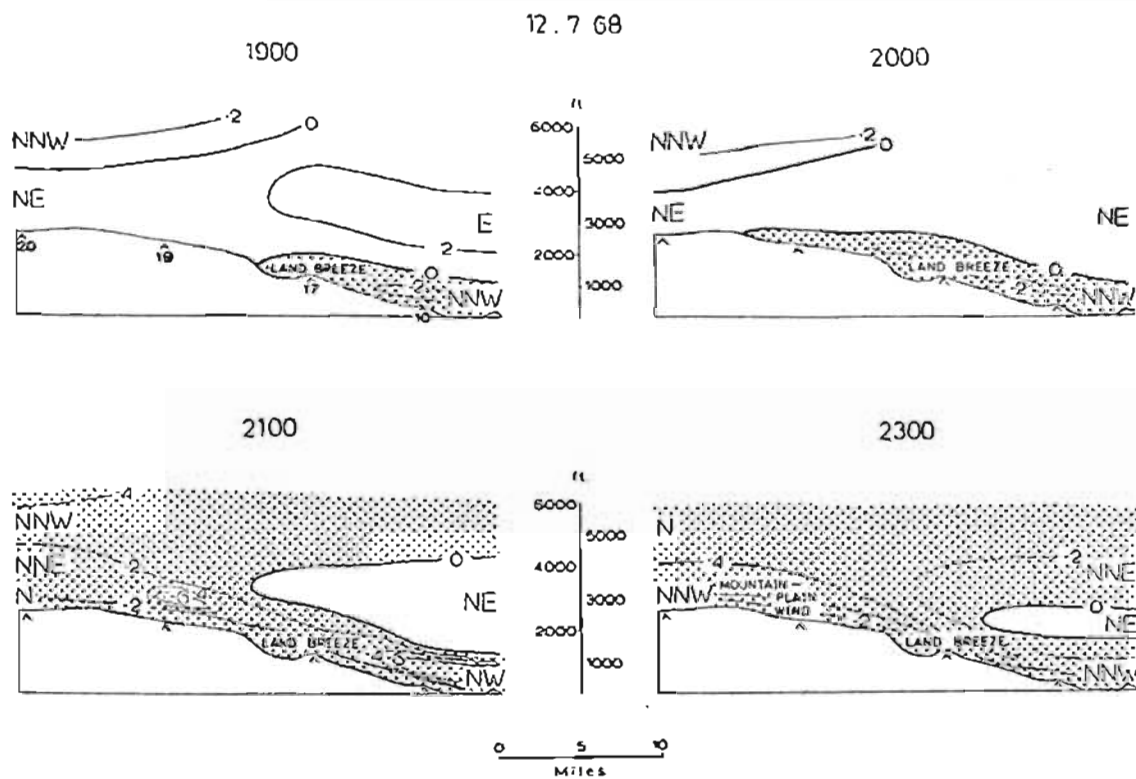


Fig. 4.11 : Mountain-plain wind - land breeze interaction on 12.7.68 between Durban and Cato Ridge. Velocity isopleths in m/sec

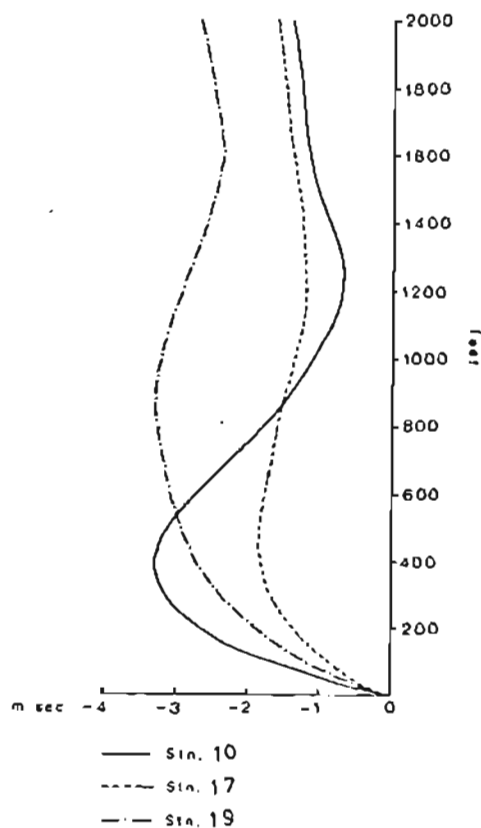


Fig. 4.12 : Mean profiles of the land breeze - mountain-plain wind for July 1968 at stations 10, 17, and 19

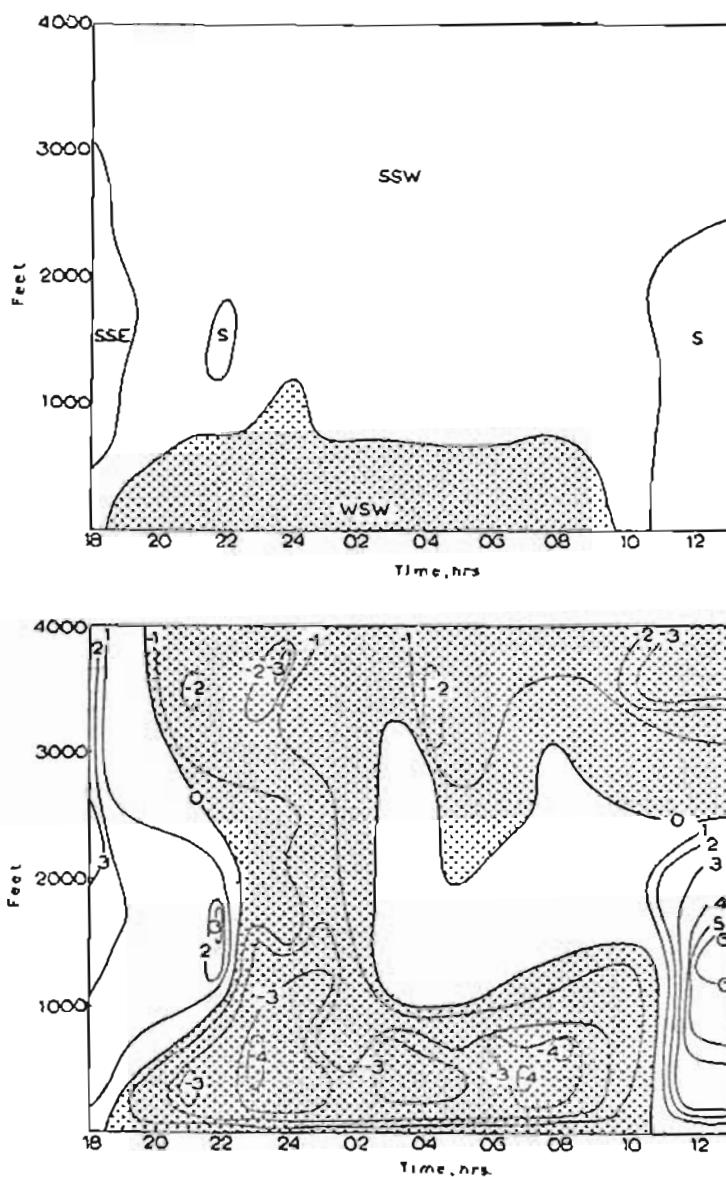


Fig. 4.13 : Time section to show depth (ft), velocity (m/sec) and direction characteristics of the land breeze under post-frontal conditions. Observations on 5-6.7.67 from station 18

the land breeze. Both profiles differ in form from that calculated for station 19, the maximum offshore component in this case lying at 900 ft. It is conceivable, therefore, that instead of immediate coalescence of the two wind systems, the mountain-plain wind overtops the land breeze at the coast.

#### 4.6 The effect of gradient winds

Although the usually strong and turbulent south-west winds that follow at the rear of a depression may suppress the development of a vigorous land breeze circulation, a weak diurnal variation of wind direction is usually perceptible. Fig. 4.13 shows that on 5-6 July 1967 a west-south-west land breeze was able to prevail throughout the night despite the presence of upper south-south-west winds. Where gradient winds parallel the coastline with low pressure at sea, seaward frictional inflow may cause low-level offshore winds. Cool land air may thus be advected seawards to strengthen the horizontal temperature gradient between land and sea and, therefore, the pressure gradient in the surface layers. This process probably contributed an added component to the weak land breeze and on this occasion strengthened the offshore wind below 1,000 ft.

An increase in gradient wind speeds may partially or totally suppress the land breeze. For instance during the early part of the night of 3-4 July 1967 a west-south-west land breeze prevailed beneath south-south-west gradient winds (Fig. 4.14). At 0200 the gradient wind speed increased and veered to south-west and it is doubtful whether the re-instated offshore wind was due to a reinvigorated land breeze. The weak offshore wind component, the excessive height of zero wind component under these conditions and the relatively unchanged wind direction near the ground suggest that some other mechanism, possibly frictional inflow towards lower pressure at sea, was responsible for the offshore component of air movement.

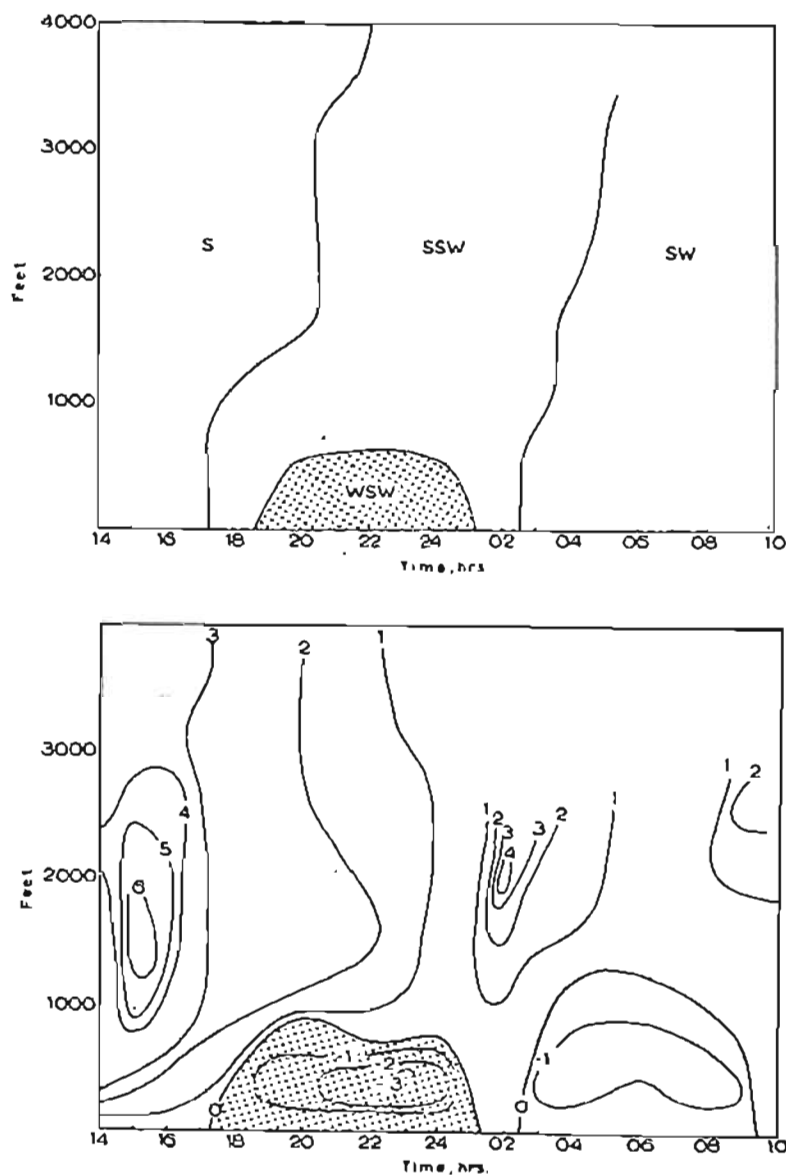


Fig. 4.14 : Time section to show depth (ft), velocities (m/sec) and direction characteristics of the land breeze under post-frontal conditions. Observations on 3-4.7.67 from station 18

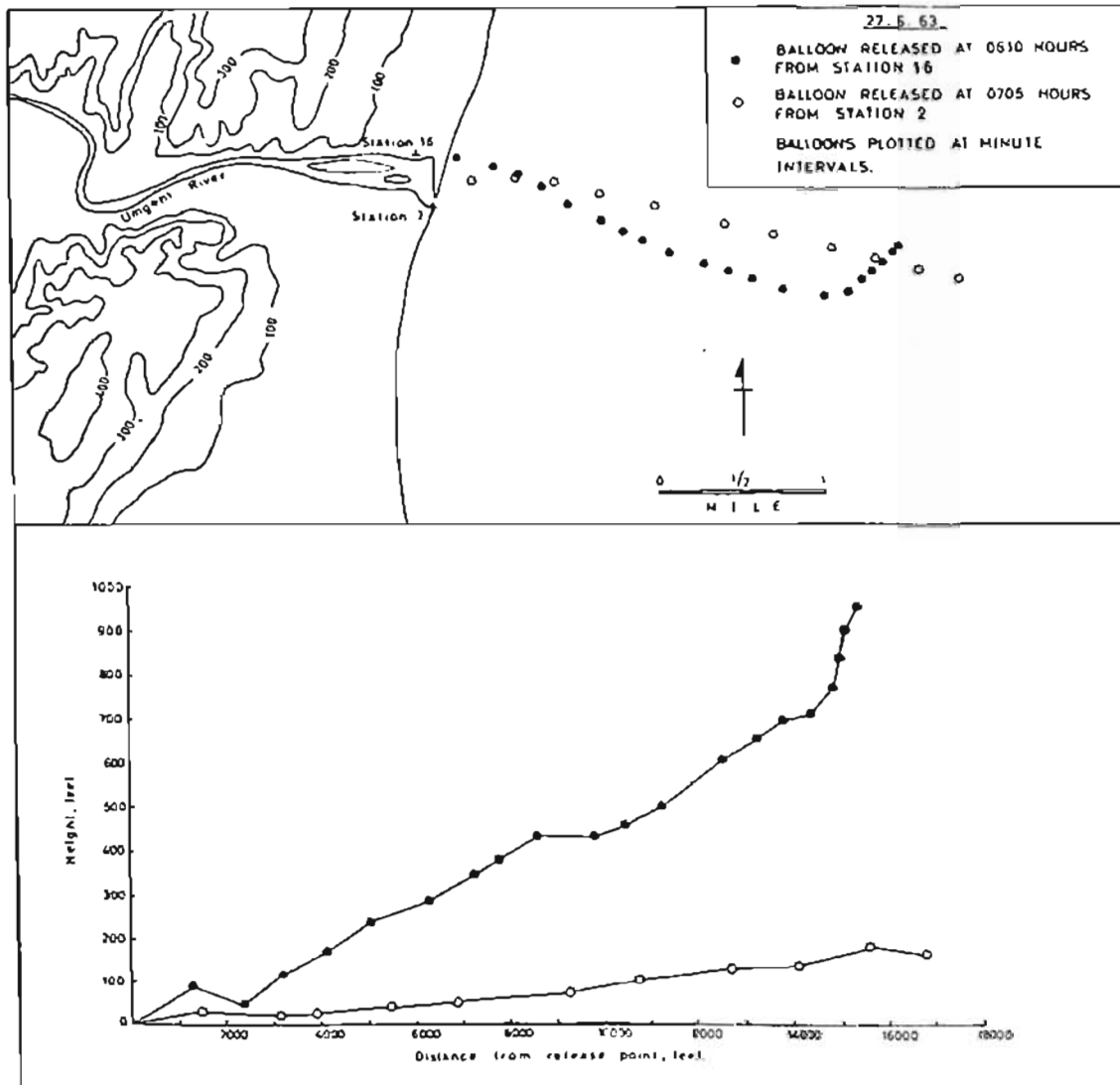


Fig. 4.15 : Seaward penetration of the land breeze under fine weather conditions. Balloon releases on 27.6.63 from stations 16 and 2

The layer of seaward moving land-cooled air is made up of drainage winds in river valleys and the land breeze strengthened by a mountain-plain wind above. In fine weather the discontinuity between the often smoke-laden land air and the cleaner sea air is clearly visible. Flights through this land-sea air front at 100 ft above sea level are invariably accompanied by turbulence. From aircraft it is also evident that cool land air penetrates an estimated 5 miles seawards although the overall drift of cool air may be locally strengthened by air drainage from river valleys. Fig. 4.15 shows westerly air movement near the mouth of the Mgeni River on 27 June 1963 veering to west-north-west further seaward. Winds draining from the Mgeni valley provided the offshore wind below 200 ft in this region. This is shown by the mean velocity of 7.5 m/sec in this layer which is in contrast to 4.5 m/sec for the mean velocity of the land breeze above 200 ft. Low south-west gradient wind speeds of the order of 1.9 m/sec were the result of a weak pressure gradient.

When wind directions over the sea are north-north-east to north-east, the land air over the sea is moved southwards down the coast. Since the air layer retains its stable characteristics until well after sunrise, air movement within this layer is relatively non-turbulent.

\* \* \* \* \*

The seaward drift of a deep layer of land-cooled air provides an ideal vehicle for the transportation of atmospheric pollution and this is visually evident on any fine winter morning. The tendency for some of this pollution to be returned to the land by weak sea breezes has already been noted. However, because of the

remarkable fetch and immense volume of air transported by the land breeze - mountain-plain wind, the potential for a pollution problem over the coast with regionally based rather than local pollution sources must be emphasised.

As with the sea breeze, the land breeze produces certain climatic phenomena. In a later chapter the diurnal variation of rainfall at Durban is examined and an attempt is made to explain the part played by the land breeze in contributing towards the high frequency of occurrence of low intensity rainfall.



## CHAPTER 5

### DRAINAGE WINDS

#### 5.1 Theoretical models

Local thermally-induced air circulations are a common feature in regions of dissected terrain and can be separated into slope and valley wind systems. Both winds are best developed under fine weather conditions when heating or cooling is at a maximum.

During periods of nocturnal cooling, slope winds are directed downslope. Radiational cooling produces a steep horizontal temperature gradient between the air near the slope surface and the air at the same level over the valley. The effect of the downslope bending of isotherms is to cause pressure surfaces to bend upslope and the air layer near the surface soon becomes strongly baroclinic. A slope wind is generated by a solenoidal circulation in this layer causing internal heat energy to be converted to kinetic energy. Tyson (1967b) points out that the energy exchange mechanism in the case of downslope winds is complicated by the conversion of geopotential energy (the product of gravitational attraction and height) into kinetic energy as well. Thus downslope winds have two components, one thermal and one gravitational.

Various attempts have been made to erect theoretical models of slope wind behaviour. Wagner (1938) recognised a binary set of circulation cells over a valley in which downslope winds at night occur in association with a vertical current in the centre of the valley. The form and extent of slope winds have also been examined by Defant (1951) and Prandtl (1942) who assume heat flow normal to a uniform slope over which a horizontal pressure gradient exists due to horizontal temperature differences. The profile advanced by

Prandtl (1942) is of the form

$$u = U_m \frac{\exp(\pi/4)}{\sin(\pi/4)} \sin(z\pi/H) \exp \{ - (z\pi/H) \} \quad (5.1)$$

where  $U_m$  is the observed wind speed maximum,  $H$  is the depth of the air stream and  $z$  is height.

A pressure gradient necessary to generate valley winds is consequent upon temperature variations in the valley. Wagner (1938) noted that the diurnal temperature variation in selected Alpine valleys up to the height of the ridge crest was more than twice as large as variations within a similar layer over the plain. This is largely due to:

- (1) The warming of a smaller mass of air within a valley to that over the plain by radiational heating over the same horizontal area and at the same altitude over the two localities. A V-shaped valley is estimated to contain about half the amount of air over the plain for the same area of insolation (Tyson, 1967a). Similarly the loss of heat by radiation at night is applied to a smaller air mass;
- (2) Slope winds add heated slope air to the valley through the circulation which descends over the valley centre. Thus the temperature in the centre of the valley continuously increases during the day and decreases at night when the circulation is reversed (Wagner, 1938).

The pressure gradient from valley to plain or vice versa thus produced is steepest near the surface and decreases with height to disappear near the ridge level.

The diurnal periodic fluctuation of topographically-induced winds has also been described by Defant (1951). This model requires that at night slope winds be initiated first followed by mountain winds and finally mountain-plain winds. Deflection of the slope winds occurs in a down-valley direction as these winds merge with the mountain wind which, constrained by the form of the valley, flows parallel to the axis of the valley. Down-valley winds fill the entire valley and slowly deepen to ridge level with a consequent reduction of slope wind effectiveness. The model, therefore, requires two wind systems to maintain conditions in the valley; one consists of flow parallel to the valley axis produced by pressure gradient forces, the other is the slope wind with flows over the ridge produced by thermal heating and cooling.

Gleeson (1953) has examined the periodic valley wind as a function of time and elevation in terms of the diurnal temperature variations, valley floor slope, horizontal pressure gradient and Coriolis force. Only the longitudinal profile of the valley was considered in the circulation equations and the heating and cooling influences of the valley sides were ignored. The maximum wind speed of the valley wind occurs at some height above the surface. Above this height velocities decrease as the differential heating and cooling of the air by the ground becomes less effective. Gleeson also suggests that a more realistic representation of the valley wind is possible when the effect of the Coriolis force is considered than when it is neglected.

The equations of motion for a compressible fluid cooled at the bottom by contact with a radiating surface of uniform slope and large extent have been derived by Feagle (1950). This model is concerned with mean flow within a cooled layer rather than with the form of wind profiles. The mean drainage velocity is expressed as a function of friction, slope and the mean rate of cooling near the surface. According to his dynamic model, so called because of inclusion of the

inertia term in the model, Feagle predicts that the mean velocity in the layer undergoing cooling,

- (a) is proportional to the net outgoing radiation,
- (b) is inversely proportional to the thickness of the layer which undergoes cooling,
- (c) begins by varying periodically and gradually becomes constant,
- (d) is inversely proportional to the slope of the ground.

The lack of a comprehensive model of topographically-induced winds as functions of all three space coordinates and velocity components of time, pressure, temperature and density, spurred Thyer and Buettner (1962) to make a numerical study of valley winds. The model thus produced shows a system of slope winds, valley winds and anti-valley winds, updrafts over the ridge and downdrafts over the valley.

Recognition of drainage winds on the Natal coast is complicated by the overriding influence of the land breeze. Since most river valleys are aligned normal to the coast line, and, therefore, parallel the land breeze direction, it is often difficult to distinguish between these two circulations. Both winds occur under conditions of thermal stability so that the vertical exchange of momentum is suppressed and drainage wind velocities of the order 2-3 m/sec may not produce an easily recognisable wind shear at the land breeze - drainage wind boundary should it exist. Nevertheless, observed vertical profiles suggest that in the lower layers at least, drainage winds may be independent of the land breeze.

## 5.2 Onset

Drainage winds in river valleys on the Natal coast frequently set in before the land breeze. This is primarily due to more rapid cooling in valleys than at ridge-top level since the loss of heat by radiation is applied to a smaller air mass than that over a horizontal surface. The drainage wind sets in once the pressure gradient in the valley reverses from up-valley to down-valley. In the example shown in Fig. 5.1 westerly down-valley flow at station 4 commenced 90 minutes before the south-westerly gradient wind was replaced by a westerly land breeze. The onset is normally sudden and occurs as a local front of cold air advances down-valley. The passage of a front is a typical characteristic of these winds and Tyson (1967b), working in Natal, has recorded temperature discontinuities of the order  $3.0 - 5.5^{\circ}\text{C}$ . In contrast the temperature drop at the mouth of the Umbilo and Mgeni River valleys is seldom more than  $2^{\circ}\text{C}$ . The small temperature discontinuity produced by the down-valley advection of cold air at the coast is due to the existence of a warm ocean which does not cool during the night (as does a plain over land). Consequently valley air which is heated above sea temperatures during the day does not cool appreciably before an offshore temperature gradient is established.

## 5.3 Damming and channelling

Cold air which issues from the mouth of the Umbilo and Mhlathuzana River valleys moves across the alluvial flats at the head of Natal Bay to dam against the western flank of the Bluff ridge. However, stagnation of this air does not take place. Instead westerly air drainage at the valley mouths and over the alluvial flats at the head of the bay becomes south-west and south-south-west as the cold air is channelled north-east between the Bluff and Berea ridges (Fig. 5.2). The lack of a significant topographic gradient in this

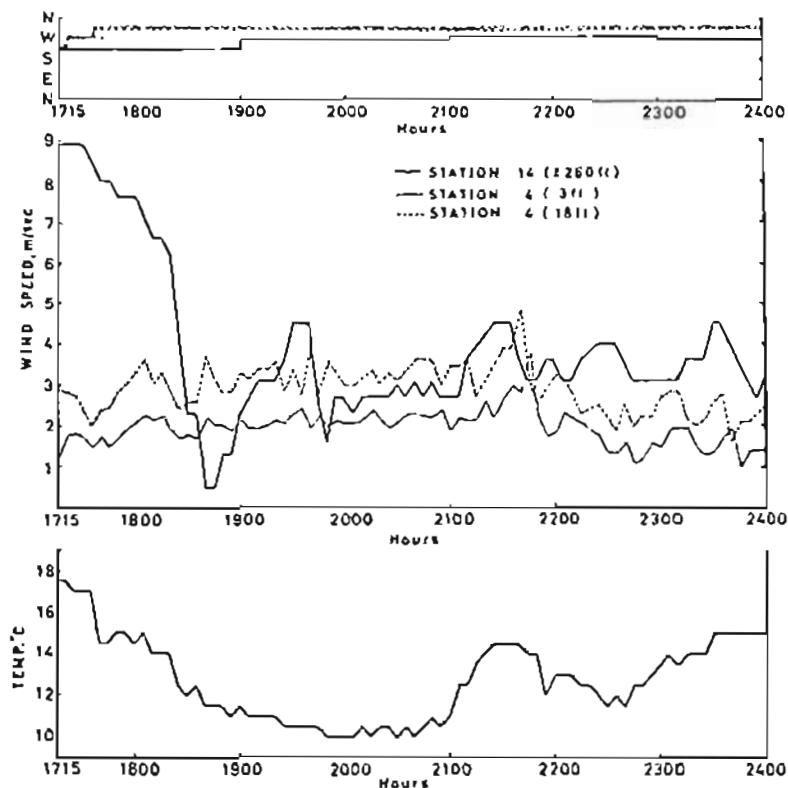


Fig. 5.1 : Comparison between wind speeds (m/sec) and direction on 7.7.64 at stations 4 and 14. Temperatures ( $^{\circ}\text{C}$ ) recorded at station 4

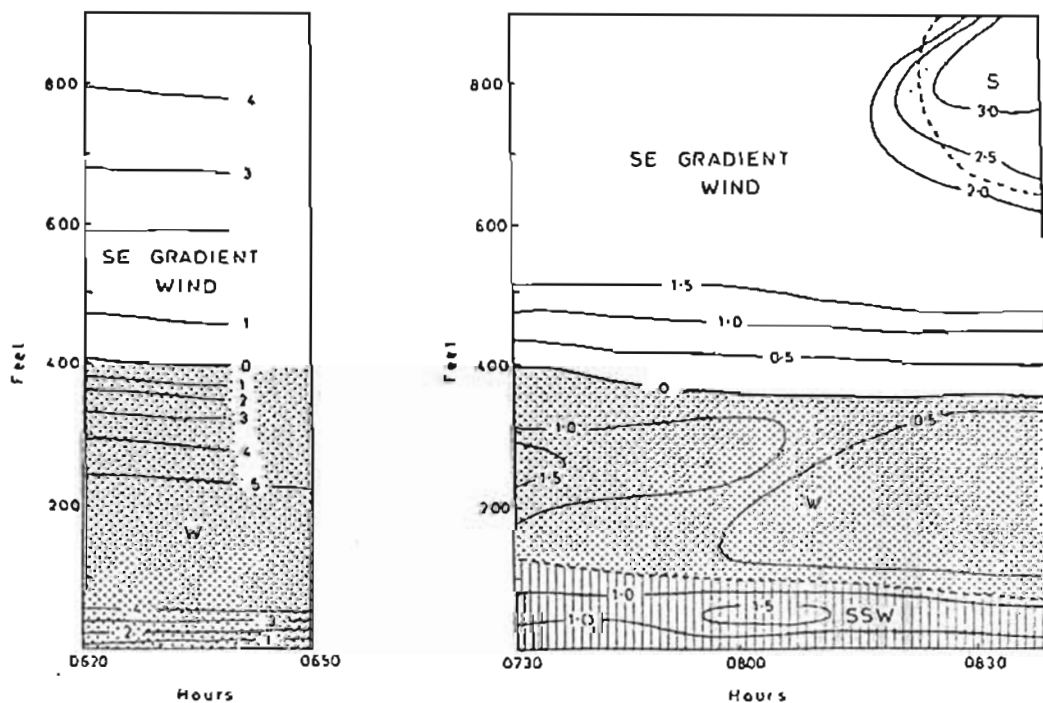


Fig. 5.2 : Time sections to show drainage winds on 17.7.63 at stations 4 and 8. Wind speed isotachs in m/sec; pecked lines indicate transitional boundaries

area means that south-westerly air movement is partly in response to a pressure gradient set up between radiationally cooled alluvial flats which are cooled further and to a greater depth by drainage winds than the warmer air over Natal Bay and the city north of the bay<sup>1</sup>. Drainage wind velocities vary between 1 and 2 m/sec.

The south-west drainage wind only sets in after a build-up period over the alluvial flats at the head of the bay. A north-west land breeze may, therefore, persist at the surface north of the alluvial flats during the pre-onset period. Surface cooling over the alluvial flats must proceed until a temperature and, therefore, pressure gradient parallel to the ridges produces air motion which is large enough to replace the land breeze. The arrival of the drainage wind at 2030 at station 9 shown in Fig. 5.3 is a good estimate of the onset time at this point under clear weather conditions.

Further damming of cold air takes place against the obstacles presented by the multi-storied buildings which line the north-west flank of Natal Bay. Some cold air moves over the city but the main exist is via the narrow harbour mouth.

The volume of air transported by drainage winds in the Natal Bay is calculated by the product of the cross-sectional area between the ridges and the mean wind speed in the layer. By assuming that a section across the Natal Bay (A-B in Fig. 2.1) is the upper side of a

---

<sup>1</sup> Topographic channelling of cold near-surface air is not common only to Durban but has also been observed at Richards Bay where the topography is essentially similar to that at Durban (Fig. 5.4). Balloon releases from station 22 revealed near-surface north-east drainage winds which paralleled the 150-200 ft high sand dunes north of the lagoon mouth (Fig. 5.5). Although not recorded by balloon traverses, it is also likely that air drainage from the Mhlatuze River valley at the head of the lagoon would initiate south-west air movement parallel to the sand dunes south of the lagoon mouth.

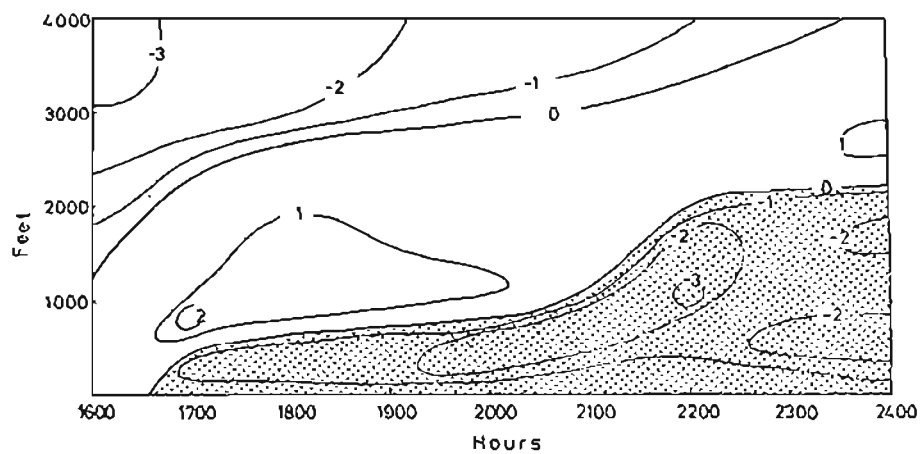
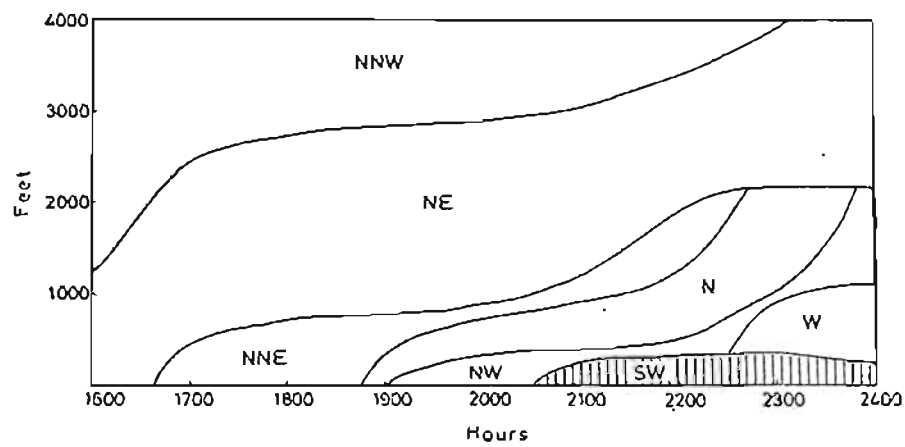


Fig. 5.3 : Time section to show the onset of south-west drainage winds at station 9. Velocity isopleths in m/sec



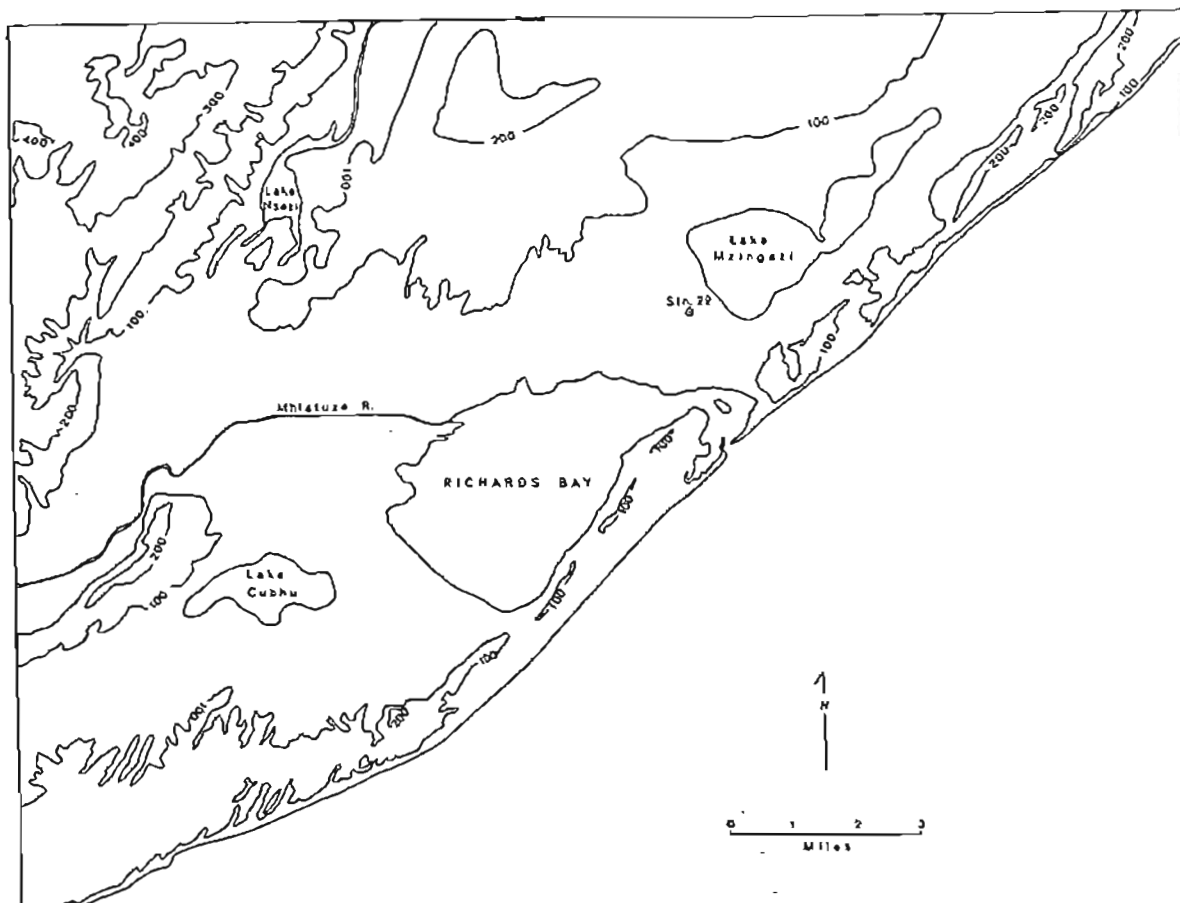


Fig. 5.4 : Relief and location map of the Richards Bay area

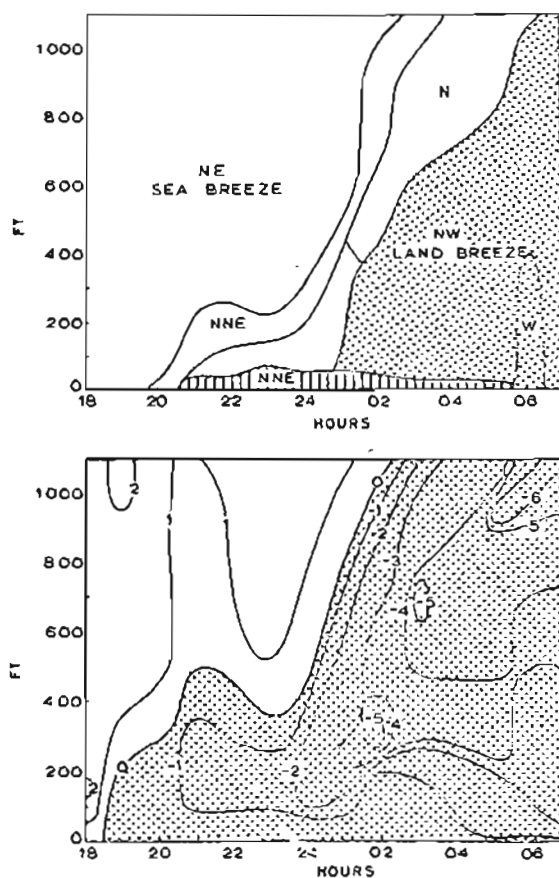


Fig. 5.5 : Time section to show depth (ft), velocity (m/sec) and direction characteristics of drainage winds recorded on 25-26.5.68 from station 22 at Richards Bay

trapezium, the area may be calculated by

$$\frac{(A + B) z}{2} \quad (5.2)$$

where A and B are parallel sides, in this case the valley base and a level above and z is the perpendicular distance between them, taken here as 200 ft. Changes in the volume of air with variations in mean wind speed are shown in Table 5.1.

Table 5.1: Volume ( $m^3$ ) of air transported by drainage winds of varying speed (m/sec) past the section in Fig. 2.1

$\bar{U}$	1.0	1.5	2.0
Vol	$3.3 \times 10^5$	$4.9 \times 10^5$	$6.6 \times 10^5$

The pattern of air movement described above remained basically unchanged on 10 out of 13 days during June-July 1963 and there is no reason to suppose that drainage winds do not occur nightly under fine weather conditions. On the 3 days during which this pattern did not emerge a strong gradient wind had overcome the local circulation.

#### 5.4 Depth

The depth of the drainage wind in the Natal Bay area is determined by a direction shear of  $70-100^\circ$  between the drainage wind and the land breeze above and during the winter of 1963 was found to be approximately 200 ft. Where no topographic barriers exist to divert drainage winds, such as at the mouth of the Mgeni River valley,

the depth of this wind is less easy to determine as drainage wind and land breeze directions are quasi-parallel.

Cold air which flows down the Mgeni River valley must pass through the narrow Springfield Gap through the Berea ridge. Schnelle (1956) has shown that where valleys narrow, air drainage is effectively impeded and damming occurs up-valley. That this also occurs in the Springfield flats is recognised by the tendency for near-surface air motion to stagnate. Fig. 5.6 shows that on 15-16 July 1968 at station 1, wind speeds 6 ft above the surface decreased gradually throughout the night. In similar calm, clear weather conditions on 9-10 July 1969, drainage wind speeds at station 2, beyond the Springfield Gap, were found to increase slightly with time. Gradually strengthening wind velocities, east of the Springfield Gap may be in proportion to deepening of the cold air layer in the Springfield flats and to a strengthening temperature and, therefore, pressure gradient between this area and the sea.

Air movement and depth characteristics of the drainage wind in the Mgeni River valley are shown in Fig. 5.7. By 0200 drainage winds were well-established and little variation in the height of the system can be recognised. The maximum offshore movement occurred at a height approximately the depth of the Mgeni River valley at the Springfield Gap and the profile of the drainage wind approximates to that predicted by Prandtl (1942) for a local wind of purely thermodynamic origin (Fig. 5.8). Although Tang (1960) maintains that the Prandtl model does not hold for slopes of less than  $11^{\circ}$  it appears that the model is valid for gentler slopes in the Natal Coast area under certain weather conditions. In addition Tyson (1967b) has shown that mountain winds in the Natal midlands which blow over slopes less than  $11^{\circ}$  also conform to the model.

The drainage wind does not normally show a finite upper

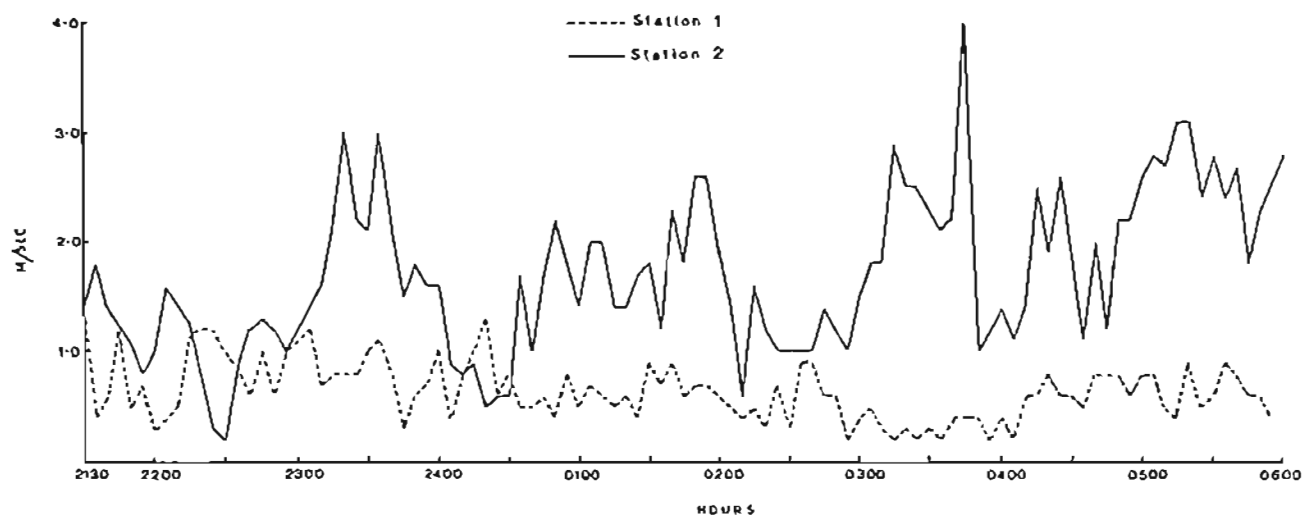


Fig. 5.6 : Comparison of drainage wind speeds at 6 ft (m/sec) measured on 15-16.7.68 at station 1 and 9-10.7.69 at station 2

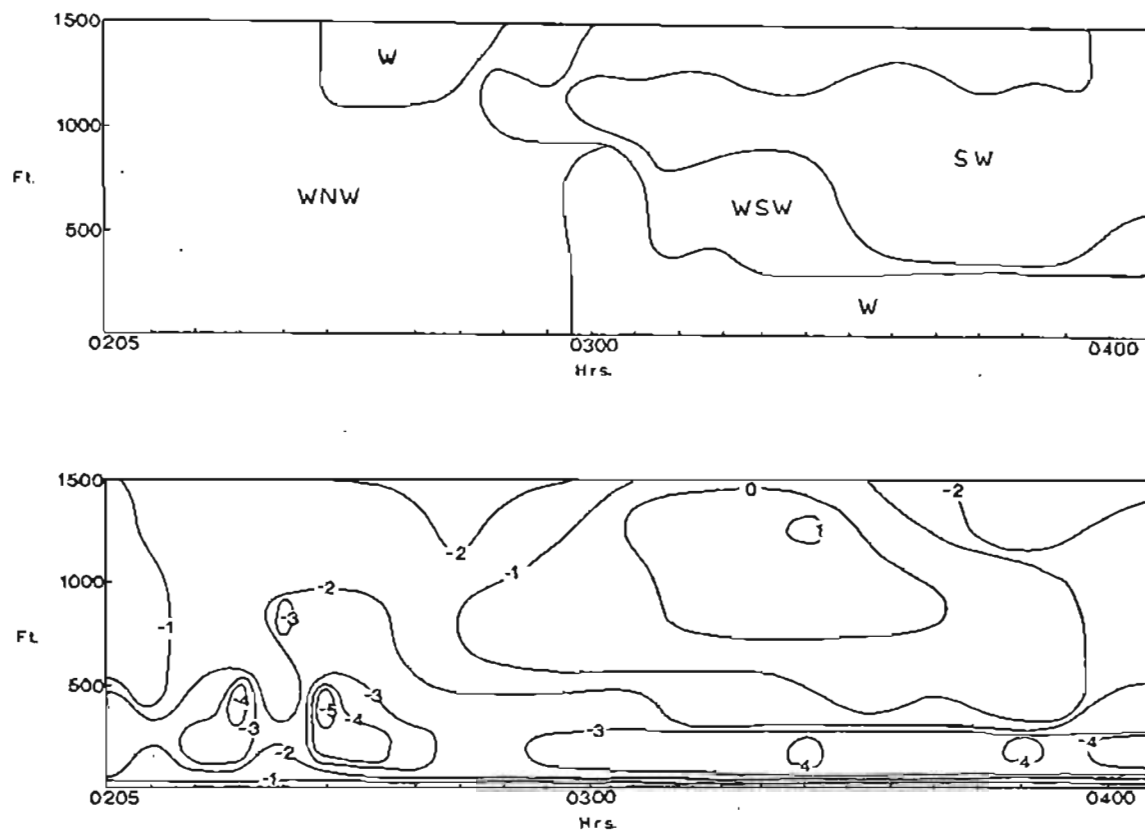


Fig. 5.7 : Time section to show depth (ft), velocity (m/sec) and direction characteristics of the drainage wind on 11.7.69 in the Mgeni River valley at station 2

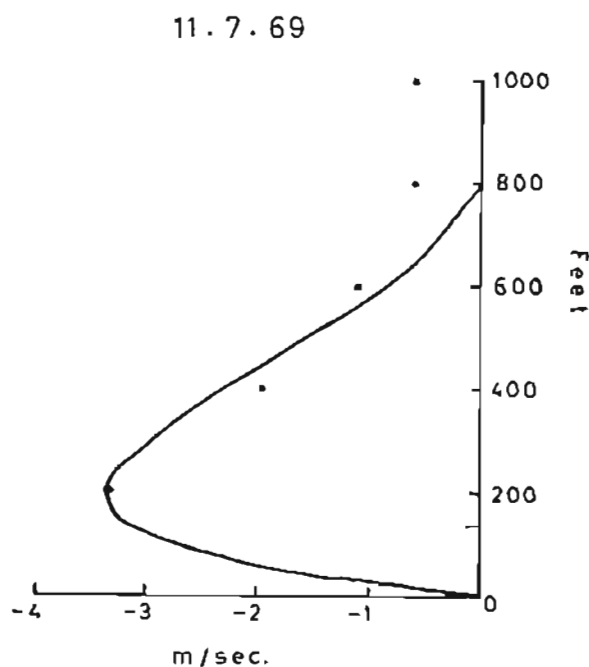


Fig. 5.8 : Comparison of the mean offshore wind component profile in the drainage wind-land breeze (dots) with the Prandtl profile (solid line), 11.7.69

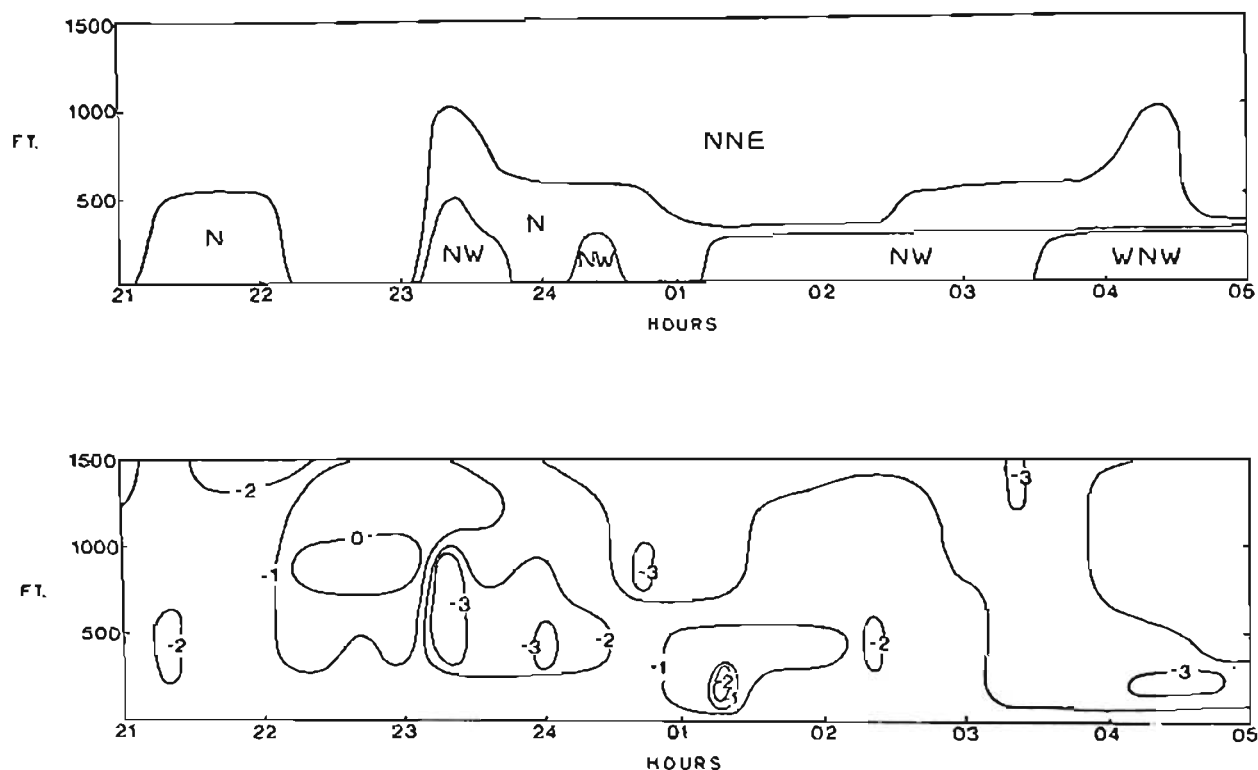


Fig. 5.9 : Time section to show depth (ft), velocity (m/sec) and direction characteristics of the drainage wind in the Mgeni River valley with upper north-north-east gradient winds. Observations on 9-10.7.69 from station 2

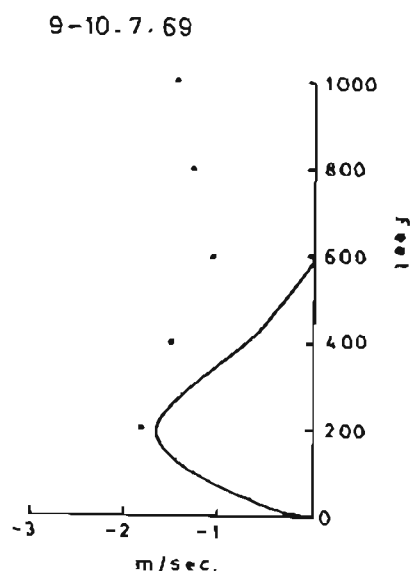


Fig. 5.10 : Comparison of the mean offshore wind component profile in the drainage wind (dots) with the Prandtl profile (solid line) 9-10.7.69

limit due to the presence of offshore land breezes above. However, if  $H$  is taken as the height of the mean minimum offshore wind component on this occasion, and  $h$  is the height of the maximum offshore wind component,  $h/H = 0.25$ . This is in contrast to the mean ratio of 0.5 computed by Davidson (1961) in Vermont valleys under clear sky conditions but is in closer agreement with measurements by Tyson (1967b) in Pietermaritzburg, Natal.

Although a low-level velocity maximum is a common feature of air movement with an offshore component in the Mgeni River valley, a finite upper limit to the wind profile required by the Prandtl model is usually only present when the upper land breeze is suppressed by a gradient wind with an onshore component. Fig. 5.9 shows that even with the small offshore component provided by north-north-east gradient winds the correlation between the observed mean wind profile and the Prandtl model is poor (Fig. 5.10).

## 5.5 Surging

The tendency for cool downslope winds to exhibit surge characteristics is well-known. Intermittency of slope winds has been described by Defant (1933), Scaetta (1935), Nitze (1936), Reiher (1936) and Küttner (1949). The last two authors were also concerned with periodicity of the surges and their measurements revealed a period of approximately 5 minutes. A longer period of 20 minutes has been recorded by Heywood (1933).

Intermittency in mountain and valley winds has been noted by Thyer and Buettner (1962) and Tyson (1968b). The latter author describes surges in the mountain wind recorded between 2 ft and 20 ft at Pietermaritzburg which varied between 45 and 75 minutes. Surges with a 20 minute fluctuation are also described in the Pietermaritzburg area, the maximum turbulent energy occurring at the 300, 400 and

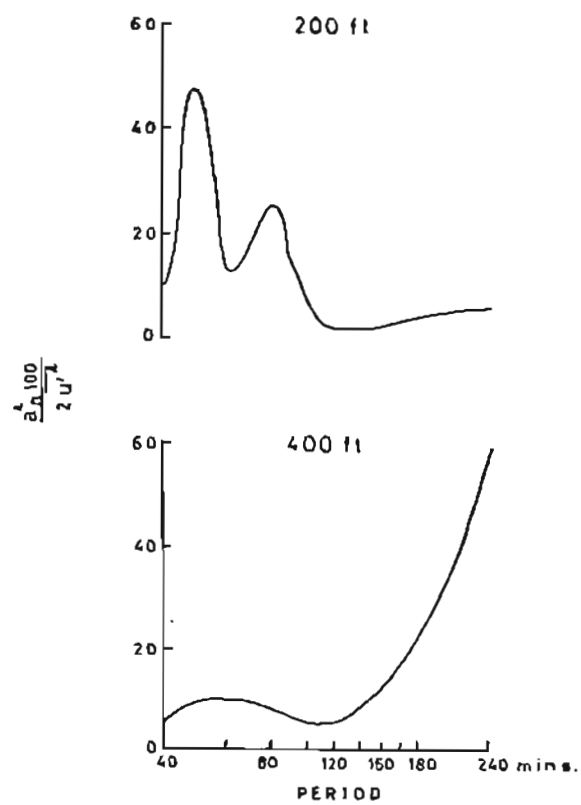


Fig. 5. 11 : Velocity spectra of the drainage wind, 0205-0405 on 11.7.69 at station 2



500 ft levels rather than near the surface.

Surges are also characteristic of drainage winds at the coast and on 11 July 1969 a marked surge period of 50 minutes with a lesser period of 80 minutes was recorded at 200 ft at station 2 in the Ngeni River valley (Fig. 5.11). Surging is clearly related only to the drainage wind and in this case disappears with increasing height.

The cause of intermittent surges in the drainage wind is not well understood. An attractive explanation is, however, advanced by Feagle (1950) who maintains that the cause of periodic wind fluctuations lies in the compressibility and consequent adiabatic heating of the atmosphere. As air accelerates downslope under the influence of a thermally-induced pressure gradient, a point is reached when adiabatic heating exceeds radiational cooling. This results in an oppositely directed pressure gradient which slows air movement until radiational cooling again reverses the pressure gradient. Thus a periodically varying velocity is produced.

## 5.6 The effect of gradient winds

Under strong north-east gradient wind conditions the amplitude of the diurnal variation of wind direction is reduced and components of air movement normal to the coast are weak. Instead of the seaward movement at night of cool land air on a regional scale, localised tongues of cold air drain from river mouths and their seaward penetration depends largely upon the strength of drainage winds as opposed to the gradient winds. These conditions were found to prevail during the night of 30 June - 1 July 1963. Pressure gradients steepened during this period as a depression approached Durban and fresh north-east gradient winds persisted throughout the night and suppressed the development of the land breeze. Fig. 5.12

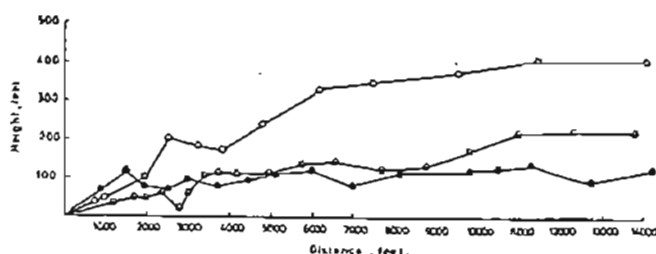
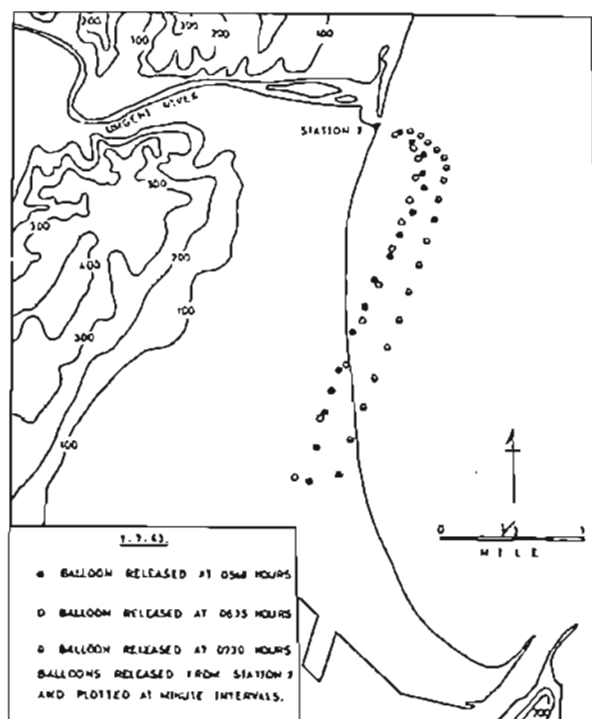


Fig. 5.12: Drainage wind - gradient wind interaction over the sea. Balloon release on 1.7.63 from station 2

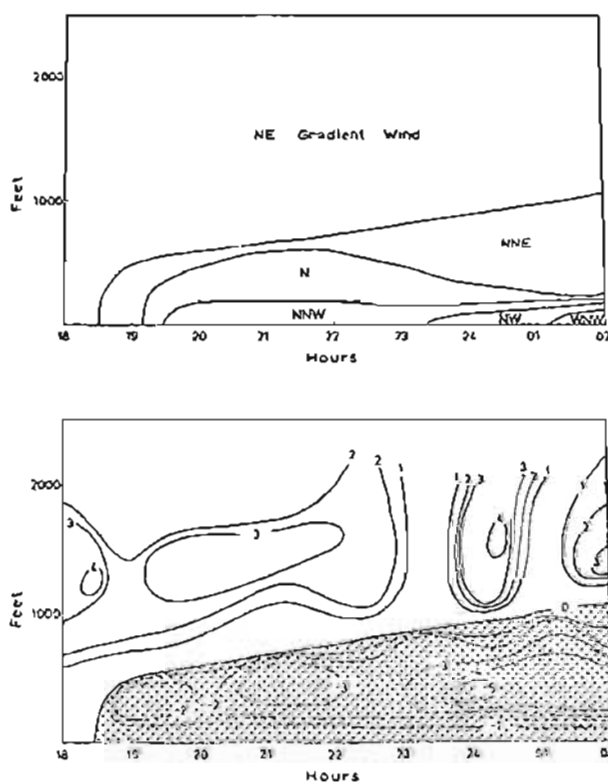


Fig. 5.13: Backing of the drainage wind with time observed on 19-20.5.67 from station 2

shows that despite the absence of a land breeze, westerly drainage winds prevailed under the sheltered conditions provided by the Mgeni River valley. The cold air which drained seawards from the valley mouth is shown to entrain into the north-east gradient wind over the sea and move back towards the land and over the city.

The suppressing effect of strong north-east or south-west gradient winds is initially felt by the land breeze. If the synoptical field between land and sea is not weakened beyond the threshold required to initiate an offshore component of air movement, a weak, shallow north-north-east or north offshore wind may appear. However, in north-west - south-east valleys, which are largely sheltered from the upper gradient winds, drainage winds may still persist and even strengthen throughout the night. Fig. 5.13 shows that on 19-20 May 1967 at station 2, a northerly land breeze prevailed below north-east gradient winds. Although drainage winds set in at 1930, one hour after the onset of a weak offshore component of air movement at the surface, they are clearly influenced by the upper gradient winds and until 2330 the direction shear separating land breeze and drainage wind was small. However, as drainage winds strengthened the influence of gradient winds became less effective and backing to a parallel-valley direction was observed near the surface.

The occurrence of drainage winds under conditions not usually conducive to the development of local circulations must be attributed to the nature of the terrain and to the presence of a warm sea. The deeply incised valleys along the Natal coast lose the sun fairly early in winter so that a lengthy period of cooling can be expected. If strong gradient winds prevail this process is slowed by turbulent mixing of cool near-surface air with warmer air above. Nevertheless, once the temperatures within the valley are lowered below those beyond the valley mouth and over the sea, the pressure gradient reverses and the onset of the drainage wind can be expected.

Even so downward turbulent transfer of momentum from gradient winds may affect the direction characteristics of drainage winds particularly beyond the valley mouth. The observed backing of this wind with time is mainly due to:

1. Steepening of the down-valley pressure gradient as falling temperatures in the valley increase the temperature differential between valley and warm sea.
2. Deepening of the layer of cold air in the valley bottom which becomes better able to resist the downward momentum transfer of upper winds.
3. The cross-valley component of air movement induced by upper northerly winds, blowing over a north-west - south-east aligned valley should cause an accumulation of air on the southern wall of the valley and a depletion of air on the northern wall. A cross-valley pressure gradient would, therefore, be directed towards the northern wall.

## 5.7 Dissipation

The nature of the vertical structure of the wind field at the time of reversal from mountain to valley wind seems to vary from place to place. Defant (1951) and Thyer and Buettner (1962) report initial ground level changes or simultaneous reversals at all levels, while Hewson and Gill (1944), Ayer (1961) and Davidson and Rao (1963) have observed dissipation of drainage winds from ridge level downwards. Tyson (1967c) has observed both characteristics over Pietermaritzburg but maintains that ground level dissipations are the more common. However, little attention seems to

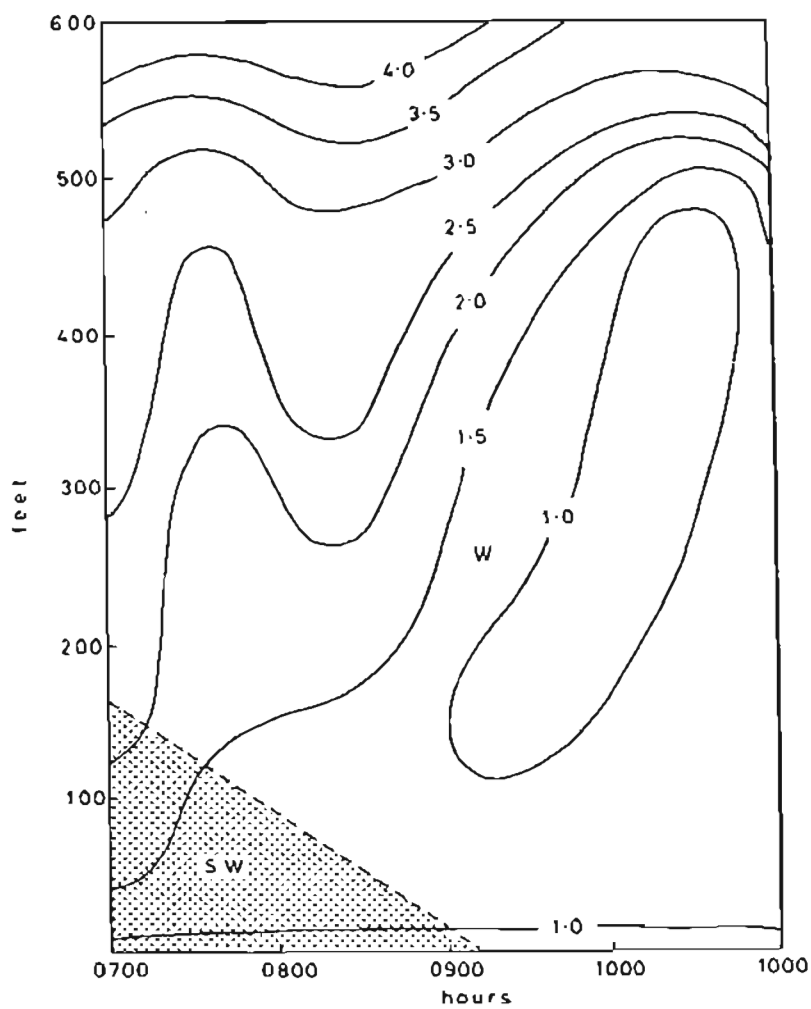


Fig. 5.14: Time section to show weakening of the drainage wind over Natal Bay. Observations on 9.7.63 from station 8. Wind speed isotachs in m/sec; pecked lines indicate transitional boundaries

have been directed towards the dissipation of drainage winds under land breeze conditions.

The dissipation of the south-west drainage wind in the Natal Bay area was found to be unvaried and was accompanied by the progressive downward penetration of the north-west land breeze. Lowering of the top of the drainage wind varied with the relative strength of the land breeze and drainage wind circulations. For instance, in Fig. 5.2 lowering at the rate of 20 ft/hr is considerably slower than the rate of 78 ft/hr shown in Fig. 5.14.

Davidson and Rao (1963) have suggested that the decay of the cold air stream from above is due to initial heating of ridge-tops and the response of the general wind to increased instability at these levels by the descent of this wind into the valley. Since most valleys along the Natal coast are aligned north-west to south-east, initial heating of north facing slopes would produce a cross-valley pressure gradient and Gleeson (1951) maintains that a component of air movement would then be generated in the direction of the warmest slope. Turbulence associated with this wind may be responsible for the establishment of convective mixing on the upper slopes of the valleys before the valley bottoms. More important, however, is that the source of cold air from valley sides is shut off by slope heating. Consequently, draining away of the cold air layer in the valley bottom would be accompanied by a reduction in the depth of the layer in the Natal Bay area.

\* \* \* \* \*

The nocturnal channelling of cold air between the Bluff and Berea ridge must be regarded as one of the most important aspects of air movement in the area. The low wind speeds, the depth of the

wind systems and the stability of the air layer means that a considerable volume of relatively non-turbulent air is moved towards the central business district from the south-west. Similarly cool land air from the Mgeni River valley is shown to reach the city after entrainment with north-east gradient winds. The potential for the transport of atmospheric pollution by these winds towards the city should be viewed in a serious light by planning authorities.

PART III

THE EFFECT OF LOCAL CIRCULATIONS UPON  
SELECTED CLIMATIC ELEMENTS



## CHAPTER 6

### THE DIURNAL VARIATION OF RAINFALL AT DURBAN

#### 6.1 Introduction

The diurnal variation of rainfall must be one of the least studied aspects of rainfall characteristics in South Africa and to the author's knowledge no detailed research into the field has been published in this country. An explanation of diurnal variations of hourly rainfall frequency and mean hourly rainfall amount can be a useful indicator of local atmospheric circulation characteristics. The purpose of this chapter, therefore, is to estimate the significance of land and sea breezes as factors in the rainfall process.

The records used in this study were obtained from an automatic raingauge at Louis Botha airport (station 15) and cover a 10 year period from 1958 to 1967. These were supplemented by 5 daily raingauges in the Durban area each with a similar 10 year record. These gauges are aligned approximately normal to the coast and inland as far as Bothas Hill. A 10 year rainfall record is too short for useful climatological analysis and no such attempt is made. Instead this study is concerned with the type and cause of rainfall and for this purpose a relatively short record length is usually adequate.

Haurwitz and Austin (1944) maintain that in maritime areas a high proportion of rainfall occurs at night. This characteristic is also found at Durban. In this chapter the diurnal variation of rainfall at Durban is analysed and it is shown that rainfall can be

attributed to undercutting of moist sea air by the land breeze, cold front activity and nocturnal thunderstorms.

## 6.2 Theories of nocturnal rainfall

In low latitudes rainfall is largely controlled by diurnal processes. In coastal areas it is the land and sea breeze regime that governs the diurnal course of rainfall and cloudiness in undisturbed weather conditions. The actual processes involved are also considerably affected by local topography so that explanatory models that fit one area may not suitably explain the rainfall characteristics of another.

Riehl (1954) shows that in undisturbed conditions at Puerto Rico an orographic-convection cell pattern at the sea breeze front produces cumulus development and showers inland from the coast during the day while the coastal region remains clear and dry. As the sea breeze weakens in the evening these clouds dissipate and cloud development and showers now occur over the coast as cool land air undercuts humid, warm air over the sea.

On the west coast of Malaya late night and early morning summer rainfall is associated with the interaction between local and meso-scale wind systems. Watts (1955) points out that line squalls (locally called 'Sumatras') which seem to originate in convection among the Sumatran ranges before sunset, later travel eastward at night. As a 'Sumatra' approaches the Malayan coast, uplift is initiated by a land breeze which undercuts conditionally unstable air over the Malacca Straits. Radiation from the top of cumulus clouds may further increase the instability and convection.

The tendency for cool offshore winds to initiate rainfall, particularly as thunderstorms, is also examined by Neumann (1951) who

shows that areas of increased nocturnal thunder activity correlate well with the frequency of offshore winds and the shape of the coastline. Where coasts contain large embayments, the quasi-radial convergence of cool air to undercut warmer sea air is sufficient to initiate thunderstorms.

The rainfall process appears to be different for the east coast of Malaya. Ramage (1964) discounts the effect of the land breeze as part of the nocturnal summer rainfall mechanism and his model is based instead upon movement of the sea breeze front. As cumulus clouds deepen at the sea breeze front, the upper return branch of the sea breeze combines with the gradient wind to cause the upper portions of the convergence cloud to drift seawards and produce showers at the coast. As the sea breeze weakens the convergence zone, with associated rainfall, retreats towards the coast and the evening rainfall maximum occurs as this zone crosses the coast.

In middle latitudes the diurnal rainfall curve is complicated by frontal discontinuities which may arrive at any time. Haurwitz and Austin (1944) maintain, however, that nocturnal radiational cooling of upper air, with little diurnal temperature change in the surface layers, produces convective instability. Frontal weather would also be affected by this process and it may be expected that frontal precipitation would be greater at night than during the day.

Various other attempts have been made to explain high nocturnal frequencies of rainfall occurrence and amount. Hewson (1937) suggests that this phenomenon could be caused by instability in the cloud layer which develops as a result of radiational cooling of the top and radiational warming of the bottom layer of the cloud. Means (1944) has criticised this idea and maintains instead that radiational cooling of the top of the cloud layer would lead to the development or intensification of a stable layer above the cloud top.

This would tend to suppress vertical motion. According to Means nocturnal rainfall, particularly from thunderstorms, could result from warm air advection in the lower layers of the atmosphere. The effect of this would be to reduce the stability of cooler air layers above.

In the Hydrometeorological Report (1947) the suggestion is made that higher relative humidities at night reduce evaporation of falling precipitation. Bleeker and Andre (1951) point out, however, that the rate of evaporation of precipitation elements is not dependent on the relative humidity of the air but on the difference in vapour pressure over the precipitation element and the air. This difference is unlikely to have a diurnal variation.

Dexter (1944) shows that warm front rainfall in the British Isles occurs with a maximum in the latter part of the night. He maintains that during the day warm sector air becomes potentially more unstable and that uplift along the warm front at night soon releases the instability. At night, however, near surface warm sector air layers become more stable and during the day must be lifted to greater altitudes up the warm front surface to release the instability.

It appears that diurnal rainfall characteristics along coastal areas are better understood in the tropics than in the middle latitudes. At Durban, situated in the sub-tropics, no simple explanation of the diurnal rainfall distribution can be advanced since rainfall is produced by processes reminiscent of both the tropics and the mid-latitudes.

### 6.3 Characteristics of the diurnal variation of rainfall

Rainfall at Durban is largely a summer phenomenon with a 3.65 times increase in rainfall amount from July, the driest month,

to February, the wettest month (Table 6.1). Rain does, nevertheless, fall in winter and the months June-August account for 12.7 per cent of the annual rainfall. This is in contrast to the interior of Natal where the division between the dry and wet seasons is more marked. For instance, rainfall over a similar period at Newcastle (27°45'S; 29°55'E) provides only 4.4 per cent of the annual rainfall.

Table 6.1: 30 year (1921-50) rainfall normals for Durban Point (after Climate of South Africa, 2, 1950)

J	F	M	A	M	J	J	A	S	O	N	D
119.6	157.5	144.5	84.6	79.3	55.4	43.2	49.0	67.8	100.6	126.5	131.6

The diurnal variation of mean hourly rainfall over Durban from 1958 to 1967 shows a predominance of evening precipitation with a maximum at 2100 (Fig. 6.1). Sixty-four per cent occurs between 1900-0600 and the remainder between 0700-1800. Hour by hour the pattern of high nocturnal precipitation is maintained throughout the year although in winter this effect is much reduced (Fig. 6.2). It is also apparent that the hourly frequency of occurrence of precipitation closely follows the pattern described above (Fig. 6.3). That there is a high correlation between rainfall amount and rainfall frequency is self evident.

In order to establish characteristics of the duration and period of precipitation, the frequencies with which a minimum of 0.1 mm rainfall was recorded between 0700-1800 and 1900-0600 were examined and found to be significantly different<sup>1</sup>. Table 6.2 shows

<sup>1</sup> At the 0.001 level.

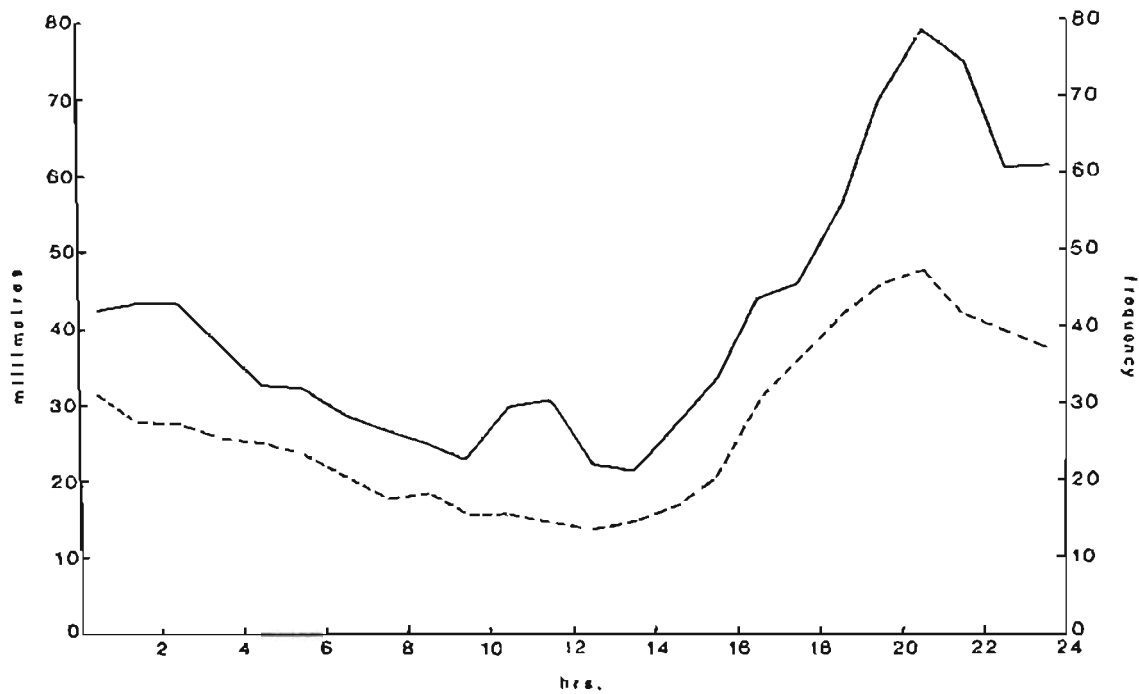


Fig. 6.1 : Mean hourly rainfall amount in mms (solid line) and mean frequency of occurrence (dashed line) at Louis Botha airport, Durban, 1958-67

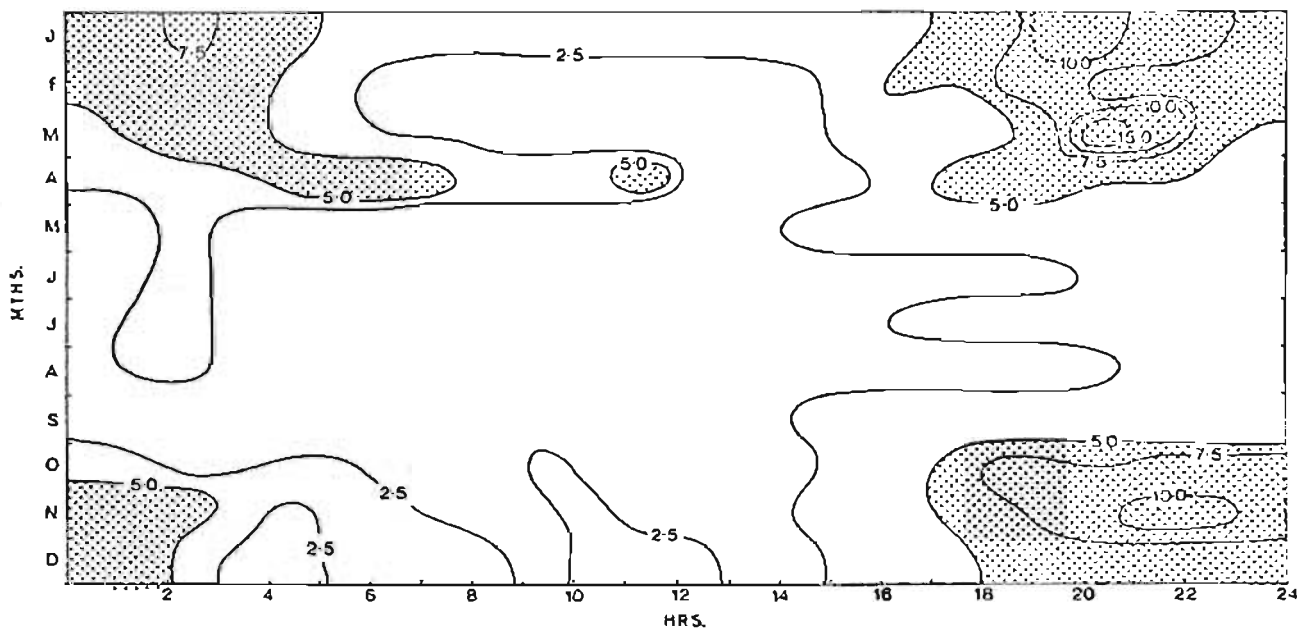


Fig. 6.2 : Mean hourly rainfall amount (mms) by month at Louis Botha airport, Durban, 1958-67

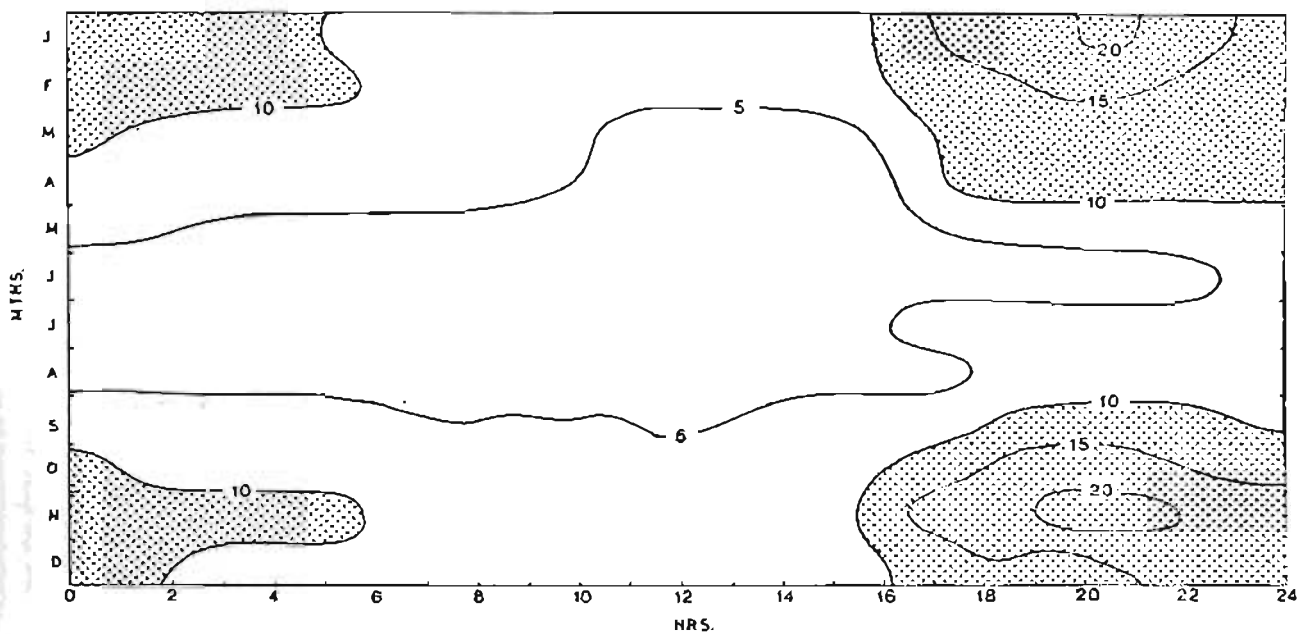


Fig. 6.3 : Percentage frequency hourly rainfall occurrences by month at Louis Botha airport, Durban, 1958-67

that 89 per cent of raindays included rainfall between 1900-0600. On 47 per cent of the raindays, precipitation occurred during the night but not during the day. This strongly suggests the existence of a precipitation process which is operative only at night.

Table 6.2: Frequency of raindays during specified hours recorded at Louis Botha airport, Durban, 1958-67<sup>1</sup>

	0700-1800		1900-0600	
	Rain	No Rain	Rain	No Rain
J	75	77	137	15
F	60	68	111	17
M	61	72	122	11
A	58	48	96	10
M	35	30	55	10
J	23	18	37	8
J	35	30	53	13
A	29	30	49	10
S	52	54	99	7
O	89	59	134	14
N	95	76	155	15
D	97	73	147	19
Total	709	635	1195	149
%	53	47	89	11

On 53 per cent of raindays, precipitation was recorded between 0700-1800. However, on only 11 per cent of the raindays did precipitation occur during the day but not during the night. It would appear that precipitation beginning during the day is likely to continue into the night, as is expected with the occurrence of general rains.

<sup>1</sup> If rain occurred throughout a day it was recorded in both categories.



The examination of correlations of mean, median and upper quartile rainfall figures for each hour at Durban indicates a higher degree of positive skewness during the summer than the winter months (Figs. 6.4 and 6.5). Hourly means are usually higher than the corresponding median which in most cases is less than 1.0 mm. In addition in 30 per cent of the summer and 12 per cent of the winter cases, hourly means also exceed the upper quartile figure.

By day and by night, irrespective of the season, it is apparent from Table 6.3 that much of Durban's rainfall occurs as gentle showers which do not produce more than 1.0 mm/hr. Precipitation less than 1.0 mm/hr accounts for 63.2 per cent of January and 58.7 per cent of July rainfall. In both January and July the major part of this low intensity rain occurs at night.

Table 6.3: Percentage frequency of rainfall intensities (mm/hr) between 0700-1800 and 1900-0600 in January and July at Louis Botha airport, Durban, 1958-1967

	January		July	
	0700-1800	1900-0600	0700-1800	1900-0600
0.1 - 1.0	20.3	42.9	22.2	36.5
1.1 - 2.5	8.3	11.0	7.5	14.7
2.6 - 5.0	2.7	7.1	5.6	4.9
5.1 - 10.0	1.7	2.5	1.8	3.0
10.1 - 15.0	1.0	0.9	1.5	1.1
15.1 - 20.0	0.0	0.8	0.4	0.4
20.1 - 25.0	0.1	0.5	0.0	0.4
> 25.1	0.1	0.1	0.0	0.0

Low intensity precipitation which is restricted to the day or night is usually of short duration and differs both in frequency

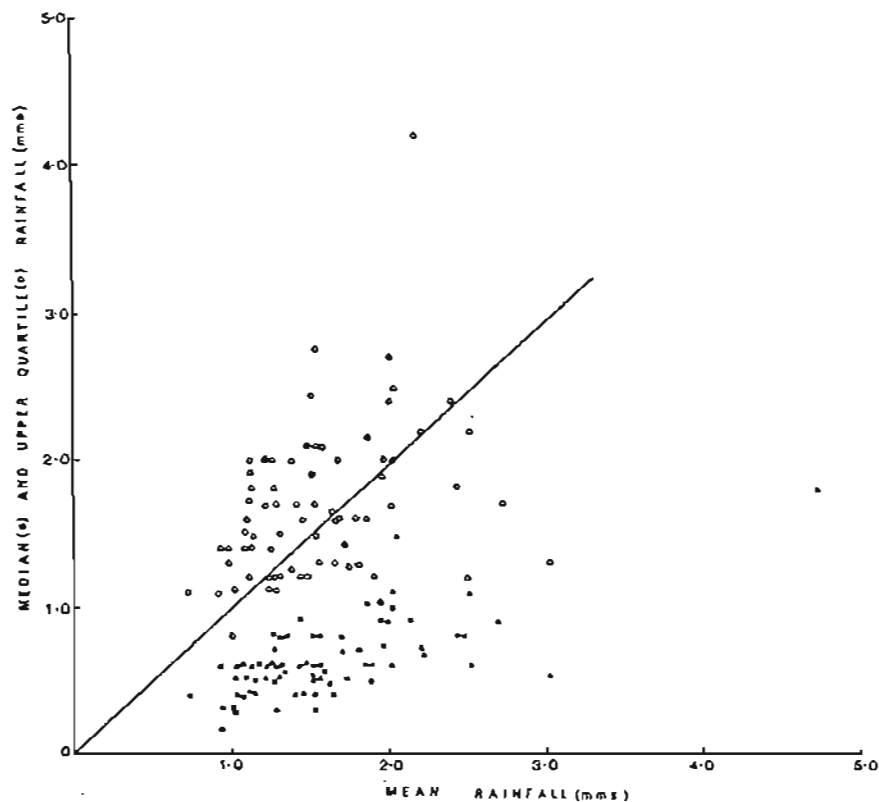


Fig. 6.4 : Median and upper quartile rainfall plotted against mean hourly rainfall (mms) recorded in December, January and February at Louis Botha airport, Durban, 1958-67. The straight line indicates equal values of upper quartiles or medians and means

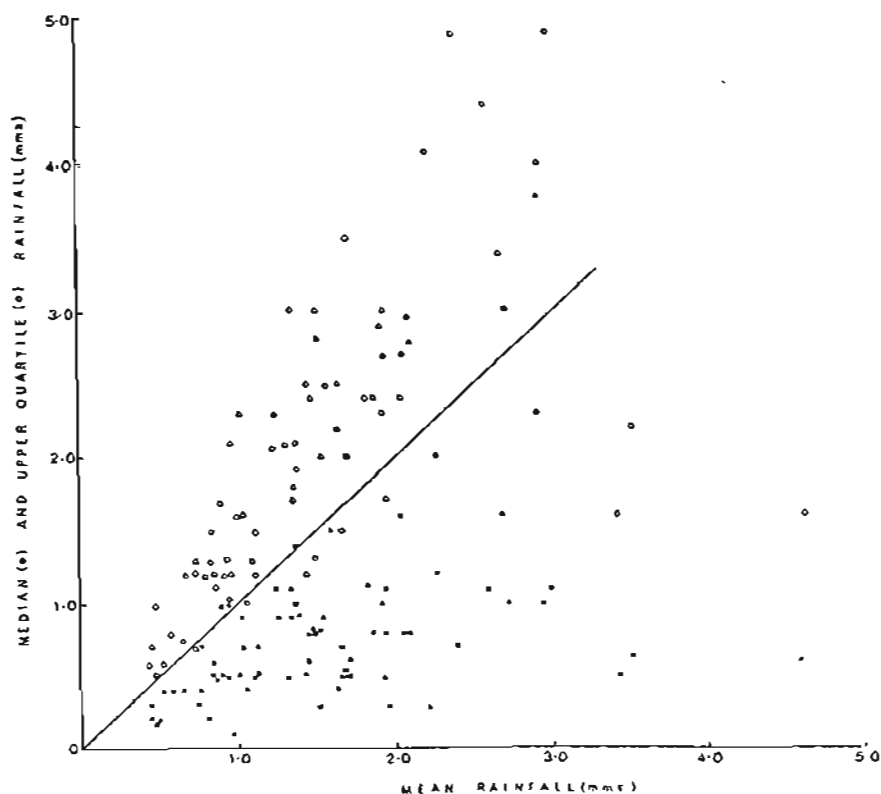


Fig. 6.5 : Median and upper quartile rainfall plotted against mean hourly rainfall (mms) recorded in June, July and August at Louis Botha airport, Durban, 1958-67. The straight line indicates equal values of upper quartiles or medians and means

and intensity from more continuous rains. Table 6.4 shows that hourly rainfall continuous by day or night over a 10-hour period<sup>1</sup>, has a low percentage frequency but high percentage contribution to the total monthly rainfall.

Table 6.4: Percentage frequency of occurrence and percentage contribution to total monthly rainfall of 10 hour continuous rainfall at Louis Botha airport, Durban, 1958-1967

	Amount	Frequency
J	25.7	7.3
F	27.7	5.3
M	18.5	2.9
A	56.2	9.2
M	53.8	12.3
J	32.7	8.3
J	41.0	7.1
A	53.9	10.0
S	31.5	7.9
O	50.5	9.3
N	25.1	6.3
D	37.2	5.3

No single factor can explain the diurnal rainfall characteristics at Durban. It may, however, be possible to classify three separate rainfall types in terms of the processes responsible for precipitation. The cause of high frequency occurrence of low intensity rainfall at night may be explained by the undercutting of moist sea air by the land breeze. Continuous rainfall of higher intensity is caused by frontal depressions. Finally, high intensity but short duration rainfall which accompanies thunderstorm activity

<sup>1</sup> An arbitrarily chosen period.

is precipitated after sunset over Durban. It seems that these storms are connected with a process involving diurnal variations and the influence of the sea breeze in this connection is suggested.

#### 6.4 A model for low intensity nocturnal precipitation over Durban

Sunset, following a relatively cloud-free day over the Natal coast, is often accompanied by the development of low stratus cloud followed by light showers. This frequently occurs after the passage of a coastal low or weak frontal depression has lowered atmospheric temperature and raised dewpoint temperature but failed to initiate precipitation. Although these weather systems may not themselves produce rain, they bring cooler, moister conditions which raise the wet bulb temperature near the surface thus making the lapse rate potentially unstable.

A rapidly cooling land surface is a feature not easy to reconcile with precipitation. The problem is clearly one of providing a mechanism by which moist air, which may contain considerable numbers of large condensation nuclei, is lifted up to condense into stratus cloud the droplets of which grow to precipitate 2-3 hours after condensation. Since a cool land breeze usually prevails at night it is suggested that this wind provides the necessary uplift by undercutting warmer air over the coastal margin.

A model which describes the air movement characteristics responsible for nocturnal cloud and precipitation at the coast is shown in Fig. 6.6. In (a) as moist air is advected over the land by the sea breeze, and strengthened in most cases by onshore gradient winds, condensation and cumulus cloud formation is initiated both by slope convection over the Kloof plateau and by the inland

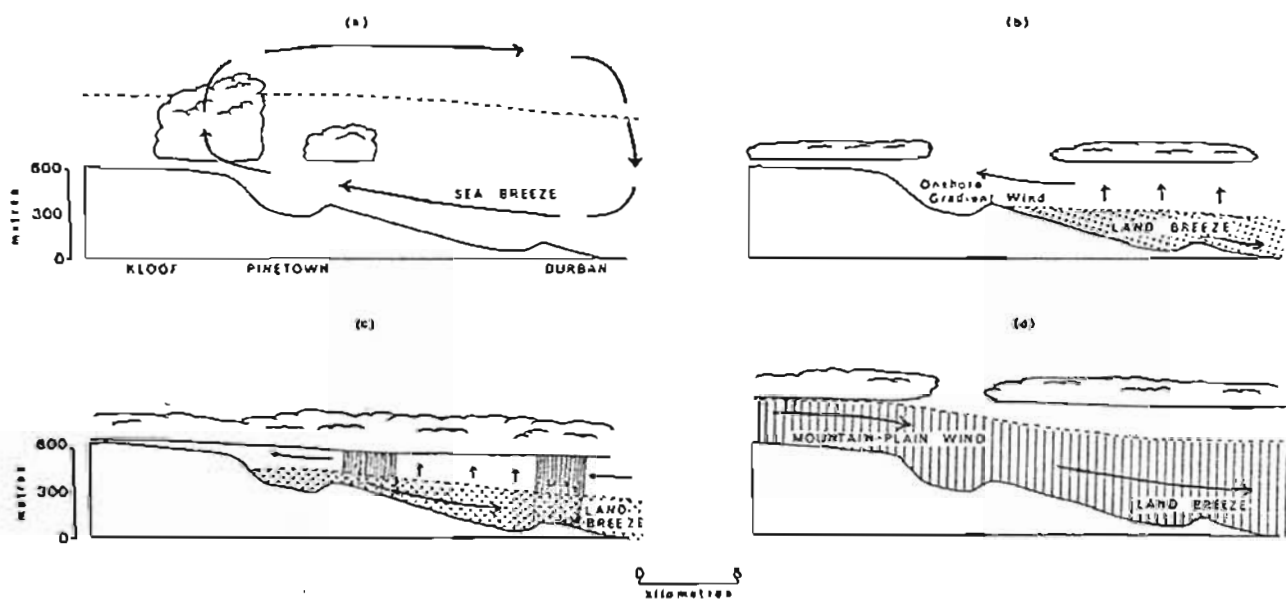


Fig. 6.6 : Diagrammatic model showing the influence of land breeze and mountain-plain winds upon nocturnal precipitation over the coast

vertical ascent normally associated with the sea breeze cell. With the cessation of the sea breeze and the weakly organised vertical motion in the sea breeze convergence zone, the cumulus cloud degenerates into a stratus cover. With the onset of the land breeze (in b) low stratus cloud begins to form over the coast due to the undercutting (and hence uplift) of warmer sea air by the cool land air. The land breeze circulation, strengthened by drainage winds in river valleys, deepens and migrates further inland with time (c). Concomitant with this is the formation of cloud and the occurrence of light showers likewise migrating inland.

Highest rainfall has been shown to occur at 2100 at Durban. Some mechanism is required to inhibit further precipitation after this time, except possibly as sporadic showers spread at intervals throughout the night. This is accomplished by the mountain-plain wind which by 2100-2200 reaches the Kloof plateau and merges with or over-rides the land breeze at the coast (d). A deep layer of cool, dry stable air now moves seaward. Little condensation is likely to take place within the land breeze-mountain-plain wind layer, and air forced to rise over the coast by the undercutting of this wind is likely to produce only shallow non-precipitating stratus.

The distribution of mean annual rainfall in the Durban-Pinetown-Kloof area shows that the highest rainfall occurs seaward of the Berea ridge crestline and over the Kloof plateau (Fig. 6.7). The rainfall distribution in the former area strengthens the case for the model. Over the Kloof plateau, however, it is difficult to separate orographic from other influences in determining the cause of rainfall.

The contention that nocturnal rainfall is associated with offshore winds is supported by Table 6.5. Over the six-month period

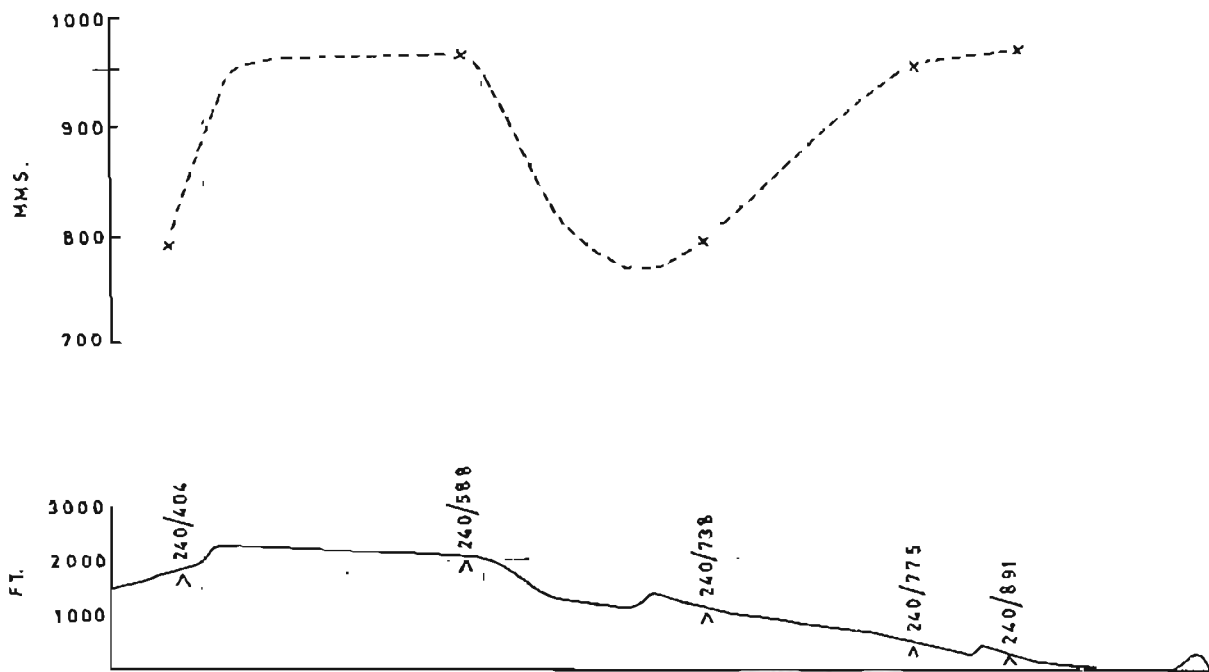


Fig. 6.7 : Mean annual rainfall distribution normal to the coast at Durban (after S.A. Weather Bureau, 1965)

Table 6.5: Frequency of occurrence at Station 12, of wind components normal to the coast during periods of rainfall from July to December 1967

Wind Components	0700 - 1800	1900 - 0600
Onshore	46	53
Offshore	29	127

examined, 70.6 per cent of rainfall was recorded at night and 49.8 per cent with offshore winds<sup>1</sup>.

## 6.5 Evening thunderstorms over Durban

Thunderstorms on the Natal coast differ in frequency and time of occurrence from those in the interior. There are approximately 100 days per annum with thunderstorms in the Drakensberg area decreasing to 20 to 30 on the coast (Climate of South Africa, 1965). These storms are largely a summer phenomenon and tend to occur in mid to late afternoon in the interior of Natal. On the coast, however, they occur most frequently during the evening (Jackson, 1966).

It is difficult to make a meaningful contribution to the understanding of coastal storms without reference first to storms in the interior of Natal. The main problem of forecasting storms lies in the recognition of the large-scale situations which are favourable

---

<sup>1</sup> The two independent samples given in Table 6.5 are significantly different at the 0.001 level.



for storm development. Severe storms in the interior of Natal are usually associated with the passage of an upper level trough eastward across the country. Strong north-westerly gradient winds which are generated on the eastern limb of the trough provide the wind shear which Newton and Newton (1959), Dessens (1960) and Ludlam (1963) have recognised as a necessary condition for the development and maintenance of storms.

It may be expected that north-westerly air flow over the Drakensberg would tend towards the formation of a lee depression in southern Natal and East Griqualand. During January 1969 the mean height of the 850 mb surface in Table 3.3, which shows lower pressure at Kokstad than at Umtata, Estcourt or Cedara, supports this contention. It has also been suggested that marine air brought onshore by the sea breeze and gradient winds is drawn towards this area of lower pressure. Thus a further necessary condition for the development of storms may be fulfilled, namely the availability of abundant moisture in the lower levels.

A field of large scale upward motion is most pronounced in strongly baroclinic zones. Jackson (1966) maintains that with the eastward movement of a trough and the barrier effect of the Lesotho mountains, westerly to south-westerly winds advect cool air around the southern edge of the mountain barrier. A zone of convergence between warm moist north to north-east winds and cooler west to south-west winds forms with almost frontal characteristics. The moisture front thus formed may be related to a similar front which extends across the highveld (Taljaard, 1959).

Because of the lack of upper air soundings in the Natal interior, instability characteristics of the prevailing air mass cannot be defined. It is nevertheless likely that during the first half of the day an inversion separates moist marine type air from drier subsiding air above the convergence zone. Fulks (1951)

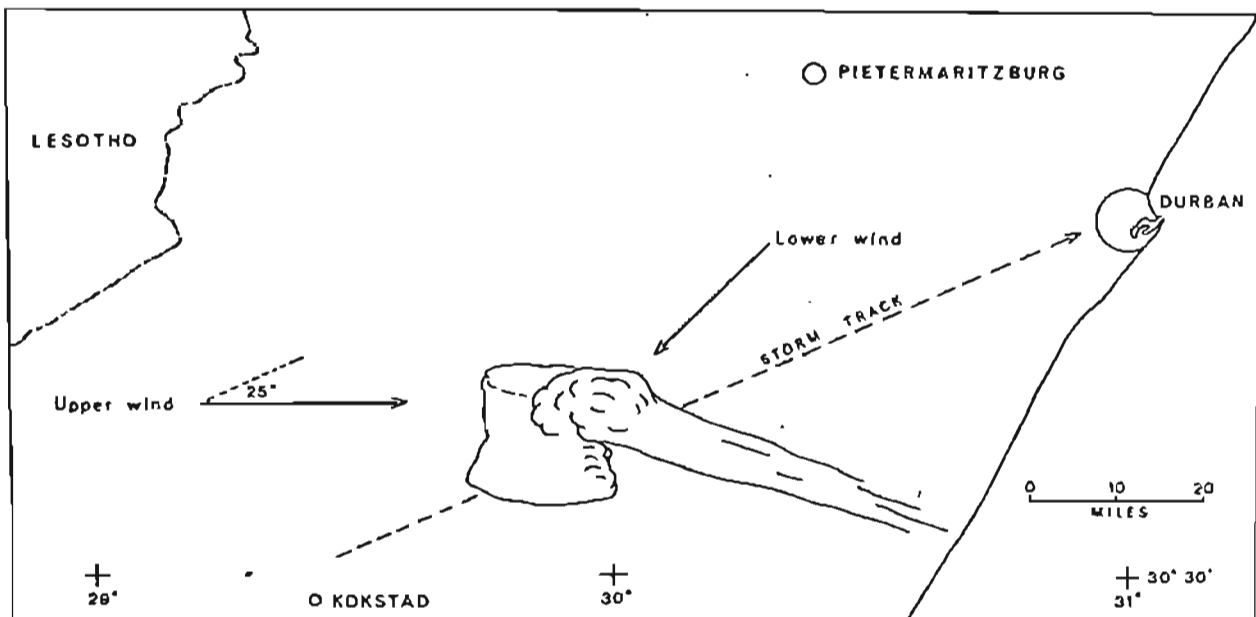


Fig. 6.8 : Track of thunderstorms which move towards Durban from the interior of Natal

emphasises the importance of an inversion during the production of an unstable air mass since it prevents the penetration of convection from the lower moist layer into the upper troposphere. Thus the lower moist layer can be increased in warmth and moisture content. If at the same time drying takes place in the upper troposphere, a progressive increase in potential instability results. With the introduction of some dynamic mechanism for the release of the instability an explosive overturning takes place.

The mechanism by which atmospheric instability in the Natal interior is released is open to debate. Beebe and Bates (1955) have shown that a stable layer may be eliminated through persistent organised vertical motion. Superposition of upper-level divergence over low-level convergence could satisfy this demand in Natal where convergence towards a lee depression by north-east winds or along a front separating north-east from south-west air flow, is probably more than compensated by divergence along the eastern limb of an upper air trough. Surface heating causing buoyant air parcels to rise to condensation level and beyond must also contribute to the instability release mechanism.

Storms that build up along lines or in areas in the Natal interior describe definite patterns of movement usually from west-south-west to east-north-east. It has been confirmed by radar observations at Durban that it is the afternoon thunderstorm development in the Kokstad district some 110 miles to the south-west which is most likely to move eastward and reach Durban by evening (Fig. 6.8; personal communication, Durban Weather Bureau forecasting staff). Jackson (1966) points out that the speed of movement of this storm system, which may be made up of a series of developing cells, can be as much as 9 m/sec.

It has been known for some years that thunderstorms in the northern hemisphere move systematically to the right of winds in the

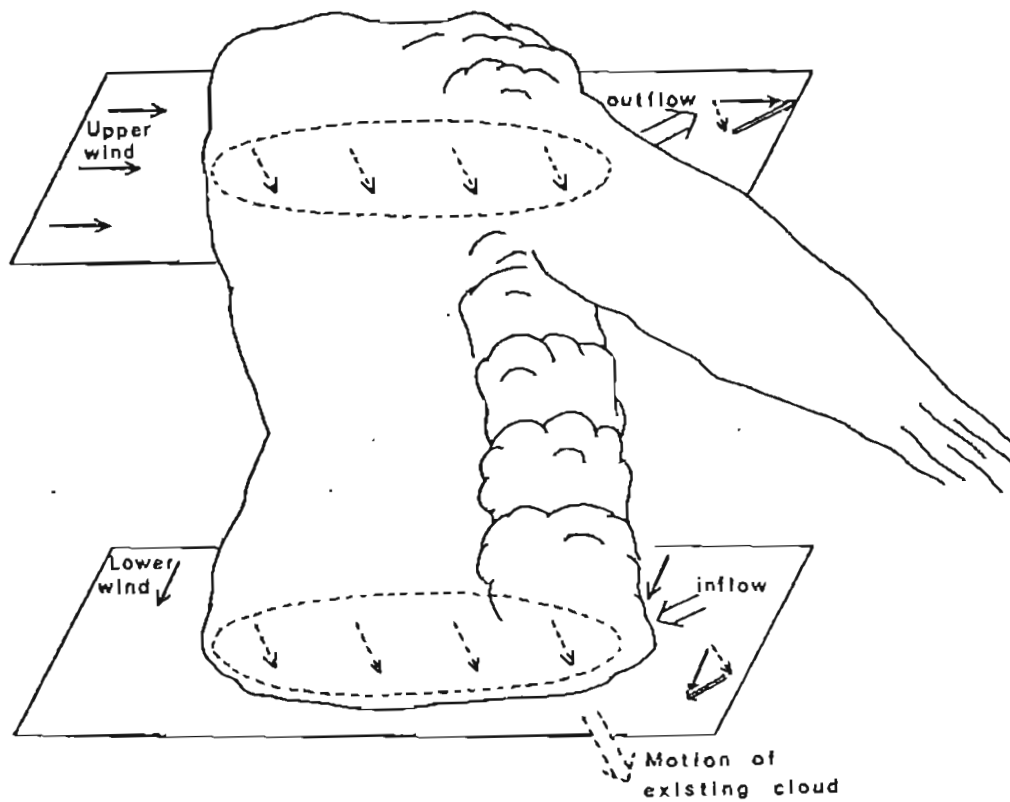


Fig. 6.9 : Model of a large isolated thunderstorm or squall-line element embedded in an environment in which the wind backs with height (after Newton, 1960)

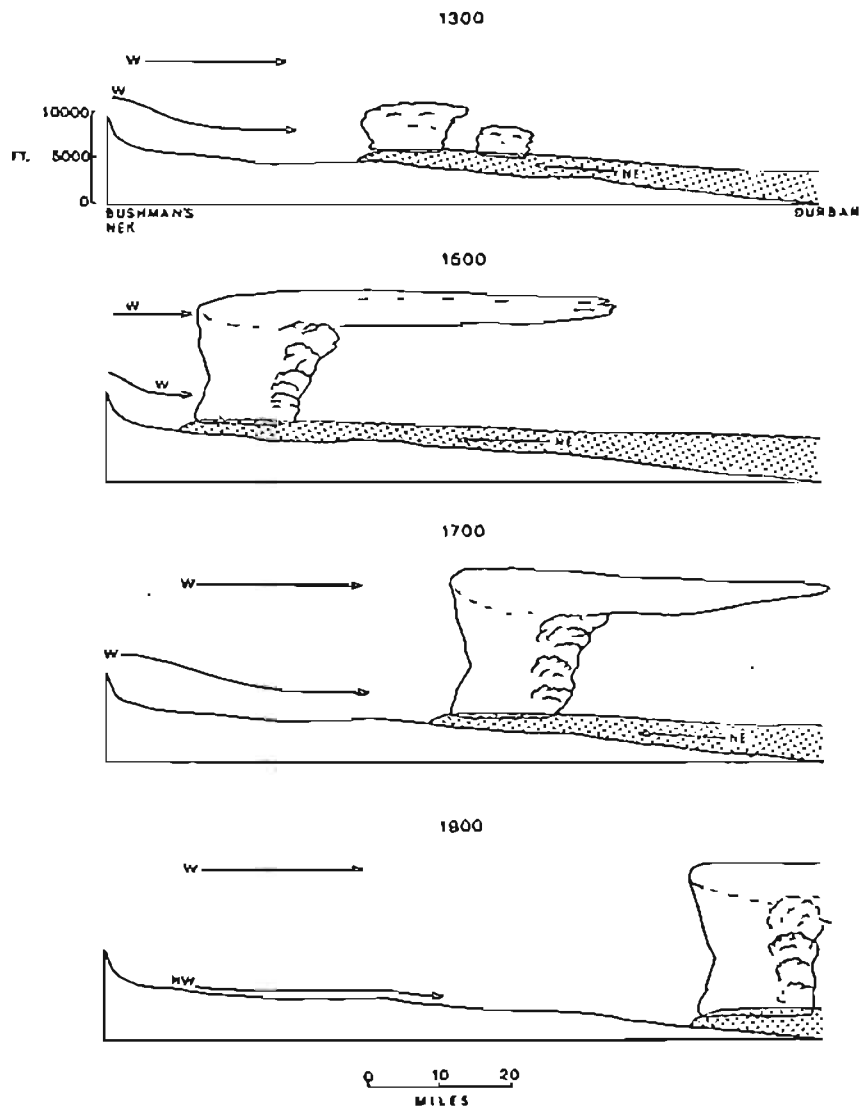


Fig. 6.10 : Diagrammatic model showing the movement of a thunderstorm towards the coast following the retreating convergence zone between onshore and offshore winds

middle and upper levels of the troposphere (Hoecker, 1957; Fugita, 1958; Hamilton, 1958; Douglas and Hitschfeld, 1959; Browning and Donaldson, 1963). This characteristic has been clearly defined by Newton and Katz (1958) who found that on average convective storms moved about  $25^{\circ}$  to the right of and 7 knots slower than the mean wind in the 850-500 mb layer. In the southern hemisphere, Carte (1966) describes a similar characteristic with the difference that storms move to the left of the mean wind. This explains the tendency for storms in Natal to move in an east-north-east direction when upper winds are westerly.

The explanation offered by Newton and Newton (1959) and Newton (1960) for this phenomenon is based on the existence of a wind shear through the atmosphere layer. Vertical mixing of momentum within the layer would produce an average in-cloud motion indicated by dashes in Fig. 6.9. The motion of the ambient air relative to in-cloud air is into the left flank in lower levels and away from that flank in upper levels. This favours growth on the left flank which when added to the tendency for existing cloud to drift with the mean wind results in the deviation of the storm motion to the left.

An explanation is now required as to why conditions, which favour thunderstorm development in the Natal interior during the afternoon, do not similarly affect the coast while in the evening this position is reversed. Clearly the lack of a well-developed sea breeze convergence zone along the coast during the day and the absence of any mechanism which could cause the release of instability should it exist mitigates against daytime thunderstorms near the coast particularly while a sea breeze prevails. It has been suggested, however, that the sea breeze near the coast and gradient and valley winds further inland are responsible for the penetration of marine air into the Natal interior. It is this air which feeds into the lower left flank of an eastward moving thunderstorm.





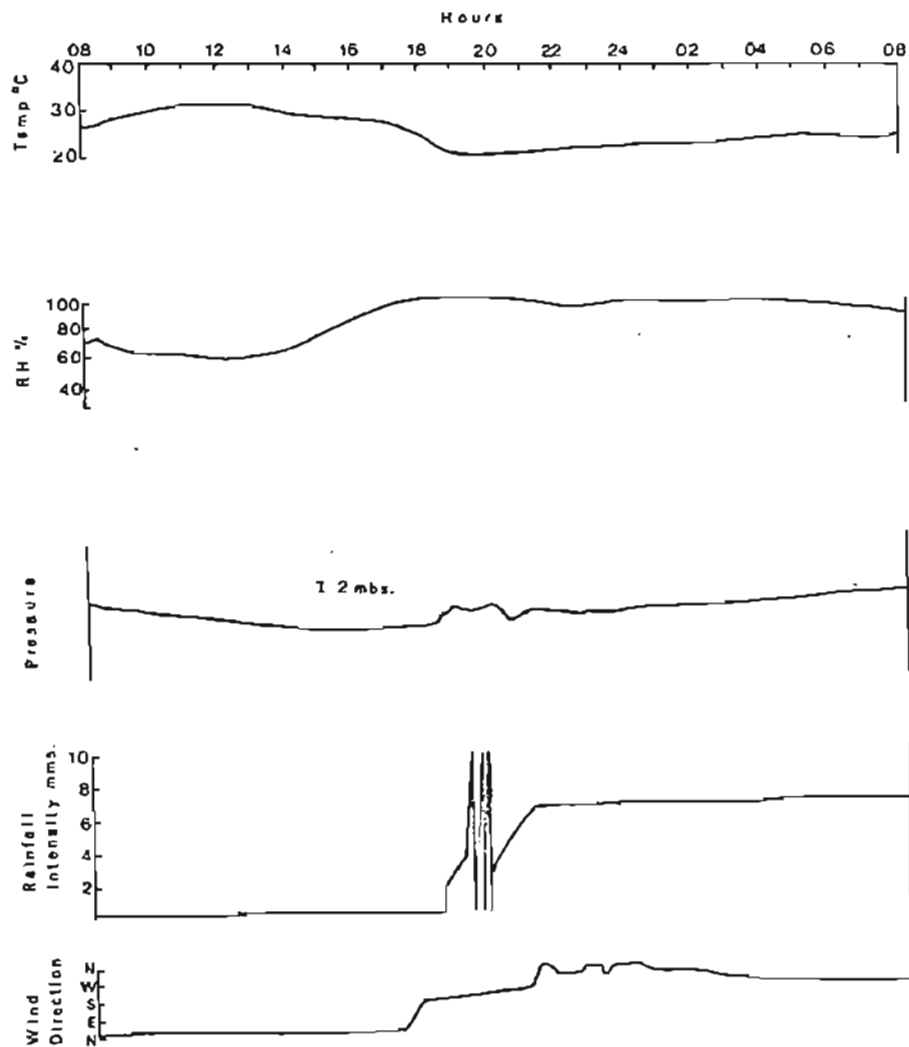


Fig. 6.12 : Autographic records during the passage of a thunderstorm past Durban on 9.1.69



As the inland directed circulation weakens during the late afternoon, the convergence zone between near surface north-easterly and south-westerly winds over the interior must withdraw towards the coast. The eastward movement of thunderstorms is probably coincident with this withdrawal. By sunset in summer this convergence zone nears the coast and thunderstorm activity may be expected at any time in the early evening (Fig. 6.10).

The model can be tested against observations and synoptic charts for 9 January 1968 and autographic records for a typical evening thunderstorm over Durban on that day are shown in Fig. 6.11 and 6.12. Lowest surface pressure east of the escarpment is shown to occur in East Griqualand and southern Natal. It is suggested that a lee depression existed in that area caused by air flow about a shallow trough over South Africa which at 1400 produced 30 knot north-westerly winds at 500 mbs and 50 knot north-westerly winds at 300 mbs over Durban. A shear zone separating onshore from offshore winds advanced inland during the morning and by 1400 wind directions at Estcourt and Cedara were onshore east-north-east. South-westerly winds were recorded at Kokstad at 1400 so that a convergence zone must have separated these two winds. The thunderstorm which reached Durban originated along this convergence zone and moved to the left of the upper winds in an east-north-east direction as shown by the west-south-west direction of the downdraft. Although the downdraft produced an immediate fall in temperature the pressure jump waited upon the onset of high intensity rainfall.

\* \* \* \* \*

While acknowledging that large-scale circulation patterns are the dominant controls of precipitation patterns over any area, it is important to recognise the influence of local circulations

upon the meso-scale occurrence and distribution of rainfall. These circulations have been shown to induce precipitation in tropical latitudes but no attempts have been made to trace similar characteristics in South Africa. However, this study indicates that parallels do exist although some characteristics common to the Natal coast do not seem to have been recognised elsewhere. In particular the effect of the mountain-plain wind in suppressing precipitation should be noted in this respect.

## CHAPTER 7

## WIND AS A FACTOR IN THE FORM OF DURBAN'S

## HEAT ISLAND

## 7.1 Introduction

Local climatic variations between a city environment and its surroundings have been well documented. Howard (1833) showed the mean urban temperature of London to be in excess of its surroundings and this characteristic has since been confirmed by Chandler (1965). Renou (1862) compared temperatures within and without Paris and found that urban temperatures had a higher minimum and smaller diurnal range. Automobile traverses by Schmidt (1927), Peppler (1929) and Riechel (1933) showed that the built-up areas of Vienna, Karlsruhe and Berlin were warmer than surrounding rural areas. More recently studies by Duckworth and Sandberg (1954), Landsberg (1956), Mitchell (1961), Bornstein (1968) and Munn *et al* (1969) have confirmed this climatic characteristic of cities.

Various explanations to account for the heat island have been advanced. Howard maintains that urban temperatures are raised by self-heating due to industrial and domestic combustion. The absorption and re-radiation of terrestrial radiation by atmospheric pollution is considered by Kratzer (1956) as the prime reason for large nocturnal urban temperature excesses. Munn (1966) points out that the upward flux of terrestrial radiation is less in urban than in rural areas, particularly where buildings are tall and narrow, while back radiation is greater. Mitchell (1961) emphasises the large heat capacity and conductivity of the urban fabric while Bornstein (1968) has suggested that with reduced evaporation and transpiration and, therefore, lowered humidities in cities, the available solar radiation must go into heating the city streets, buildings and air. Chandler (1965) maintains that by day upward

turbulent transfer of heat will lower the urban temperature excess, at times below that of surrounding areas. However, Mitchell (1961) visualises buildings as barriers to the penetration of cool air into the city.

Clearly the heat island effect is the net result of several competing physical processes each of which acting alone could produce relatively large temperature contrasts between the city and its surroundings. For instance, radiation exchanges in the city are complicated by the numerous vertical surfaces and by atmospheric pollution, evaporating surfaces are reduced, thermal capacity and heat storage capacity is high and the city is also an emitter of heat by combustion. In general, however, the mean temperature differential between city and country is not large so that a tendency for cancellation of these processes obviously exists. Myrup (1969) suggests, for instance, that a decrease in evaporation towards the city centre, which should account for increased temperatures, is balanced by the increasing size of buildings and this augments the diffusion of heat upwards by mechanical turbulence. In a numerical model Myrup (1969) shows that the most important parameters which determine the size of the heat island are the reduction of evaporation in the city, the thermal properties of buildings and paving materials and wind speed. During the day reduced evaporation is the most important parameter; during the night the thermal properties of the urban fabric.

Heat islands are more intense by night than by day. Although perhaps not a general rule, some cities such as Vienna, Bath and London have been shown by Kraus (1945), Balchin and Pye (1949) and Chandler (1965) respectively to have summer daytime temperatures which on occasions are lower than surrounding areas. In contrast Duckworth and Sandberg (1954) describe a nocturnal temperature differential of the order  $11.0^{\circ}\text{C}$  on one occasion in San Francisco.

In some cases the thermal response of a built-up area may

be partly influenced by local circumstances. For instance, the high albedo of near-white limestone, which is widely used for buildings in Bath, is suggested by Balchin and Pye (1949) to contribute towards a low urban temperature by day. In general, however, city-country temperature differentials are variable from day to day and appear to be affected by particular meteorological conditions. In an attempt to define the underlying causes of the temperature difference between the urban heat island and the surrounding rural areas, Sundborg (1950) developed for Upsala empirical equations for day and night of the form

$$\Delta T \text{ (day)} = 1.4^{\circ} - 0.01C - 0.09U - 0.01T - 0.04e \quad (7.1)$$

$$\Delta T \text{ (night)} = 2.8^{\circ} - 0.1C - 0.38U - 0.02T + 0.03e \quad (7.2)$$

where  $\Delta T$  is the temperature differential in  $^{\circ}\text{C}$ ,  $C$  is cloudiness in tenths,  $U$  is wind velocity in m/sec,  $T$  is temperature in  $^{\circ}\text{C}$  and  $e$  is vapour pressure in mbs. The equations show that by night the influence of cloud upon  $\Delta T$  increases by a factor of 10 and wind by a factor of 4, relative to day conditions. By day only the wind parameter has some modifying effect upon the undefined constant which essentially represents all the static city influences such as heat conductivity and radiative screening of built-up areas. With increasing wind speed the temperature differential decreases. An expression of this form has been calculated by Chandler (1965) for London and the general direction of the above relationships have also been substantiated by Duckworth and Sandberg (1954) for San Francisco.

During the day and the night the urban heat island is usually characterised by an isotherm configuration which, assuming low relief, conforms to the shape of the city. The nature of this cellular form may, however, show day to day changes particularly when influenced by winds which tend to displace the heat island in a down-wind direction (Munn et al, 1969). However, mean temperatures should indicate any tendency for the heat island to be persistently displaced

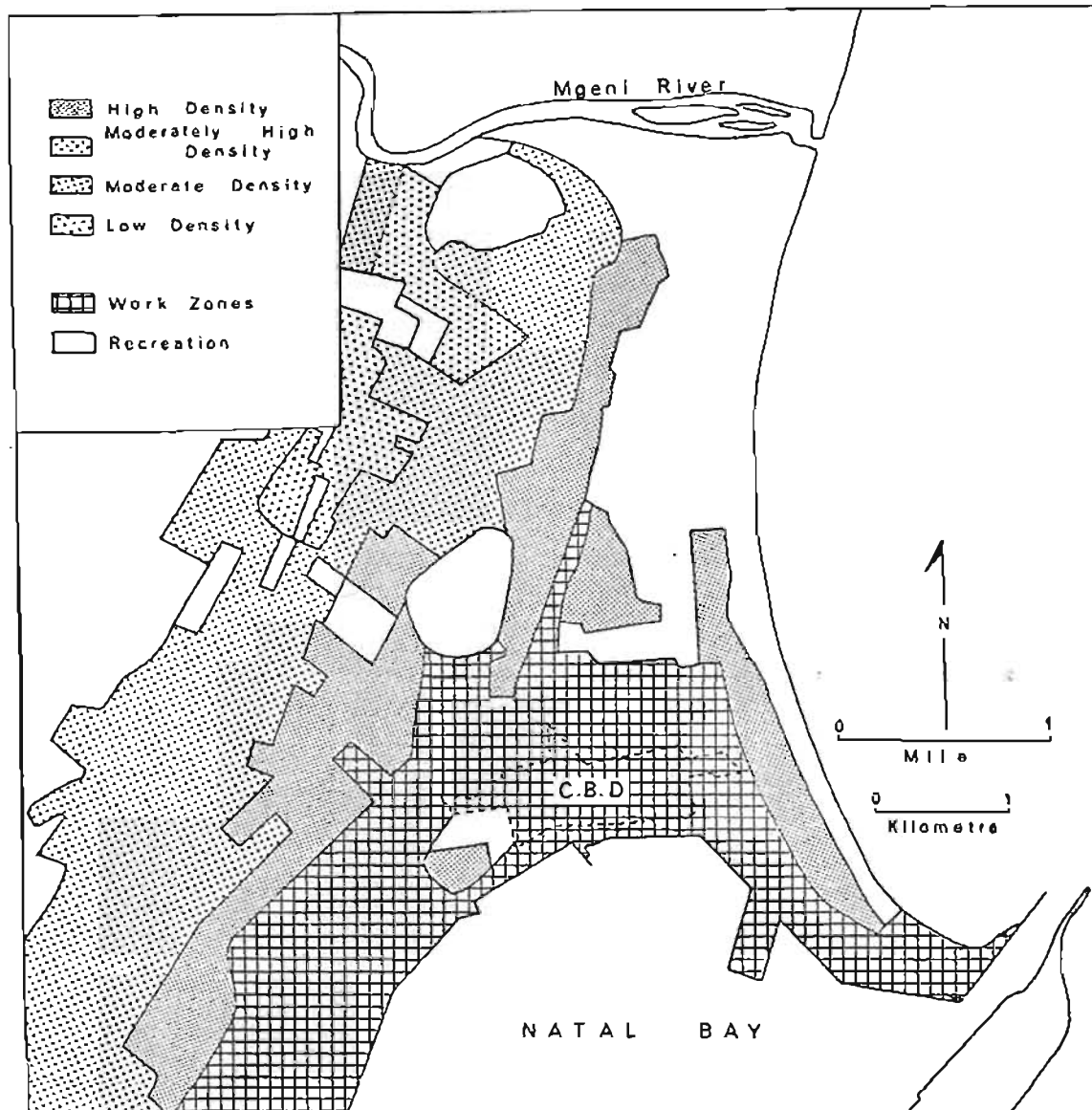


Fig. 7.1 : Residential density, work zone and recreational regions in the Durban area (after Davies, 1960; Davies and Rajah, 1965)

by the wind. Local circulations at Durban could produce such an effect and this chapter is concerned with an examination of the changing form of Durban's heat island and the development of an empirical model to describe the mean spatial distribution of temperature across the heat island.

## 7.2 The urban setting

The work zone shown in Fig. 7.1 is located on alluvial flats that surround the harbour at Durban and occupies land less than 30 ft above sea level. From the point of view of the urban temperature field, the unifying characteristics of the region are the close proximity of buildings, which are bounded within a grid network of macadamised streets, the high density of motor vehicle traffic and the lack, with one exception, of large open recreational space. Multi-storied apartments which line the seashore cause the high residential density in that area.

The alluvial flats are backed by the Berea ridge, which rises with a 7 degree slope to an altitude exceeding 400 ft. The decrease in residential density up the Berea ridge is accompanied by a corresponding change in the urban fabric. The region of high residential density located along the lower slopes of the Berea ridge consists of single-storied, closely-spaced houses set in small properties in narrow macadamised streets. With increasing elevation up the ridge, decreasing residential density coincides with larger houses set in more spacious properties.

## 7.3 Land breeze - drainage wind modification of the temperature field

4B

The measurement of nocturnal temperatures in the Durban

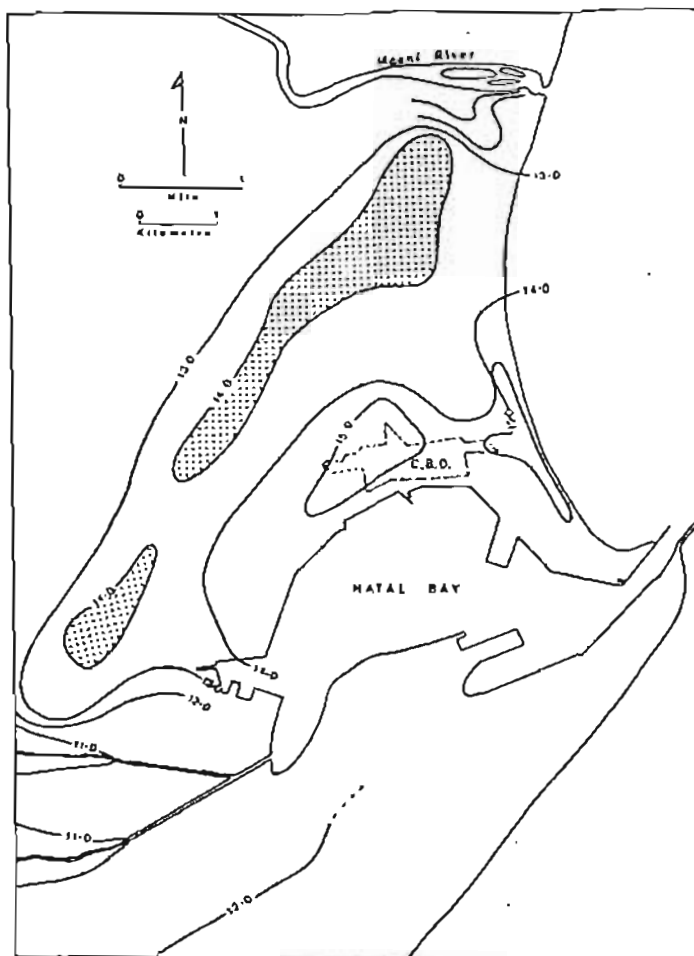


Fig. 7.2 : Isotherms ( $^{\circ}\text{C}$ ) of mean minimum temperature, July 1968 in the Durban area

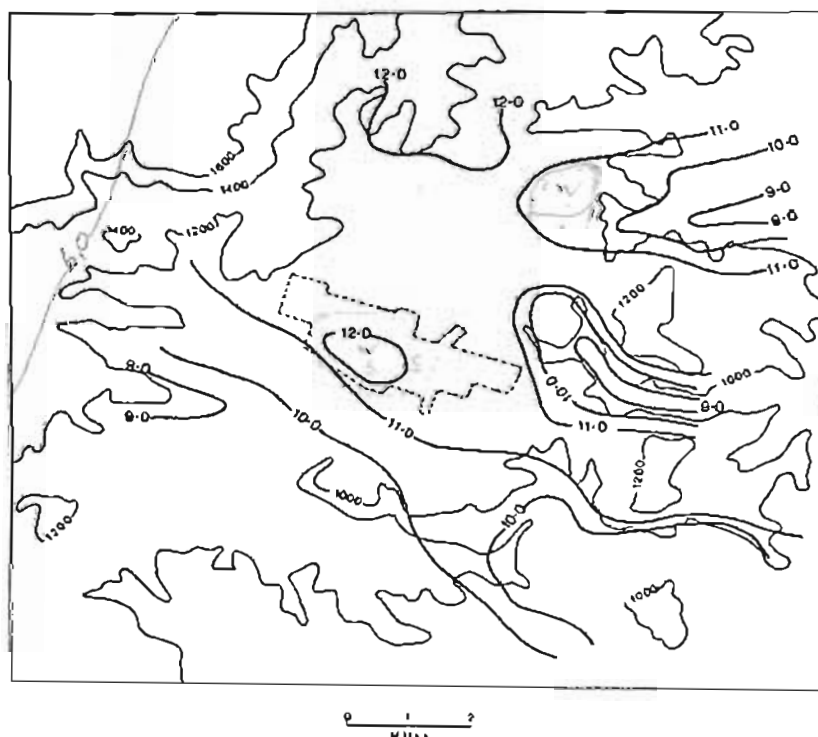


Fig. 7.3 : Isotherms ( $^{\circ}\text{C}$ ) of mean minimum temperature in the Pinetown basin, July 1968



area was only undertaken in clear settled winter weather, local circulations being best developed under these conditions. An isotherm map based on mean 0400-0500 temperatures recorded during July 1968 is shown in Fig. 7.2. A two-cell urban heat island is evident over the city, the eastern cell located in the high density residential zone which flanks the seashore and the western cell situated over the western edge of the central business district. Temperatures in the work zone region are higher than other areas on the low-lying alluvial flats but compare with the thermal belt located along the Berea ridge. Predictably, lowest temperatures are found in the river valleys.

Drainage winds from the Umbilo and Mhlatusana River valleys are largely responsible for the low mean temperatures in the respective valleys and over the alluvial flats at the head of the Natal Bay<sup>1</sup>. Channelling of these winds between the Bluff and Berea ridges accounts for temperatures along the northern and western bayside which are lower than are to be found within the two heat island cells. It may also be expected that the drainage winds receive an added velocity component in response to the temperature and, therefore, pressure gradient between the alluvial flats to the south and the urban heat island to the north of the bay. The characteristic of local winds to be attracted towards urban heat islands has been noted by Pooler (1963), Crow (1964) and Smith (1967).

---

<sup>1</sup> The effect of topographically-induced winds upon temperature is also clearly evident from 0400-0500 mean winter temperatures over the Pinetown basin (Fig. 7.3). Low temperatures, usually with a steep local temperature gradient, are restricted to the river valleys located to the east of the basin where drainage winds are likely to be well-developed. The temperature gradient within the basin is shallow north of the built-up area but steeper in the shallow south-draining valley south-west of this area. The urban heat island is situated squarely over the business district and there is no evidence of its displacement by the land breeze.

The existence over the city of two separate heat island cells is due to penetration of cool stable air into much of the work zone area. Consequently maximum urban temperatures are only to be found west of the main stream of cold air and in the sea front zone where heat is trapped behind closely-spaced apartment blocks. It is also conceivable that the higher temperatures evident in the eastern heat island may be partly due to displacement of heat generated within the business district by westerly to north-westerly land breezes.

It has been shown that drainage winds from the Mgeni River valley are entrained into north-easterly gradient winds over the sea with the result that cool air is moved southwards. Temperatures along the seashore and alluvial flats south of the Mgeni River mouth are lowered partly by this phenomenon and partly by radiational cooling.

A temperature inversion up-slope at night is an expected phenomenon and in this case radiational cooling of the lower Berea slopes is assisted by drainage winds. The well-developed thermal belt that extends almost the length of the Berea ridge is partly due to this phenomenon and partly due to lowering of temperatures along the ridge crest by the cool land breeze. Although the thermal belt is located on the leeward side of the Berea ridge away from the direct influence of the land breeze, nocturnal temperatures must also be kept high in this area by the urban fabric and by the well-developed vegetation cover.

#### 7.4 Sea breezes and the urban temperature field

The measurement of day temperatures over Durban were undertaken from 1230-1330, approximately at the time of maximum surface temperature. To evaluate Durban's heat island in terms of

## Correction Factor

purely urban conditions, height effects were eliminated by reducing all mean maximum temperatures to sea level using the observed lapse rate of  $0.4^{\circ}\text{C}/100\text{ m}$  that prevailed between the lowest and highest stations. This lapse rate was determined by regression analysis of temperature on heights based on data from 9 Weather Bureau stations in the area ranging in height above sea level from 23 ft to 2,292 ft.

Fig. 7.4 is based on mean summer temperature traverses under north-east sea breeze conditions. These breezes, strengthened by gradient winds, blow strongly during the summer months. Table 7.1 shows the high frequency of the north-east sea breeze which blows obliquely off the sea.

Table 7.1: Percentage frequency of wind observations from December to February at Durban (after Weather on the coasts of Southern Africa 1941)

Knots	N	NE	E	SE	S	SW	W	NW	Calm
3 - 13	3	30	12	12	10	2	-	-	4
14 - 27	-	5	1	-	10	10	-	-	-
28 - 40	-	-	-	-	-	1	-	-	-

It is apparent that an elongated heat island extends along the foot of the Berea ridge with its centre situated west of the central business district over a relatively flat area occupied by a market, an extensive car park, wide streets and buildings which are lower than those in the business district. This anomaly is due to the displacement of the heat island by the sea breeze away from the heat sources provided by the business district. The energy of the sea breeze as it blows over the aerodynamically rough surface of the central business district is reduced near the surface so that wind

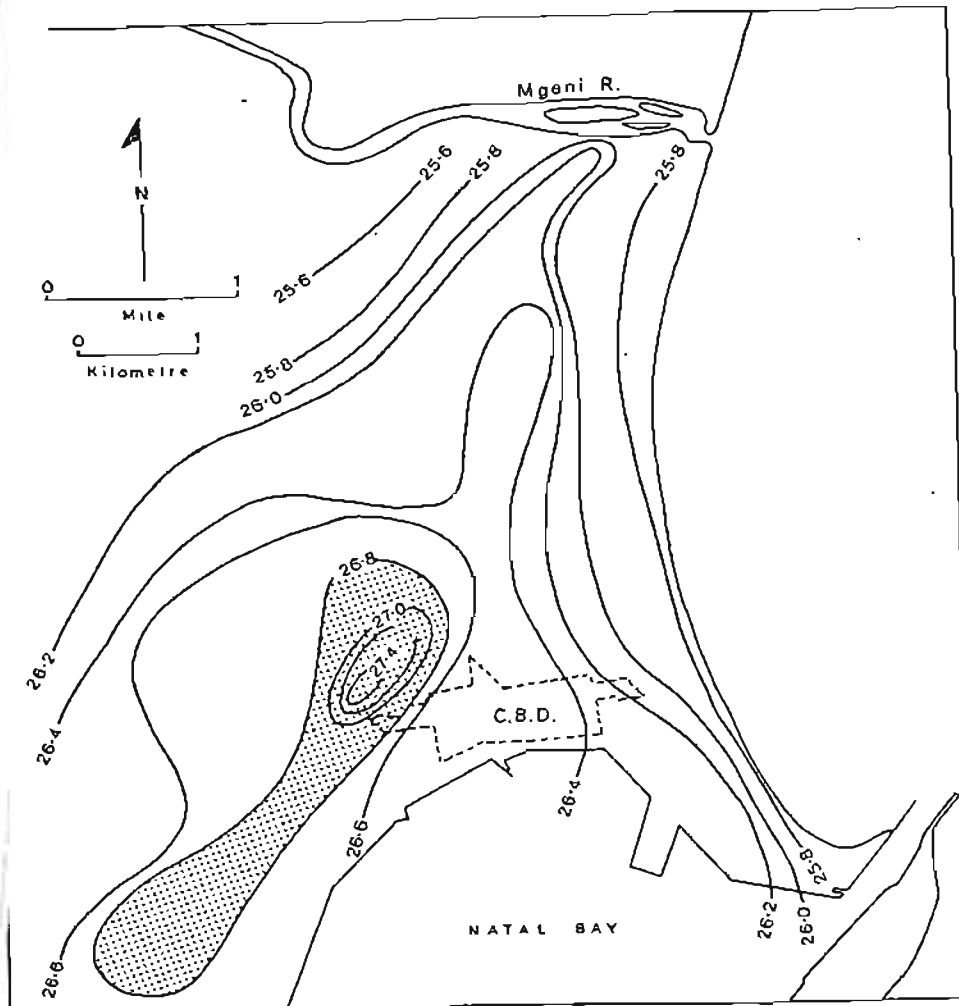


Fig. 7.4 : Isotherms ( $^{\circ}\text{C}$ ) of mean midday corrected temperatures under north-east sea breeze conditions, November-February 1969

speeds in the heat island area are low. Turbulent diffusion of accumulated heat is, therefore, also low.

Temperature gradients are relatively steep along the seashore east of the work zone and along the foot of the Berea ridge. The gradient is due in the former area to the presence of multi-storied apartments which block penetration of the sea breeze into the work zone; in the latter area to variations in the character of the residential setting. In general, however, reduced temperatures are lowest along the seashore and crest of the Berea ridge.

#### 7.5 Gradient wind modification of the temperature field

North-east sea breezes prevail in warm anticyclonic weather conditions in which skies are cloud-free and gradient winds, supplemented by the sea breeze, produce only moderate winds. However, with the passage of a depression and accompanying steep pressure gradients, winds strengthen and veer to south-west, temperatures drop, a low stratus cloud cover forms and precipitation may occur. It would not be surprising, therefore, to find that under these weather conditions surface temperatures over Durban would be generally lower than in the sea breeze case. This is confirmed by Fig. 7.5. With south-west winds the mean temperature over the work zone is lowered by 0.8 - 1.0°C relative to the mean temperature under north-east sea breeze conditions.

It has been shown that during the day south-westerly winds back to south and south-south-east in response to a sea breeze effect. These winds are responsible for the displacement of heat provided by the business district to a position north-west of this area. An elongated heat island still extends along the foot of the Berea ridge but with two centres of equal intensity located north-west of the heat island shown in Fig. 7.4. Furthermore, frictional slowing of

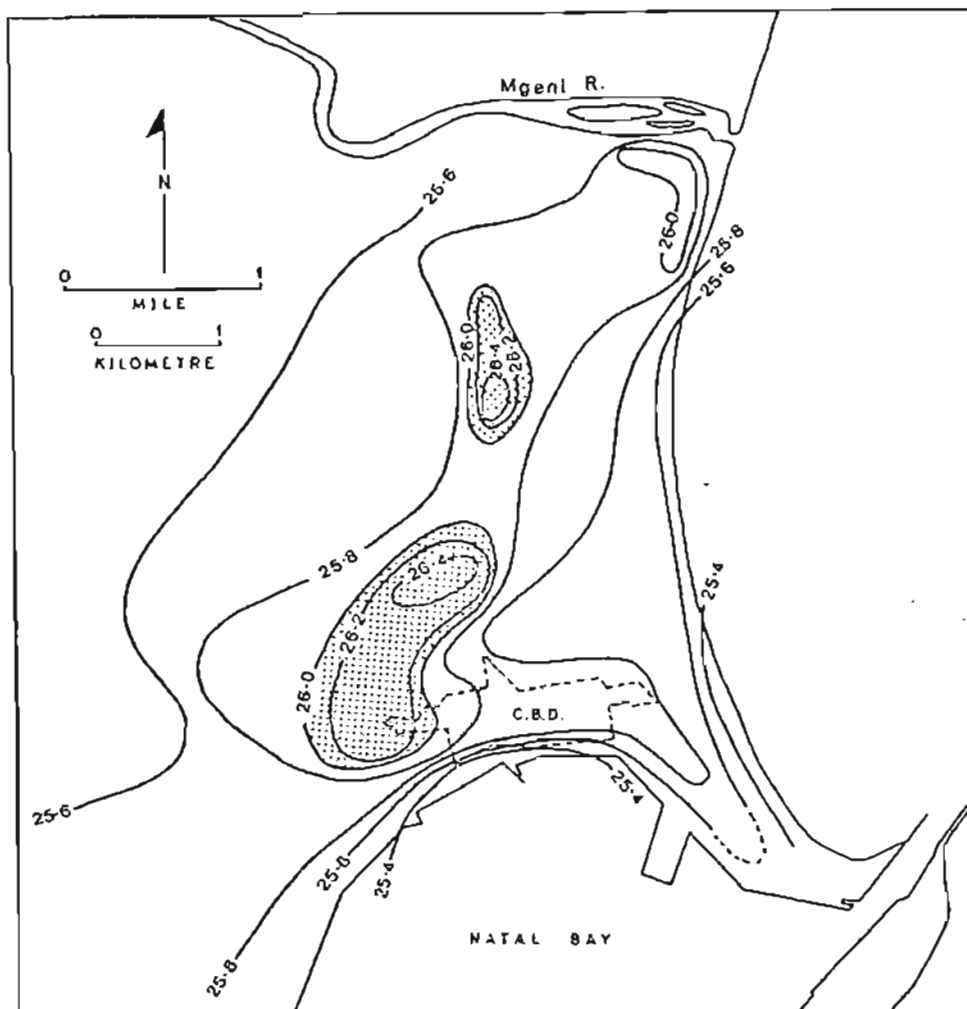


Fig. 7.5 : Isotherms ( $^{\circ}\text{C}$ ) of mean midday corrected temperatures under southerly wind conditions, November-February 1969

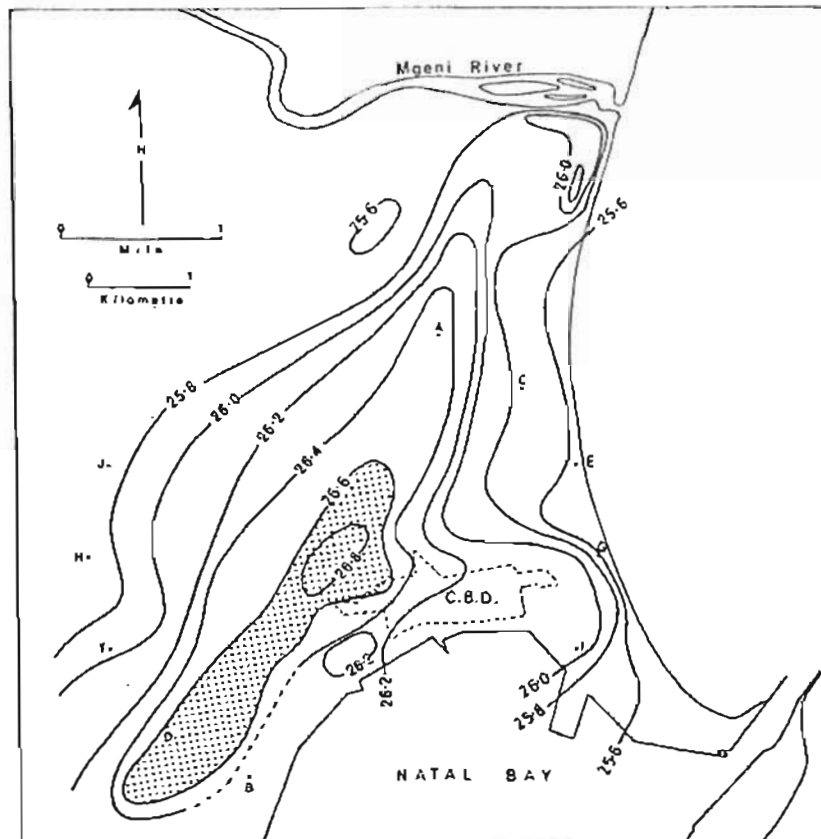


Fig. 7.6 : Isotherms ( $^{\circ}\text{C}$ ) of mean midday corrected temperatures, November-February 1969

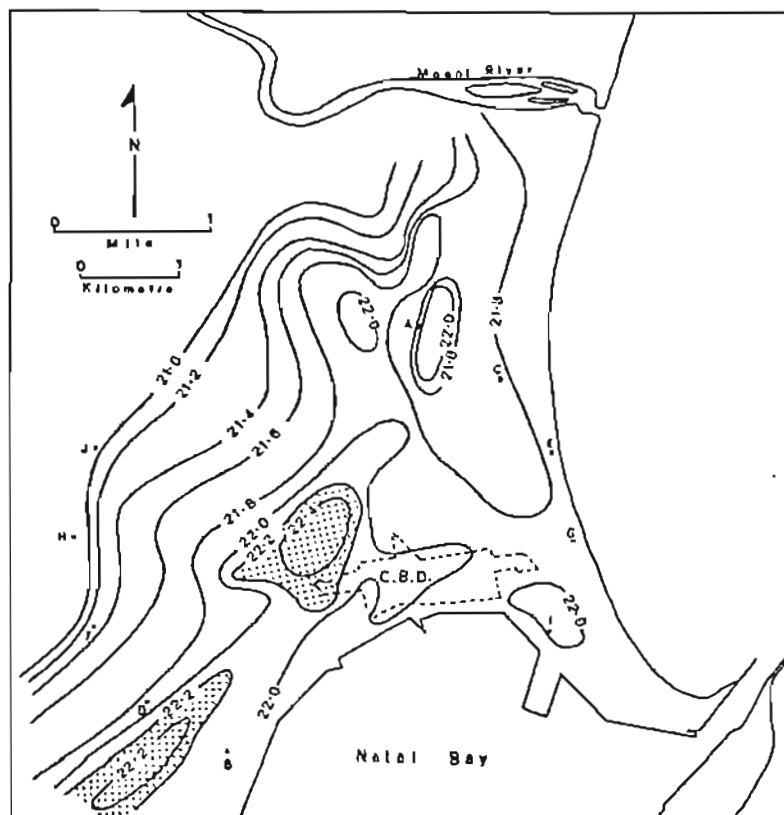


Fig. 7.7 : Isotherms ( $^{\circ}\text{C}$ ) of mean midday corrected temperatures, June 1969

surface winds over the aerodynamically rough surface of the work zone lowers wind speeds both in the business district and in the lee of this region, i.e. over the heat island. Eddy diffusion of heat in this latter region is consequently low.

#### 7.6 Comparison of mean summer and winter reduced temperature

Contrary to the findings of Balchin and Pye (1949) for Bath where summer day temperatures were found to be less in the city than without, mean midday temperatures over Durban show the existence of a heat island in summer as well as in winter (Figs. 7.6 and 7.7). Because of the high frequency of north-east sea breezes in both seasons, the centre of the heat island is displaced away from the central business district and is located at the foot of the Berea ridge.

Mean temperatures over Durban are expectedly lower in the winter months and in addition the seasonal temperature range increases with distance away from the coast (Table 7.2). This suggests that an additional component, namely distance from the sea, must be considered as a factor in the urban energy balance at Durban.

Table 7.2: Seasonal range and mean extreme temperatures ( $^{\circ}\text{C}$ ) along the east-west section G-H through the heat island

	Berea crest (H)	Heat island	Seashore (G)
Summer	25.8	26.8	25.6
Winter	21.0	22.4	21.8
Range	4.8	4.4	3.8



During winter sea breezes, weakened by reduced baroclinity, are less effective as a cooling agent on the coast and this is shown by a weak temperature gradient along the seashore relative to summer. However, in this season the development of an urban heat island would, in addition to normal production and retention of heat within the city structure, be assisted by reduced mechanical turbulence due to low mean wind speeds and by increased counter-radiation from an atmosphere that frequently remains polluted for much of the day. It is surprising, therefore, to find in Table 7.3 that the mean winter temperature differential between the heat island and the coast differs from the mean summer value by a factor of 2.

Table 7.3: Mean seasonal temperature differentials,  $\Delta T^{\circ}\text{C}$ , between the seashore, heat island and Berea crest, along the section line G-E

	Heat island - Berea crest	Heat island - seashore
Summer	1.0	1.2
Winter	1.4	0.6

An explanation for the low winter  $\Delta T$  value between the heat island and the seashore must be sought in the energy balance characteristics of the work zone region. At noon the azimuth angle of the sun is  $0^{\circ}$  but the solar elevation varies from  $84.6^{\circ}$  at mid-summer to  $35.6^{\circ}$  at mid-winter. By midday in winter because of the low elevation of the winter sun, the main streets, which are aligned approximately east-west, are still in deep shade with only the tops of tall north facing buildings receiving insolation. The street blocks are long, from 600 - 1,000 ft and this reduces warming of the city by solar heating of the narrow north-south aligned cross streets. In addition, the increased winter air pollution concentration must reduce solar energy reaching the ground (Sheppard, 1958). In combination these

factors serve to weaken the heat island in winter.

The value of  $\Delta T$  between the heat island and the Berea crest is higher in winter than in summer and is caused by lower temperatures on the Berea ridge relative to summer months. The high temperature range on the ridge given in Table 7.2 shows this to be true. Once again the lack of solar heating in winter is attributed to this phenomenon. At midday the low solar elevation means that many buildings on the south-east facing Berea ridge are in shade or casting long shadows.

#### 7.7 A spatial model of the urban heat island

As an alternative to describing day by day changes of the urban temperature field, an empirical model of the spatial distribution of mean midday temperatures recorded in Durban during the summer and winter of 1968-1969 is presented. To develop a quantitative model of the spatial variation of Durban's heat island, 12 equidistant points were linearly extrapolated along the section lines given in Fig. 7.8 and submitted to harmonic analysis (Conrad and Pollak, 1950; Brooks and Carruthers, 1953). The resulting equation describing the temperature field is of the form given in Equation 2.2 so that

$$\bar{T} = \bar{T}_s + \sum_{k=1}^6 a_k \sin \left( \frac{2\pi kd}{12} + \phi_k \right) \quad (7.3)$$

where  $\bar{T}_s$  is the space mean temperature,  $a_k$  the amplitude of wave number  $k$  with phase angle  $\phi_k$  and where  $d = 0, 1, \dots, 11$  measured in units of 0.3 miles from the points of origin A, C, E, G and I on the section lines of Fig. 7.8.

The heat island can be precisely described by determining

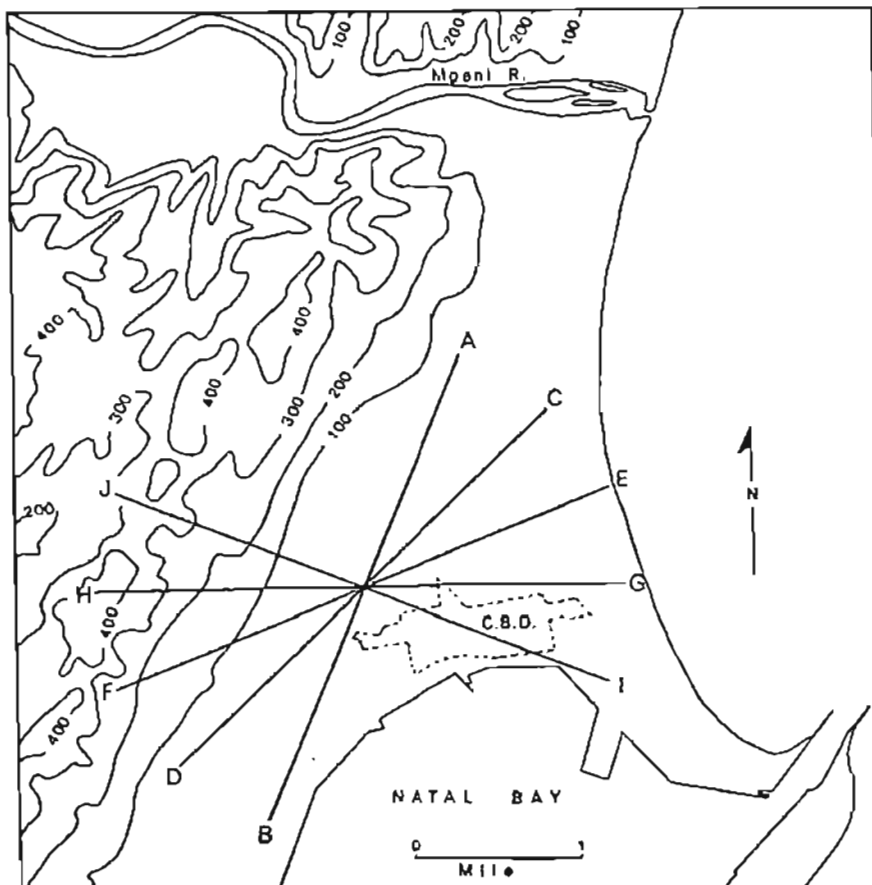


Fig. 7.8 : Location of section lines for the harmonic analysis of mean spatial temperatures over Durban

the amplitudes and phase angles of the temperature variations along the section lines cutting the heat island. Table 7.4 shows the spatial variation of these parameters for mean summer and winter reduced temperatures.

Table 7.4: Spatial distribution of mean summer and winter reduced temperature ( $^{\circ}\text{C}$ ) expressed by Equation 7.3.  $S_k$  denotes cumulative percentage contribution to the total variance.

Section	$\bar{T}_s$	Summer								
		$a_1$	$\phi_1$	$a_2$	$\phi_2$	$a_3$	$\phi_3$	$S_1$	$S_2$	$S_3$
A-B	26.5	0.24	297	0.07	113	0.04	360	88	95	98
C-D	26.5	0.43	242	0.17	200	0.14	249	75	87	95
E-F	26.2	0.56	255	0.08	139	0.06	304	94	96	97
G-H	26.2	0.45	281	1.10	65	0.08	323	90	95	98
I-J	26.2	0.42	285	0.17	90	0.11	333	81	94	99
Mean	26.3	0.42	272	0.12	121	0.09	314	86	93	97

Winter										
A-B	22.1	0.22	256	0.11	157	0.07	270	72	89	95
C-D	22.0	0.27	276	0.13	109	0.06	303	76	84	88
E-F	21.9	0.39	283	0.16	57	0.06	326	80	94	96
G-H	21.8	0.47	304	0.18	49	0.15	0	74	85	93
I-J	21.8	0.47	313	0.18	71	0.14	21	70	80	87
Mean	21.9	0.36	286	0.15	89	0.09	184	74	86	92

The degree to which a particular wave fits the observed temperature variation through the heat island is given by the percentage variance contribution of the wave to the total variance and is expressed by Equation 2.7. The lowest percentage variance contribution of each of the first three sine terms in Equation 7.3 to the total variance about the space mean summer temperature is shown in Table 7.4 to account for 75 per cent, 87 per cent and 97 per cent of the total variance; the highest percentage variance contribution

accounts for 94 per cent, 96 per cent and 99 per cent of the total variance. The percentage variance contribution of the first three sine terms about the space mean winter temperature is also high and the lowest variance contribution for each wave accounts for 70 per cent, 80 per cent and 87 per cent of the total variance.

Phase angles for successive harmonics calculated along each section line do not vary greatly and amplitudes are approximately constant fractions of the space mean temperatures. Mean amplitudes and phase angles may, therefore, be taken as representative of the area covered. Mean values of  $a_1$ ,  $a_2$ ,  $a_3$  are respectively 1.6 per cent, 0.46 per cent and 0.34 per cent of the mean summer  $\bar{T}_s$  and 1.6 per cent, 0.68 per cent and 0.41 per cent of the mean winter  $\bar{T}_s$ . The expressions

$$\begin{aligned}\bar{T} \text{ (Summer)} = \bar{T}_s + .016 \bar{T}_s \sin(kd + 272^\circ) + .0046 \bar{T}_s \sin(2kd + 121^\circ) \\ + .0034 \bar{T}_s \sin(3kd + 314^\circ)\end{aligned}\quad (7.4)$$

$$\begin{aligned}\bar{T} \text{ (Winter)} = \bar{T}_s + .016 \bar{T}_s \sin(kd + 286^\circ) + .0068 \bar{T}_s \sin(2kd + 89^\circ) \\ + .0041 \bar{T}_s \sin(3kd + 184^\circ)\end{aligned}\quad (7.5)$$

where  $k = 30$  degrees for  $d=0,1,\dots,11$  describes, therefore, the mean spatial temperature distribution for the two seasons.

Harmonic analysis provides a technique to ascertain the degree to which a symmetrical heat island over a city can be adequately described in a quantitative sense. The close correspondence of the mean spatial temperature wave over Durban to a single sine wave is demonstrated by the model which also provides for the prediction, from relatively few measuring points, of the spatial variation of temperatures over the city. The extent of other influences such as winds

which persist from one quarter to produce a steep temperature gradient at the edge of the built-up area are also reflected in the amplitude of the succeeding harmonics and the contribution of each wave to the total variance about the space mean temperature.

\* \* \* \* \*

Although day by day isotherm patterns over Durban are largely dependent upon the nature of the weather conditions and upon the direction of gradient and local winds, the mean summer and winter isotherm pattern describes a heat island cell which persists by day along the foot of the Berea ridge on the westward side of the central business district. In planning for climate and human comfort the empirical model developed for determining space mean temperatures over the city and across the heat island would be particularly useful. However, temperature alone is not a completely satisfactory measure for determining climatic comfort for man and a model which defines the spatial variation of a climatic discomfort index is also desirable. This is examined in more detail in the following chapter.

## CHAPTER 8

## PHYSIO-CLIMATIC VARIATIONS IN THE DURBAN AREA

## 8.1 Introduction

The effect of atmospheric conditions on comfort and health has been well documented. One of the earliest accounts based on scientific enquiry came from Benjamin Franklin (1750) who considered the cooling effect of evaporation on human skin. Other empirical studies were made by Lining (1748), Ellis (1758), Blagden (1775), Haldane (1904) and Leferre (1911). In addition the association of climatic conditions and human behaviour was reported at length by Huntingdon (1939, 1945, 1951).

More recently workers in this field have attempted to define a comfort zone for humans. This zone has been placed between  $32.2^{\circ}\text{C}$  and  $23.2^{\circ}\text{C}$  by Bedford (1950) and  $15.6^{\circ}\text{C}$  and  $24.4^{\circ}\text{C}$  with relative humidity at noon varying from 40 to 70 per cent by Markham (1947). Brooks (1950) maintains that the comfort zone lies between  $14.4^{\circ}\text{C}$  and  $21.1^{\circ}\text{C}$  in Britain,  $20.6^{\circ}\text{C}$  and  $26.7^{\circ}\text{C}$  in the United States and  $23.3^{\circ}\text{C}$  and  $29.4^{\circ}\text{C}$  in the tropics with relative humidity between 30 and 70 per cent. The comfort zone does not have distinct boundaries; instead a sensation of thermal neutrality, slight stress and discomfort shade into one another. The problem is further complicated by individual physiological responses while thermal requirements also vary with age and sex (Olgyay, 1962).

The problem of translating physical data about the atmosphere into physiologically useful indices has been discussed by Landsberg (1960). Terjung (1966) has attempted to fulfil this need by the development of a physio-climatic classification. However,

detailed knowledge of the manner in which weather and climate are related to human physiology clearly precede this development and this problem has been investigated by Lind (1964), Blum (1964), Jankowiak (1964), Gold (1964) and Kreider (1964).

It has been shown that urban areas are generally warmer than surrounding areas both by day and by night, the isotherm configuration of the urban heat island normally conforming to the shape of the built-up area. Both absolute and relative humidities are usually lower (Chandler, 1965; Kratzer, 1956) although studies in Leicester by Chandler (1967) suggest that while relative humidity responds to the thermal effect of the heat island as well as to the vapour content of the air, vapour pressure may frequently be higher within cities than without. In addition increased friction encountered by winds over cities results in lowered mean wind speeds (Maurain, 1947). In hot climates these conditions may combine to produce an intolerable degree of discomfort yet, to the author's knowledge, no attempts have been made to map physio-climatic variations in urban areas.

To what extent the urban environment contributes towards illness and morbidity has been the object of considerable research most of which has been directed towards the air pollution problem (Prindle, 1964). However, Brezowsky (1964) emphasises the close relationship that exists between temperature, vapour pressure and man and points out that a warm, humid environment, as well as being responsible for discomfort, is also accompanied by an increase in infections. Where cities are located in warm climates, the added heat component derived from the high heat capacity of the urban fabric may increase temperatures beyond the comfort threshold. The tendency towards this condition is assisted by high absolute humidities and low wind speeds.

Ventilation of built-up areas in hot climates is of



paramount importance if thermal comfort is to be maintained. Not only is air temperature lowered by turbulent diffusion of heat but the cooling sensation, due to heat loss by convection and evaporation from the skin, is increased. High absolute humidities may be accompanied by a sense of depression which becomes noticeable when vapour pressure exceeds 20 mbs; beyond this mark each additional millibar of pressure can be countered with 0.59 m/sec wind speed (Olgyay, 1963).

Numerous indices have been developed to measure heat stress upon humans. In some, such as the Index of Physiological Effect (Robinson et al, 1945), the Thermal Acceptance Ratio (Plummer et al, 1945), the Predicted Four Hour Sweat Rate (Wyndham et al, 1952) and the Belding-Hatch Heat Stress Index (Belding and Hatch, 1955), many variables are involved, some of which require direct measurement on the body. In others, such as the Effective Temperature Index (Houghton and Yaglou, 1923; Yaglou and Miller, 1925), the Wet Bulb Globe Index (Yaglou, 1923) and the Temperature-Humidity Index (Thom, 1959) an attempt is made to combine into a single value the thermal effect of climatic elements such as temperature, humidity, radiation and wind. These latter indices have been criticised by the tendency towards a progressive reduction in accuracy at high stress levels (Lind, 1964). However, they are simple to use and in areas which experience environmental temperatures which are not excessive can be of great value. The Effective Temperature Index is a sensory scale of warmth combining air temperature, humidity and air movement in a single index. The Wet Bulb Globe Temperature Index is determined from dry bulb, wet bulb and black globe temperatures. Air movement is not measured since this is reflected by globe temperatures. The temperature-Humidity Index, now used by the United States Weather Bureau in several parts of the country as well as in its daily forecasts, is most convenient to use being expressed by

$$THI = 0.4 (T_d + T_w) + 15 \quad (8.1)$$

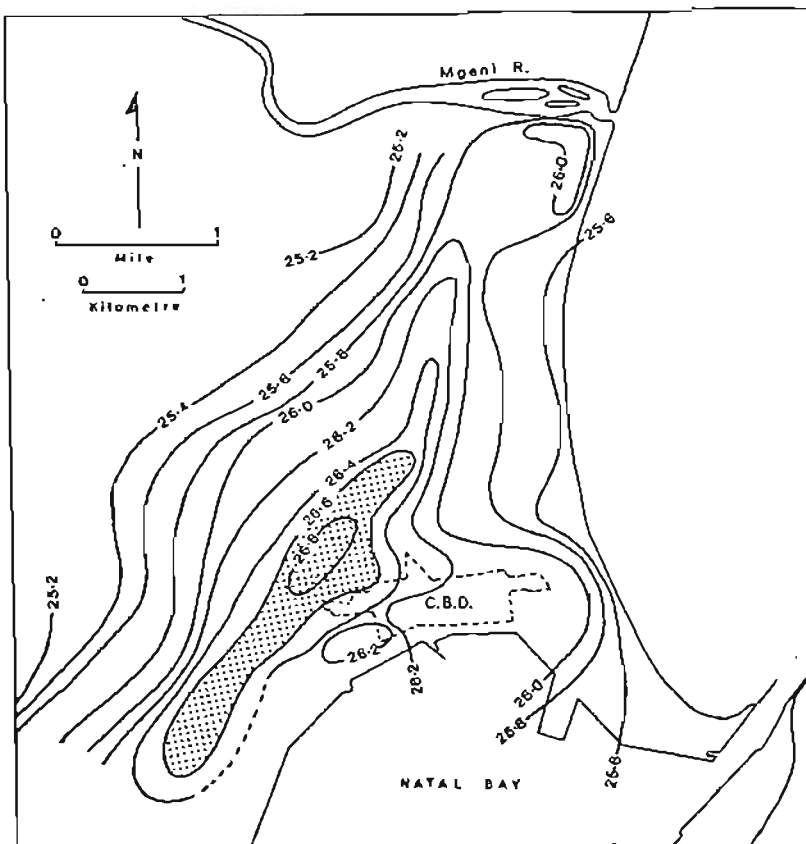


Fig. 8.1 : Isotherms ( $^{\circ}\text{C}$ ) of mean midday uncorrected temperatures, November-February 1969

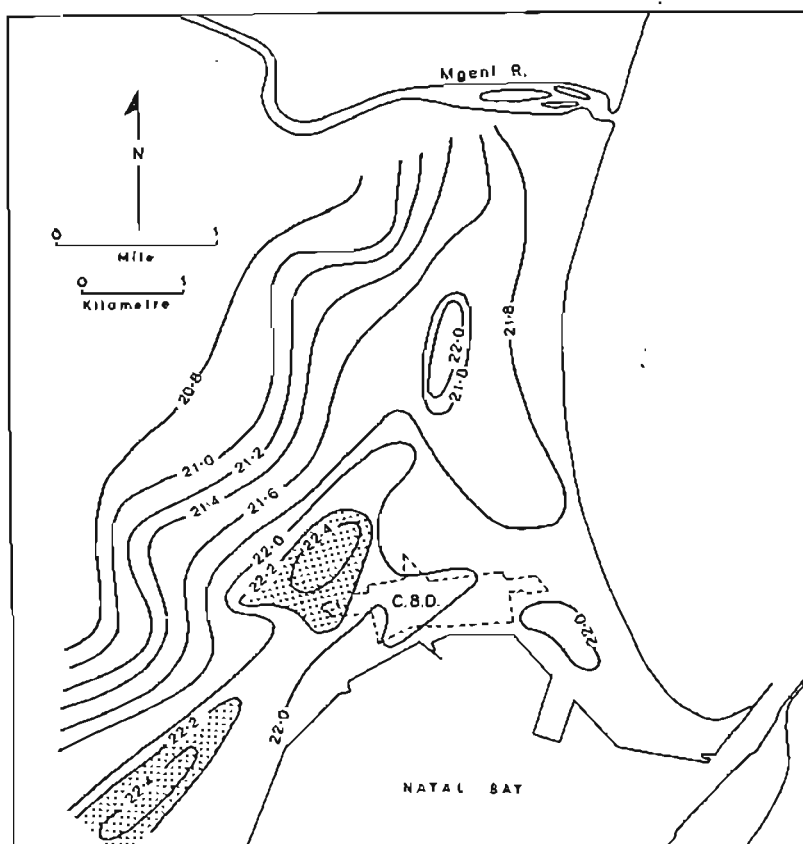


Fig. 8.2 : Isotherms ( $^{\circ}\text{C}$ ) of mean midday uncorrected temperatures, June 1969

where  $T_d$  is dry bulb temperature and  $T_w$  is wet bulb temperature in degrees Fahrenheit.

The Temperature-Humidity Index requires only two variables and is, therefore, suitable for the measurement of dry bulb and wet bulb temperatures at a large number of stations. Largely because of this it was used as the discomfort index, the spatial variation of which is discussed in this chapter. According to Thom (1959) people feel discomfort as the index rises above 70, with over half uncomfortable with the index over 75. All are uncomfortable by the time the index number reaches 79, some feeling discomfort acutely.

## 8.2 The spatial variation of temperature

It has been shown that both in summer and in winter an elongated heat island extends along the foot of the Berea ridge with its centre situated west of the central business district over a relatively open area occupied by a market, an extensive car park, wide streets and buildings which are lower than those in the business district. It was suggested that this anomaly was due to the displacement of the heat island by the north-east sea breeze and by south-south-east gradient winds away from the heat provided by the business district. In general mean temperatures were found to be lowest along the Berea crest and the seashore.

The distribution of mean temperatures uncorrected for altitude are given in Figs. 8.1 and 8.2 and Berea crest temperatures are shown to be lower than in Figs. 7.6 and 7.7. In terms of human comfort, however, the occurrence of stronger winds along the ridge crest and the seashore than in the built-up area is more important than the altitude effect, a cooling sensation being enhanced by greater evaporation from the skin. This is particularly important during

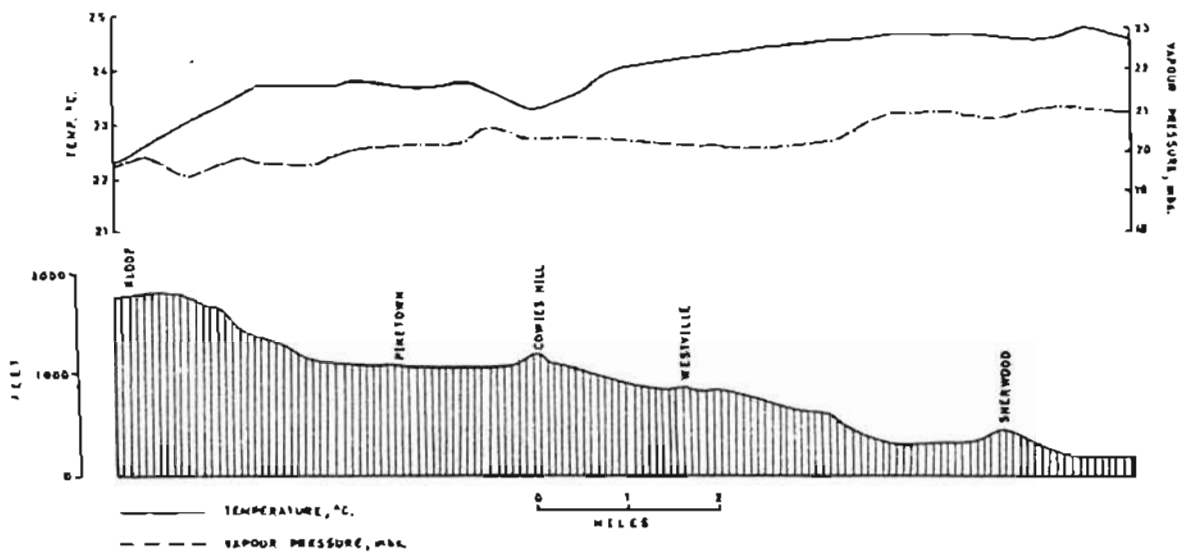


Fig. 8.3 : Section to show the reduction of mean summer temperature ( $^{\circ}\text{C}$ ) and vapour pressure (mbs) with distance inland from the Berea crastline

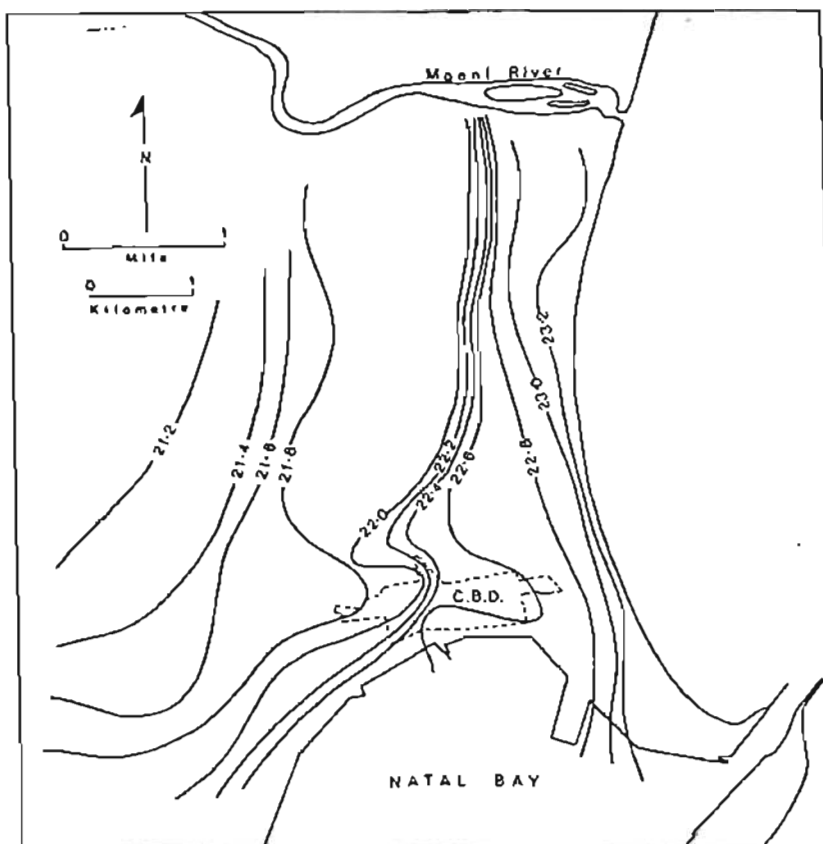


Fig. 8.4 : Mean midday vapour pressure isopleths under north-east sea breeze conditions, November-February 1969

the summer months.

From the Berea crest to the Kloof plateau the land rises approximately 1,400 ft, with an average gradient of 1 : 38. A steady decrease of mean midday temperature with height is shown in Fig. 8.3 and regression analysis of mean temperature,  $\bar{T}$  °C, against distance inland in miles,  $d$ , yields an equation of the form

$$\bar{T} = 24.82 - 0.16 d \quad (8.2)$$

### 8.3 The spatial variation of vapour pressure

Spatial and temporal variations of vapour pressure over Durban are largely controlled by diurnal, synoptic and seasonal changes in temperature and air movement. The advection of warm, moist air from sea to land by the north-east sea breeze is the main diurnal control and Fig. 8.4 shows that, not unexpectedly, highest mean midday vapour pressure occurs along the seashore with a steep vapour pressure gradient over the alluvial flats south of the Mgeni River mouth. This area is largely used for recreation and is not built over so that onshore penetration of moist air is unimpeded. The vapour pressure gradient is steep along the foot of the Berea ridge but further ascent up the ridge produces surprisingly little variation. This may be ascribed to the nature of the urban fabric on the lower slopes of the Berea ridge, closely spaced houses set in small properties being a characteristic of the area. Frictional slowing of the wind and reduced eddy diffusion inhibits mixing of air in this area. However, with increasing elevation up the ridge and more spacious properties, turbulent diffusion maintains a normal day-time humidity lapse.

The vapour pressure gradient over the work zone region is

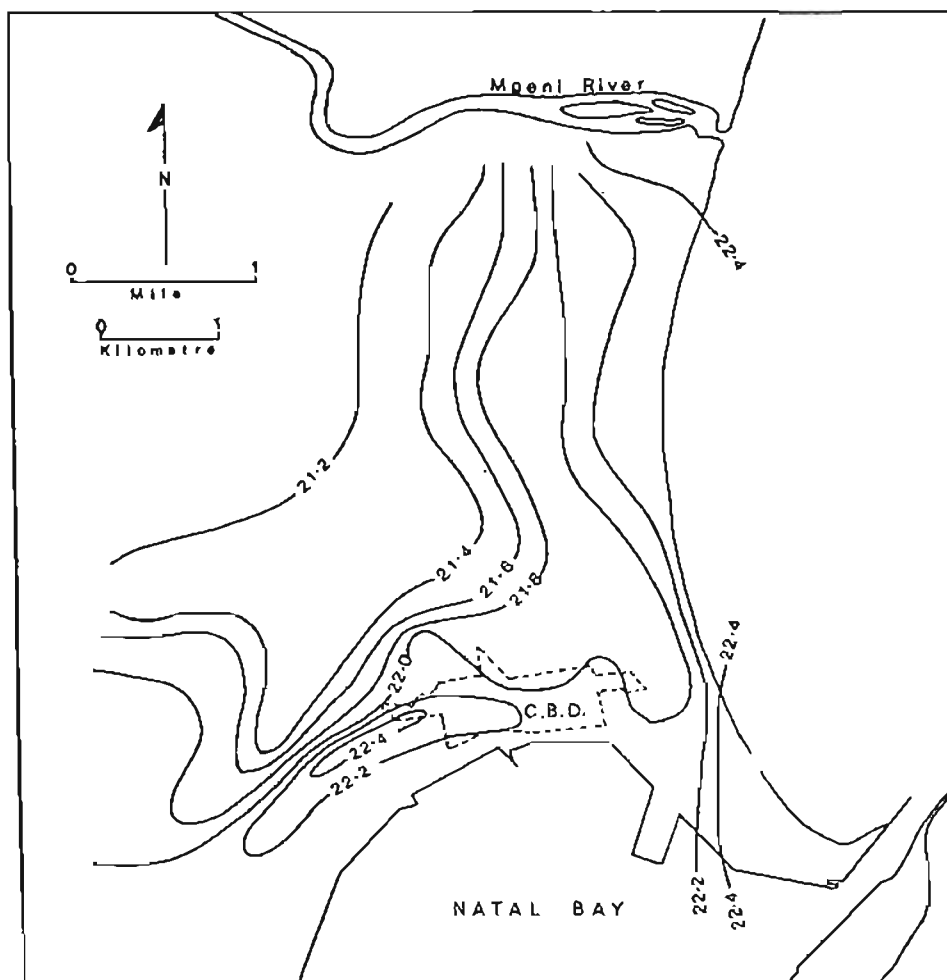


Fig. 8.5 : Mean midday vapour pressure isopleths under southerly wind conditions, November - February 1969

steep along its eastern and western edge but gentle over the central business district. Tall apartments that line the seashore block penetration of moisture into the built-up area and this accounts for the steep vapour pressure gradient along the seashore. Moist air which does penetrate into the city is trapped between buildings and because of lowered mean wind speeds over the city mixing with drier air from above is reduced. The relatively steep vapour pressure gradient along the western edge of the business district marks the transition to better mixed, drier air over the slopes of the Berea ridge.

After the passage of a low, winds veer to south and south-south-east in response to a sea breeze effect. This explains the high vapour pressure values slightly west of the central business district (Fig. 8.5). Low wind speeds in the work zone region relative to the Berea ridge inhibit mixing of moist air trapped between buildings and west of the business district the transition to drier air along the Berea ridge is sharp.

A marked seasonal change in the spatial variation of water vapour over the city is shown by an increase in mean summer vapour pressure values relative to winter by a factor of 1.85 in the business district, 1.80 along the seashore and 1.88 along the Berea crest (Figs. 8.6 and 8.7). This is primarily due to a higher water vapour capacity of the warmer air, weakening of the influence of anti-cyclones and associated near surface subsidence in this season and strengthened onshore advection of moist air by the sea breeze. In both seasons the orientation of high mean vapour pressure isolines is east-west over the work zone, evidence of trapping between buildings of moist air advected into the area by southerly winds. North of the work zone moist air advection by the north-east sea breeze is responsible for vapour pressure isolines with an inland gradient that parallel the coast.

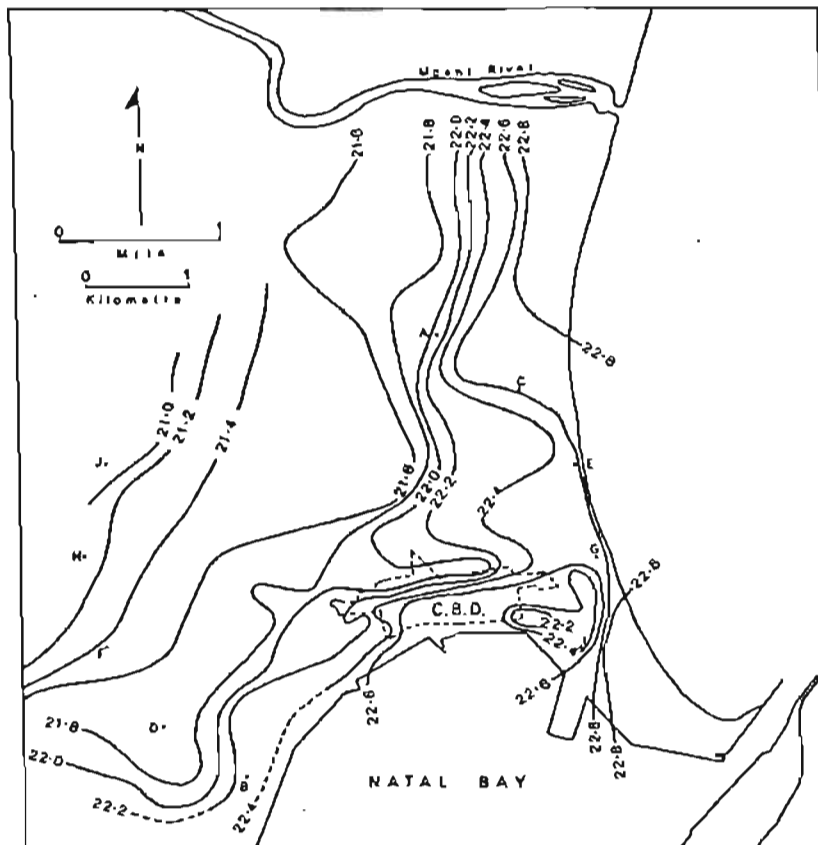


Fig. 8.6 : Mean midday vapour pressure isopleths,  
November-February 1969

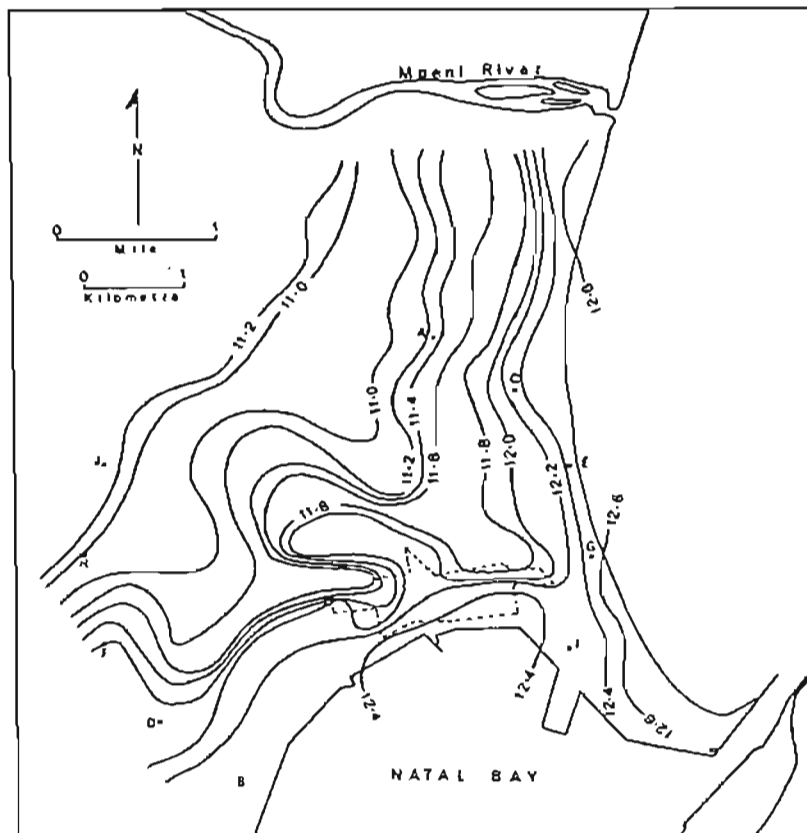


Fig. 8.7 : Mean midday vapour pressure isopleths,  
June 1969



The difference in vapour pressure values between the seafront and the Berea crest is approximately the same in both seasons; 1.7 mb in summer and 1.4 mb in winter. The gradient is steepest over the alluvial flats north of the work zone region and gentle with ascent up the Berea ridge. This phenomenon may be explained by the existence during the day of a humidity lapse which is produced by vertical mixing of air by relatively strong turbulent winds along the Berea ridge. However, in the badly ventilated high and medium density residential areas, moisture is trapped between buildings and this reduces the mixing of moist air with drier air above.

Local variations of vapour pressure are of interest. For instance, the cell of relatively low vapour pressure on the eastern side of the work zone in summer lies landward of a 30 ft high sand dune that parallels the seashore. The effect of the dune in blocking penetration of the north-east sea breeze is accentuated by multi-storied apartment blocks constructed along the crest of the dune.

Regression analysis of the decrease of mean vapour pressure,  $\bar{e}$ , along section line G-H (Fig. 7.8) results in expressions of the form

$$\bar{e} \text{ (mbs) summer} = 21.2 - 0.369 d \quad (8.3)$$

$$\bar{e} \text{ (mbs) winter} = 10.9 - 0.387 d \quad (8.4)$$

where  $d$  is distance in miles. It is interesting to note that although the value of the intercept varies between summer and winter, the slope constant remains approximately the same.

The decrease of mean summer vapour pressure values from the Berea crest to the Kloof plateau is less steep (Fig. 8.3), and may be expressed by

$$\bar{e} \text{ (mbs)} = 21.0 - 0.18 d \quad (8.5)$$

#### 8.4 A spatial model of physio-climatic variations

The aim of the Temperature-Humidity Index is to estimate the impact on human comfort of combined temperature and humidity during the summer months. This index was based on earlier estimations of 'Effective Temperature' which were developed to indicate values of temperature, relative humidity and air movement that gave the same degree of 'average comfort'. The Temperature-Humidity Index is an empirically derived expression that agrees closely with Effective Temperatures at extremes of temperature and humidity (Field, 1964).

The spatial variation of the Temperature-Humidity Index, THI, west of the city from the Berea crest to the Kloof plateau may be described by simple regression analysis of discomfort index on distance in miles,  $d$ . The resulting equation describing the variation is of the form

$$\overline{\text{THI}} = 73.59 - 0.14 d \quad (8.6)$$

Areas of high temperature in the Durban area are associated with relatively high humidities and it is, therefore, not surprising that maximum discomfort areas should correspond closely to the elongated heat island which extends along the foot of the Berea ridge (Fig. 8.8). The 75.0 discomfort index line, which determines the point at which half the population feels heat discomfort, conforms closely to the shape of the work zone region. Two cells with a discomfort index more than 75.2 are located on the western side of this region. A third area encompassed by a 75.0 discomfort index isoline is located over the high density residential area at the foot of the Berea ridge and north of the work zone region. As with the mean summer temperature map, the mean gradient is relatively steep along the seashore east of the work zone and along the foot of the Berea

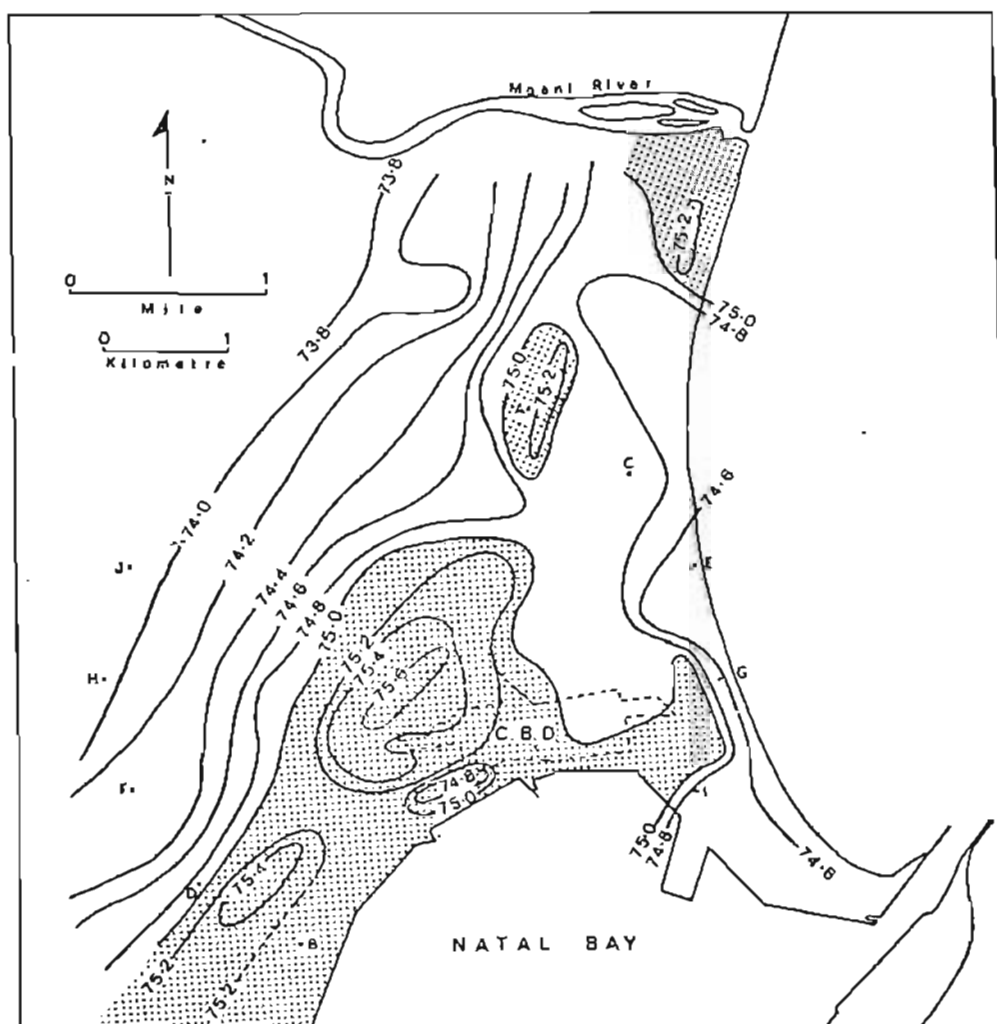


Fig. 8.8 : Mean midday isopleths of the Temperature-Humidity Index, November-February 1969

ridge. Due largely to the cooling influence of the sea breeze, areas of relative maximum comfort are located along the seashore and crest of the Berea ridge.

By the use of harmonic analysis the spatial variation of the Temperature-Humidity Index over the city can be precisely described by determining the amplitude and phase angles along the section lines cutting the cell of maximum discomfort index. Table 8.1 shows the spatial variation of these parameters.

Table 8.1: Spatial variation of mean summer Temperature-Humidity Index.  $S_k$  denotes cumulative percentage contribution to the total variance.

Section	THI	$a_1$	$\phi_1$	$a_2$	$\phi_2$	$a_3$	$\phi_3$	$S_1$	$S_2$	$S_3$
A-B	75.3	0.32	234	0.13	123	0.02	224	82	96	97
C-D	75.2	0.35	265	0.07	126	0.02	269	89	93	93
E-F	74.9	0.58	284	0.15	79	0.06	326	92	98	99
G-H	74.9	0.56	302	0.16	57	0.12	351	84	90	94
I-J	74.9	0.56	312	0.26	53	0.13	7	79	94	98
Mean	75.0	0.47	279	0.15	88	0.07	235	85	94	96

The first three terms in Equation 2.2 are shown in Table 8.1 to account for more than 79 per cent, 90 percent and 93 per cent of the variance about the space mean discomfort index. As in the case of the heat island model, phase angles for successive harmonics calculated along each section line do not vary greatly and amplitudes are approximate constant values of the space mean Temperature-Humidity Index. Mean amplitudes and phase angles may, therefore, be taken as representative of the area covered by the section lines. Mean values of  $a_1, a_2, a_3$  are respectively 0.63 per cent, 0.2 per cent and 0.09 per cent of the mean discomfort index and the expression

$$\begin{aligned} \overline{\text{THI}} = \overline{\text{THI}}_s + .0063 \overline{\text{THI}}_s \sin(kd + 279^\circ) + \\ + .002 \overline{\text{THI}}_s \sin(2kd + 88^\circ) + .0009 \overline{\text{THI}}_s \sin(3kd + 235^\circ) \quad (8.7) \end{aligned}$$

where  $k = 30^\circ$  for  $d=0,1,\dots,11$  describes the mean spatial distribution of the index.

The empirical expression developed for the spatial variation of climatic discomfort is similar to that developed to describe the heat island over Durban. The close correspondence of the mean spatial Temperature-Humidity Index wave over Durban to a single sine wave is demonstrated by the model. The value of this model clearly lies in the provision for the determination, from relatively few measuring points, of the spatial variation of a discomfort index over the city.

\* \* \* \* \*

During summer in sub-tropical latitudes, ventilation of urban areas is essential in order to reduce the sensation of discomfort which is induced by combined high temperature and humidity. The effect of poor ventilation upon climatic discomfort is clearly shown by the relative difference between mean summer Temperature-Humidity Index values in the area of closely-spaced housing along the foot of the Berea ridge and the better ventilated Berea crest and sea-front. This pattern may well change with the implementation of planning schemes. However, the present distribution of mean summer Temperature-Humidity Index values over Durban should be of interest to the architect and town planner.

PART IV

CONCLUSIONS

## CHAPTER 9

### SUMMARY AND CONCLUSIONS

It has been shown that certain characteristics of weather and climate along the Natal coast are intimately related to local wind systems. The main features of these circulations together with their influence upon selected climatic elements are briefly summarised as follows:

#### A. Sea breezes

1. The sea breeze is a periodic and predictable wind of thermodynamic origin which blows during the day and throughout the year from sea to land. At first the circulation is associated with a marked onshore component of air movement. However, this component weakens as sea breeze velocities increase and the circulation grows horizontally with time. This takes place as the wind backs in response to the Coriolis force to assume a direction parallel to the coast.

2. During summer months, increased surface heating ensures a higher frequency of sea breezes than during winter months. The sum of north-north-east, north-east and east-north-east wind frequencies per 500 for the 12 daytime hours at Durban (S.A. Weather Bureau, 1960) increase in January relative to July by a factor of 1.5. Mean wind speeds for the same directions increase correspondingly by a factor of 1.14.

3. The onset of the sea breeze circulation takes place some 2 hours earlier in summer than winter but maximum hourly wind

velocities in both seasons occur approximately at the time of maximum land-sea temperature difference.

4. The duration of the sea breeze under fine weather conditions is a function of surface heating, gradient wind direction and speed. The onset of the sea breeze is seldom delayed by offshore gradient winds along the Natal coast and in summer onshore winds appear over the coast by 0900 and prevail thereafter for about 11 hours. In winter, however, the onset of the sea breeze awaits upon the breakdown of a deep nocturnal inversion. This must be accomplished by surface heating which is weak in winter. Starting at about 1100 the sea breeze usually prevails for about 7 hours in this season.

5. Normally gradient winds over the Natal coast blow with an onshore component of air movement. Although sea breeze velocities are strengthened by this addition, the sea breeze circulation as a whole is weakened. Advection of cool sea air with a large inland fetch inhibits the rise in temperature of the atmosphere over the land and consequently the development of a steep horizontal temperature gradient within a thick layer of atmosphere. Under these conditions the onset of the sea breeze can seldom be identified by a sea breeze front.

6. Day to day variations in the depth of the sea breeze are determined by a number of factors which include changes in lapse rate, direction and speed of gradient winds and surface heating. Despite these changes the level of zero wind component, which separates onshore from offshore wind components, usually occurs below 3,000 ft.

7. The wind profile is a useful indicator of the depth and mean velocity characteristics of the sea breeze particularly where onshore gradient winds are deep. Maximum onshore wind components



in the sea breeze occur below 1,000 ft, usually between 600 - 800 ft.

8. Steepened pressure gradients ahead of a coastal low or cold front cause strong north-east gradient winds. The sea breeze circulation is weakened by the reduction of the land-sea temperature gradient under these conditions and it becomes difficult to separate the two wind components.

9. Under post-frontal weather conditions strong, cool south-west gradient winds tend to subdue the sea breeze circulation. Despite adverse conditions for sea breeze development, a component of this wind may frequently be recognised by backing of the wind to south-east during the day. This is followed by a return to south-west at night.

10. Surging of sea breeze velocities is recognised. As sea breeze velocities increase the land-sea solenoidal field may be weakened by heat diffusion and cool air advection. The resulting reduction of the sea breeze component of the onshore wind lowers the mean wind speed. A decrease in heat diffusion allows the solenoidal field to strengthen and the return of the sea breeze to its former strength occurs as a surge.

11. The periodicity of surges in the sea breeze varies with changes in gradient wind velocities and the land-sea temperature gradient. Surges tend to be confined to the zone of maximum wind velocity below 1,000 ft and were found to occur with periods ranging from 60 - 120 minutes.

12. The sea breeze, strengthened by gradient winds, advances inland as a shear line marked by a wind shift separating winds with an onshore and offshore component of motion. It is recorded as penetrating at least 40 miles inland and may extend even further.

13. Valley wind systems extend from the coast to the Drakensberg escarpment during the day to produce east-south-east to south-east winds over Natal. However, the observation in this study of east-north-east and north-east winds in the 40 mile wide coastal belt, suggests that onshore sea breezes, strengthened by gradient winds, may overlie the valley wind system in this area. Where deepening of the valley wind takes place to above ridge level, the resultant wind may be easterly.

14. Maximum upward vertical motion associated with the sea breeze circulation is normally located at the convergence zone between onshore and offshore winds. However, the deep inland penetration of onshore gradient winds prevents the development of a convergence zone of this form in the immediate coastal hinterland and local deepening of the sea breeze over the Kloof plateau is probably due to orographic convergence. The bank of cumulus clouds that line the escarpment under these conditions bears testimony to the presence of this vertical motion.

15. The location of the Natal coast in sub-tropical latitudes places this region in a belt within which climate and weather is characteristic of both tropical and middle latitudes. Surface heating in summer is more typical of tropical latitudes but increased gradient wind speeds and Coriolis force is more characteristic of middle latitudes.

#### B. Land breezes

1. In fine weather over the Natal coast the land breeze blows from land to sea as a north-west wind with speeds less than 3.5 m/sec. The Coriolis force is insignificant due to the low velocities and small fetch of this wind.

2. In both summer and winter the duration of the land breeze exceeds that of the sea breeze. This is caused by more effective nocturnal cooling of the near-surface air layer than daytime heating. At night, thermal stability in the lower atmospheric layer inhibits turbulent mixing so that in cloudless weather, radiational cooling takes place in relatively undisturbed conditions. Consequently the maximum nocturnal land-sea temperature difference is larger than daytime values by a factor of 3.25 in winter and 1.74 in summer. This results in a land breeze duration of 16 hours in winter and 13 hours in summer.

3. The deeply dissected and wide Mgeni River valley west of the Kloof plateau is reduced to a comparatively narrow gorge north-east of the plateau (Fig. 9.1). The onset of the mountain wind over the plateau takes place as cold air accumulates upstream of the gorge, deepens and finally overflows onto the plateau. With similar development in other valleys a mountain-plain wind develops, at first as a shallow wind but deepening throughout the night.

4. The land breeze circulation is shallow at first and restricted to a narrow coastal belt. As the circulation grows with time, the belt of offshore winds deepen and migrate inland ultimately to surmount the Kloof plateau by 2100. Concomitant with this development is the deepening to above ridge level of mountain winds in Natal river valleys and the subsequent development of a mountain-plain wind blowing towards the coast. Integration of the mountain-plain wind into the land breeze takes place over the Kloof plateau (Fig. 9.2).

5. The pre-dawn winter depth of the land breeze over Durban was found to be about 800 ft. This is in excess of most published observations of the land breeze depth.

6. When land breeze and mountain-plain wind directions coincide, the upper limit of the land breeze is difficult to define. Under

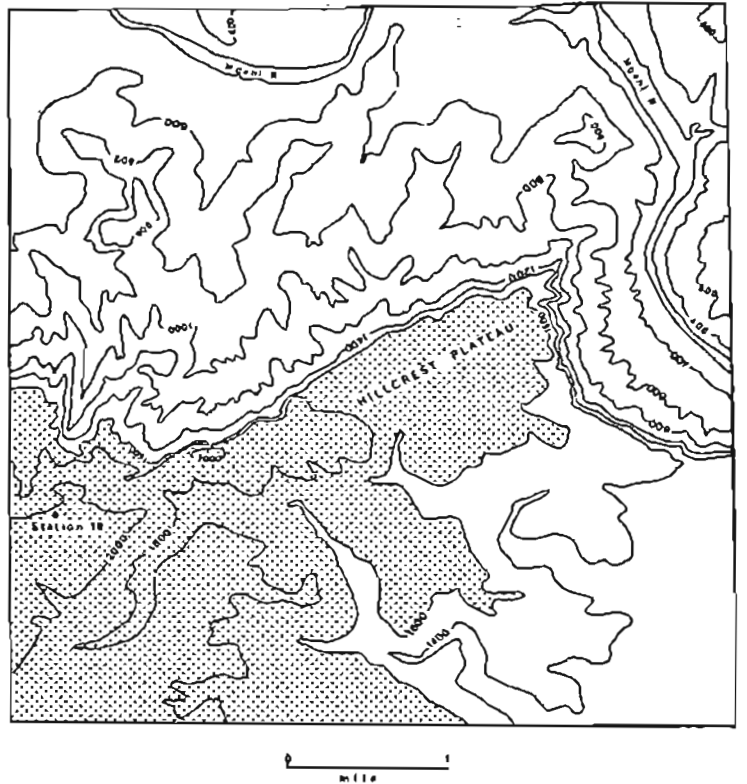


Fig. 9.1: Relief and location map of the Hillcrest scarp region

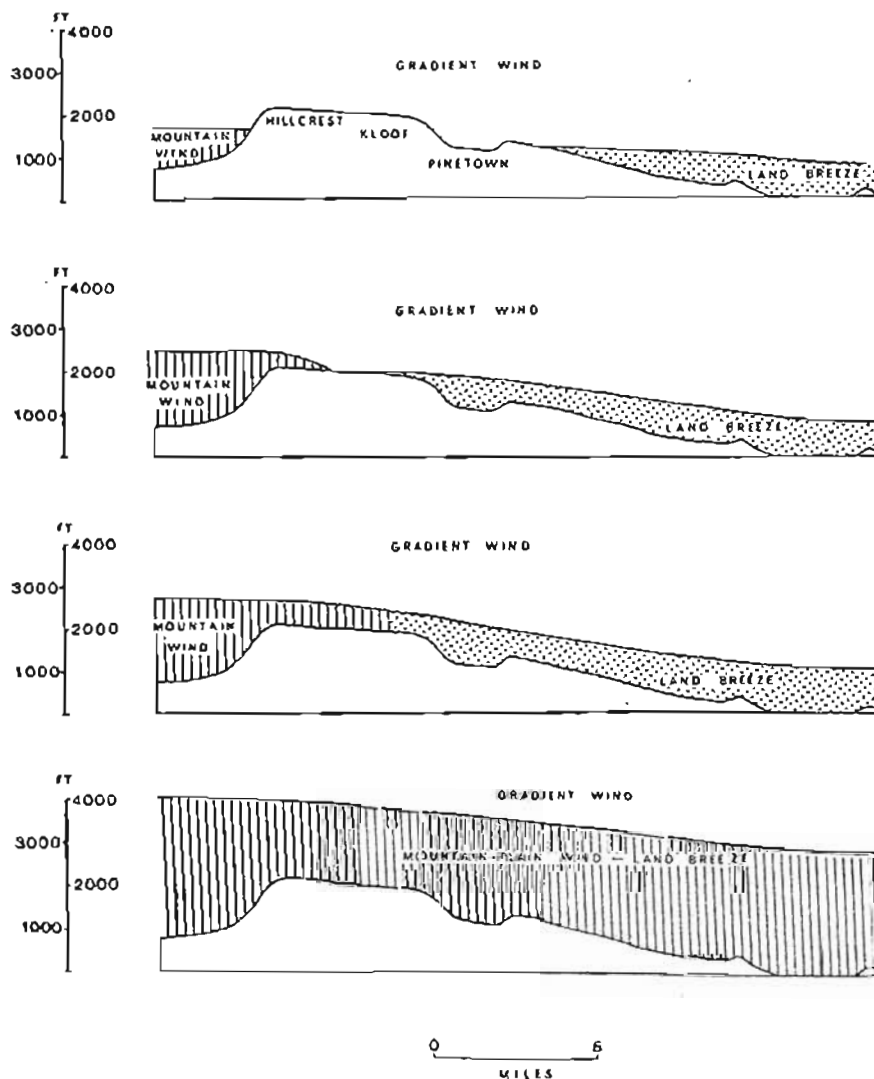


Fig. 9.2: Model to show stages of mountain wind deepening and overflow onto the Kloof-Hillcrest plateau

these conditions the combined circulations may deepen during the night to above 3,000 ft.

7. The seaward movement of the land breeze at first takes place in a shallow layer which later deepens by addition of the mountain-plain wind component. By sunrise a layer of cool land air may extend to the base of the subsidence inversion and penetrate some 5 miles seawards. The discontinuity between the land and sea air is frequently sharp and clearly visible due to accumulated atmospheric pollution in the land air.

#### C. Drainage winds

1. The onset of drainage winds in coastal valleys takes place at night when the thermally-induced pressure gradient reverses from upvalley to downvalley. The arrival of the drainage wind is marked by an abrupt temperature drop as a local front of cold air advances downvalley.

2. The temperature change associated with the onset of drainage winds is smaller than recorded in the Natal midlands. On summer days the mean maximum land-sea temperature difference is only of the order of  $2.0^{\circ}\text{C}$ . Since the diurnal temperature change over the sea is small, land heated air is not required to cool as far as that in inland areas before the temperature gradient is reversed in river valleys.

3. In the Durban area cold air, which drains from the mouth of the Umbilo River valley, moves across the alluvial flats at the head of Natal Bay, dams against the Bluff ridge and is then channelled northwards between the Bluff and Berea ridges. Low velocity south-west drainage winds in the Natal Bay area occur nightly in fine winter weather.

4. The mean depth of south-west drainage winds over Natal Bay is approximately 200 ft.

5. Where land breezes and drainage winds have the same direction, it becomes difficult to separate the land breeze component from the drainage wind. Under these conditions the wind profile of the downvalley component of motion does not normally show a finite upper limit. The maximum velocity of this component is shown to occur at 200 ft in the Mgeni River valley and, by comparison with drainage winds in the Natal Bay area, this suggests some integration of drainage winds and land breezes.

6. Periodic surging seems to be a characteristic of low-level air movements in the Mgeni River valley. A measured 50 minute period at 200 ft falls within the time range for periodic surges in the mountain wind over Pietermaritzburg.

7. Under strong gradient wind conditions, the development of a land breeze circulation is inhibited before the suppression of drainage winds. On occasions cold air movement is restricted to river valleys and the seaward penetration of this air depends upon the relative strength of the drainage and gradient winds.

8. Westerly drainage winds from the Mgeni River valley entrain cold air into the gradient wind over the sea. When this latter wind is north-east the valley air is returned to land and moves over the Durban central business district.

9. After sunrise the source of cold air from valley sides is shut off by slope heating and accompanying convective mixing. Without replacement of the cold air in the valley bottoms, the depth of the drainage wind in the Natal Bay area is progressively reduced. The dissipation of the wind is usually accompanied by downward penetration of the north-west land breeze.

- D. The influence of local winds upon selected climatic elements in the Durban area

*Nocturnal precipitation*

1. Throughout the year the diurnal variation of rainfall frequency and amount over Durban is higher by night than by day. Both measures reach a peak at 2100 and decline sharply thereafter. Precipitation is largely a summer phenomenon, however, and the mean February rainfall amount exceeds the mean July amount by a factor of 3.65.
2. The frequency distribution of hourly rainfall occurrence between specified limits is positively skewed with 63.2 per cent of January and 58.7 per cent of July rainfall occurrences producing precipitation less than 1.0 mm/hr. Much of this low intensity rainfall is precipitated at night, 42.9 per cent in January and 36.5 per cent in July.
3. On 47 per cent of raindays precipitation over the period 1958-67 was restricted to the night period alone. However, when rain does fall during the daytime it is most likely to continue into the night. On only 11 per cent of raindays was precipitation restricted to the daytime period. The operation of two main rainfall processes is thus suggested.
4. Low intensity but high frequency nocturnal rainfall occurs most frequently in relatively unstable air at the rear of coastal depressions. By undercutting moist, unstable sea air the land breeze acts as a trigger to release the instability and rainfall results. This precipitation is inhibited after 2100 by the arrival of mountain-plain winds over the coast.

5. Rainfall which occurs through the day and night is the product of frontal depressions and is not related to local circulations.

6. A third rainfall process, less distinctive on rainfall records because of its low frequency of occurrence, is caused by thunderstorms. These storms occur mainly after sunset during summer.

7. Radar observations show that thunderstorms which reach Durban in the evening, originate during the early afternoon in the Kokstad area some 110 miles south-west of the city. The suitability of this area as a breeding ground for storms is suggested by the possible existence, under particular synoptic conditions, of a lee depression in this area into which moist onshore winds converge from the north-east.

8. It is suggested that thunderstorms are maintained at the convergence zone between onshore and offshore winds over Natal. The onshore component within 40 miles of the coast is maintained by sea breezes as well as gradient winds so that the seaward movement of storms must await upon the weakening of this zone. This takes place towards evening as the sea breeze circulation dies and the subsequent movement of thunderstorms towards the coast is probably in phase with the retreating convergence zone.

#### *Temperature*

9. Cold air which drains south-west in the Natal Bay dams against tall buildings that line its northern shore. Part of this air flow is diverted towards the bay entrance while the remainder penetrates the work zone region from the south. Consequently the mean winter nocturnal heat island is split into two cells one lying



west of the main stream of cold air and the other in the sea front zone.

10. A thermal belt extends the length of the Berea ridge on winter nights. This is primarily caused by lowering of ridge top temperatures by the land breeze and along the base of the ridge by radiational cooling and drainage winds.

11. By midday in summer, the mean position of the urban heat island is displaced westward of the central business district by the north-east sea breeze. Turbulent dissipation of the energy of the sea breeze over the aerodynamically rough surface of the business district, results in low wind speeds in the heat island area. Consequently diffusion of accumulated and locally generated heat is low.

12. When winds blow south-east the mean position of the midday summer heat island is displaced north-west of the central business district. Tall buildings that line the northern bayside are, however, partly effective in blocking penetration of these winds into the city and this is shown by a steep temperature gradient in this area.

13. Mean midday temperatures in the Durban area show a heat island situated on the western flank of the central business district in both summer and winter. This is in contrast to the expected pattern in which the centre of the heat island coincides with the centre of the city as in Johannesburg (Goldreich, 1969).

14. By midday under both north-east and south-west gradient wind conditions, a sea breeze component causes onshore winds over Durban. Strengthened onshore winds which advect cool sea air over the city cause temperatures to be lowered most along the seashore and Berea ridge crest.

15. Both in summer and in winter the mean spatial temperature wave over Durban corresponds closely to a single sine wave. This is largely due to the sea breeze which lowers temperature along the seashore and ridgetop and displaces the mean midday heat island to a position approximately midway between these areas. This enables the spatial variation of mean temperature across the heat island to be described by a simple harmonic model. This model also facilitates the prediction of the spatial variation of temperature over the city from relatively few measuring points.

*Physio-climatic variations*

16. In the summer months, climatic discomfort in sub-tropical regions is caused largely by combined high temperature and humidity. Under these conditions the role of wind in the partial alleviation of heat discomfort is important.

17. As with the spatial variation of temperature over the city, vapour pressure variations are also influenced by air movement and the urban fabric. Under north-east sea breeze conditions, highest summer midday vapour pressures are located over the seashore and these values decrease inland. Along the foot of the Berea ridge low wind speeds, induced by the physical nature of the high density residential area, reduce the rate of mixing of air. Consequently the vapour pressure gradient is steep in this region relative to more elevated areas along the ridge.

18. Tall apartments that line the seashore east of the central business district block moist air advection over this region by the sea breeze. Consequently mean midday summer vapour pressure is slightly lower over the business district than north of the work zone in less built-up areas.

19. With south to south-east winds the zone of steep vapour pressure gradient is located along the foot of the Berea ridge north-west of Natal Bay.

20. A twofold increase in mean vapour pressure values takes place between winter and summer with highest humidity in the latter season.

21. Because of the association of high temperature with relatively high humidity over Durban, maximum discomfort areas, defined by the Temperature-Humidity-Index, correspond closely to the elongated heat island that extends along the foot of the Berea ridge.

22. The spatial variation of the Temperature-Humidity Index over the city is precisely described by a simple harmonic model. As with temperature, the mean spatial discomfort index wave shows a high correspondence to a single sine wave.

The nature and characteristics of local wind systems on the Natal coast which are described in this study also provide a means of assessing the potential for the transport or dispersal of atmospheric pollution. While it is not the intention to examine Durban's air pollution problem, it is perhaps appropriate to conclude by indicating briefly the manner in which the information in this study may be used to show how polluted air can be transported over the city and coast.

In fine winter weather, pollution emitted at night from sources along the Natal coast is moved seawards by the land breeze-mountain-plain wind. Pollution emitted from a single source under these conditions stays visible for a considerable distance and can

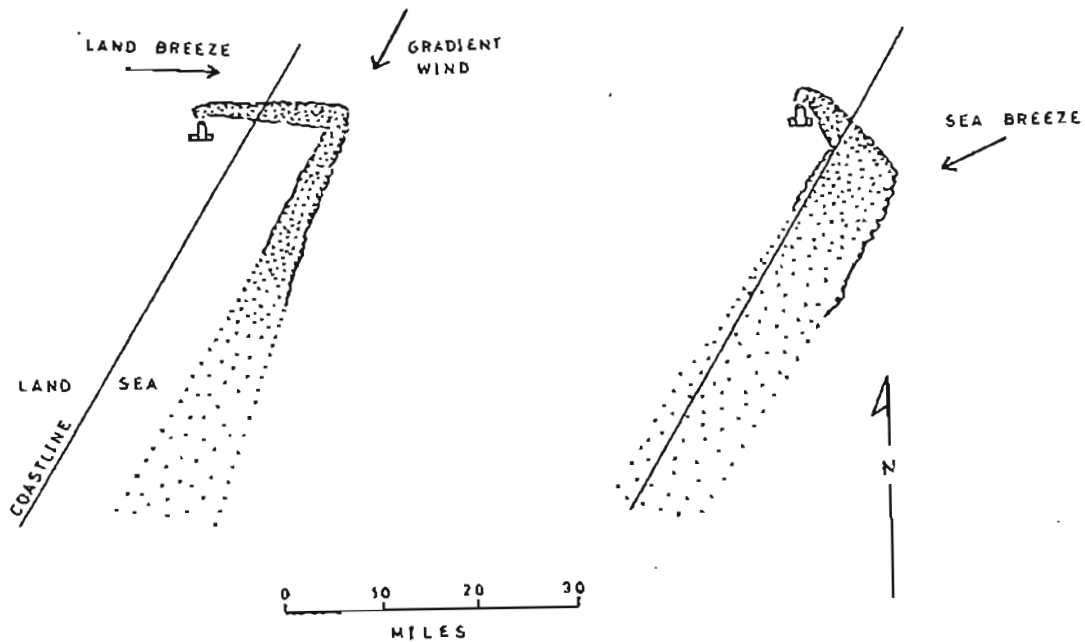


Fig. 9.3 : The movement of atmospheric pollution from a single source by local circulations and gradient winds on the Natal coast

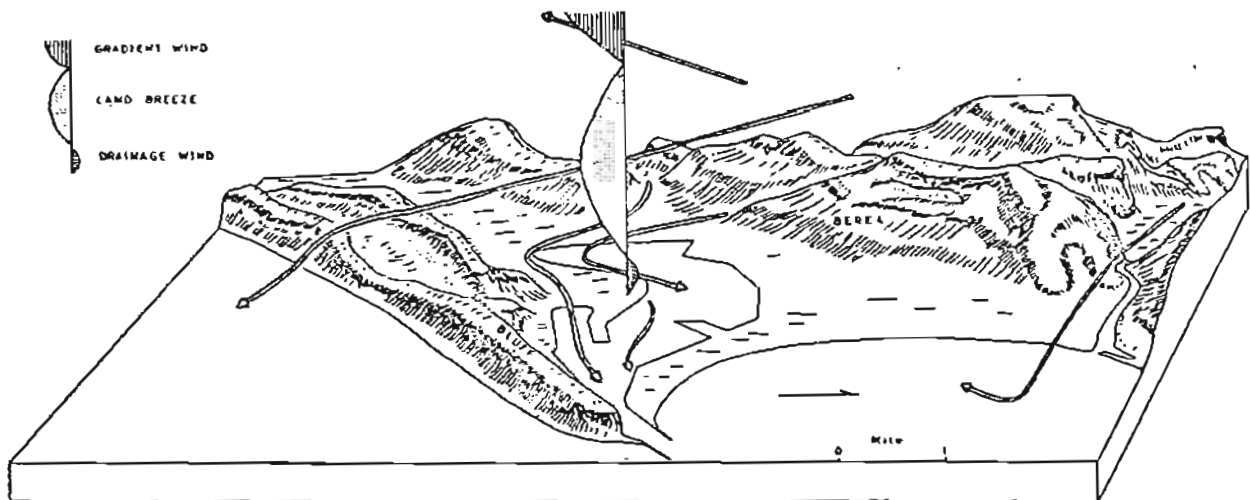


Fig. 9.4 : Diagrammatic model to show nocturnal local air circulations during winter in the Durban area

be used as an indicator of local circulation characteristics. Aircraft observations indicate that the north-west land breeze veers to north or north-north-east over the sea at the land breeze-gradient wind boundary. Consequently a plume at first carried seaward by the land breeze-mountain-plain wind soon turns to parallel the coast. Individual plumes which behave in this manner have been visually traced by the use of aircraft for over 60 miles (Fig. 9.3). Veering of the gradient wind to east-north-east or the onset of a weak sea breeze can return this pollution to the land many miles downwind from its source. The existence of these winds and their potential for the transport of atmospheric pollution should be regarded as a primary consideration for all planning along the Natal coast.

Atmospheric stability during the winter months, the nature of the topography and the characteristics of local topographically-induced winds as well as land and sea breezes are major factors which could produce a serious air pollution problem over Durban. At night the upper level of the nocturnal radiation inversion is frequently found to be associated with a low-lying subsidence inversion and under these conditions turbulence in near surface winds is damped out and ventilation of the area between the Bluff and Berea ridges is particularly poor.

Air drainage down the Umbilo and Mhlathuzana River valleys and over the alluvial flats at the head of Natal Bay provides a vehicle for the nocturnal transportation of polluted air from these areas. Since this air is diverted to move between the Bluff and Berea ridges below 200 ft, pollutants in the drainage wind may contribute to the contamination of the air over the city (Fig. 9.4).

Polluted air from the Springfield flats is initially moved eastward by the drainage wind and its seaward penetration depends upon the strength of the drainage winds relative to gradient winds



over the sea. Entrainment of the cool land air into a north-east gradient wind may cause an advection of the polluted air over the city. As the advection is slowly retarded by gentle convergence with the south-west drainage wind from the opposite direction, the situation is exacerbated. Consequent upon this condition, if climate alone is considered, the Springfield flats is a highly unfavourable location for industrial development.

\* \* \* \* \*

While it must be acknowledged that large-scale circulation patterns are the dominant controls of weather and climate, this study clearly shows that the influence of local air circulations upon the mesoclimate of Durban should also be recognised. The considerable effect of land and sea breezes upon mean urban temperatures has been described. In addition these winds are shown to be closely associated with certain precipitation processes along the Natal coast. Finally, the significance of local winds as a means of transporting air pollution has been briefly mentioned. It is to be hoped that future planning along the Natal coast will take these features into consideration.

## REFERENCES

- Arnold, A., 1948 : On the accuracy of winds aloft at low altitudes. Bull.Amer.Met.Soc., 29, 140.
- Ayers, H., 1958 : A sample of single theodolite wind errors in the coast range of Oregon. Bull.Amer.Met.Soc., 39, 279.
- ... 1961 : On the dissipation of drainage wind systems in valleys in morning hours. Jour.Met., 18, 560.
- Ball, F.K., 1960 : Finite tidal waves propagated without change of shape. Jour.Fluid Mech., 9, 506.
- Balchin, W.G.V. and N. Pye, 1949 : Temperature and humidity variations in an urban area of diversified relief. Jour.Manchester Geog.Soc., 55, 1.
- Bedford, T., 1950 : Environmental warmth and human comfort. Brit. Jour.Appl.Phys., Feb., 33.
- Beebe, R.G. and F.C. Bates, 1955 : A mechanism for assisting in the release of convective instability. Mon.Wea.Rev., 83, 1.
- Belding, H.S. and T.F. Hatch, 1955 : Index for evaluating heat stress in terms of resulting physiologic strains. Heating, Piping and Air Conditioning. August, 129.
- Bjerknes, V., J. Bjerknes, H. Solberg and J.T. Bergeron, 1933 : Physikalische hydrodynamik. Verlag von Julius Springer, Berlin.
- Blagden, C., 1775 : Experiments and observations in a heated room. Phil.Trans.Roy.Soc.Lond., 65, 111.
- Blecker, W. and M.J. Andre, 1951 : On the diurnal variations of precipitation particularly over central U.S.A. Quart. Jour.Roy.Met.Soc., 77, 260.
- Blum, H.F., 1964 : Effects of sunlight on the human body. Medical climatology, (Ed. Licht,S.). Elizabeth Licht, New Haven.
- Bornstein, R.D., 1968 : Observations of the urban heat island effect in New York City. Jour.Appl.Met., 7, 575.

- Brezowsky, H., 1964 : Morbidity and weather. Medical climatology, (Ed. Licht, S.). Elizabeth Licht, New Haven.
- Brooks, C.E.P., 1950 : Climate in everyday life. Ernest Bemm, London.
- Brooks, C.E.P. and N. Carruthers, 1953 : Handbook of statistical methods in climatology. H.M.S.O., London.
- Browning, K.A. and R.J. Donaldson, 1963 : Airflow and structure of a tornado storm. Jour.Atmos.Sci., 20, 533.
- Bryson, R.A., 1957 : Fourier analysis of the annual march of precipitation in Australia. Technical report on meteorology and climatology of arid regions, No.5, Inst. of Atmos. Physics, University of Arizona.
- Carte, R., 1966 : Features of Transvaal thunderstorms. Quart.Jour.Roy.Met.Soc., 92, 290.
- Chandler, T.J., 1965 : The climate of London. Hutchinson, London.
- ... 1967 : Absolute and relative humidity in towns. Bull.Amer.Met.Soc., 48, 394.
- Conrad, V. and L.W. Pollak, 1950 : Methods in climatology. Harvard University Press, Cambridge, Massachusetts.
- Crow, L.W., 1964 : Airflow related to Denver air pollution. Jour.Air Poll. Control Assn., 14, 56.
- Davidson, B., 1961 : Valley wind phenomena and air pollution problems. Jour.Air Poll. Control Assn., 11, 364.
- Davidson, B. and K.P. Rao, 1963 : Experimental studies of the valley-plain wind. Int.Jour.Air Water Poll., 7, 907.
- Defant, F., 1951 : Local winds. Compendium of meteorology, (Ed. Malone, T.F.). American Meteorological Society, Boston.
- Dessens, H., 1950 : Severe hailstorms are associated with very strong winds between 6000 and 12000 m. Physics of precipitation. Geophys. Monograph, No.5, Amer.Geophys.Un., Washington D.C.
- Dexter, R.V., 1944 : The diurnal variation of warm frontal precipitation and thunderstorms. Quart.Jour.Roy.Met.Soc., 70, 129.
- ... 1958 : The sea breeze hodograph at Halifax. Bull.Amer.Met.Soc., 39, 241.



- Douglas, R.H. and W. Hirschfeld, 1959 : Patterns of hailstorms in Alberta. Quart.Jour.Roy.Met.Soc., 85, 105.
- Duckworth, F.S. and J.S. Sandberg, 1954 : The effect of cities upon horizontal and vertical temperature gradients. Bull.Amer.Met.Soc., 35, 198.
- Ellis, H., 1758 : An account of the heat of the weather in Georgia. Phil.Trans.Roy.Soc.Lond., 50, 754.
- Estoque, M.A., 1962 : The sea breeze as a function of the prevailing synoptic situation. Jour.Atmos.Sci., 19, 244.
- Feagle, R.G., 1950 : A theory of air drainage. Jour.Met., 7, 227.
- Field, F., 1964 : Measurement of weather. Medical climatology, (Ed. Licht, S.). Elizabeth Licht, New Haven.
- Fisher, E.L., 1960 : An observational study of the sea breeze. Jour.Met., 17, 645.
- ... 1961 : A theoretical study of the sea breeze. Jour.Met., 18, 216.
- Franklin, B., 1758 : Letter from Benjamin Franklin to John Lining, London, June 17, 1758. The works of Benjamin Franklin. Boston.
- Frizzola, J.A. and E.L. Fisher, 1963 : A series of sea breeze observations in the New York City area. Jour.Appl. Met., 2, 722.
- Fugita, T., 1958 : Meso-analysis of the Illinois tornadoes of 9 April 1952. Jour.Met., 5, 77.
- Fulks, J.R., 1951 : The instability line. Compendium of Meteorology, (Ed. Malone, T.F.). American Meteorological Society, Boston.
- Geiger, R., 1965 : Climate near the ground. Harvard University Press, Cambridge, Massachusetts.
- Gleeson, T.A., 1951 : On the theory of cross-valley winds arising from differential heating of the slopes. Jour.Met., 8, 398.
- ... 1953 : Effects of various factors on valley winds. Jour.Met., 13, 279.
- Godske, C.L., 1934 : Über bildung und vernichtung der zirkulationsbewegungen einer flüssigkeit. Astrophys.Norv., 1, 11.

- Gold, J., 1964 : Pathologic effects of heat exposure. Medical climatology, (Ed. Licht, S.). Elizabeth Licht, New Haven.
- Goldreich, Y., 1969 : A preliminary study of aspects of Johannesburg's urban climate. Unpub. Ph.D. Thesis, University of Witwatersrand, Johannesburg.
- Haldane, J.S., 1904 : Report to the Secretary of State for the Home Department on the health of Cornish miners. London.
- Hamilton, J.W., 1958 : Some features in the use of radar in forecasts and warnings of heavy hail, damaging winds and/or tornadoes. Proc. Seventh Weather Radar Conf., American Meteorological Society, Boston.
- Hattle, J.B., 1944 : Tech. Note No. 27. South African Air Force Meteorological Section, Pretoria.
- Haurwitz, B., 1947 : Comments on the sea breeze circulation. Jour. Met., 4, 1.
- Haurwitz, B. and J.M. Austin, 1944 : Climatology. McGraw Hill, New York.
- Hewson, E.W., 1937 : The application of wet bulb potential temperature to air mass analysis III; rainfall in depressions. Quart.Jour.Roy.Met.Soc., 63, 323.
- Hewson, E.W. and G.C. Gill, 1944 : Meteorological investigation in the Columbia River valley near Trail. U.S. Bureau Mines Bull., 453, 23.
- Heywood, G.S.P., 1933 : Katabatic winds in a valley. Quart.Jour.Roy. Met.Soc., 49, 29.
- Hoecher, W.H., 1957 : Abilene, Texas, area tornadoes and associated radar echoes of May 27, 1956. Proc. Sixth Weather Radar Conf., American Meteorological Society, Boston.
- Horn, L.H. and R.A. Bryson, 1960 : Harmonic analysis of the annual march of precipitation over the United States. Annls. Assn.Amer.Geog., 50, 157.
- Houghton, F.C. and C.F. Yaglou, 1923 : Determining equal 'comfort' lines. Trans.Amer.Soc.Heat and Vent. Engrs., 29, 163.
- Howard, L., 1833 : The climate of London deduced from meteorological observations made in the metropolis at various places around it. Longman and Co., London.

Huntingdon, E., 1939 : Civilisation and climate. Yale University Press, New Haven.

... 1945 : Mainsprings of civilisation. John Wiley and Sons, New York.

... 1951 : Principles of human geography. John Wiley and Sons, New York.

Hydrometeorological Report, No. 5, 1947 : Thunderstorm rainfall. Hydrometeorological section, U.S.A.

Jackson, J.K., 1966 : Some aspects of the weather on the air routes over Natal. Weather Bureau News Letter, No. 209, 140.

Jackson, S.P., 1947 : Airmasses and the circulation over the plateau and coast of South Africa. South African Geog.Jour., 29, 1.

... 1954 : Sea breeze studies in South Africa. South African Geog.Jour., 36, 13.

Jankowiak, J., 1964 : Effects of wind on man. Medical climatology, (Ed. Licht, S.). Elizabeth Licht, New Haven.

Jeffreys, H., 1922 : On the dynamics of wind. Quart.Jour.Roy.Met.Soc., 48, 29.

Kimble, G.H.T., 1946 : Tropical land and sea breezes. Bull.Amer.Met.Soc., 27, 99.

Koschmeider, H., 1941 : Danziger seewindstudien. Forsch-Arb. Meteor. Inst.Danzig, 10.

Kraus, E., 1945 : Climate made by man. Quart.Jour.Roy.Met.Soc., 71, 397.

Kratzer, P.A., 1956 : Das stadtklima die wissenschaft. Fried. Vieweg und Sohn, Braunschweig.

Kreider, M.B., 1964 : Pathologic effects of extreme cold. Medical climatology, (Ed. Licht, S.). Elizabeth Licht, New Haven.

Küthner, J., 1949 : Periodische luftlawinen. Met.Rundsch., 2, 183.

Landsberg, H.E., 1956 : The climate of towns. Man's role in changing the face of the earth, (Ed. Thomas, W.L.). University of Chicago Press, Chicago.

... 1960 : Bioclimatic work in the Weather Bureau. Bull.Amer.Met.Soc., 41, 184.

- Leferre, J., 1911 : Chaleur animale et bioenergetique. Paris.
- Leopold, L.B., 1949 : The interaction of trade wind and sea breeze, Hawaii. Jour.Met., 6, 312.
- Lind, A.R., 1964 : Physiologic responses to heat. Medical climatology, (Ed. Licht, S.). Elizabeth Licht, New Haven.
- Lining, J., 1748 : Concerning the weather in South Carolina; with abstracts of the tables of his meteorological observations in Charles-Town. Phil.Trans.Roy.Soc.Lond., 45, 336.
- Lucas, D.H., G. Spurr and F. Williams, 1957 : The use of balloons in atmospheric pollution research. Quart.Jour.Roy.Met.Soc., 83, 508.
- Ludlam, F.H., 1963 : Severe local storms; a review. Meteorological Monographs, Vol. 5, American Meteorological Society, Boston.
- Markham, S.F., 1947 : Climate and the energy of nations. Oxford University Press, London.
- Maurain, C.H., 1947 : Le climat Parisien. Presses Universitaires, Paris.
- Means, L., 1944 : The nocturnal maximum occurrence of thunderstorms in the mid-western states. Dept.Met.Univ.Chicago Misc. Rep. No. 16.
- Meteorological Office, 1959 : The measurement of upper winds by means of pilot balloons. H.M.S.O., London.
- McGee, O.S. and S.L. Hastenrath, 1966 : Harmonic analysis of the rainfall over South Africa. Notos, 15, 79.
- Mitchell, J.M., 1961 : The temperature of cities. Weatherwise, 14, 224.
- Munn, R.E., 1966 : Descriptive micrometeorology. Academic Press, New York.
- Munn, R.E., M.S. Hirst and B.F. Findlay, 1969 : A climatological study of the urban temperature anomaly in the lake-side environment at Toronto. Jour.Appl.Met., 8, 41.
- Myrop, L.O., 1969 : A numerical model of the urban heat island. Jour. Appl.Met., 8, 908.

- Neumann, J., 1951 : Land breezes and nocturnal thunderstorms. Jour.Met., 8, 60.
- Newton, C.W., 1960 : Morphology of thunderstorms and hailstorms as affected by vertical wind shear. Geophys. Monographs, 5, 339.
- Newton, C.W. and S. Katz, 1958 : Movement of large convective rainstorms in relation to winds aloft. Bull.Amer. Met.Soc., 32, 129.
- Newton, C.W. and H.R. Newton, 1959 : Dynamical interactions between large convective clouds and environment with vertical shear. Jour.Met., 16, 483.
- Nitze, F.W., 1936 : Untersuchung der nächtlichen zirkulationsströmung am berghang durch stereophotogrammetrisch vermessene balloonbahnen. Biokl. B., 3, 125.
- Olgyay, V., 1963 : Design with climate. A bioclimatic approach to architectural regionalism. Princeton University Press, New Jersey.
- Panofsky, H.A. and G.W. Brier, 1963 : Some applications of statistics to meteorology. Pennsylvania State University Press, Pennsylvania.
- Pearce, R.P., 1962 : A simplified theory of the generation of sea breezes. Quart.Jour.Roy.Met.Soc., 88, 20.
- Peppler, A., 1929 : Das auto als hilfsmittel der meteorologischen forschung. Zeitschrift für angewandte meteorologie, 46, 305.
- Plummer, J.H., M. Ionides and P.A. Siple, 1945 : Thermal balance of the human body and its application as an index of climatic stress. Report from Climatology and Environmental Protection Section, Office of the Quartermaster General.
- Pooler, F., 1963 : Airflow over a city in terrain of moderate relief. Jour.Appl.Met., 2, 446.
- Prandtl, L., 1942 : Strömungslehre. F. Veitweg and Son, Braunschweig.
- Prindle, R.A., 1964 : Air pollution and community health. Medical climatology, (Ed. Licht, S.). Elizabeth Licht, New Haven.
- Ramage, C.S., 1964 : Diurnal variation of summer rainfall of Malaya. Jour.Trop.Geog., 19, 62.

- Reiher, M., 1936 : Nächtlicher kalte Luftfluss an Hindernissen.  
Biokl. B., 3, 152.
- Renon, E., 1862 : Différences de température entre Paris et  
Choisy-le-Roi. Société Météorologique de France,  
Annuaire, 10, 105.
- Riechel, E., 1933 : Ein Beispiel grosser Temperaturunterschiede  
zwischen Stadt- und -Freiland-Stationen.  
Preussisches Meteorologisches Institut, Veröffentlichungen,  
Bericht, 402, 72.
- Riehl, H., 1954 : Tropical meteorology. McGraw Hill, New York.
- Robinson, S., E.S. Turrell and S.K. Gerking, 1945 : Physiologically  
equivalent conditions of air temperature and humidity.  
Amer. Jour. Phys., 143, 21.
- Sabbagh, M.E. and R.A. Bryson, 1962 : Aspects of the precipitation  
climatology of Canada investigated by the method of  
harmonic analysis. Annls. Assn. Amer. Geog., 52, 426.
- Scaetta, H., 1935 : Les avalanches d'air dans les Alpes et dans les  
hautes montagnes de l'Afrique centrale. Ciel et Terre,  
51, 79.
- Schmidt, F.H., 1947 : An elementary theory of the land and sea breeze  
circulation. Jour. Met., 4, 9.
- Schmidt, W., 1927 : Die Verteilung der Minimum-Temperaturen in der  
Frostnacht des 12. Mai 1927 im Gemeindegebiet von Wien.  
Fortschritte der Landwirtschaft, 2, 687.
- Schnelle, F., 1956 : Ein Hilfsmittel zur Feststellung der Höhe von  
Frostlagen in Mittelgebirgstälern. Met. Rundsch., 9,  
180.
- Sheppard, P.A., 1958 : The effect of pollution on radiation in the  
atmosphere. Int. Jour. Air Water Poll., 1, 31.
- Smith, D., 1967 : A study of air pollution in Johnstown. Unpub. M.Sc.  
thesis, Pennsylvania State University.
- South African Weather Bureau, 1954 : Climate of South Africa, Part I.  
Govt. Printer, Pretoria.
- ... : Climate of South Africa, Part 2.  
Govt. Printer, Pretoria.
- ... 1960 : Climate of South Africa, Part 6.  
Govt. Printer, Pretoria.

- South African Weather Bureau, 1965 : Climate of South Africa, Part 8.  
Govt. Printer, Pretoria.
- ... 1965 : Climate of South Africa, Part 9.  
Govt. Printer, Pretoria.
- ... 1965-66 : Radiosonde Rawin data. Govt.  
Printer, Pretoria.
- ... 1965-67 : Daily synoptic charts. Govt.  
Printer, Pretoria.
- Staley, D.O., 1957 : The low level sea breeze of N.W. Washington.  
Jour.Met., 14, 458.
- ... 1959 : Some observations of surface wind oscillations  
in a heated basin. Jour.Met., 16, 364.
- Sundborg, A., 1950 : Local climatological studies of the temperature  
conditions in an urban area. Tellus, 2, 221.
- Sutton, O.G., 1953 : Micrometeorology. McGraw Hill, New York.
- Taljaard, J.J., 1955 : Stable stratification in the atmosphere over  
Southern Africa. Notos, 4, 217.
- ... 1959 : South African air masses, their properties,  
movement and the associated weather. Unpub. Ph.D.  
thesis, University of Witwatersrand, Johannesburg.
- ... 1967 : Development, distribution and movement of  
cyclones and anticyclones in the southern hemisphere  
during the I.G.Y. Jour.Appl.Met., 6, 973.
- Taljaard, J.J., W. Schmidt and H. van Loon, 1961 : Frontal analysis  
with application to the southern hemisphere. Notos,  
10, 25.
- Taljaard, J.J. and H. van Loon, 1962 : Cyclogenesis, cyclones and  
anticyclones in the southern hemisphere during the  
winter and spring of 1957. Notos, 11, 3.
- ... 1963 : Cyclogenesis, cyclones and  
anticyclones in the southern hemisphere during  
summer 1957-58. Notos, 12, 37.
- Tang, W., 1960 : Analysis of wind structure. Final report; contract  
no. DA - 36 - 039 - sc - 78091 - phase 1, U.S. Army  
Signal Research and Development Lab., New York  
University.

- Terjung, W.H., 1966 : Physiologic climates of the counterminuous United States: a bioclimatic classification based on man. Annls.Assn.Amer.Geog., 56, 141.
- Thom, E.C., 1959 : A discomfort index. Weatherwise, 12, 57.
- Thyer, N. and K.J.K. Buettner, 1962 : Part A : On valley and mountain winds III; Part B : Valley wind theory. Final report University of Washington AF contract 19 (604) - 7201.
- Tyson, P.D., 1964 : Berg winds of South Africa. Weather, 19, 7.
- ... 1966 : Examples of local air circulations over Cato Ridge during July 1965. South African Geog.Jour., 48, 13.
- ... 1967a : An investigation of some topographically-induced local wind systems in Natal. Unpub. Ph.D. thesis, University of Witwatersrand, Johannesburg.
- ... 1967b : Some characteristics of the mountain wind over Pietermaritzburg. South African Geog.Soc. Jubilee Conf.Proc., 103.
- ... 1968a : South-easterly winds over Natal. Jour. for Geog., 111, 237.
- ... 1968b : Velocity fluctuations in the mountain wind. Jour.Atm.Sci., 25, 381.
- ... 1969 : Time series : a problem of numerical analysis in geography. Jour.for Geog., 3, 451.
- Van Bemmelen, W., 1922 : Land und seebrisen in Batavia. Beitrage zur physik der freien atmosphäre, 10, 169.
- Van Lingen, M.S., 1944 : The coastal low of the south and south-east coasts of the Union of South Africa. Tech. Note No. 33, South African Air Force Met. Section.
- Van Loon, H., 1961 : Charts of average 500 mb absolute topography and sea level pressures in the southern hemisphere in January, April, July and October. Notos, 10, 105.
- Vowinckel, E., 1955 : Southern hemisphere weather map analysis: five year mean pressures: Part 2. Notos, 4.
- Wagner, A., 1938 : Theorie und beobachtung der periodischen gebergswinde. Ger.Beit.Geophys., 52, 408.



- Wallington, C.E., 1959 : The structure of the sea breeze front as revealed by gliding flights. Weather, 14, 263.
- Watts, I.E.M., 1955 : Equatorial weather. University of London Press, London.
- Weather on the coasts of Southern Africa, 1941 : vol. 2, Part 4, Meteorological Service of the Royal Navy and South African Air Force, Pretoria.
- Wellington, J., 1955 : Southern Africa Vol. 1. Cambridge University Press, Cambridge.
- Wexler, R.W., 1946 : Theory and observation of land and sea breezes. Bull.Amer.Met.Soc., 27, 272.
- Wyndham, C.J., W. Bouwer, M.G. Devine, H.E. Patterson and D.K.C. MacDonald, 1952 : Examinations of use of heat exchange equations for determining changes in body temperature. Jour.Appl.Phys., 5, 299.
- Yaglou, C.P., 1935 : Indices of comfort. Physiology of heat regulation and science of clothing. (Ed. Newburg, L.H.). W.B. Saunders Co., Philadelphia.
- Yaglou, C.P. and W.E. Miller, 1925 : Effective temperature with clothing. Trans.Amer.Soc. Heat and Vent Engrs., 31, 89.